



HAL
open science

Random access for dense networks: Design and Analysis of Multiband CSMA/CA

Baher Mawlawi

► **To cite this version:**

Baher Mawlawi. Random access for dense networks: Design and Analysis of Multiband CSMA/CA. Networking and Internet Architecture [cs.NI]. INSA Lyon, 2015. English. NNT: . tel-01258500

HAL Id: tel-01258500

<https://theses.hal.science/tel-01258500>

Submitted on 2 Feb 2016

HAL is a multi-disciplinary open access archive for the deposit and dissemination of scientific research documents, whether they are published or not. The documents may come from teaching and research institutions in France or abroad, or from public or private research centers.

L'archive ouverte pluridisciplinaire **HAL**, est destinée au dépôt et à la diffusion de documents scientifiques de niveau recherche, publiés ou non, émanant des établissements d'enseignement et de recherche français ou étrangers, des laboratoires publics ou privés.



Distributed under a Creative Commons Attribution - NoDerivatives 4.0 International License

N° d'ordre 2015ISAL0112
Année 2015

Thèse

Random access for dense networks: Design and Analysis of Multiband CSMA/CA

Présentée devant
L'institut national des sciences appliquées de Lyon

Pour obtenir
Le grade de docteur

Formation doctorale
Traitement du Signal et de l'Image

École doctorale
École doctorale EEA

Par
Baher Mawlawi
(Ingénieur)

Soutenue le 26 novembre 2015 devant la Commission d'examen

Jury MM.

M. Débbah	Professeur (CentraleSupélec), Président du jury
R. Verdone	Professeur (Université de Bologne, Italie), Rapporteur
M. Coupechoux	HDR, Maître de Conférence (Telecom ParisTech), Rapporteur
I. Guérin-Lassous	Professeur (Université Lyon I), Examinatrice
J-P. Cancès	Professeur (ENSIL), Examineur
J-M. Gorce	Professeur (INSA Lyon), Directeur de thèse
J-B. Doré	Docteur Ingénieur (CEA-Leti), Encadrant CEA

Laboratoires de recherche :

Laboratoire CITI – Lyon
CEA-Leti DRT/DSIS/STCS/LSP - Grenoble

Acknowledgments

Je tiens en tout premier lieu à remercier vivement Jean-Marie Gorce d'avoir accepté de prendre la direction de mes travaux et à le remercier pour ses nombreux et pertinents conseils durant toute la durée de mon doctorat.

Je tiens à remercier très particulièrement mon encadrant Jean-Baptiste Doré pour l'excellence de son accompagnement, ainsi que pour la confiance et la grande autonomie qu'il m'a accordé pendant ces trois années, tout en étant très disponible dès que j'en exprimais le besoin, et ce, malgré ses nombreuses contraintes. Je lui suis tout reconnaissant pour son aide infini et pour les responsabilités enrichissantes qu'il a accepté de me confier pendant le doctorat.

J'exprime ma gratitude à Vincent Berg, chef du laboratoire LSP au CEA-Leti, pour ses nombreux encouragements ainsi que pour la richesse de ses conseils. Je le remercie également de m'avoir accueilli dans le laboratoire et témoigné une grande confiance.

Je tiens également à exprimer toute ma reconnaissance à Dominique Noguet, chef du service STCS au CEA-Leti, pour ses nombreux conseils et pour l'opportunité qui m'a offert de pouvoir contribuer au standard IEEE 1900.7 et d'être un membre actif de sein du comité de standardisation.

Je remercie Messieurs Roberto Verdone et Marceau Coupechoux pour l'intérêt qu'ils ont porté à mes travaux en ayant accepté de les rapporter et de participer au jury de la thèse. Je remercie également Mérouane Debbah, Isabelle Guérin-Lassous et Jean-Pierre Cancès pour leur participation à mon jury.

Je veux également remercier tous les membres des équipes LSP, LESC au CEA-Leti et CITI à l'INSA – Lyon qui ont tous largement contribué à la réussite des travaux par leurs encouragements et leurs aides.

Je tiens également à exprimer ma gratitude au CEA-Leti de m'avoir accordé une bourse pour financer mes travaux de thèse. Merci également de m'avoir permis de participer à des différentes conférences qui m'ont enrichi au niveau professionnel autant qu'au niveau personnel. Également, un très grand merci pour notre assistante de direction Sandrine Bertola pour son aide indispensable dans toutes les démarches administratives.

Enfin, je tiens à remercier très affectueusement ma famille – mes parents, frères et sœur ainsi que mes amis pour l'aide qu'ils m'ont apporté, mais aussi leur soutien et leur patience pendant ces trois années qui m'ont permis d'avancer et de progresser dans mes travaux et largement contribué à la réussite de mes trois années de doctorat.

Abstract

Random protocols are promising candidates for future wireless systems dedicated to machine to machine (M2M) communication. Such protocols are usually based on a random access with simple techniques of medium sensing and deferring to reduce collisions while avoiding the use of complex schedulers. Among different protocols, Carrier sense multiple access/collision avoidance with a Request-To-Send/Clear-To-Send (CSMA/CA-RTS/CTS) is an opportunistic protocol which could be adopted for M2M scenarios. Such approach is efficient to avoid collisions between data packets but in a very dense network, the random access used to send the RTS suffers itself from a high probability of collision which degrades the performance. In order to mitigate this effect, RTS collisions should be reduced. This thesis proposes to address this issue by splitting the common channel in sub-channels for transmitting the RTS messages. While the common channel is used as a whole for data transmission. Multiple nodes can then contend in time and frequency for these RTS sub-channels, thereby reducing RTS collisions and increasing overall efficiency. In this work, we thus derive a complete protocol solution relying on CSMA/CA - RTS/CTS multiplexing a multi-channel configuration for RTS messages and a unique channel for data transmission. An enhanced version based on users scheduling is integrated as well. In this thesis, the proposed protocol is investigated from a joint PHY-MAC point of view. This strategy is shown to provide better system performance particularly for loaded networks. An accurate analytical model derived as a straightforward extension of the Bianchi model is analyzed and validated by simulations. Performance in terms of saturation throughput, transmission delay and packet drop probability is discussed.

Résumé

Les protocoles de communications à accès aléatoires sont des candidats prometteurs pour les futurs systèmes de communications sans fil dédiés aux applications machine à machine (M2M). Ces méthodes d'accès sont généralement basées sur des techniques d'accès aléatoires mettant en œuvre des concepts simples de sondage de canal et de report de la transmission pour réduire les collisions, tout en évitant l'utilisation d'ordonnanceurs complexes. Parmi les différents protocoles, Carrier sense multiple access/collision avoidance with a Request-To-Send/Clear-To-Send (CSMA/CA-RTS/CTS) est un protocole qui pourrait être adopté pour les scénarios de M2M. Cette approche est efficace pour éviter les collisions entre les paquets de données. Cependant dans le cas d'un réseau très dense, les performances sont dégradées à cause de la forte probabilité de collisions. Pour atténuer cet effet, les collisions entre les messages de contrôles RTS doivent être réduites.

Cette thèse propose de résoudre ce problème en divisant le canal commun en sous-canaux pour transmettre les messages de contrôle de demande d'accès au canal ; le canal commun est utilisé dans son ensemble pour la transmission de données. L'ajout d'un degré de liberté pour le message de demande d'accès permet de réduire la probabilité de collision, et donc d'améliorer les performances du système notamment dans des scénarios avec des nombres importants de nœuds souhaitant communiquer. Dans ce travail, nous dérivons ainsi une solution complète de méthode d'accès en s'appuyant sur le CSMA / CA - RTS / CTS et en multiplexant une configuration multi-canal pour les messages RTS et un canal unique pour la transmission de données. Une version améliorée, basée sur l'ordonnement des utilisateurs, est également étudiée. Un modèle analytique a été développé, analysé et validé par simulations. Celui-ci est une extension du modèle Bianchi. Les performances en termes de débit saturé, de temps de transmission et de la probabilité de rejet de paquets sont discutées. Enfin, les impacts liés à la prise en compte d'une couche physique de type multi porteuses sont discutés dans le dernier chapitre.

Résumé des travaux de thèse

Motivation

De nos jours, les appareils sans fil sont largement déployés dans notre société. Dans les années à venir, il est prévu une explosion du nombre de terminaux pouvant communiquer, avec et sans intervention humaine. Dans ce contexte, des études sont actuellement menées pour la définition d'un futur réseau 5G [1]. Les besoins identifiés sont très divers et parfois même antinomiques. Au-delà de 2020, il est prévu que la plupart des appareils soient connectés. Les utilisateurs pourront interagir à travers des dispositifs multiples et connectés qui nécessiteront, globalement, une bande passante ultra-large [2].

Par exemple, [3] mentionne la possibilité d'applications gourmandes en bande passante comme la communication vidéo instantanée. Celles-ci génèrent un volume important de trafic avec des contraintes de latence faibles. Le débit de données d'utilisateur doit être délivré de façon uniforme dans la zone de couverture (même sur les bords des cellules), et doit être d'au moins 50 Mbps [3]. Les communications entre machines autonomes (M2M) sont d'autres applications cibles de la 5G. Elles interviennent dans les processus de production (contrôle/commande de machines industrielles autonomes, engins autonomes), la surveillance et la sécurité en environnements contraints (drones, robots mobiles en environnements difficiles, télésurveillance/détection d'intrusion, réseaux de capteurs), les systèmes de contrôle et de sécurité des circulations automobiles (Intelligent Transport Systems, analyse de trafic autoroutier). Dans ce contexte, les données échangées peuvent être sporadiques (surveillance, alarmes) ou répétitives (contrôle/commande) avec des tailles de paquets échangés importantes, de l'ordre de plusieurs Kilo-octets (images fixes ou animées). Ces débits importants sont associés à une communication fiable et robuste, avec une latence maîtrisée dans un contexte de réseaux chargés. Au niveau de la couche d'accès, des protocoles robustes doivent être intégrés. Parmi les candidats, les méthodes d'accès aléatoires peuvent avoir un intérêt particulier. Ces dernières pourraient être adoptées pour de nombreuses raisons : elles permettent de fonctionner avec toute la bande passante disponible dans un environnement de nombre inconnu de dispositifs [4], fonctionnent d'une manière répartie [5] et conduisent à un déploiement moins coûteux que les méthodes ordonnancées car elles ne nécessitent pas de planification, d'interopérabilité et de complexité de gestion [6].

Parmi les méthodes d'accès aléatoire couramment utilisées, le CSMA / CA - RTS / CTS (Carrier Sense Multiple Access / Collision Avoidance – Request To Send / Clear To Send) est un candidat privilégié. Il est utilisé dans de nombreux réseaux sans fil et son succès, à travers son utilisation dans le WiFi, en fait une méthode d'accès éprouvée. Le CSMA/CA - RTS/CTS est un protocole d'accès aléatoire qui permet aux émetteurs d'accéder à un canal partagé tout en assurant à long terme des débits égaux entre utilisateurs. Celui-ci est également intéressant pour lutter contre le problème des nœuds cachés [7].

Cependant, le CSMA / CA a un point faible majeur. Dans le cas d'un réseau chargé, lorsque le nombre de nœuds actifs est important, les performances du système sont nettement dégradées à cause des collisions entre les paquets. Pour mettre en exergue cet effet, prenons un exemple simple. Considérons les paramètres de la couche physique de l'IEEE 802.11n [8] avec un débit égal à 72.2 Mbps et analysons les débits en mode saturé en fonction de la charge du réseau. La Figure 1 montre le débit normalisé en fonction du nombre des nœuds

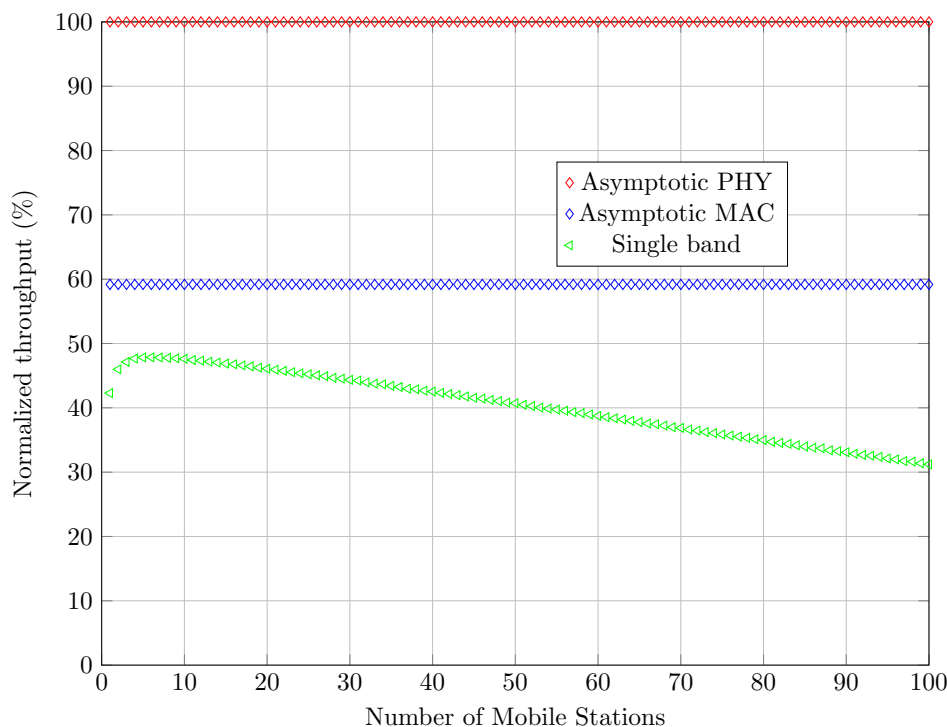


Figure 1: Performance de la couche d'accès CSMA/CA RTS/CTS.

mobiles pour différentes configurations. La courbe “asymptotic PHY” sert de référence ; elle décrit le débit en présence d’une simple couche physique, avec une couche d’accès parfaite (sans collision). La courbe “asymptotic MAC” correspond à la borne supérieure du protocole CSMA/CA - RTS/CTS ; ces performances intègrent les pertes dues aux mécanismes de poignée de main. Une fois encore on considère qu’il n’y a pas de collisions. Il est clair que le débit du CSMA/CA - RTS/CTS se dégrade rapidement quand le nombre de nœuds actifs dans le réseau augmente. En considérant 100 nœuds, les performances du CSMA/CA sont de 30% inférieures à la borne asymptotique. Cet exemple concret montre les limites du système actuel dans des configurations de réseaux chargés et ouvre à des perspectives d’améliorations.

Le but de cette thèse est donc d’étudier comment améliorer les performances des protocoles d’accès pour s’approcher des bornes asymptotiques. Plus particulièrement, nous nous sommes intéressés dans ce travail aux protocoles de type CSMA/CA.

Objectifs de la thèse

Dans ce travail, l’impact du nombre élevé de nœuds sur les performances du CSMA / CA - RTS / CTS est étudié. Plus particulièrement nous avons cherché à :

- Identifier les causes de la dégradation des performances du système lorsque le nombre de nœuds est élevé.
- Proposer un nouveau protocole afin d’améliorer les performances dans le cadre de réseaux chargés.
- Analyser d’une manière analytique les performances - calculer les expressions du débit en mode saturé dans certaines conditions pour deux cas : lorsque la limite de retransmission est fini et infini.
- Analyser et évaluer la performance des solutions proposées en fonction de plusieurs paramètres.

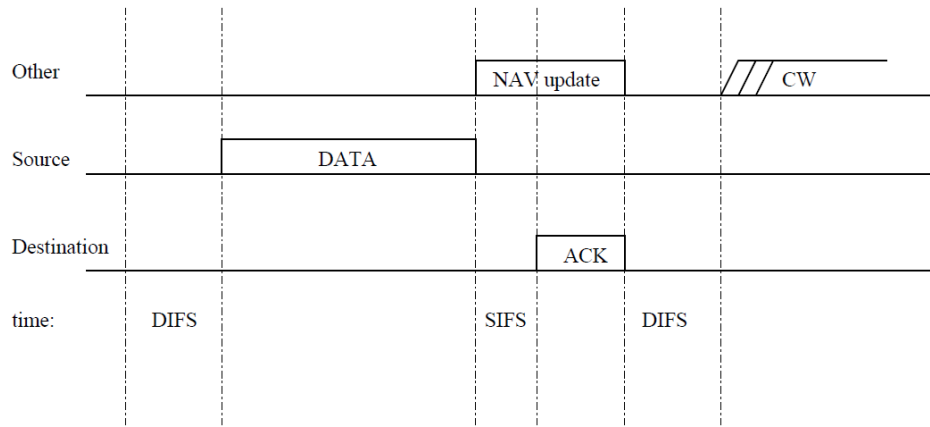


Figure 2: CSMA/CA Basique [9]

- Étudier l'impact d'une couche physique de type multiporteuse sur le protocole proposé. En particulier, calculer des expressions analytiques pour le rapport signal sur interférence (*SIR*) en tenant compte de l'effet de la couche physique.

Chapitre 2 - Généralité sur les protocoles d'accès

Dans ce chapitre nous présentons un état de l'art en rapport avec les différents types de méthodes d'accès. Tout d'abord, le concept général de protocole d'accès est introduit. Nous nous focaliserons sur les méthodes d'accès ordonnancées et aléatoires. Dans un second temps, nous expliciterons la théorie fondamentale d'analyse des performances des protocoles de type CSMA/CA qui se repose sur les chaînes de Markov. Basé sur le modèle original, nous introduirons un modèle modifié pour résoudre le problème « d'entonnoir » que l'on explicitera. Nous discuterons enfin des travaux antérieurs dans la dernière partie de ce chapitre.

Le CSMA/CA

Considérons la version basique du CSMA/CA, représentée sur la Figure 2. Chacun des nœuds ayant un paquet à transmettre doit d'abord sonder le canal. Si le canal est détecté comme inactif pendant une période supérieure à une durée prédéfinie (DIFS), le nœud envoie son paquet de données. Après la réception correcte d'un paquet de données, un accusé de réception (ACK) est renvoyé. Si le canal n'est pas libre, le nœud diffère sa transmission. Un compteur d'attente aléatoire est alors généré dans l'intervalle $[0, CW-1]$ où CW est une variable appelée « fenêtre de contention ». Lorsque le canal est détecté libre, le compteur d'attente est décrémenté d'une unité. Si le canal est détecté occupé le compteur sera figé. Le nœud envoie son paquet de données lorsque le compteur atteint 0. Si un accusé de réception est bien reçu, la transmission est réussie et la variable CW est initialisée à la valeur CW_{min} . En cas d'échec de transmission, la variable CW est doublée jusqu'à ce qu'elle atteigne une valeur maximale, CW_{max} .

Lorsque le mode RTS/CTS est activé par le nœud possédant un paquet à transmettre, ce dernier transmet un message de demande d'accès RTS comme représenté sur la Figure 3. Si le paquet RTS est reçu sans collision, un CTS est renvoyé pour informer tous les nœuds dans la cellule que le canal est réservé. Tous les nœuds reportent leurs transmissions pour la durée spécifiée dans le message RTS : ce mécanisme est appelé détection virtuelle. Après la réception réussie d'un paquet de données, un paquet d'acquiescement (ACK) est renvoyé. Si le canal n'est pas libre, le nœud diffère sa transmission. Un compteur d'attente aléatoire est alors généré dans l'intervalle $[0, CW-1]$. Sous l'hypothèse d'une transmission sans perturbation et

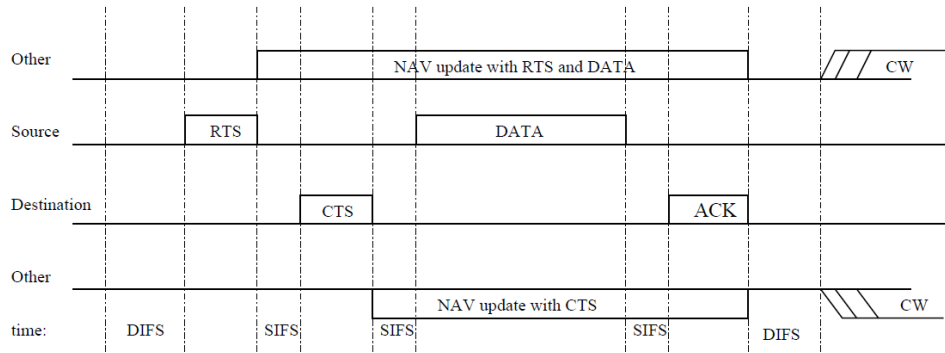


Figure 3: CSMA/CA - RTS/CTS [9]

d'un sondage parfait du canal, les collisions ne peuvent se produire que sur les paquets RTS et CTS. La transmission des paquets de données peut donc se dérouler sans interférence des autres nœuds.

Outils d'analyse pour le CSMA/CA

Considérons un réseau de plusieurs nœuds avec un point d'accès. Si le canal est occupé, les nœuds choisissent aléatoirement un compteur temporel dans l'intervalle $[0, CW)$ avec CW la fenêtre de contention. CW est un entier entre CW_{min} et CW_{max} . Ce compteur sera décrémenté par d'une unité par slot de temps à chaque fois que le canal est libre. Quand le canal est occupé, le compteur est bloqué. Il sera décrémenté à nouveau une fois que le canal redeviendra libre pour une durée au moins égale à une période DIFS. Après chaque collision, la variable CW est doublée jusqu'à une valeur maximale égale à $CW_{max}-1$.

Dans le but d'analyser les performances du protocole CSMA/CA, Bianchi [10] propose de répartir l'analyse en 2 ensembles. En se basant sur un modèle à base d'une chaîne de Markov, une probabilité stationnaire π qui correspond à la probabilité d'émission d'un paquet dans un intervalle de temps est calculée. Le débit en mode saturé peut être calculé en fonction de cette probabilité π et en étudiant les événements qui peuvent avoir lieu dans un slot de temps (collision, succès et attente).

Probabilité de transmission de paquet

Soit N le nombre de nœuds actifs en mode saturé (chaque nœud possède toujours un paquet prêt pour la transmission) présent dans le réseau. Chaque état de la chaîne de Markov est représenté par $\{s(t), b(t)\}$, avec $b(t)$ est un processus stochastique qui représente le compteur temporel (backoff) pour un nœud donné et $s(t)$ est le processus stochastique qui représente l'état de backoff $(0, 1, \dots, m)$ pour le nœud en temps t . Une échelle de temps discret et entier est adoptée ; les instants t et $(t + 1)$ signifient le début de deux slot de temps consécutives. La probabilité d'une collision p peut être calculée en supposant les hypothèses suivantes [11] :

- Pas de nœuds cachés ni de "capture effect".
- Les échecs de transmissions ne se produisent qu'à la suite d'une collision.
- Tous les nœuds sont en mode saturé, ayant donc toujours des paquets à envoyer.
- La probabilité de collision pour un nœud, p , est constante et indépendante de l'historique de collision du nœud et de tous les autres nœuds.
- La probabilité de collision ne dépend pas de la phase d'attente à laquelle la transmission est effectuée.

- Tous les nœuds ont les mêmes débits et la même durée de temps de transmission.

Aussi, nous définissons p comme étant la probabilité que, dans une tranche de temps, au moins un des $N - 1$ nœuds transmet. Cette probabilité peut être exprimée par :

$$p = 1 - (1 - \pi)^{(N-1)} \quad (1)$$

Avec π la probabilité qu'un nœud transmet un paquet. Elle peut être exprimée par :

$$\pi = \sum_{i=0}^m b_{i,0} \quad (2)$$

Avec $b_{i,k} = \lim_{t \rightarrow \infty} P\{s(t) = i, b(t) = k\}$, $i \in (0, m)$, $k \in (0, CW_i - 1)$ la distribution stationnaire de la chaîne. $b(i, 0)$ est considérée car la transmission aura lieu une fois le backoff égal à 0. En considérant la chaîne de Markov illustrée sur la Figure 4, $b_{i,0}$ peut être exprimée en fonction de p :

$$b_{i,k} = \frac{W_i - k}{W_i} \begin{cases} (1 - p) \sum_{j=0}^m b_{j,0} & i = 0 \\ pb_{i-1,0} & 0 < i \leq m \\ p(b_{m-1,0} + b_{m,0}) & i = m \end{cases} \quad (3)$$

Après normalisation et en considérant l'équation 3, $b_{0,0}$ peut être exprimée en fonction de p :

$$\begin{aligned} 1 &= \sum_{i=0}^m \sum_{k=0}^{CW_i-1} b_{i,k} \\ &= \frac{b_{0,0}}{2} \left[W_{min} \left(\sum_{i=0}^{m-1} (2p)^i + \frac{(2p)^m}{1-p} \right) + \frac{1}{1-p} \right] \end{aligned} \quad (4)$$

Avec $W_{min} = CW_{min} - 1$. Finalement, en combinant les équations (2),(3), et (4), la probabilité d'accès au canal π est égale à :

$$\begin{aligned} \pi &= \sum_{i=0}^m b_{i,0} \\ &= \frac{b_{0,0}}{1-p} \\ &= \frac{2(1-2p)}{(1-2p)(W_{min} + 1) + pW_{min}(1 - (2p)^m)} \end{aligned} \quad (5)$$

Ces deux équations, (1) et (5), forment un système de deux équations non linéaires qui aura une solution unique et peut être résolu numériquement.

Débit saturé

Le débit en mode saturé, qui représente le rapport de la quantité d'informations transmise sur la durée totale de transmission, peut être exprimé en utilisant l'expression suivante [9] :

$$\begin{aligned} \tau &= \frac{E[\text{Quantité d'information durant un slot de temps}]}{E[\text{Durée du slot de temps}]} \\ &= \frac{P_s P_{tr} L}{P_s P_{tr} T_s + P_{tr}(1 - P_s) T_c + (1 - P_{tr}) T_{id}} \end{aligned} \quad (6)$$

Avec $P_{tr} = 1 - (1 - \pi)^N$ la probabilité qu'il y ait au moins une transmission dans un slot de temps; L est la quantité d'informations; T_s est la durée moyenne nécessaire pour transmettre

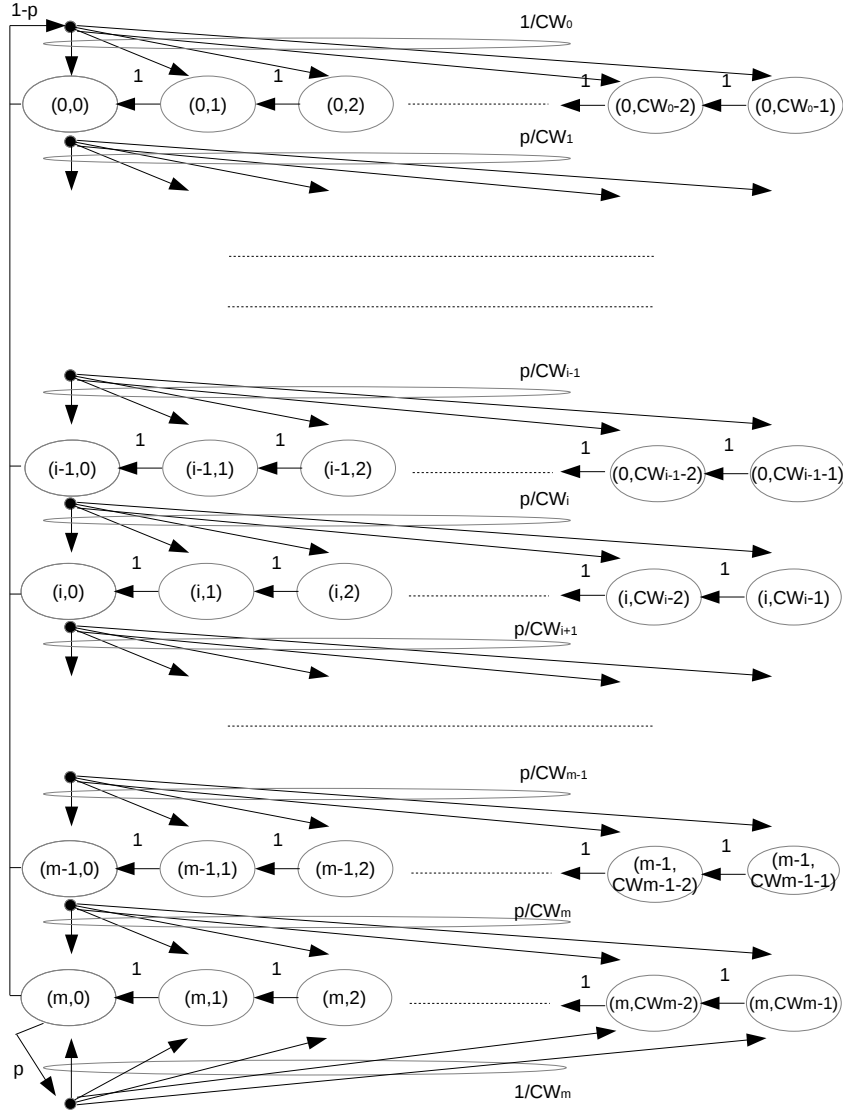


Figure 4: Modèle de Bianchi pour l'analyse du CSMA/CA [10].

un paquet de taille L ; $P_s = \frac{N\pi(1-\pi)^{N-1}}{1-(1-\pi)^N}$ est la probabilité d'une transmission avec succès; T_{id} est la durée d'une période d'attente (un slot de temps); et T_c est la durée moyenne passée dans la collision. T_c et T_s peuvent être calculées pour le mode de transmission RTS/CTS avec [9]:

$$\begin{cases} T_s = RTS + SIFS + \sigma + CTS + SIFS + \sigma + H + P \\ \quad + SIFS + \sigma + ACK + DIFS + \sigma \\ T_c = RTS + DIFS + \sigma \end{cases} \quad (7)$$

avec H , P , and ACK les durées nécessaires pour transmettre respectivement l'entête du paquet, le paquet, et l'acquittement. σ est la durée de propagation.

Chapitre 3 - Multibande CSMA/CA - RTS/CTS

Dans ce chapitre, nous présentons les motivations qui nous ont amenées à proposer une nouvelle méthode d'accès : le Multiband CSMA / CA-RTS / CTS (M-CSMA / CA-RTS / CTS). Une description complète du M-CSMA/CA - RTS/CTS est donnée suivie d'une étude de cas.

Nous dérivons un modèle analytique qui permet d'analyser les performances du système et de comparer ses performances par rapport aux performances du protocole déjà décrit dans l'état de l'art (CSMA/CA - RTS/CTS). Enfin, nous discutons de deux méthodes d'allocation des nœuds qui ajoutent un nouveau degré de liberté pour les concepteurs.

M-CSMA/CA-RTS/CTS

Sans perte de généralité, nous considérons un scénario où une pluralité de nœuds transmettent des paquets à un point d'accès (PA). Les performances du système sont étroitement liées au nombre de collisions entre les paquets transmis simultanément. Considérant un canal symétrique et idéal (couche physique parfaite sans perte de paquets) avec un mécanisme RTS/CTS, les collisions entre paquet ne peuvent se produire que pendant la transmission des messages RTS.

Le multiplexage fréquentiel (orthogonal) des messages RTS est proposé. Ainsi, un seul canal est divisé en n sous-canaux lors de la transmission des RTS. Il convient de mentionner que la durée d'un paquet RTS est dans ce cas multipliée par un facteur n lorsque la bande de fréquence est réduite d'un facteur n , et ce pour préserver la capacité de la liaison. Cette propriété sera discutée plus en détail dans le chapitre dédié à l'analyse de la méthode en présence d'une couche physique de type multiporteuse.

Nous supposons que tous les nœuds ont la connaissance de la taille des sous-canaux et de leurs fréquences centrales. La stratégie proposée est utilisée pour réduire les collisions entre les paquets de différents utilisateurs (nœuds source), qui sont disposés à accéder en même temps à un point d'accès commun (nœud destinataire) et cela en introduisant un degré de liberté supplémentaire avec le choix d'un sous-canal. Le récepteur doit être à l'écoute de tous les sous-canaux simultanément.

On suppose qu'il a été alloué, pour chaque nœud (STA), un sous-canal de RTS parmi les n possibles. Si un signal est détecté sur au moins un sous-canal, le canal est déclaré occupé. Ensuite, une période (exprimée en nombre de slot de temps) d'un compteur d'attente est choisie aléatoirement dans l'intervalle $[0, CW-1]$, où CW est une fenêtre de contention. Une fois que le canal est détecté disponible sur une durée DIFS, le compteur de temporisation est décrémenté d'une unité (un slot de temps). Le compteur d'attente se fige quand le canal est occupé, et reprend lorsque le canal est de nouveau disponible.

Lorsque le compteur d'attente arrive à zéro, la source (STA) envoie un message de demande d'autorisation (RTS) vers le nœud de destination en utilisant son sous-canal. Il attend alors de recevoir un message d'autorisation (CTS) du nœud de destination (point d'accès) avant de transmettre ces données. Du côté du nœud destination, tous les sous-canaux sont écoutés simultanément. Si un ou plusieurs RTS sont détectés, le point d'accès (PA) diffuse un message CTS sur tous les sous-canaux indiquant quel nœud est autorisé à communiquer.

Le nœud gagnant envoie alors ses données et attend de recevoir l'acquittement du PA. Les données et le message d'acquittement (ACK) sont envoyés sur l'agrégation de tous les sous-canaux.

Décrivons un exemple simple qui considère le cas de trois STA : STA3, STA20, STA26 et un PA. La figure 5 illustre la façon dont la collision peut être réduite en divisant le canal RTS en deux sous-canaux. Le premier sous-canal a été alloué aux STA20 et STA26. Le deuxième sous-canal a été alloué au nœud STA3. Chacun des nœuds tente d'envoyer un signal RTS sur son sous-canal. Du côté de récepteur, une collision se produit sur le sous-canal 1 alors que le message RTS peut être décodé sur le sous canal 2. Le PA choisit donc la STA3 et envoie un message CTS sur tous les sous-canaux présents indiquant que la STA3 a gagné l'accès au canal. Tous les nœuds reçoivent et décodent le CTS et seul STA3 tente d'envoyer ses paquets au cours d'une quantité définie de temps. Une communication réussie a lieu lorsque le PA répond par un acquittement qui est diffusé sur tous les sous-canaux.

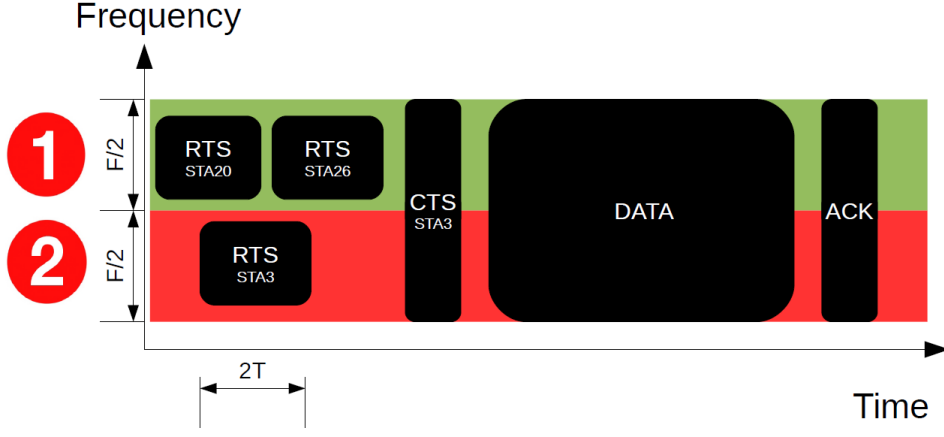


Figure 5: Exemple de scénario pour le M CSMA/CA - RTS/CTS

Modélisation Analytique du M-CSMA/CA

Dans cette section, la méthode d'accès proposée est modélisée analytiquement par des chaînes de Markov dans le cas d'un nombre infini de retransmission [12]. En d'autres termes, cela signifie que le nœud essaie de transmettre un paquet jusqu'au succès en restant bloqué dans l'état d'une fenêtre contention égale à CW_{max} .

Dans cette partie, nous dérivons analytiquement l'expression du débit en mode saturé (tous les nœuds ont toujours un paquet à envoyer) pour le protocole proposé. Pour cela, nous suivons le même raisonnement que Bianchi [10, 13]. L'extension au cas multi canal est proposée en prenant en compte la division en plusieurs sous canaux du message RTS.

Le débit saturé, qui est la charge utile moyenne d'information dans une tranche de temps sur la durée moyenne d'une tranche de temps, peut être exprimé en utilisant l'expression [10]:

$$S^n = \frac{E[\text{information utile transmise dans un slot temps}]}{E[\text{Durée de slot de temps}]} \quad (8)$$

$$= \frac{P_s^n \times P_{tr}^n L}{P_s^n \times P_{tr}^n T_s^n + P_{tr}^n \times (1 - P_s^n) T_c^n + (1 - P_{tr}^n) T_{id}}$$

Cette formulation est strictement équivalente à celle proposée par Bianchi [10], mais nous allons voir par la suite comment ces variables changent en fonction de n , le nombre de sous canaux.

Les exposants se réfèrent au nombre des bandes de RTS ; P_{tr}^n est la probabilité qu'il y aura au moins une transmission dans le système qui considère n canaux de RTS dans le temps considéré ; L est la taille moyenne de paquets de données utiles ; T_s^n est le temps moyen nécessaire pour transmettre un paquet de la taille L (y compris les périodes d'espacement inter-trames [10]) ; P_s^n est la probabilité d'une transmission réussie ; T_{id} est la durée de la période d'inactivité (un seul slot de temps) ; et T_c^n est le temps moyen passé dans un état de collision. T_c^n et T_s^n peuvent être calculés pour le mode de transmission RTS / CTS avec:

$$\begin{cases} T_s^n = n \times RTS + SIFS + \sigma + CTS + SIFS + \sigma + H \\ \quad + P + SIFS + \sigma + ACK + DIFS + \sigma \\ T_c^n = n \times RTS + DIFS + \sigma \end{cases} \quad (9)$$

Où H , P , et ACK correspondent aux durées de transmission nécessaires pour envoyer l'en-tête des paquets, la charge utile, et l'acquittement, respectivement. σ est le délai de propagation. L'objectif est de calculer P_{tr}^n et P_s^n .

La probabilité de transmission et la probabilité de succès pour n sous-canaux prises en compte dans le système sont données par:

Théorème 1 :

$$P_{tr}^n = 1 - \prod_{i=1}^n (1 - \pi_i)^{N_i} \quad (10)$$

$$P_s^n = \frac{1 - \prod_{i=1}^n (1 - N_i \pi_i (1 - \pi_i)^{N_i - 1})}{1 - \prod_{i=1}^n (1 - \pi_i)^{N_i}} \quad (11)$$

N_i est le nombre de nœuds actifs affectés au sous-canal i et π_i est la probabilité qu'un nœud associé au sous-canal i émette dans un slot de temps choisi d'une façon aléatoire. Les équations 10 et 11 montrent que les probabilités de transmission et de succès pour l'ensemble du système sont équivalentes à au moins une transmission avec succès sur un sous-canal. Maintenant, nous proposons de calculer l'expression de π_i qui sera exprimée par le théorème 2.

Théorème 2 :

$$\pi_i = \frac{2}{1 + W_{min_i} + p_i W_{min_i} \sum_{k=0}^{m_i - 1} (2p_i)^k} \quad (12)$$

Cette probabilité d'accès au canal est inversement proportionnelle à la fenêtre de contention minimale et à la probabilité de collision liée à chaque état de backoff. Dans le cas où le nombre d'utilisateurs actifs présents dans le système est réparti de manière égale sur tous les sous-canaux, les probabilités de transmission et de succès pour l'ensemble du système peuvent être exprimées de la manière suivante :

cas 1: N est multiple de n :

Dans ce cas, $\pi_1 = \pi_2 = \dots = \pi_i = \dots = \pi_n = \pi$ and $N_1 = N_2 = \dots = N_i = \dots = N_{n-1} = N_n = \frac{N}{n}$

$$P_{tr}^n = 1 - (1 - \pi)^N \quad (13)$$

$$P_s^n = \frac{1 - (1 - \frac{N}{n} \pi (1 - \pi)^{\frac{N}{n} - 1})^n}{1 - (1 - \pi)^N} \quad (14)$$

Il faut noter que le cas $n = 1$ correspond au résultat donné par Bianchi [10].

case 2: N n'est pas multiple de n :

La répartition des nœuds sur les bandes peut être exprimée par l'équation 15.

$$\begin{aligned} N_1 &= \left\lfloor \frac{N}{n} \right\rfloor \\ N_2 &= \left\lfloor \frac{N - N_1}{n - 1} \right\rfloor \\ N_i &= \left\lfloor \frac{N - \sum_{k=1}^{i-1} N_k}{n - k} \right\rfloor \\ N_n &= N - \sum_{k=1}^{n-1} N_k \end{aligned} \quad (15)$$

Les probabilités de succès et de transmission liées à ces cas sont données par les équations 10 et 11.

Validation

Afin de valider l'expression analytique du débit, nous considérons le cas de deux sous-canaux RTS avec une allocation a priori équi-repartie des nœuds. Nous considérons également une couche physique du type IEEE 802.11n dont les paramètres sont rapportés dans le tableau 1.

La figure 6 représente l'erreur relative entre le modèle analytique et les résultats de simulation du protocole proposé en fonction du nombre de nœuds dans le réseau. La différence qui apparait est négligeable (inférieure à 5 %). Cette erreur peut s'expliquer par les hypothèses de modélisation que nous avons considérées :

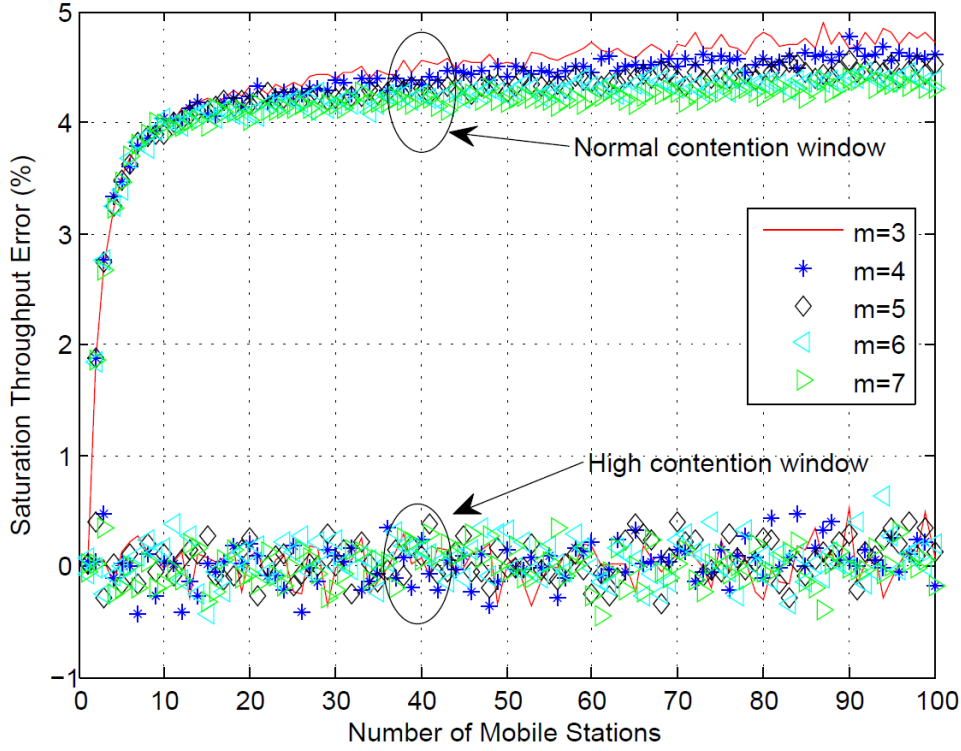


Figure 6: Erreur (%) entre le modèle analytique et la simulation.

Packet payload	8184 bits
MAC header	272 bits
PHY header	128 bits
ACK length	112 bits + PHY header
RTS length	160 bits + PHY header
CTS length	112 bits + PHY header
Channel Bit Rate	72.2 Mbit/s
Propagation Delay	1 μ s
SIFS	10 μ s
Slot Time	9 μ s
DIFS	28 μ s

Table 1: Paramètres de la couche physique 802.11n 20Mhz

- La probabilité de collision, p_i , est constante et indépendante de l'historique des collisions du nœud et de tous les autres nœuds.
- La probabilité de collision ne dépend pas de la phase de temps au cours de laquelle la transmission est faite.

Ces hypothèses se vérifient dans le cas d'une fenêtre de contention minimale importante et la présence d'un grand nombre de nœuds mobiles (loi des grands nombres).

Remarque : la simulation avec une fenêtre minimale de contention de taille importante ($CW_{min} = 2^{20}$) a été réalisée et l'erreur tend vers zéro. Même si ce paramètre n'a pas d'intérêt pratique, il sert à valider la modélisation. Ces courbes sont illustrées sur la figure 6 pour différent nombre d'état de backoff légendées par « high ».

Il faut noter que cette méthode d'accès améliore les performances du système en termes de débit et de délai par rapport au CSMA/CA classique fonctionnant sur un seul canal (adopté dans le standard Wifi par exemple) et plus particulièrement pour les réseaux chargés.

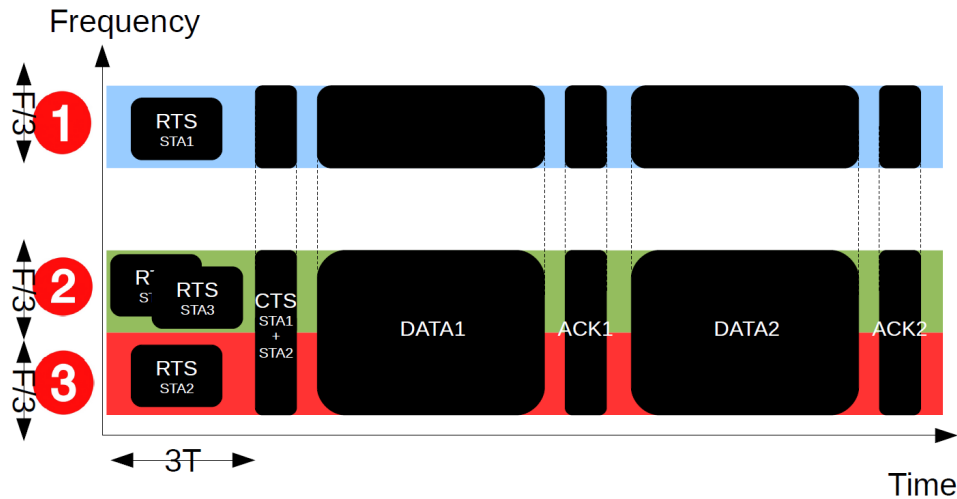


Figure 7: M-CSMA/CA ordonnance avec une taille d'ordonnanceur de 2

Chapitre 4 - M- CSMA/CA - RTS/CTS avec ordonnancement

Une nouvelle technique basée sur le M-CSMA/CA-RTS/CTS est proposée dans ce chapitre. L'idée vient du constat suivant : dans certains cas on peut recevoir une pluralité de messages RTS sans collision. L'idée est donc d'ordonner les nœuds sans qu'ils aient à refaire toute une nouvelle procédure d'accès au canal.

Dans un premier temps, on présentera la technique proposée. Ensuite, on étudiera et on analysera les performances du système. Finalement, cette nouvelle technique sera comparée à celle présentée dans le chapitre précédent.

Description de la technique

Considérons un réseau composé de quatre nœuds STA0, STA1, STA2, STA3 prêts à transmettre et un point d'accès (PA). La Figure 7 illustre le scénario considéré. Les nœuds STA1 et STA2 choisissent la 1ère et la 3ème sous-bande. Les nœuds STA0 et STA3 choisissent la seconde sous-bande. Tous les nœuds transmettent leur message RTS sur les sous-bandes choisies. Le PA détecte les messages RTS des STA1 et STA2 mais ne sera pas capable de decoder le message RTS sur la 2ème sous-bande à cause de la collision. Le PA choisit de servir STA1 puis STA2 et il diffuse le message CTS sur toutes les sous-bandes avec les informations d'ordonnement. Le choix des nœuds peut être aléatoire ou peut dépendre d'autres facteurs (priorité du service, distance...). Le nombre de nœuds pouvant être servis par le PA dépend de la taille de l'ordonnanceur. Dans le cas illustré, la taille de l'ordonnanceur est égale à deux. Tous les nœuds reçoivent et décodent le CTS et seulement STA1 et STA2 peuvent transmettre. Une fois l'ACK pour STA1 reçu, le canal devient libre et STA2 sera autorisé à transmettre ses données. Lorsque l'ACK de STA2 est diffusé, indiquant le succès de la transmission, le canal redevient libre pour une nouvelle procédure de backoff.

Cette stratégie permet de servir successivement les nœuds en réduisant la probabilité de collision des messages RTS et en diminuant aussi le temps nécessaire pour effectuer une transmission ; dans le cas du second nœud STA2, il n'a pas été nécessaire de refaire toute la procédure d'accès au canal.

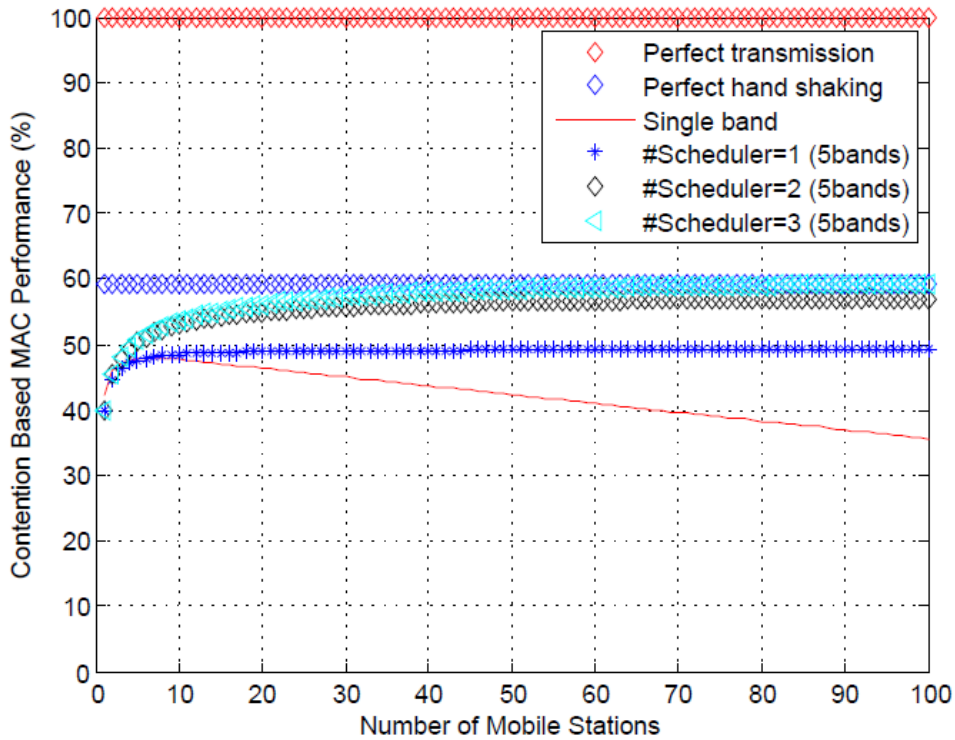


Figure 8: Les performances des méthodes d'accès à contention.

Étude des performances

Dans cette partie on propose d'étudier les performances du débit normalisé en mode saturé pour la technique proposée. Les performances sont également comparées avec les bornes usuelles (couche physique pure et couche MAC pure). La Figure 8 montre le débit normalisé en mode saturé du multi bande CSMA/CA-RTS/CTS avec la technique proposée en considérant 5 sous-bandes en fonction du nombre de nœuds présents dans le réseau.

La courbe PHY sert comme référence et correspond à la performance d'une communication sans aucune perte. La courbe MAC correspond aux performances maximales du CSMA/CA-RTS/CTS. Ces résultats montrent que dans le cas d'un réseau chargé, il est possible d'atteindre les bornes supérieures de la couche MAC en considérant la technique proposée dans ce chapitre avec 5 sous-bandes et une taille d'ordonnancement égale à 3. Ce chiffre est à mettre en relief avec les performances du CSMA/CA-RTS/CTS classique (perte 64%).

Synthèse

En guise de synthèse, une comparaison entre le comportement du CSMA/CA-RTS/CTS, M-CSMA/CA-RTS/CTS et le M-CSMA/CA-RTS/CTS ordonné est illustrée sur les figures 9 et 10.

Dans le cas de réseaux chargés, le M-CSMA/CA-RTS/CTS montre sa suprématie comparé au CSMA/CA-RTS/CTS. Les performances sont améliorées en introduisant la technique d'ordonnancement. Au contraire, pour un cas de réseau peu chargé, le CSMA/CA-RTS/CTS possède des performances meilleures que le M-CSMA/CA-RTS/CTS, même en introduisant la technique d'ordonnancement. Il faut également mentionner que le M-CSMA/CA-RTS/CTS nécessite légèrement plus d'information de « signaling » comparé au CSMA/CA-RTS/CTS conventionnel.

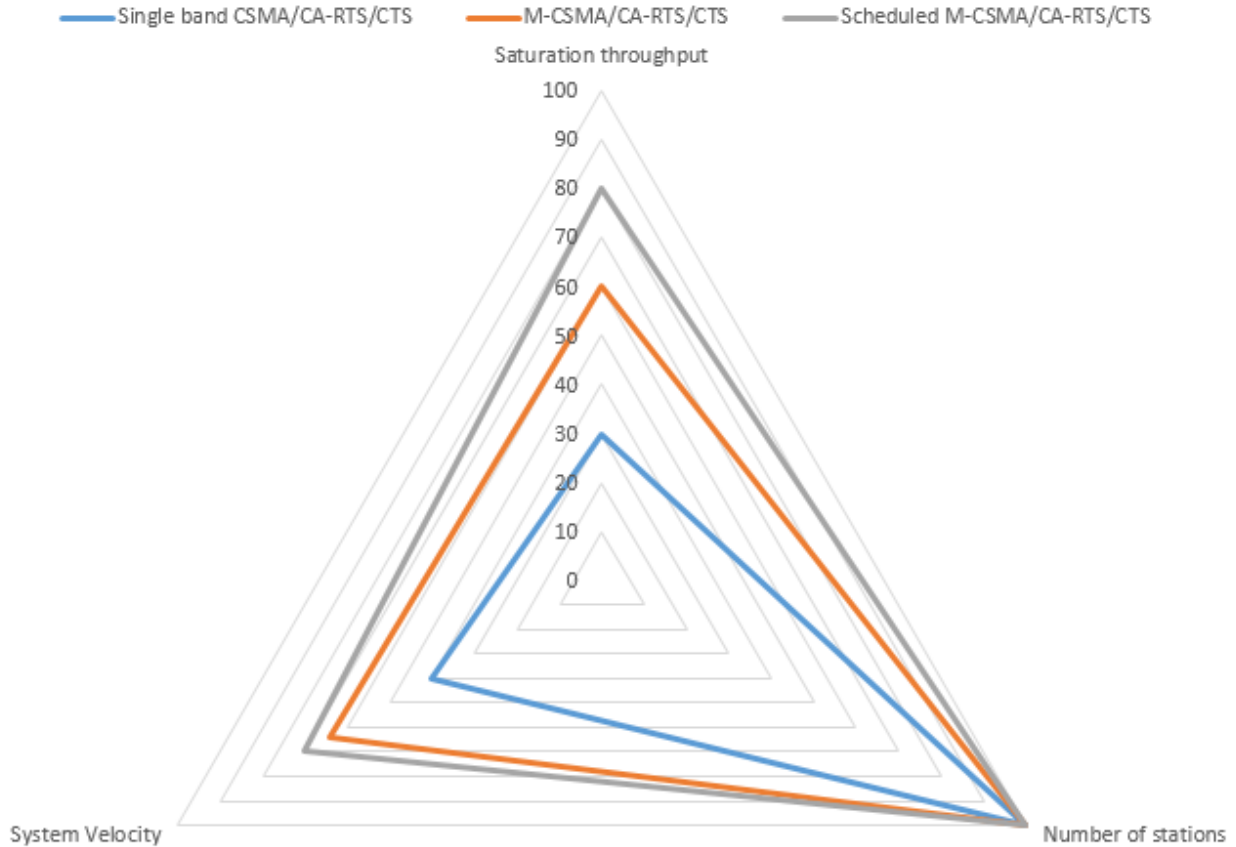


Figure 9: Synthèse du CSMA/CA – RTS/CTS pour le cas des réseaux chargés.

PHY standard	Subcarrier range	Pilot subcarriers	Subcarriers (total/data)
802.11n, 20MHz	-28 to -1, +1 to +28	$\pm 7, \pm 21$	56 total, 52 usable (7% pilots)

Table 2: Channel description attributes for legacy mode.

Chapitre 5 - Couche Conjointe Multi bande CSMA/CA - RTS/CTS

Une étude étendue du M-CSMA/CA-RTS/CTS en prenant en compte d'une couche physique fait l'objet de ce chapitre. Dans un premier temps, on présentera la couche physique de type multiporteuse du standard 802.11n. Ensuite, on développera un modèle correspondant à la couche physique en prenant en compte les effets de "capture" et d'interférence inter bande causés par des transmissions asynchrones sur des bandes adjacentes. Finalement, les performances du système seront évaluées et comparées au cas d'une couche physique parfaite discutée dans les chapitres précédents 3 et 4.

Dans ce chapitre on adopte le mode « legacy » du standard 802.11n. La table 2 montre l'allocation des porteuses de données et celle des pilotes. Les porteuses pilotes sont destinées à la mesure du canal. La Figure 11 montre la répartition des sous porteuses.

Effet de la couche physique

On considère une version simplifiée du standard 802.11n. Pour cela, on considère que les données sont transmises sur 52 sous-porteuses en utilisant la modulation OFDM. La durée nécessaire T pour transmettre un paquet de taille P est donnée par la relation suivante:

$$T = 20\mu s + M(N_c + GI)/B \quad (16)$$

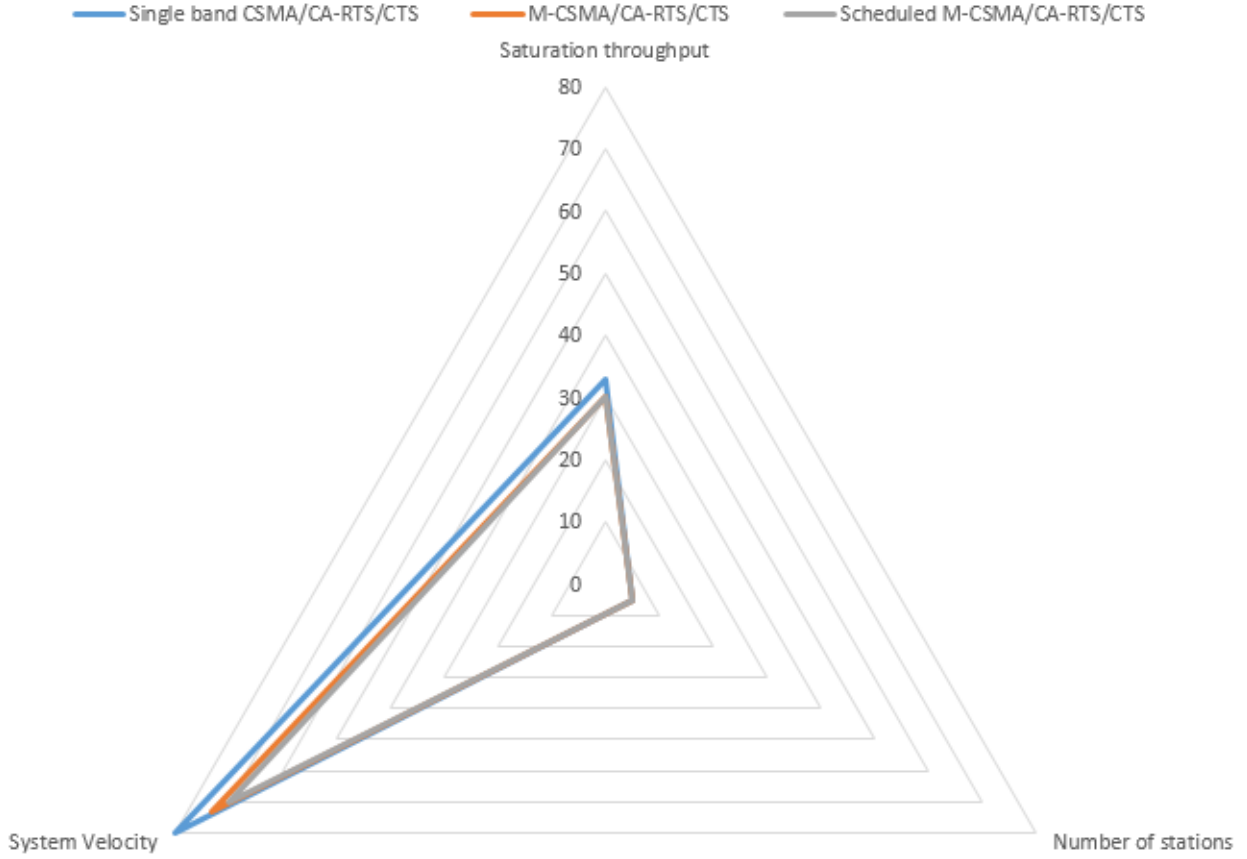


Figure 10: Synthèse du CSMA/CA – RTS/CTS pour le cas des réseaux non chargés.

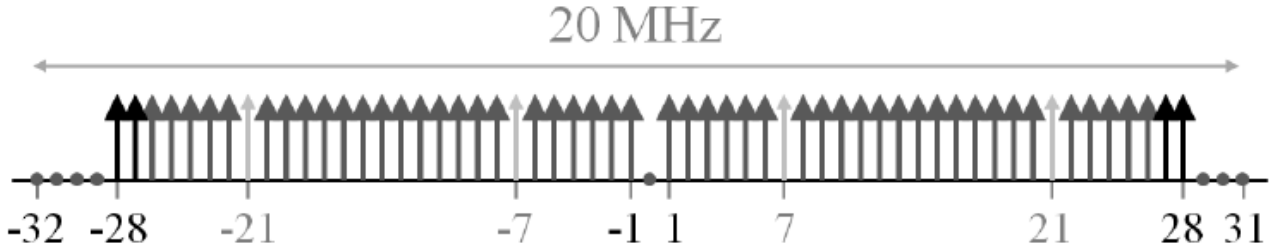


Figure 11: Sous porteuses WiFi pour le mode "legacy" [14].

avec M le nombre des symboles OFDM, N_c le nombre des sous-porteuses actives et B est la largeur de bande. GI représente l'intervalle de garde.

Effet de Capture

Dans les communications sans fil, lorsque plusieurs utilisateurs partagent le même canal de communication, ils génèrent des interférences les uns sur les autres. La qualité de communication se caractérise par le rapport signal sur interférence SIR . Ce rapport est donné par l'équation suivante qui servira pour les simulations:

$$SIR(k, i) = \frac{\frac{1}{R_i^\alpha}}{\sum_{\substack{j=1 \\ j \neq i}}^{g_k} \frac{1}{R_j^\alpha}} \quad (17)$$

R_i présente la distance entre le nœud i et le PA. Et α présente l'atténuation du trajet.

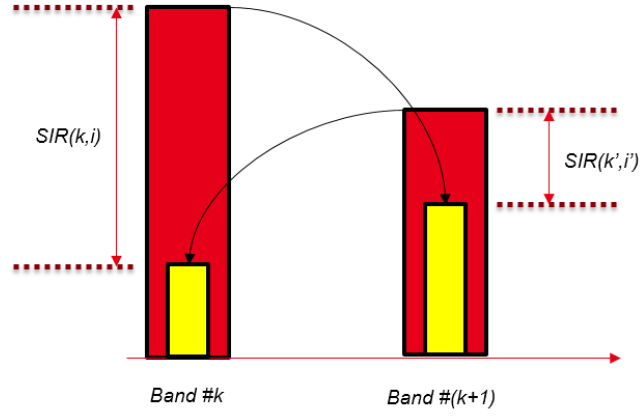


Figure 12: Interférence entre les bandes.

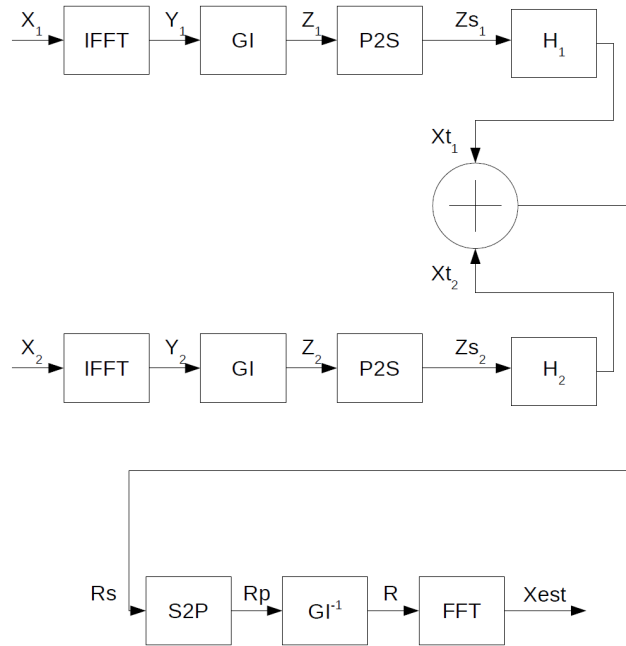


Figure 13: Cas du M-CSMA/CA-RTS/CTS avec 2 sous bandes.

Interférence Interbande

Comme la modulation OFDM n'est pas bien localisée en fréquence [15], elle cause des interférences entre deux transmissions parallèles sur deux sous-canaux adjacents quand ceux-ci ne sont pas synchronisés (à l'intervalle de garde prêt). La figure 12 montre le cas de deux transmissions en parallèle sur les deux bandes adjacentes k et $k + 1$. Les rectangles rouge et jaune sont associés au signal et à l'interférence. Lorsque la puissance du signal est forte elle cause plus d'interférence sur la bande adjacente. L'objectif est de calculer l'interférence causée par une bande adjacente sur la bande d'intérêt pour pouvoir estimer le SIR mesuré sur cette dernière.

La figure 13 présente un cas de M-CSMA/CA-RTS/CTS avec 2 sous bandes. A_1 et A_2 sont les matrices qui contiennent les informations des messages RTS transmis sur la 1ère et la 2ème sous-bande. La taille de ces matrices est $\frac{N}{2} \times M$ qui contiennent chacune $N_a \times M$ éléments actifs.

$$A_1 = \begin{bmatrix} a_{11}^1 & a_{12}^1 & a_{13}^1 & \dots & a_{1M}^1 \\ a_{21}^1 & a_{22}^1 & a_{23}^1 & \dots & a_{2M}^1 \\ \dots & \dots & \dots & \dots & \dots \\ a_{\frac{N}{2}1}^1 & a_{\frac{N}{2}2}^1 & a_{\frac{N}{2}3}^1 & \dots & a_{\frac{N}{2}M}^1 \end{bmatrix} = \begin{bmatrix} 0 & 0 & 0 & \dots & 0 \\ \dots & \dots & \dots & \dots & \dots \\ 0 & 0 & 0 & \dots & 0 \\ a_{51}^1 & a_{52}^1 & a_{13}^1 & \dots & a_{5M}^1 \\ a_{61}^1 & a_{62}^1 & a_{63}^1 & \dots & a_{6M}^1 \\ \dots & \dots & \dots & \dots & \dots \\ a_{N_a1}^1 & a_{N_a2}^1 & a_{N_a3}^1 & \dots & a_{N_aM}^1 \end{bmatrix}$$

Les 4 premières lignes de A_1 sont nulles (ce qui correspond aux sous-porteuses -32, -31, -30 et -29).

$$A_1 = N_1 B_1 \quad (18)$$

$$N_1 = \begin{bmatrix} 0_4 \\ I_{N/2-4} \end{bmatrix}$$

B_1 correspond aux éléments non nuls de A_1 et 0_4 est une colonne de 4 zéros.

$$A_2 = \begin{bmatrix} a_{11}^2 & a_{12}^2 & a_{13}^2 & \dots & a_{1M}^2 \\ a_{21}^2 & a_{22}^2 & a_{23}^2 & \dots & a_{2M}^2 \\ \dots & \dots & \dots & \dots & \dots \\ a_{\frac{N}{2}1}^2 & a_{\frac{N}{2}2}^2 & a_{\frac{N}{2}3}^2 & \dots & a_{\frac{N}{2}M}^2 \end{bmatrix} = \begin{bmatrix} 0 & 0 & 0 & \dots & 0 \\ a_{21}^2 & a_{22}^2 & a_{23}^2 & \dots & a_{2M}^2 \\ a_{31}^2 & a_{32}^2 & a_{33}^2 & \dots & a_{3M}^2 \\ \dots & \dots & \dots & \dots & \dots \\ a_{N_a1}^2 & a_{N_a2}^2 & a_{N_a3}^2 & \dots & a_{N_aM}^2 \\ 0 & 0 & 0 & \dots & 0 \\ \dots & \dots & \dots & \dots & \dots \\ 0 & 0 & 0 & \dots & 0 \end{bmatrix}$$

La première et les trois dernières lignes de A_2 sont nulles (sous-porteuses 0, 29, 30 et 31).

$$A_2 = N_2 B_2 \quad (19)$$

$$N_2 = \begin{bmatrix} 0 \\ I_{N/2-4} \\ 0_3 \end{bmatrix}$$

B_2 correspond aux éléments non nuls de A_2 et 0_3 est une matrice de 3 zéros.

X_1 et X_2 sont les matrices de taille $N \times M$ qui contiennent A_1 et A_2 . Donc, X_1 et X_2 peuvent être exprimées de la manière suivante :

$$X_1 = \begin{bmatrix} A_1 \\ 0 \end{bmatrix}$$

$$X_2 = \begin{bmatrix} 0 \\ A_2 \end{bmatrix}$$

Y_1 et Y_2 sont les transformées de Fourier de X_1 et X_2 respectivement, de taille $N \times M$ et sont données par les équations suivantes :

$$Y_1 = F^H X_1 \quad (20)$$

$$Y_2 = F^H X_2 \quad (21)$$

Après une conversion parallèle-série, Z_{s1} et Z_{s2} peuvent être exprimées par les équations suivantes :

$$Z_{s1} = [y_{N-GI+1,1}^1 \dots y_{N,1}^1 \ y_{1,1}^1 \ y_{2,1}^1 \dots y_{N,1}^1 \ y_{N-GI+1,2}^1 \dots y_{N,2}^1 \dots y_{N,M}^1] \quad (22)$$

$$Z_{s2} = [y_{N-GI+1,1}^2 \dots y_{N,1}^2 \ y_{1,1}^2 \ y_{2,1}^2 \dots y_{N,1}^2 \ y_{N-GI+1,2}^2 \dots y_{N,2}^2 \dots y_{N,M}^2] \quad (23)$$

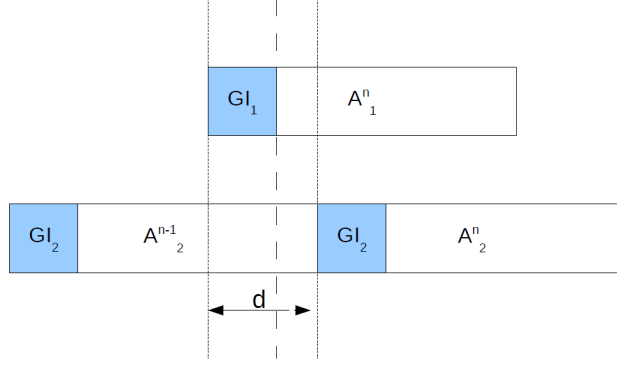


Figure 14: Messages d'RTS asynchrones.

Après convolution du canal, les messages Xt_1 et Xt_2 sont exprimés par les équations

$$Xt_1 = h_1 * Zs_1 \quad (24)$$

$$Xt_2 = h_2 * Zs_2 \quad (25)$$

Le signal reçu (R_s) est égal à la somme des deux signaux transmis. Alors,

$$\begin{aligned} R_s &= Xt_1 + Xt_2 \\ R_s &= h_1 * Zs_1 + h_2 * Zs_2 \end{aligned} \quad (26)$$

Suite à une conversion parallèle-série, le signal reçu sera mappé dans une matrice de taille $(N - GI + 1) \times M$ pour former le signal R_p . Alors, R de taille $N \times M$ est obtenu en supprimant l'intervalle de garde. Le signal X de taille $N \times M$ est calculé en appliquant la FFT sur R . On note par A_i^n le paquet transmis sur la bande i durant la période n . La Figure 14 montre le cas d'une transmission asynchrone dans le cas où deux paquets arrivent au PA avec un retard de d .

Pour décoder le paquet transmis sur la première sous bande, le récepteur doit se synchroniser sur ce paquet (paquet d'intérêt). Le récepteur commence à décoder au début de GI_1 jusqu'à la fin du paquet sur toutes les sous-bandes. Le récepteur décode A_1^n et une partie de A_2^{n-1} et de A_2^n . Le signal reçu R_p peut être écrit de la manière suivante:

$$\begin{aligned} R_p &= Z_1^n + U_d Z_2^n + V_{N+GI-d} Z_2^{n-1} \\ R_p &= I_{GI} Y_1^n + U_d I_{GI} Y_2^n + V_{N+GI-d} I_{GI} Y_2^{n-1} \end{aligned} \quad (27)$$

Y_1^n est lié au paquet reçu sur la première sous bandes. $U_d I_{GI} Y_2^n$ et $V_{N+GI-d} I_{GI} Y_2^{n-1}$ correspondent aux parties décodées du $n - 1^{th}$ et n^{th} paquets reçu sur la deuxième sous-bande. U_d et V_{N+GI-d} sont de taille $(N + GI) \times (N + GI)$ et peuvent être exprimées par les matrices suivantes:

$$\begin{aligned} U_d &= \begin{bmatrix} 0 & I_d \\ 0 & 0 \end{bmatrix} \\ V_{N+GI-d} &= \begin{bmatrix} 0 & 0 \\ 0 & I_{N+GI-d} \end{bmatrix} \end{aligned}$$

I_{-GI} est la matrice de taille $N \times (N + GI)$ qui supprime l'intervalle de garde, donc elle est composée de GI colonnes de zéros suivie d'une matrice identité.

$$I_{-GI} = \begin{bmatrix} 0 & I \end{bmatrix}$$

Comme le récepteur est synchronisé sur la première sous bande, le message transmis sur la deuxième sous-bande est retardé de d par rapport à la première sous-bande. On considère

ici simplement l'effet de l'asynchronisme. H_1 est une matrice identité et H_2 est une matrice identité décalée. Une fois l'intervalle de garde enlevé, R peut être exprimée :

$$\begin{aligned} R &= Y_1^n + I_{-GI}V_{N+GI-d}I_{GI}Y_2^n + I_{-GI}U_dI_{GI}Y_2^{n-1} \\ R &= F^H X_1^n + I_{-GI}V_{N+GI-d}I_{GI}F^H X_2^n + I_{-GI}U_dI_{GI}F^H X_2^{n-1} \end{aligned} \quad (28)$$

Enfin, le signal décodé X_{est} est donné par :

$$\begin{aligned} X_{est} &= FR \\ X_{est} &= X_1^n + FI_{-GI}U_dI_{GI}F^H X_2^n + FI_{-GI}V_{N+GI-d}I_{GI}F^H X_2^{n-1} \\ X_{est} &= X_1^n + QX_2^n + Q'X_2^{n-1} \end{aligned} \quad (29)$$

Q et Q' représentent les coefficients d'interférence introduits par la deuxième sous-bande sur la bande d'intérêt. En fait, le signal reçu peut être exprimé par la matrice suivante :

$$\begin{bmatrix} \widetilde{A}_1 \\ \widetilde{A}_2 \end{bmatrix} = \begin{bmatrix} A_1^n \\ 0 \end{bmatrix} + \begin{bmatrix} Q_{11} & Q_{12} \\ Q_{21} & Q_{22} \end{bmatrix} \begin{bmatrix} 0 \\ A_2^n \end{bmatrix} + \begin{bmatrix} Q'_{11} & Q'_{12} \\ Q'_{21} & Q'_{22} \end{bmatrix} \begin{bmatrix} 0 \\ A_2^{n-1} \end{bmatrix}$$

La première matrice est liée au signal et le reste représente l'interférence introduite sur la sous-bande d'intérêt. Le signal d'intérêt peut être exprimé par :

$$\widetilde{A}_1 = A_1^n + Q_{12}A_2^n + Q'_{12}A_2^{n-1} \quad (30)$$

La puissance sur la sous-bande d'intérêt peut être calculée de la manière suivante :

$$\begin{aligned} P_{Signal} &= E[\text{trace}(A_1^n A_1^{nH})] \\ P_{Signal} &= \text{trace}(E[A_1^n A_1^{nH}]) \\ P_{Signal} &= \text{trace}(E[N_1 B_1^n (N_1 B_1^n)^H]) \\ P_{Signal} &= \text{trace}(E[N_1 B_1^n B_1^{nH} N_1^H]) \\ P_{Signal} &= \beta \text{trace}(N_1 N_1^H) = \alpha \end{aligned} \quad (31)$$

et la puissance de l'interférence est donnée par:

$$\begin{aligned} P_{Interference} &= E[\text{trace}((Q'_{12}A_2^{n-1})(Q'_{12}A_2^{n-1})^H)] + E[\text{trace}((Q_{12}A_2^n)(Q_{12}A_2^n)^H)] \\ P_{Interference} &= \text{trace}(E[(Q'_{12}N_2 B_2^{n-1})(Q'_{12}N_2 B_2^{n-1})^H]) + \text{trace}(E[(Q_{12}N_2 B_2^n)(Q_{12}N_2 B_2^n)^H]) \\ P_{Interference} &= \beta(\text{trace}(E[Q'_{12}N_2 N_2^H Q'_{12}^H]) + \text{trace}(E[Q_{12}N_2 N_2^H Q_{12}^H])) \end{aligned} \quad (32)$$

Avec, $\beta = \text{trace}(E[B_1^n B_1^{nH}]) = \text{trace}(E[B_1^{n-1} B_1^{n-1H}]) = \text{trace}(E[B_2^n B_2^{nH}]) = \text{trace}(E[B_2^{n-1} B_2^{n-1H}])$. Ainsi, le SIR mesuré sur la première sous-bande peut être exprimé par:

$$\begin{aligned} SIR_1 &= \frac{P_{Signal}}{P_{Interference}} \\ SIR_1 &= \frac{\alpha}{\beta(\text{trace}(E[Q'_{12}N_2 N_2^H Q'_{12}^H]) + \text{trace}(E[Q_{12}N_2 N_2^H Q_{12}^H]))} \\ SIR_1 &= \frac{\text{trace}(N_2 N_2^H)}{\text{trace}(E[Q'_{12}N_2 N_2^H Q'_{12}^H]) + \text{trace}(E[Q_{12}N_2 N_2^H Q_{12}^H])} \end{aligned} \quad (33)$$

Analyse des performances

Dans cette section on analyse les performances du système en prenant en considération la couche physique 802.11n. On évalue numériquement le débit en mode saturé (exprimé en Mbps) en tenant compte de l'effet de capture et de la nature non synchrone des transmissions.

Indice de MCS	Débit de codage	Modulation
0	1/2	QPSK
1	2/3	QPSK
2	3/4	QPSK
3	1/2	16QAM
4	2/3	16QAM
5	3/4	16QAM
6	1/2	64QAM
7	2/3	64QAM
8	3/4	64QAM

Table 3: Liste des différentes stratégies de modulation et codage.

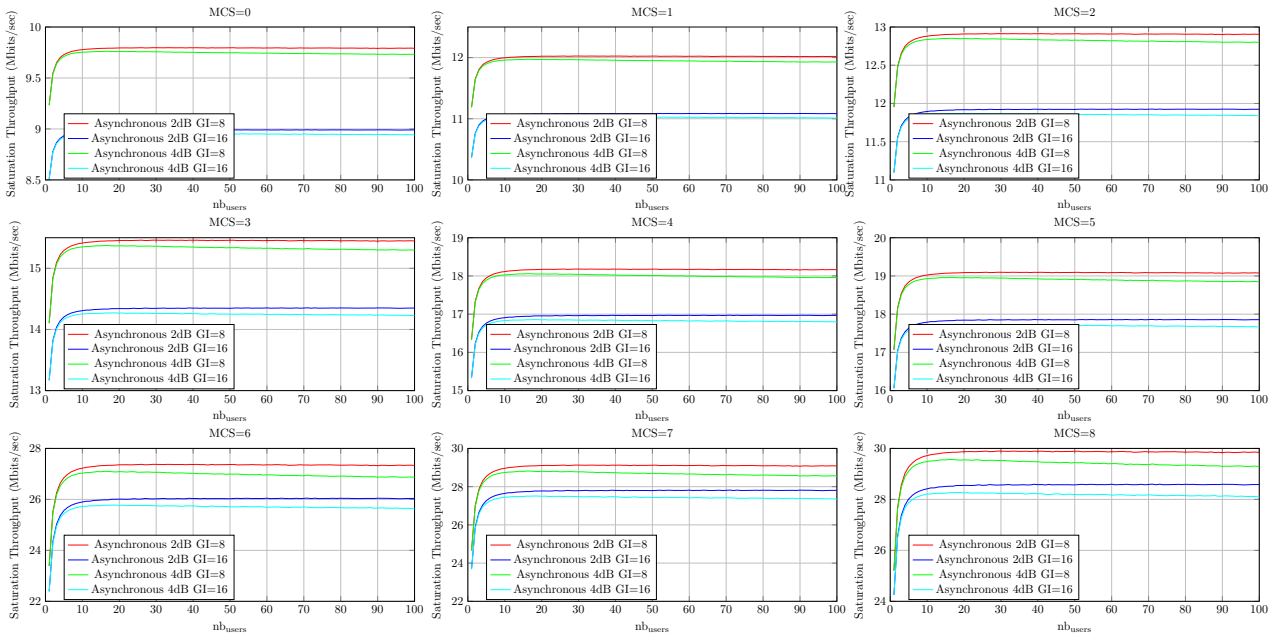


Figure 15: Débit en mode saturé en Mbps en fonction du nombre des nœuds en présence de l'interférence inter bande pour différentes valeurs d'intervalle de garde avec un canal AWGN.

Plusieurs schémas de modulation et du codage (MCS) sont définis et reportés dans le tableau 3.

On considère dans cette étude que le MCS lié aux messages RTS et CTS est le même et est égal à 0. Cette valeur de MCS correspond au schéma le plus robuste. Cela permet de minimiser la probabilité d'erreur même pour des nœuds en limite de cellule ou de sensibilité.

Les figures 15 et 16 illustrent le débit en mode saturé en Mbps en fonction du nombre des nœuds pour les différents valeurs de MCS en considérant l'effet de l'interférence inter bande avec des intervalles de gardes différents pour deux types de canaux: AWGN et D avec évanouissement.

Ces figures montrent que le débit en mode saturé du canal AWGN est meilleur que le canal D car le seuil de SIR est plus faible. Cela permet au récepteur de mieux décoder les messages RTS. On peut également remarquer que le débit du M-CSMA/CA-RTS/CTS est toujours meilleur.

Cette étude montre que le M-CSMA/CA-RTS/CTS possède de meilleures performances comparé au CSMA/CA-RTS/CTS, notamment pour le cas des réseaux chargés et lorsque le seuil de décodage est élevé.

De plus, nous avons étudié le taux de transmission avec succès des paquets en fonction de la distance séparant les nœuds et le PA pour les deux systèmes : mono bande et M-

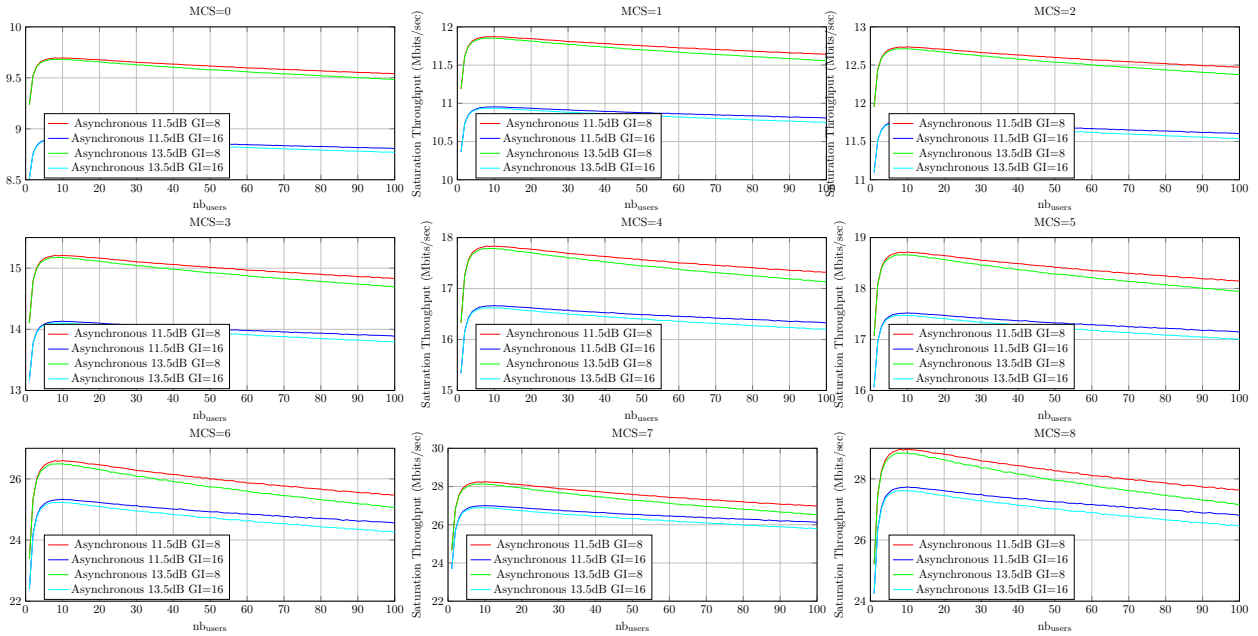


Figure 16: Débit en mode saturé en Mbps en fonction du nombre des nœuds en présence de l'interférence inter bande pour différentes valeurs d'intervalle de garde avec un canal D.

CSMA/CA – RTS/CTS. Ainsi, nous avons montré que le M-CSMA/CA – RTS/CTS possède une meilleure qualité de service pour les nœuds loin du PA par rapport au mono bande CSMA/CA – RTS/CTS. Cet aspect rend notre schéma plus intéressant pour les applications où la qualité de service est une métrique à respecter.

Conclusion

Cette thèse analyse le comportement du CSMA/CA – RTS/CTS lorsqu'un nombre important de nœuds essayent de communiquer simultanément. Dans la première partie de ce travail nous avons introduit les motivations qui nous en amener à développer ce travail. Comme le CSMA/CA est le cœur de ce travail, nous avons décrit son fonctionnement en se basant sur la théorie proposée initialement par Bianchi [10].

Dans le chapitre 3, nous avons montré que les performances du CSMA/CA sont dégradées à cause du nombre important de collisions. Dans le but de réduire les effets des collisions nous avons proposé un nouveau modèle d'accès. Le modèle se repose sur du multi bande CSMA/CA – RTS/CTS (M-CSMA/CA – RTS/CTS) et est basé sur des transmissions orthogonales des messages de RTS sur des sous bandes différentes. Un modèle analytique a été développé et validé par des simulations. Les performances du système ont été analysées en termes de débit en mode saturé, délai de transmission et le taux de réjection des paquets. Ces résultats ont montré que la technique proposée peut améliorer le débit en mode saturé et réduire le délai de transmission et le taux de réjection des paquets. Cette technique semble particulièrement adaptée pour des réseaux chargés basée sur une méthode d'accès aléatoires.

Dans le chapitre 4, nous avons proposé une amélioration du M-CSMA/CA – RTS/CTS en introduisant une technique d'ordonnancement pour servir plusieurs nœuds à la suite. Nous avons montré par des simulations que cette technique permet d'améliorer les performances en termes de débit en mode saturé, délai de transmission et de taux de rejection des paquets. Une synthèse a été également réalisée pour comparer les différentes méthodes. Cette synthèse montre que le CSMA/CA RTS/CTS est bien adapté dans le cas de réseaux non chargés tandis que les performances du M-CSMA/CA – RTS/CTS avec ou sans ordonnancement sont meilleures dans les scénarios chargés. Pour pouvoir analyser les effets de la couche physique sur

les performances de ces méthodes d'accès, une étude conjointe (PHY-MAC) a été proposée dans le chapitre 5. Nous avons tout d'abord décrit la couche physique du standard IEEE 802.11n. Ensuite, nous avons proposé un modèle qui permet d'étudier les performances de ces méthodes en présence d'une couche physique. En particulier nous avons étudié le « capture effect » et l'effet de l'interférence inter bande causés par les transmissions asynchrones des messages RTS. Les performances de ces méthodes ont été évaluées par des simulations en considérant deux types de canaux : AWGN et canal D avec évanouissement. Les résultats des simulations ont montré que le M-CSMA/CA – RTS/CTS a de meilleures performances dans le cas des réseaux chargés. Enfin, nous avons aussi démontré que le M-CSMA/CA-RTS/CTS est plus spatialement équitable par rapport au CSMA/CA - RTS/CTS. En fait il permet aux nœuds loin de PA de pouvoir transmettre même en présence de nœuds proches de PA avec une probabilité supérieure à celle du cas classique.

Pour conclure, le M-CSMA/CA – RTS/CTS améliore efficacement la méthode d'accès et permet de garantir un meilleur débit dans le cas des réseaux chargés.

Contents

1	Introduction	1
1.1	Context and motivations	1
1.2	Thesis objectives	3
1.3	Thesis outline	3
1.4	List of patents, publications and contributions.	4
2	Overview of access protocols	7
2.1	Introduction	7
2.2	The concept of access protocols	7
2.3	Scheduled access techniques	8
2.3.1	Frequency Division Multiple Access	8
2.3.2	Time Division Multiple Access	9
2.3.3	Code Division Multiple Access	9
2.4	Random access protocols	9
2.4.1	ALOHA Class	9
2.4.2	Carrier Sense Multiple Access	10
2.5	Analysis tools for CSMA/CA	13
2.5.1	Packet Transmission Probability	14
2.5.2	Saturation Throughput	16
2.5.3	Numerical Analysis	16
2.6	Improvement of CSMA/CA	17
2.6.1	Contention window optimization	17
2.6.2	CSMA/CA - Enhanced Collision Avoidance	23
2.6.3	Related Works	24
2.7	Conclusion	25
3	M-CSMA/CA - RTS/CTS	27
3.1	Introduction	27
3.2	Motivations	27
3.3	Description	28
3.3.1	System Model	28
3.3.2	M-CSMA/CA - RTS/CTS Case Study	29
3.4	Analytical Model	30
3.4.1	Infinite Retry Limit Analysis	31
3.4.2	Finite Retry Limit Analysis	36
3.5	Performance Analysis	38
3.5.1	Model Validation	38
3.5.2	Performance Discussion	40
3.6	Upper bounds	46
3.7	Allocation Methods	48
3.8	Conclusion	49

4	Scheduled M-CSMA/CA - RTS/CTS	51
4.1	Introduction	51
4.2	Description	51
4.3	Performance Analysis	53
4.3.1	Time Repartition	53
4.3.2	Saturation Throughput	54
4.3.3	Transmission Delay	56
4.3.4	Packet Drop Probability	56
4.4	Upper bounds	58
4.5	Conclusion	61
5	Joint PHY-MAC analysis of M-CSMA/CA - RTS/CTS	65
5.1	Introduction	65
5.2	Physical layer description	65
5.2.1	802.11n description	65
5.2.2	Physical layer effect	67
5.2.3	Capture effect	69
5.2.4	Interband interference	70
5.3	Performance analysis	84
5.3.1	Physical layer	85
5.3.2	Capture effect	85
5.3.3	Asynchronous transmission	89
5.4	Conclusion	92
6	Conclusions and Future works	95
6.1	Conclusions	95
6.2	Suggestions for future works	96

List of Figures

1	Performance de la couche d'accès CSMA/CA RTS/CTS.	2
2	CSMA/CA Basique [9]	3
3	CSMA/CA - RTS/CTS [9]	4
4	Modèle de Bianchi pour l'analyse du CSMA/CA [10].	6
5	Exemple de scénario pour le M CSMA/CA - RTS/CTS	8
6	Erreur (%) entre le modèle analytique et la simulation.	10
7	M-CSMA/CA ordonnance avec une taille d'ordonnanceur de 2	11
8	Les performances des méthodes d'accès à contention.	12
9	Synthèse du CSMA/CA – RTS/CTS pour le cas des réseaux chargés.	13
10	Synthèse du CSMA/CA – RTS/CTS pour le cas des réseaux non chargés.	14
11	Sous porteuses WiFi pour le mode "legacy" [14].	14
12	Interférence entre les bandes.	15
13	Cas du M-CSMA/CA-RTS/CTS avec 2 sous bandes.	15
14	Messages d'RTS asynchrones.	17
15	Débit en mode saturé en Mbps en fonction du nombre des nœuds en présence de l'interférence inter bande pour différentes valeurs d'intervalle de garde avec un canal AWGN.	19
16	Débit en mode saturé en Mbps en fonction du nombre des nœuds en présence de l'interférence inter bande pour différentes valeurs d'intervalle de garde avec un canal D.	20
1.1	Use case categories definition [1]	1
1.2	Contention based MAC performance	2
2.1	OSI model [16]	7
2.2	Multiplexing/Demultiplexing process	8
2.3	Deterministic access techniques [17]	8
2.4	Random access protocols [18]	9
2.5	ALOHA [18]	10
2.6	Slotted ALOHA [18]	10
2.7	CSMA Modes [18]	11
2.8	CSMA/CD Scheme [19]	12
2.9	CSMA/CA's three strategies [18]	12
2.10	Basic CSMA/CA Algorithm [9]	13
2.11	CSMA/CA - RTS/CTS Algorithm [9]	13
2.12	Markov Chain model for the backoff window size.	15
2.13	Saturation throughput comparision between basic and RTS/CTS CSMA/CA [9].	17
2.14	802.11 and proposed backoff strategy.	18
2.15	Markov chain model of backoff window size in proposed CSMA/CA.	19
2.16	Relative error vs. number of mobile stations.	21
2.17	Saturation throughput for proposed strategy with RTS/CTS transmission.	21
2.18	Saturation throughput for classical 802.11 with RTS/CTS transmission.	22

2.19	CDF of access delay for $m = 3$ with 50 mobile stations. Delay is expressed in second.	23
2.20	CSMA/ECA description [20]	24
3.1	Single channel CSMA/CA - RTS/CTS time repartition vs. number of mobile stations.	28
3.2	Multi channel CSMA/CA - RTS/CTS.	29
3.3	Illustration of the hidden and exposed node problem	31
3.4	Backoff model for the proposed CSMA/CA with infinite retry limit. Compared to Bianchi [9], the probability is p_i instead of p	34
3.5	Backoff model for the proposed CSMA/CA with finite retry limit.	36
3.6	Saturation throughput for 2 RTS sub-channels based on the analytical model.	39
3.7	Saturation throughput for 2 RTS sub-channels based on simulation.	39
3.8	Error (%) between analytical model and simulation.	40
3.9	Collision probability gain vs. number of mobile stations for various number of RTS sub-channels.	41
3.10	CSMA/CA - RTS/CTS time repartition vs. number of mobile stations for 3 RTS sub-bands.	42
3.11	CSMA/CA - RTS/CTS time repartition vs. number of mobile stations for 5 RTS sub-bands.	43
3.12	Saturation throughput vs. number of mobile stations for various number of RTS sub-channels.	44
3.13	Saturation throughput (bits/sec) vs. number of mobile stations for various number of RTS sub-channels with $m=r=3$	44
3.14	Saturation throughput gain vs. number of mobile stations for various number of RTS sub-channels.	45
3.15	Transmission delay gain vs. number of mobile stations for various number of RTS sub-channels.	46
3.16	Packet drop probability for single channel vs. number of backoff stages for various retransmission limits.	46
3.17	Packet drop probability for #sub-channels=2 vs. number of backoff stages for various retransmission limits.	47
3.18	Packet drop probability for #sub-channels=3 vs. number of backoff stages for various retransmission limits.	47
3.19	Contention Based MAC Performance.	48
3.20	Saturation throughput difference (%) between Pre and Postallocation techniques vs. the number of mobile station for various number of sub-channels.	50
4.1	Flow chart of the proposed strategy.	52
4.2	Flow chart of the proposed strategy.	53
4.3	Scheduled multiband CSMA/CA with RTS/CTS mechanism with scheduler size=2.	54
4.4	CTS frame format.	54
4.5	CSMA/CA - RTS/CTS time repartition vs. number of mobile stations for 5 RTS sub-bands with scheduler size=3.	54
4.6	Saturation Throughput Gain (%) vs. number of nodes for scheduler size=1.	55
4.7	Saturation Throughput Gain (%) vs. number of nodes for scheduler size=2.	56
4.8	Saturation Throughput Gain (%) vs. number of nodes for scheduler size=3.	57
4.9	Saturation Throughput Gain (%) vs. number of nodes for scheduler size=1.	57
4.10	Saturation Throughput Gain (%) vs. number of nodes for scheduler size=2.	58
4.11	Saturation Throughput Gain (%) vs. number of nodes for scheduler size=3.	58
4.12	Delay Gain (%) vs. number of nodes for various number of sub-bands with scheduler size=1.	59

4.13	Delay Gain (%) vs. number of nodes for various number of sub-bands with scheduler size=2.	59
4.14	Delay Gain (%) vs. number of nodes for various number of sub-bands with scheduler size=3.	60
4.15	Packet Drop Probability for scheduler size=1.	60
4.16	Packet Drop Probability for scheduler size=2.	61
4.17	Packet Drop Probability for scheduler size=3.	61
4.18	Contention Based MAC Performance.	62
4.19	CSMA/CA - RTS/CTS synthesis for loaded scenario.	63
4.20	CSMA/CA - RTS/CTS synthesis for unloaded scenario.	64
5.1	80211n WLAN frame, Legacy Mode [21].	66
5.2	WLAN frame modifications to allow for MIMO operation, Mixed Mode [21].	66
5.3	802.11n WLAN frame, Green Field [21].	66
5.4	Legacy Signal Field (L-SIG) [22].	67
5.5	WiFi subcarriers according to legacy mode [14].	67
5.6	Block diagram of the transmitter.	68
5.7	Interband Interference.	71
5.8	Architecture of OFDM transmitter.	71
5.9	Architecture of OFDM receiver.	72
5.10	Architecture of single band TX-RX.	72
5.11	Architecture of M-CSMA/CA-RTS/CTS TX-RX with n RTS sub-bands.	75
5.12	Block diagram of M-CSMA/CA-RTS/CTS TX-RX with 2 RTS sub-bands.	75
5.13	Developped M-CSMA/CA-RTS/CTS with 2 sub-bands architecture.	76
5.14	Asynchronous RTS messages.	77
5.15	Interference matrices	79
5.16	Synchronous RTS messages.	80
5.17	Quasi synchronous RTS messages.	80
5.18	SIR (dB) vs. d.	81
5.19	Leakage (dB) vs. d.	82
5.20	Application scenario.	83
5.21	Saturation throughput in Mb/s for various number of users and for all MCS index with GI=8.	84
5.22	Saturation throughput in Mb/s for various number of users and for all MCS index with GI=16.	85
5.23	Captured saturation throughput in Mb/s for various number of users and for all MCS index with GI=8 and Th=3.5dB.	86
5.24	Captured saturation throughput in Mb/s for various number of users and for all MCS index with GI=16 and Th=3.5dB.	87
5.25	Captured saturation throughput in Mb/s for various number of users and for all MCS index with GI=8 and Th=5.5dB for AWGN channel.	87
5.26	Captured saturation throughput in Mb/s for various number of users and for all MCS index with GI=16 and Th=5.5dB for AWGN channel.	88
5.27	Captured saturation throughput in Mb/s for various number of users and for all MCS index with GI=8 and Th=11.5dB for D fading channel.	89
5.28	Captured achievable throughput in Mb/s for various number of users and for all MCS index with GI=16 and Th=11.5dB for D fading channel.	89
5.29	Captured saturation throughput in Mb/s for various number of users and for all MCS index with GI=8 and Th=13.5db.	90
5.30	Captured saturation throughput in Mb/s for various number of users and for all MCS index with GI=16 and Th=13.5db.	90

5.31	STR for AWGN Channel with circular map of radius = 300m, x and y axis presents the cartesian coordinates.	91
5.32	STR for D Fading Channel with circular map of radius = 300m, x and y axis presents the cartesian coordinates.	91
5.33	Saturation throughput in Mbits/s vs. number of users for all MCS index considering interband interference with different guard interval for AWGN channel.	92
5.34	Saturation throughput in Mbits/s vs. number of users for all MCS index considering interband interference with different guard interval for D fading channel.	92

List of Tables

1	Paramètres de la couche physique 802.11n 20Mhz	10
2	Channel description attributes for legacy mode.	13
3	Liste des différentes stratégies de modulation et codage.	19
2.1	PHY layer parameters	20
2.2	Delay (<i>ms</i>) and gain (%) values in both backoff strategies for many CDF values with $m = 3$	22
2.3	Delay (<i>ms</i>) and gain (%) values in both backoff strategies for many CDF values with $m = 7$	22
3.1	PHY layer parameters for 802.11n 20Mhz	38
5.1	Channel description attributes for legacy mode.	67
5.2	List of MCS Index Values.	84

Nomenclature

Abbreviations and Acronyms

MAC	Medium Access Control
PHY	Physical
WLAN	Wireless Local Area Network
M2M	Machine to Machine
NGMN	Next Generation Mobile Networks
HD	High Definition
AP	Access Point
BS	Base Station
CSMA	Carrier Sense Multiple Access
CSMA/CA	Carrier Sense Multiple Access / Collision Avoidance
CSMA/CD	Carrier Sense Multiple Access / Collision Detection
CSMA/ECA	Carrier Sense Multiple Access / Enhanced Collision Avoidance
RTS	Request to Send
CTS	Clear to Send
ACK	Acknowledge
<i>SIR</i>	Signal to Interference Ratio
M-CSMA/CA	Multiband Carrier Sense Multiple Access
OSI	Open Systems Interconnection
TX	Transmitter
RX	Receiver
FDMA	Frequency Division Multiple Access
TDMA	Time Division Multiple Access
CDMA	Code Division Multiple Access
D2D	Device to Device
IFS	Interframe Space
CW	Contention Window
CW_{min}	Minimal Contention Window
CW_{max}	Maximal Contention Window
DIFS	Distributed Inter-Frame Space
NAV	Network Allocation Vector
EIFS	Extended Inter-Frame Space
TS	Time Slot
CDF	Cumulative Density Function
VoIP	Voice over Internet Protocol
STA	Station
PDP	Packet Drop Probability
CIR	Channel Impulse Response
CP	Cyclic Prefix
FFT	Fast Fourier Transform
IBI	Inter Band Interference
IEEE	Institute of Electrical and Electronics Engineers
IFFT	Inverse Fast Fourier Transform
OFDM	Orthogonal Frequency Division Multiple Access
QAM	Quadrature Amplitude Modulation
QoS	Quality of Service

QPSK	Quadrature Phase Shift Keying
PLCP	Physical Layer Convergence Protocol
HT	High Throughput
MIMO	Multiple Input Multiple Output
L-STF	Legacy Short Training Field
L-LTF	Legacy Long Training Field
L-SIG	Legacy Signal Field
BPSK	Binary phase-shift keying
PSDU	PLCP Service Data Unit
FEC	Forward Error Correction
LDPC	Low Density Parity Check
MCS	Modulation and Coding Scheme
BER	Bit Error Rate
GI	Guard Interval
P2S	Parrallel to Serial
S2P	Serial to Parallel
PERT	Packet Error Rate Target
NLOS	Non Line of Sight
SISO	Single Input Single Output
MISO	Multiple Input Single Output
SIMO	Single Input Multiple Output
MIMO	Multiple Input Multiple Output
OFDM	Orthogonal Frequency Division Multiplexing
FBMC	Filter Bank based MultiCarrier
STR	Successful Transmission Ratio

Chapter 1

Introduction

1.1 Context and motivations

“5G is an end-to-end ecosystem to enable a fully mobile and connected society. It empowers value creation towards customers and partners, through existing and emerging use cases, delivered with consistent experience, and enabled by sustainable business models.” reported from NGMN 5G Vision [1]. Very diverse and sometimes extreme requirements are demanded by the 5G use cases. The requirements are specified according to the “Use Case Categories” defined in the Figure 1.1. For each use case category, one set of requirement values is given, which is representative of the extreme use cases in the category. As a result, in order to satisfy the requirements of a category, the requirements of all the use cases in this category should be satisfied. Broadband Machine to Machine (M2M) requires high resolution person-to-person

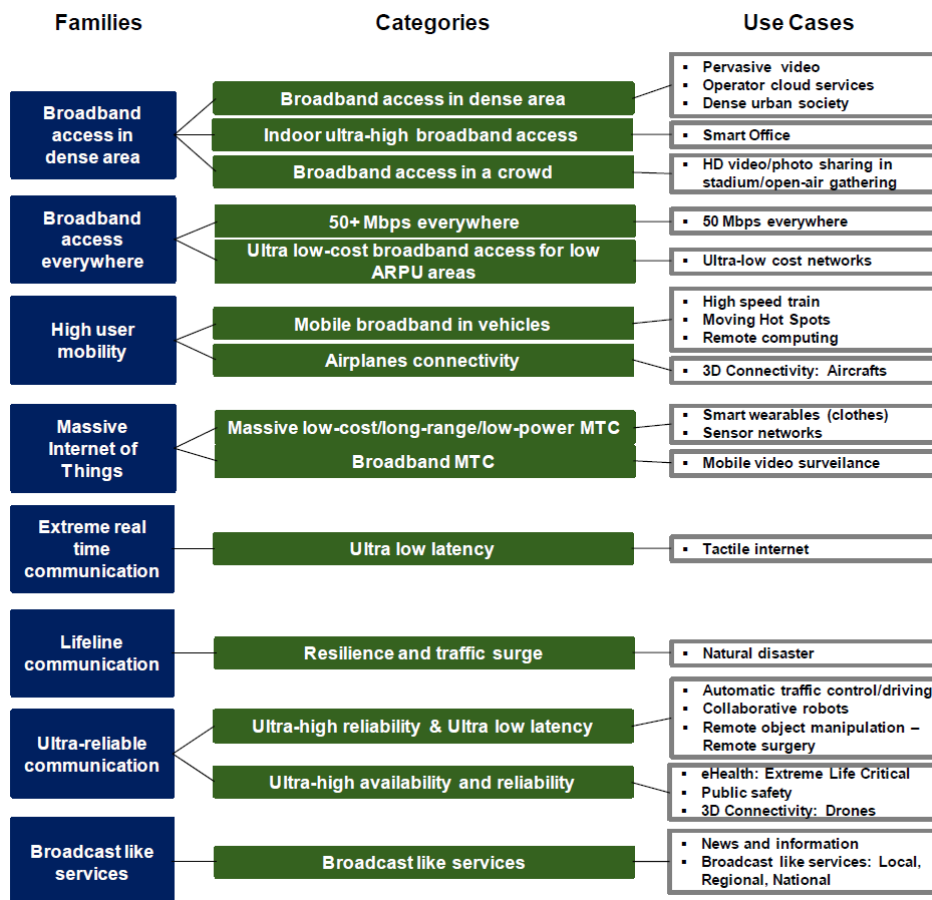


Figure 1.1: Use case categories definition [1]

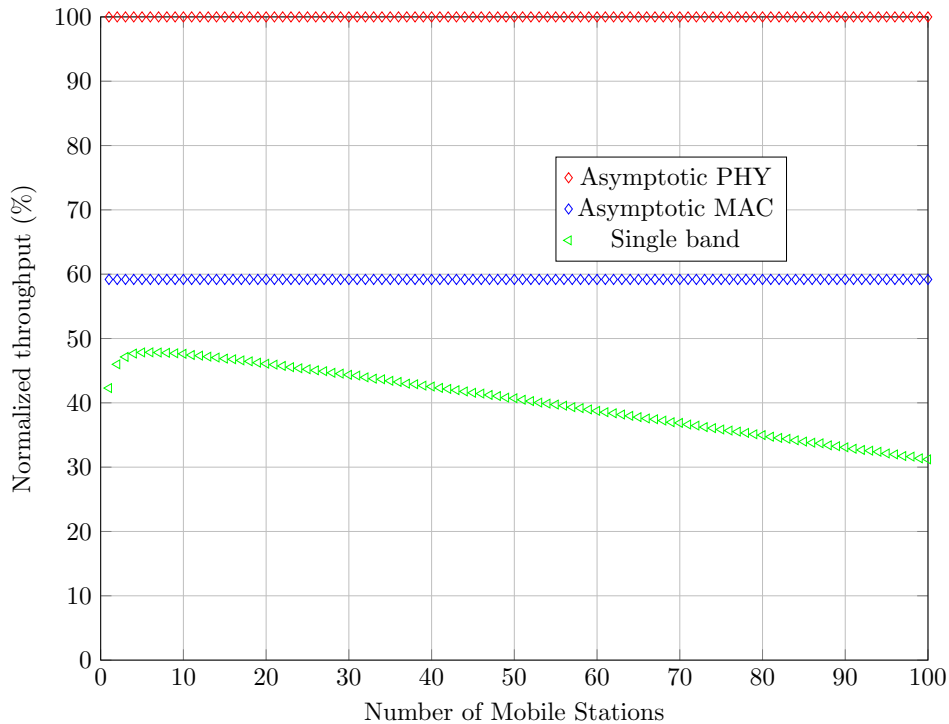


Figure 1.2: Contention based MAC performance

or person-to-group video communication which will have much wider usage with much more advanced and extreme capabilities in the near future [23]. Beyond 2020, it is envisioned that most of the devices will be wirelessly connected. Users will interact through multiple and wirelessly connected devices which require ultra-high bandwidth for high-speed services execution [2]. Bandwidth-intensive applications like instant video communication generate ultra-high traffic volume with sensitive delay. High connection density takes place in HD video/photo sharing in stadium/open-air gathering. Then, several hundred thousand users per km^2 may be served with ultra-high connection density, high data rate and low latency [1]. Moreover, the mobile and connected society will need broadband access to be available everywhere including the more challenging situations in terms of coverage (from urban to suburban and rural areas). The minimum user data rate has to be delivered consistently across the coverage area (i.e. even at the cell edges) and shall be at least 50 Mbps [3]. Considering such scenarios a robust MAC protocol should be integrated and be able to combat the collisions caused in these dense applications. The deployment should be straightforward and efficient. The network should integrate self-organized resource management for scalability. The huge amount of devices shall work opportunistically and without need to be synchronized with a predefined device (i.e. access point (AP) or base station (BS)). To fulfill these requirements random access protocols are a possible choice. The Carrier Sense Multiple Access - Request To Send / Clear To Send (CSMA/CA - RTS/CTS) could be adopted for many reasons: it allows to operate in an environment with an unknown number of devices with the entire available bandwidth [4], operates in distributed manner [5] and leads to a cheaper deployment since it doesn't require much planning, interoperability and management complexity [6]. CSMA/CA - RTS/CTS is widely used in many random access wireless networks especially to combat hidden node problem [7] as it can reduce potential collisions and improves the overall network performance. CSMA/CA - RTS/CTS is an opportunistic random access protocol which allows transmitters to access equally the wireless channel, incurring equal throughput in long term regardless of the channel conditions. Since high number of devices are supposed to transmit high packets size with opportunistic manner, the system performance should be studied in saturated conditions.

Unfortunately, CSMA/CA has a major weak point. If CSMA/CA - RTS/CTS is considered, the throughput and delay performances of the system are significantly degraded when the number of active nodes increases (dense networks). Considering the physical layer parameters of 802.11n standard with channel bitrate equals to 72.2 Mbps, Figure 1.2 depicts the normalized throughput vs. the number of mobile stations for Asymptotic physical layer (PHY), Asymptotic Medium Access Control (MAC) layer based on CSMA/CA - RTS/CTS and single band CSMA/CA-RTS/CTS. Asymptotic PHY curve is only considered for comparison purposes and corresponds to error free transmission, while Asymptotic MAC curve is the upper bound of the CSMA/CA-RTS/CTS protocol. It is seen clearly that when the number of nodes increases the throughput of the single band CSMA/CA-RTS/CTS degrades. Also for dense scenario (100 nodes in saturation conditions) the single band CSMA/CA-RTS/CTS is far of 30% from the MAC upper bound. The goal of this thesis is to improve the normalized throughput in order to be the closest as possible to the asymptotic MAC performance. This concrete example shows the limits of the current system within the dense networks configurations and open some prospects for improvement.

1.2 Thesis objectives

In this dissertation, the impact of high number of nodes on the CSMA/CA-RTS/CTS performance is addressed. As a matter of fact, we would like to:

- Identify the causes of the system performance degradation when high number of nodes is considered.
- Propose a novel system model (MAC layer) taking into account the improvements on the current protocol in order to get better system performance especially in dense scenarios.
- Based on the system model, derive closed-form expressions of the saturation throughput under some conditions for both case: finite and infinite retransmission limit.
- Analyze and evaluate the performance of the proposed MAC based on several metrics.
- Moreover investigate the impact of the interference on the system performance from joint PHY-MAC point of view. Therefore, compute analytical expressions for the *SIR* taking into account the physical layer effect.

1.3 Thesis outline

Chapter 2 - Overview of access protocols

Chapter 2 is devoted to introduce the background and the main state of the art related to the different concepts to be used throughout this thesis. First, the general concept of access protocols is provided based on deterministic and random access. Next, we give the fundamental theory of CSMA/CA techniques which relies on Markov chain and allows to analyze the system performance. Among CSMA/CA models, we introduce a modified model to solve the bottleneck problem at the first level. Furthermore, several previous works relying on single band CSMA are reviewed. We finally discuss some previous related works in the last part of this chapter.

Chapter 3 - MAC Layer Multiband CSMA/CA-RTS/CTS

In this chapter, we first give the motivations behind the proposed Multiband CSMA/CA-RTS/CTS (M-CSMA/CA-RTS/CTS) protocol. Then a full description of the M-CSMA/CA-RTS/CTS is given followed by a case study. We derive the related analytical model for finite and infinite retransmission limit cases in order to analyze the system performance. Next,

we suggest to compare the system performance of this protocol regarding the single band CSMA/CA-RTS/CTS and to some upper bounds. Finally, we discuss two different allocation methods which allow nodes to share the common communication channel.

Chapter 4 - MAC Layer Scheduled Multiband CSMA/CA-RTS/CTS

In this chapter, we propose a new technique based on M-CSMA/CA-RTS/CTS to schedule several winners in order to serve them successively. We describe first the proposed technique for both retransmission modes. Then, using the new degree of freedom offered by the M-CSMA/CA-RTS-CTS we study and analyze the related system performance. Finally, we compare this technique with the protocol introduced in the previous chapter and with the other bounds.

Chapter 5 - Joint PHY-MAC Multiband CSMA/CA-RTS/CTS

In this chapter, we study the joint PHY-MAC design of M-CSMA/CA-RTS/CTS. First, we describe the physical layer according to the 802.11n standard. Then, we derive a complete model related to the physical layer, capture effect and interband interference caused by asynchronous transmission. Finally, the system performance is evaluated and compared to the case of perfect physical layer addressed in the chapters 3 and 4.

Chapter 6 - Conclusions and Future works

This chapter draws the final conclusions by highlighting the main contributions of this dissertation. Possible future research are provided at the end.

1.4 List of patents, publications and contributions.

The contributions of this thesis are presented in the following references.

Patents

1. **Baher Mawlawi** and Jean-Baptiste Doré “Multiple access method and system with frequency multiplexing of requests for authorisation to send data” , US 14/318,838.
2. **Baher Mawlawi**, Jean-Baptiste Doré and Jean-Marie Gorce “Multiple access method and system with frequency multiplexing of several request to send messages per source node” , US 14/533480.
3. **Baher Mawlawi** and Jean-Baptiste Doré “Submitted”.

Journal Papers

1. **Baher Mawlawi**, Jean-Baptiste Doré and Jean-Marie Gorce, “A Multiband CSMA/CA Strategy for Crowded Single Band Multicarriers Wireless LAN” , under preparation.
2. **Baher Mawlawi** and Jean-Baptiste Doré, “A PHY-MAC Cross Layer Study for WRAN based on FBMC Waveforms” , under preparation.

Conference Papers

1. **Baher Mawlawi**, Jean-Baptiste Doré, “CSMA/CA Bottleneck Remediation In Saturation Mode With New Backoff Strategy” , 6th International Workshop on Multiple Access Communications,16-17 December 2013, Vilnius, Lithuania.

2. **Baher Mawlawi**, Jean-Baptiste Doré, Nikolai Lebedev and Jean-Marie Gorce, “Analysis of Frequency Channel Division Strategy for CSMA/CA with RTS/CTS Mechanism”, Eighth International Conference on Sensing Technology (ICST), 2-5 September 2014, Liverpool, Uk.
3. **Baher Mawlawi**, Jean-Baptiste Doré, Nikolai Lebedev and Jean-Marie Gorce, “Performance Evaluation Of Multiband CSMA/CA With RTS/CTS For M2M Communication With Finite Retransmission Strategy”, International Conference on Selected Topics in Mobile and Wireless Networking (MoWNet), 8-9 September 2014, Rome, Italy.
4. **Baher Mawlawi**, Jean-Baptiste Doré, Nikolai Lebedev and Jean-Marie Gorce, “Multiband CSMA/CA with RTS-CTS Strategy”, IEEE 10th International Conference on Wireless and Mobile Computing, Networking and Communications (WiMob), 8-10 October 2014, Larnaca, Cyprus.
5. **Baher Mawlawi**, Jean-Baptiste Doré, Nikolai Lebedev, Jean-Marie Gorce “CSMA/CA with RTS/CTS Overhead Reduction for M2M communication”, IEEE WCNC 2015 - Workshop - NGWIFI, 9-12 March 2015, New Orleans, LA USA.
6. **Baher Mawlawi**, Jean-Baptiste Doré, and Vincent Berg “Optimizing Contention Based Access Methods for FBMC Waveforms”, International Conference on Military Communications and Information Systems ICMCIS (former MCC), May 2015, Cracow, Poland.
7. **Baher Mawlawi** and Jean-Baptiste Doré “CSMA/CA with RTS/CTS Overhead Reduction for M2M Communication with Finite Retransmission Strategy”, IEEE International Wireless Communications & Mobile Computing Conference, August 2015, Dubrovnik, Croatia.
8. **Baher Mawlawi**, Jean-Baptiste Doré, Nikolai Lebedev, Jean-Marie Gorce “Modélisation Analytique du protocole Multi-Bande CSMA/CA”, 25ème colloque Grets, 8-11 Septembre 2015, Lyon, France.
9. Stanislav Anatolievich Filin, Dominique Noguét, Jean-Baptiste Doré, **Baher Mawlawi**, Olivier Holland, Muhammad Zeeshan Shakir, Hiroshi Harada and Fumihide Kojima “IEEE 1900.7 Standard for White Space Dynamic Spectrum Access Radio Systems”, IEEE International Conference on Standards for Communications and Networking, 28-30 October 2015, Tokyo, Japan.

Grants

COST Action IC 0902, Best tutorial days participant, 11-13 February 2013, Castelldefels-Barcelona, Spain.

Technical Contributions

1. Jean-Baptiste Doré, **Baher Mawlawi**, Dominique Noguét, “MAC Draft Standard”, IEEE 1900.7 White Space Radio, 26-29 August 2014, Piscataway, NJ, USA.
2. **Baher Mawlawi**, Jean-Baptiste Doré, Dominique Noguét, “MAC Functional Description”, IEEE 1900.7 White Space Radio, 08-10 April 2014, Grenoble, France.
3. **Baher Mawlawi**, Jean-Baptiste Doré, Dominique Noguét, “MAC Architecture”, IEEE 1900.7 White Space Radio, 08-10 April 2014, Grenoble, France.
4. **Baher Mawlawi**, Jean-Baptiste Doré, Dominique Noguét, “Novel backoff strategy for bottleneck remediation”, IEEE 1900.7 White Space Radio, 02-05 December 2013, Tokyo, Japan.
5. **Baher Mawlawi**, Jean-Baptiste Doré, Dominique Noguét, “Dynamic Spectrum Access Techniques”, IEEE 1900.7 White Space Radio, 26-29 August 2013, Arlington, USA.

6. **Baher Mawlawi**, Jean-Baptiste Doré, Dominique Noguét, “CSMA/CA Analysis”, IEEE 1900.7 White Space Radio, 26 June 2013, Grenoble, France.
7. **Baher Mawlawi**, Jean-Baptiste Doré, Dominique Noguét, “Analysis of Scenarios from an Access Scheme Perspective”, IEEE 1900.7 White Space Radio, 13 March 2013, Grenoble, France.
8. **Baher Mawlawi**, Jean-Baptiste Doré, Dominique Noguét, “White Space Dynamic Spectrum Access Radio Systems”, IEEE 1900.7 White Space Radio, 20 February 2013, Grenoble, France.

Chapter 2

Overview of access protocols

2.1 Introduction

In this chapter, we refer to the literature to extract an overview of access protocols. The concept of these access protocols will be explained in the Section 2.2. Then, two types of access techniques will be investigated in Sections 2.3 and 2.4 respectively. We focus during this study on the carrier sense multiple access (CSMA/CA) protocol for several reasons already described in the first chapter. For that we report in Section 2.5 the analysis tools for CSMA/CA from the literature. Section 2.6 describes the improvement of CSMA/CA envisaged by the state of the art and by our first contribution to this field. Finally, this chapter will be concluded in Section 2.7.

2.2 The concept of access protocols

One of the main problem in telecommunications is the access to a shared channel. When two transmitters communicate simultaneously over the same channel, it may risk a collision which leads to system performance degradation. In order to solve this problem, it was necessary to develop some access methods which are kind of algorithms able to reduce or to cancel the collision phenomena. The Medium Access Control (MAC) data communication networks protocol is a sub-layer of the data link layer specified in the seven-layer Open Systems Interconnection (OSI) model as showed in the Figure 2.1. The medium access layer was made necessary by systems that share a common communications medium [24]. We can distinguish two big families of access techniques: scheduled and random access techniques.

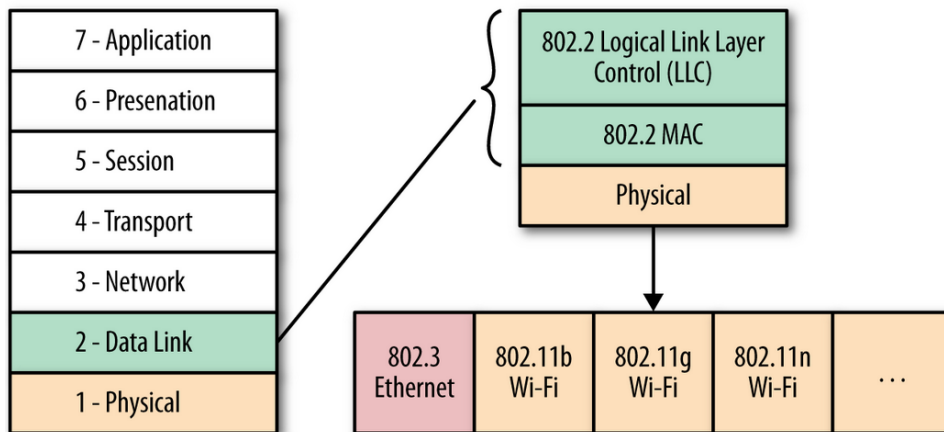


Figure 2.1: OSI model [16]

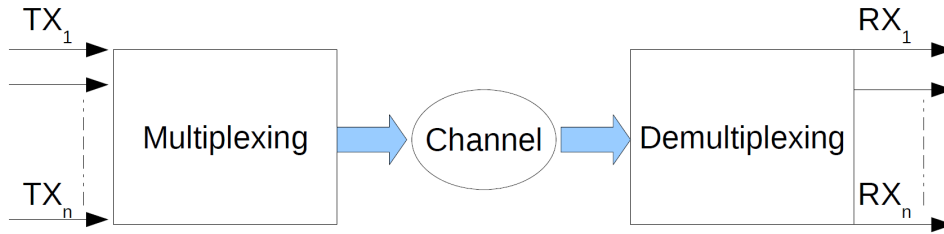


Figure 2.2: Multiplexing/Demultiplexing process

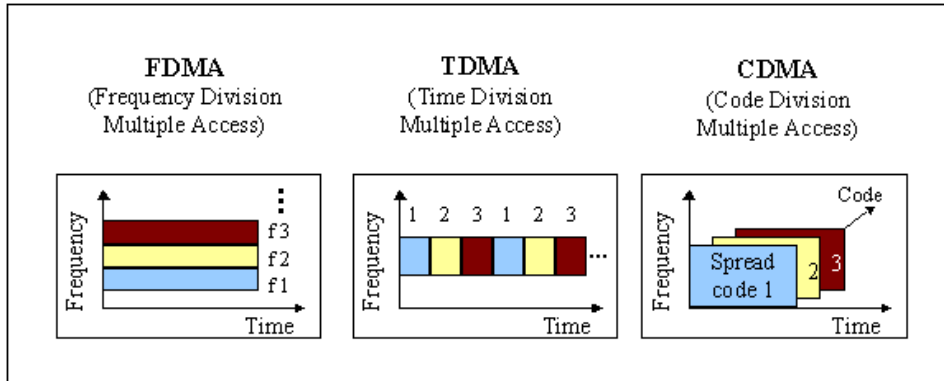


Figure 2.3: Deterministic access techniques [17]

2.3 Scheduled access techniques

In general the communication channel is used by many transmitters within a network. Since the channel capacity is limited and in order to not lose the efficiency, the channel access should be coordinated within the transmitters. Then, scheduled access techniques as showed in Figure 2.3 are needed to share the channel among the transmitters. In telecommunications we consider the three basic types of channel access (see Figure 2.3): Frequency Division Multiple Access (FDMA), Time Division Multiple Access (TDMA) and Code Division Multiple Access (CDMA).

In fact, these protocols require a central station to manage other nodes and to decide when is the best time to transmit. Hence, there is a need for control channels, resources allocations,...

2.3.1 Frequency Division Multiple Access

FDMA [25] is the most common analog system which divides the spectrum into frequencies assigned to users. With FDMA, at any given time only one subscriber is assigned to a channel. The channel therefore is closed to other conversations until the initial call is finished, or until it is handed-off to a different channel. A full-duplex FDMA transmission requires two channels, one for transmitting and the other for receiving. FDMA has been used for first generation analog systems. FDMA takes a dedicated receiver channel to listen which requires special filters to avoid interference between channels. Moreover, the channel assignment is simple and FDMA algorithms are easy to implement. Also, the maximum data rate for every channel is small and fixed with impossibility for receiver to receive the data from more than one node at the same time.

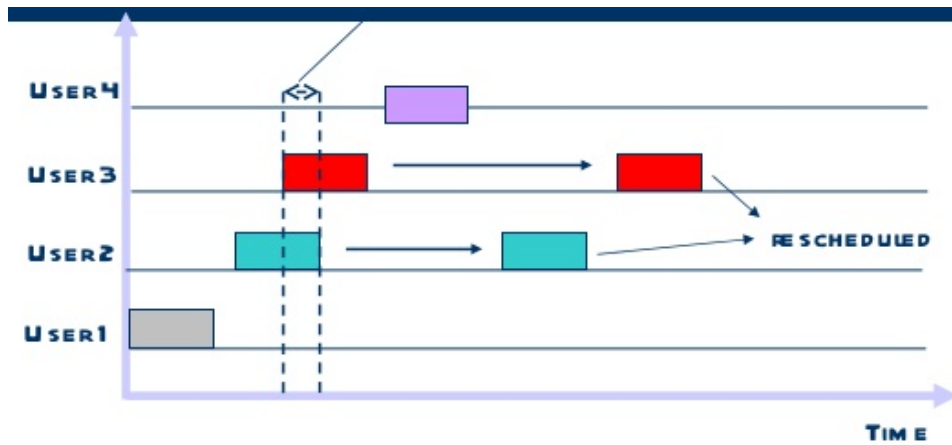


Figure 2.4: Random access protocols [18]

2.3.2 Time Division Multiple Access

TDMA [26] improves spectrum capacity by dividing each frequency into time slots. TDMA allows each user to access the complete radio frequency channel for the time slot. Other users share this same frequency at different time slots. The base station continually switches from user to another one on the same channel. TDMA was the dominant technology for the second generation mobile cellular networks. TDMA provides the user with extended battery life and talk time without interference from other simultaneous transmissions. However, transmitters must be synchronized to not use the channel simultaneously and multipath distortion could affect its performance.

2.3.3 Code Division Multiple Access

CDMA [27] is based on spread spectrum technology [28]. It has long been used for military purposes since it is suitable for encrypted transmissions. CDMA increases spectrum capacity by allowing all users to occupy all channels at the same time. Transmissions are spread over the whole radio band, and each voice or data call is assigned with a unique code to be differentiated from the other calls carried over the same spectrum. CDMA allows terminals to communicate with several base stations at the same time (soft hand-off [29]). The dominant radio interface for third-generation mobile is a wideband version of CDMA. Since CDMA uses both time and frequency it has a very flexible spectral capacity that can accommodate more users per MHz channel. But synchronization or advanced power control remain a real issue.

2.4 Random access protocols

When a node has a packet to send it may transmit at full channel data rate with no prior coordination among other nodes. If more than one transmission takes place, collision may happen. Random access protocols [30] specify how to detect collisions and how to recover from collisions via some adapted strategies (e.g. via delayed retransmissions as showed in Figure 2.4).

2.4.1 ALOHA Class

2.4.1.1 ALOHA

ALOHA also called pure ALOHA [31] relies on direct transmission whenever the node has packet to send. If collision occurs, the node waits for a random period of time and re-sends

it again (see Figure 2.5). ALOHA is simple to implement and no synchronization is required among users. However, it has a very low throughput (maximum throughput equals to 18% of channel capacity [19]) under heavy load because the probability of collision increases with the number of users.

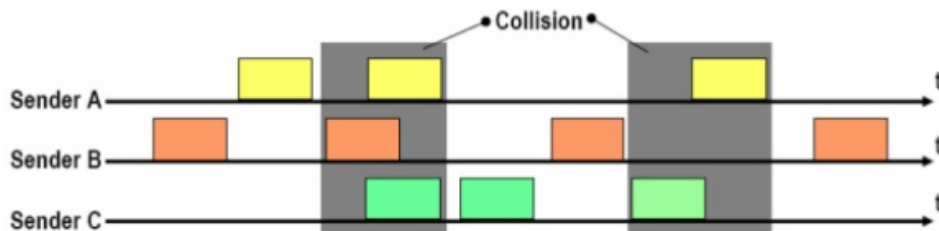


Figure 2.5: ALOHA [18]

2.4.1.2 Slotted ALOHA

In slotted ALOHA [32], time resource is divided into equal length slots and the AP transmits a beacon signal to synchronize the clocks of all nodes. When a user has a packet to transmit, the packet is buffered and transmitted at the beginning of the next time slot as showed in Figure 2.6. This protocol avoid partial packet collision but the throughput remains quite low (maximum throughput equals to 36% of channel capacity [19]).

Actually, ALOHA class is simple to implement but it has low efficiency. High number of collisions can be avoided by listening before transmitting, hence carrier sense multiple access (CSMA) may have better performance.

2.4.2 Carrier Sense Multiple Access

A user wishing to transmit first senses the communication channel to see if another transmission is in progress. If the channel is idle, the user may transmit, else it must wait. We can enumerate three type of CSMA as showed in Figure 2.7: 1-persistent, nonpersistent and p-persistent.

1-persistent CSMA [33] considers that the node keeps listening to see if the channel is free and, as soon as becomes idle, it transmits.

Nonpersistent CSMA [34] considers that the user waits for a random period of time before trying to sense again when the channel is busy. This access technique is less greedy.

p -persistent CSMA [35] requires a slotted system. When the channel is idle during the current slot, it may transmit with probability p or may defair until next slot with probability $1 - p$.

Cheng [19] shows that better performance can be achieved if user continues to listen to the medium while transmitting and stops transmission immediately if collision is detected.

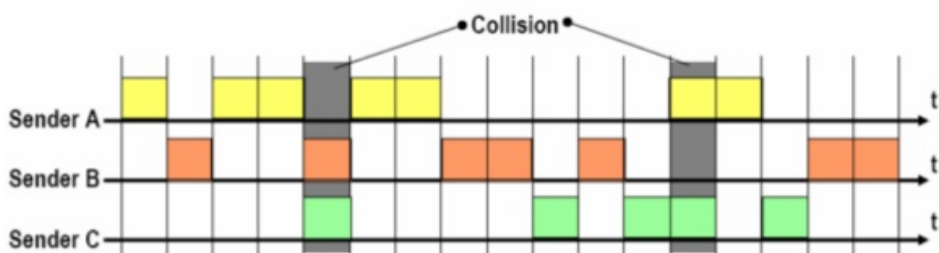


Figure 2.6: Slotted ALOHA [18]

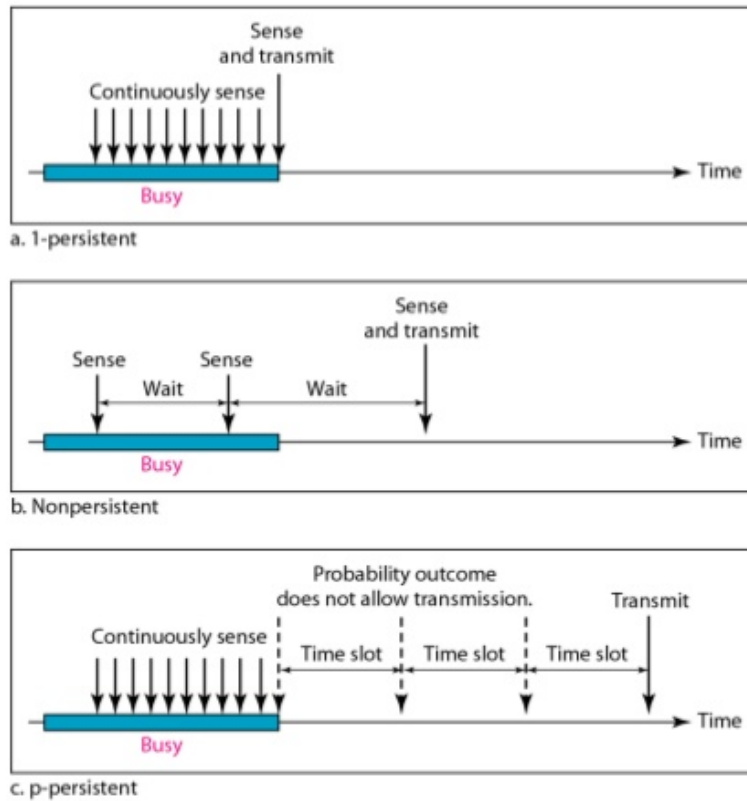


Figure 2.7: CSMA Modes [18]

2.4.2.1 Carrier Sense Multiple Access / Collision Detection

A user wishing to transmit using Carrier Sense Multiple Access / Collision Detection (CSMA/CD) [36] shall first of all listen if the channel is idle. If the channel is free, it transmits. Else it keeps listening until the channel becomes free, then transmits immediately. During the transmission phase, it keeps listening to detect collision. If a collision is detected, it stops transmitting immediately, and waits a random period of time before resensing the channel again. Figure 2.8 depicts an example of transmission using the CSMA/CD protocol. A packet is transmitted from node A to node B at time 0. Let τ be end-to-end propagation time. At time τ a collision happens. Hence a noise burst get back to A at time 2τ . Since the worst case time to detect collision is 2τ , frames should be long enough to allow collision detection prior to the end of transmission. Otherwise, CSMA/CD performance's degrades to the CSMA performance [19]. Collisions cannot be easily detected in wireless medium as power of transmitting overwhelms receiving antenna [19]. Hence, a different access method is required for wireless medium.

2.4.2.2 Carrier Sense Multiple Access / Collision Avoidance

Carrier Sense Multiple Access / Collision Avoidance (CSMA/CA) [37] was invented for wireless network where we cannot detect collisions. Collision are avoided through the use of (CSMA/CA's) three strategies [18] as showed in Figure 2.9: the interframe space (IFS), the contention windows (CW) and acknowledgement (ACK). The IFS can also be used to define the priority of a node or a frame. If the node senses the channel busy it stops the contention window timer and restarts it when the channel becomes free. CW intervals are used for contention and transmission of packet frames and the backoff counter is used only if more than one node compete for transmission.

CSMA/CA access methods have particular benefits in case of un-coordinated and/or Device to Device (D2D) communications networks. Each user can access the channel with equal priority through contention at each time instant. Two types of CSMA/CA access methods

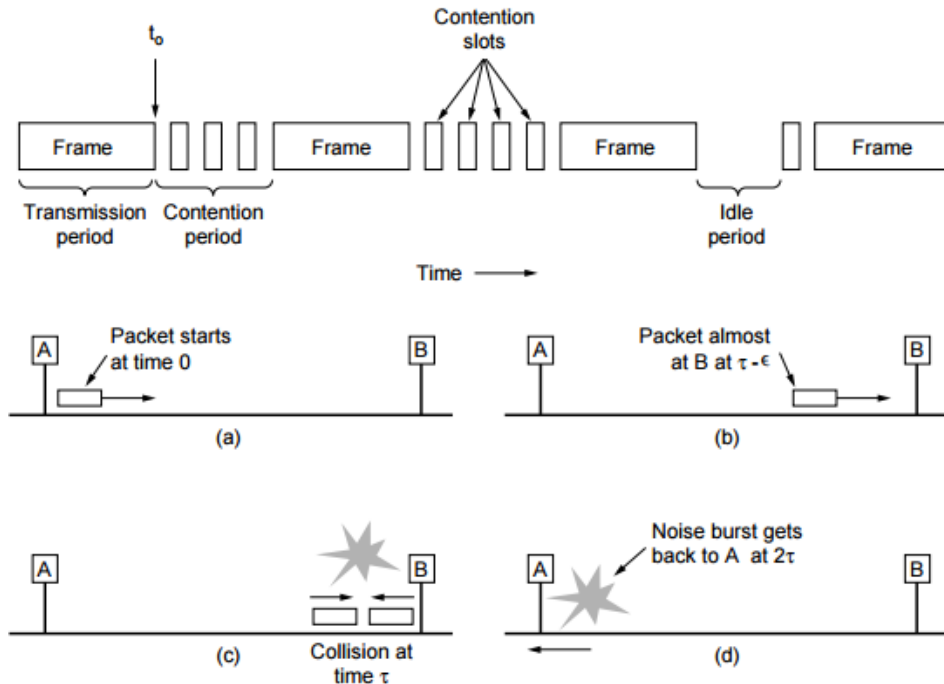


Figure 2.8: CSMA/CD Scheme [19]

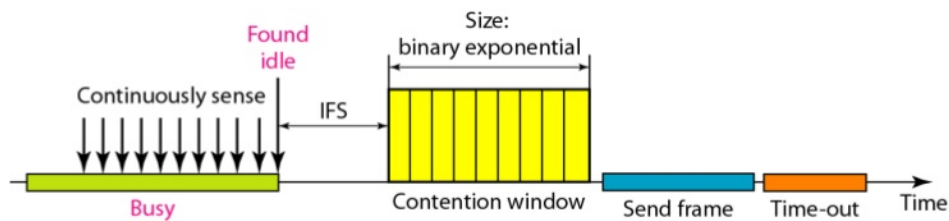


Figure 2.9: CSMA/CA's three strategies [18]

are commonly used, basic and Request to Send/Clear to Send (RTS/CTS) reservation modes. The latter is employed in order to improve performance as it reduces collision duration and addresses the hidden node problem [7]. Due to the four-way handshake mechanism, gain is achieved particularly when long data packets are transmitted.

2.4.2.2.1 Basic Carrier Sense Multiple Access / Collision Avoidance When the basic CSMA/CA is considered and as depicted in the Figure 2.10, each node with a packet to transmit should first sense the channel. If the channel is sensed to be idle for a time period greater than the distributed inter-frame space (DIFS) time, the node sends its data packet. After the successful reception of a data packet, an acknowledgment (ACK) packet is sent back. If the channel is not sensed idle, the node defers transmission. A random backoff timer is then generated in the interval $[0, CW-1]$ where CW is the contention window. When the channel is sensed idle, the backoff timer is decremented by one. If the channel is sensed busy the backoff timer is frozen. The node sends its data packet when the backoff timer reaches 0. If an acknowledge packet is received, the transmission is declared successful and CW is set to CW_{min} . In case of unsuccessful transmission, CW is doubled up until it reaches a maximum value, CW_{max} .

2.4.2.2.2 Carrier Sense Multiple Access / Collision Avoidance - Request To Send / Clear To Send When RTS/CTS mode is activated the node with a packet to transmit

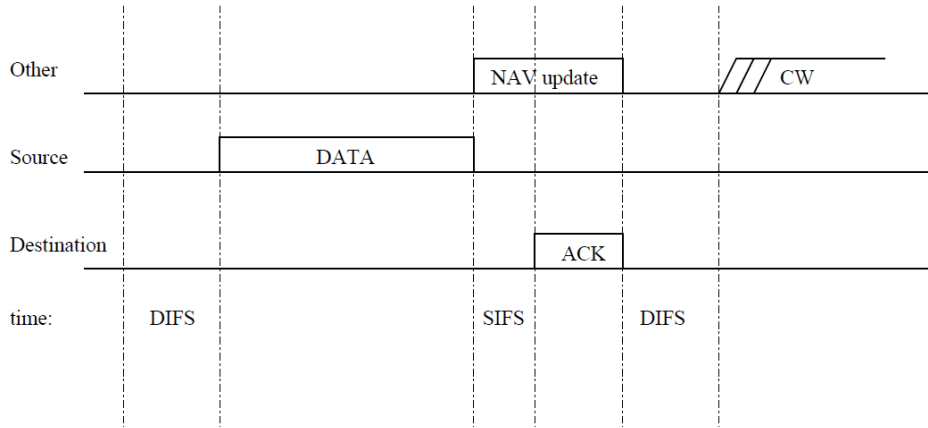


Figure 2.10: Basic CSMA/CA Algorithm [9]

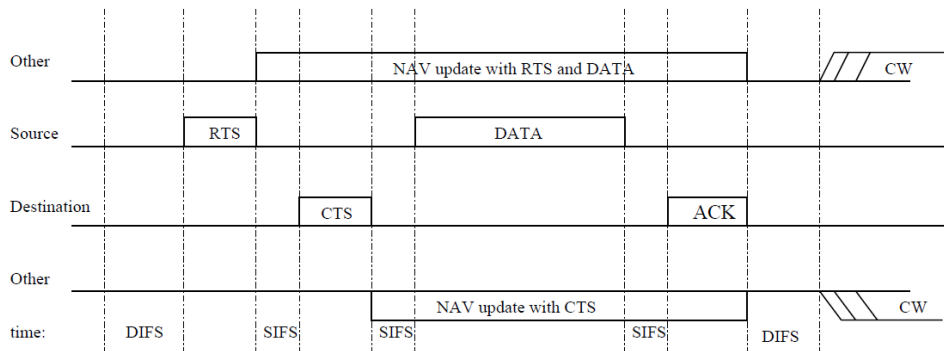


Figure 2.11: CSMA/CA - RTS/CTS Algorithm [9]

sends a RTS packet as depicted in the Figure 2.11. If the RTS packet is received without collision, a CTS is sent back to inform all nodes in the cell that the channel is reserved. All nodes defer their transmission for the duration specified by the RTS: this mechanism is called virtual sensing. After the successful reception of a data packet, an ACK packet is sent back. If the channel is not sensed idle, the backoff procedure is invoked. Under the hypothesis of a perfect transmission, collisions may only occur on RTS packets and transmission of data packets can proceed without interference from other nodes.

The CSMA/CA could be adopted for many reasons: it allows to operate in an environment with an unknown number of devices with the entire available bandwidth [4], operates in distributed manner [5] and leads to a cheaper deployment since it doesn't require much planning, interoperability and management complexity [6]. CSMA/CA - RTS/CTS is widely used in many random access wireless networks especially to combat hidden node problem [7] as it can reduce potential collisions and improves the overall network performance.

2.5 Analysis tools for CSMA/CA

Let's consider a network with many terminals and one access point. If the channel is busy for the transmitters, each one chooses randomly a backoff time (measured in time slots) in the interval $[0, CW)$ where CW is the *contention window*. As long as the channel is sensed idle, the timer (backoff) is decreased by one. When the channel is busy the timer counter is blocked and it resumes when the channel is idle again for at least a DIFS period. CW is an integer between CW_{min} and CW_{max} . After each unsuccessful transmission, CW is doubled up to the maximum value equal to $CW_{max}-1$. The source transmits an RTS frame when the backoff

reaches zero and waits for transmission permission (CTS) from the potential receiver before sending the current data packet. All nodes located in the sender's range that hear the RTS packet should update their NAVs (Network Allocation vector) and defer their transmissions for the duration specified by the RTS. By this strategy, the transmission of data packets and the corresponding ACK can proceed without interference from other nodes. In addition, whenever erroneous frame is detected by a node, it defers its transmission by a fixed duration indicated by EIFS, i.e., *extended inter-frame space* time. The contention window is initialized to CW_{min} (minimum contention window). Dense networks cause collisions between transmitters. Each node involved in the collision doubles the size of its contention window. In case of a successful transmission, the transmitter re-initializes its contention window by CW_{min} .

In order to analyze the performance of the CSMA/CA protocol, Bianchi [10] proposes to divide the analysis into two distinct parts. First, the behavior of a single node with a Markov model is studied, then the stationary probability π that the node transmits a packet in a slot time could be derived. This probability doesn't depend on the access mechanism (i.e. Basic or RTS/CTS) employed. The throughput of both basic and RTS/CTS access methods may be expressed as function of the computed value π by studying the events that can occur within a generic slot time (collision, success and idle).

2.5.1 Packet Transmission Probability

Considering a fixed number N of active contending nodes in saturation conditions (each node has always a packet available for transmission), all packets being "consecutive", each node needs to wait for a random backoff time before transmitting [10]. Each state of this Markov process is represented by $\{s(t), b(t)\}$, where $b(t)$ is the stochastic process representing the backoff time counter for a given node and $s(t)$ is the stochastic process representing the backoff stage $(0, 1, \dots, m)$ of the node at time t [9]. A discrete and integer time scale is adopted where $t, (t + 1)$ stands for the beginning of two consecutive slot times. The probability of a packet transmission failure p due to collision could be computed by assuming the following hypothesis [11]:

- No hidden terminal or capture effect.
- Failed transmissions only occur as a consequence of collision.
- All nodes are saturated, always having packets to send.
- For any given node, the probability of collision, p , is constant and independent of the collision history of the node and all other nodes.
- The probability of collision does not depend on the backoff stage at which the transmission is made.
- All users have same bitrates and same amount of time to transmit.

Also, we define p as the probability that, in a slot time, at least one of the $N - 1$ remaining nodes transmits. This probability can be expressed as:

$$p = 1 - (1 - \pi)^{(N-1)} \quad (2.1)$$

Where π is the probability that a node transmits a packet. It can be written by:

$$\pi = \sum_{i=0}^m b_{i,0} \quad (2.2)$$

Where $b_{i,k} = \lim_{t \rightarrow \infty} P\{s(t) = i, b(t) = k\}$, $i \in (0, m)$, $k \in (0, CW_i - 1)$ is the stationary distribution of the chain. Only $b(i, 0)$ are considered because a transmission occurs when the backoff time

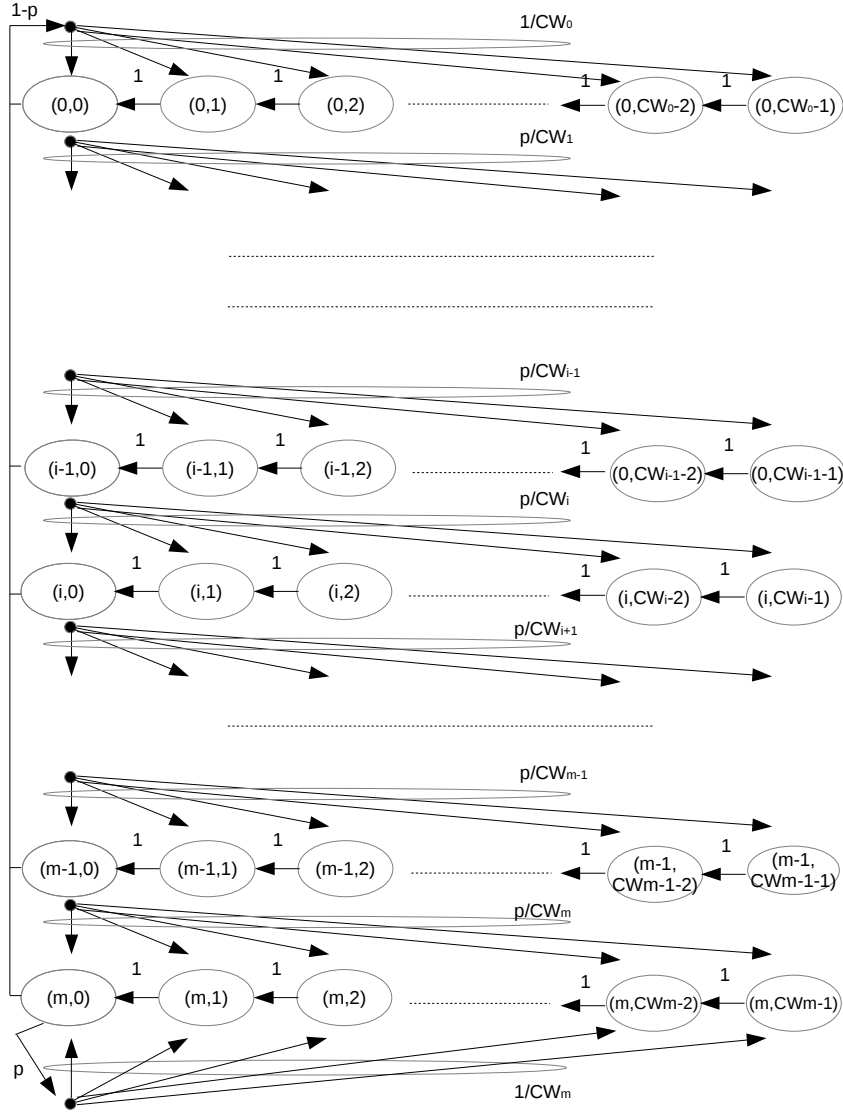


Figure 2.12: Markov Chain model for the backoff window size.

counter is equal to zero. By considering the Markov chain as referred in Figure 2.12, $b_{i,0}$ can be expressed as a function of p :

$$b_{i,k} = \frac{W_i - k}{W_i} \begin{cases} (1-p) \sum_{j=0}^m b_{j,0} & i = 0 \\ pb_{i-1,0} & 0 < i \leq m \\ p(b_{m-1,0} + b_{m,0}) & i = m \end{cases} \quad (2.3)$$

By imposing the classical normalization condition and considering equation (2.3), $b_{0,0}$ can be expressed as a function of p :

$$\begin{aligned} 1 &= \sum_{i=0}^m \sum_{k=0}^{CW_i-1} b_{i,k} \\ &= \frac{b_{0,0}}{2} \left[W_{min} \left(\sum_{i=0}^{m-1} (2p)^i + \frac{(2p)^m}{1-p} \right) + \frac{1}{1-p} \right] \end{aligned} \quad (2.4)$$

Where $W_{min} = CW_{min} - 1$. Finally, combining equations (2.2),(2.3), and (2.4), the channel access probability π is equal to:

$$\begin{aligned}\pi &= \sum_{i=0}^m b_{i,0} \\ &= \frac{b_{0,0}}{1-p} \\ &= \frac{2(1-2p)}{(1-2p)(W_{min}+1) + pW_{min}(1-(2p)^m)}\end{aligned}\tag{2.5}$$

These two equations, (2.1) and (2.5), form a system of two nonlinear equations that has a unique solution and can be solved numerically for the values of p and π .

2.5.2 Saturation Throughput

The saturation throughput, which is the average information payload in a slot time over the average duration of a slot time, can be expressed using the classical expression [9]:

$$\begin{aligned}\tau &= \frac{E[\text{Payload information transmitted in a slot time}]}{E[\text{Duration of slot time}]} \\ &= \frac{P_s P_{tr} L}{P_s P_{tr} T_s + P_{tr}(1-P_s)T_c + (1-P_{tr})T_{id}}\end{aligned}\tag{2.6}$$

where $P_{tr} = 1 - (1 - \pi)^N$ is the probability that there is at least one transmission in the considered slot time; L is the average packet payload size; T_s is the average time needed to transmit a packet of size L (including the inter-frame spacing periods [10]); $P_s = \frac{N\pi(1-\pi)^{N-1}}{1-(1-\pi)^N}$ is the probability of a successful transmission; T_{id} is the duration of the idle period (a single slot time); and T_c is the average time spent in the collision. T_c and T_s can be calculated for RTS/CTS transmission mode with [9]:

$$\begin{cases} T_s = RTS + SIFS + \sigma + CTS + SIFS + \sigma + H + P \\ \quad + SIFS + \sigma + ACK + DIFS + \sigma \\ T_c = RTS + DIFS + \sigma \end{cases}\tag{2.7}$$

where H , P , and ACK are the transmission times needed to send the packet header, the payload, and the acknowledgment, respectively. σ is the propagation delay.

2.5.3 Numerical Analysis

In this Section we present the numerical solution results of the Bianchi model [9]. The channel bitrate has been assumed equal to 6 Mbps for 802.11a standard [38]. The packet payloads are assumed all equal to 1000-octet long. Figure 2.13 shows the saturation throughput of IEEE 802.11b [39] network using Bianchi model with basic transmission mode and with RTS/CTS packets. Each curve correspond to a different value of the maximum backoff stage, i.e., m . For high number of mobile stations, as expected, the RTS/CTS transmission mode shows better throughput performance as collision between the long data packets are avoided [9]. Also, the saturation throughput increases for the higher maximum backoff stages. It should be mentioned that the Bianchi model does not take into account the retransmission limit and the maximum backoff stage as defined by the IEEE standard specification [40]. Since the RTS/CTS mechanism introduces higher throughput than the basic one for dense network scenario and for bigger payload, this work will focus on the improvement of the CSMA/CA with RTS/CTS mechanism.

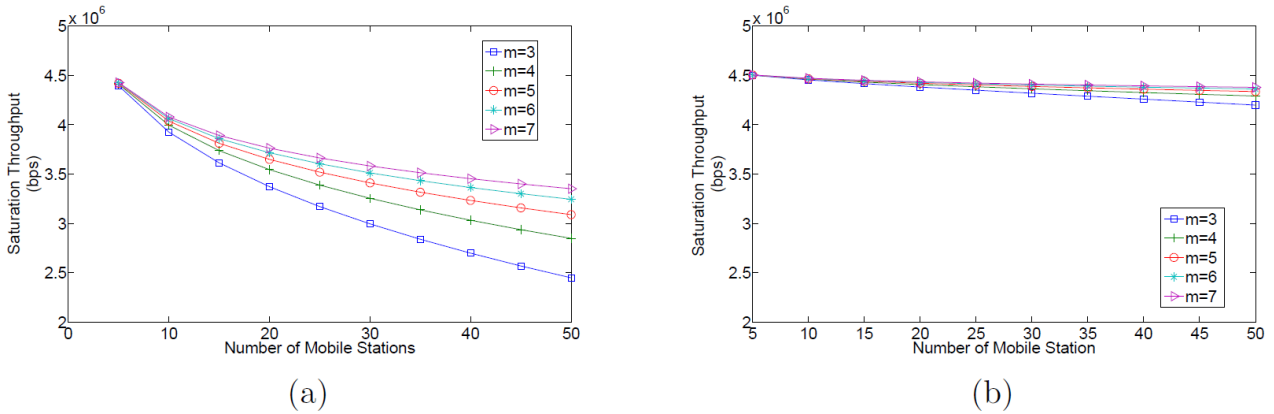


Figure 2.13: Saturation throughput comparison between basic and RTS/CTS CSMA/CA [9].

2.6 Improvement of CSMA/CA

2.6.1 Contention window optimization

Several works try to improve the throughput performance by attempting to optimize the contention window [41], [42] and [43], but they remain a tiny tuning of the contention window which is not introducing high improvement. Other researchers tried to adapt the backoff scheme based on network contention/traffic estimation [44], but unfortunately such estimations are not reliable due to unpredictable traffic patterns variations [45].

In [46], the throughput and the average access delay for different backoff algorithms were studied by simulation only. In the classical CSMA/CA protocol with 802.11 backoff strategy modeled by Bianchi [10], [13], it's clear that the first state is the bottleneck of the system, especially in crowded scenario. In order to improve the throughput and the system delay we proposed and developed a new mathematical model for a new backoff strategy based on Markov chain. We analytically prove that the outcome of the new strategy is better than the classical one in terms of saturation throughput and statistical access delay. Hence, we explain the proposed backoff strategy and we give a throughput analytical model. Then, we present the numerical results of the proposed protocol and a comparison with the classical one.

2.6.1.1 Analytical Model

As explained in the previous Section, when a node transmits successfully it returns directly to the first backoff stage. This fact introduces a high collision probability as well as an enormous additive transmission delay due to the high number of users in the same backoff stage ($m = 1$). This situation is seen as bottleneck problem. The proposed CSMA/CA is quite similar to the standard, the main difference remains in the case of a successful (i.e. collision-free) transmission, the transmitting node reduces the value of its contention window by half, so as to keep its contention window at least equal to CW_{min} (see Figure 2.14).

Using the Bianchi's model described in the previous Section, we model the proposed protocol by a Markov chain of $m + 1$ backoff stages as illustrated in Figure 3.4. Each stage of the Markov chain modelled the backoff counter. The number of states per stage is equal to the maximum authorized value of the backoff counter, i.e CW_i . It should be mentioned that we use notations described in [9], i.e $CW_i = 2^i(CW_{min} + 1)$.

When a collision occurs a transition from stage i to $(i + 1)$ is considered and a random backoff will be chosen between 0 and $CW_i - 1$ with probability of $\frac{p}{CW_i}$. A successful transmission is modelled by a transition from stage $(i + 1)$ to i and a random backoff will be chosen between 0 and $CW_{i-1} - 1$ with probability of $\frac{1-p}{CW_{i-1}}$.

Each state of this Markov process is represented by $\{s(t), b(t)\}$, where $b(t)$ is the stochastic

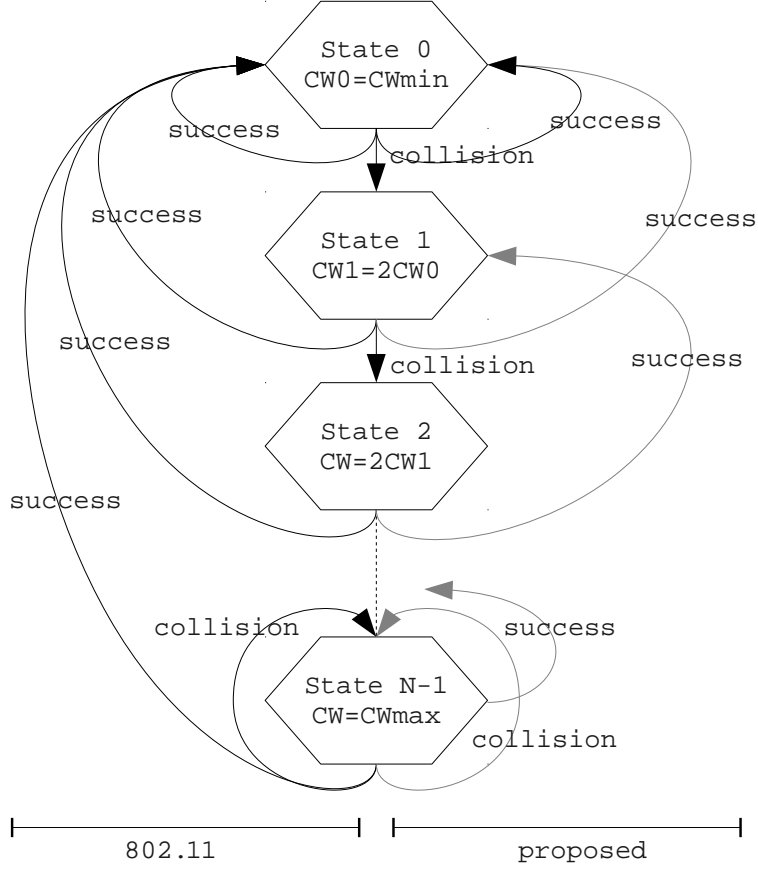


Figure 2.14: 802.11 and proposed backoff strategy.

process representing the backoff time counter for a given node and $s(t)$ is the stochastic process representing the backoff stage $(0, 1, \dots, m)$ of the node at time t [9]. A discrete and integer time scale is adopted where $t, (t + 1)$ stands for the beginning of two consecutive slot times.

We define p as the probability that, in a slot time, at least one of the $N - 1$ remaining nodes transmits. This probability can be expressed by:

$$p = 1 - (1 - \pi)^{(N-1)} \quad (2.8)$$

Where π is the probability that a node transmits a packet. It can be written as:

$$\pi = \sum_{i=0}^m b_{i,0} \quad (2.9)$$

Where $b_{i,k} = \lim_{t \rightarrow \infty} P\{s(t) = i, b(t) = k\}$, $i \in (0, m)$, $k \in (0, CW_i - 1)$ is the stationary distribution of the chain. Only $b_{i,0}$ are considered because a transmission occurs when the backoff time counter is equal to zero. By considering the proposed Markov chain, $b_{i,0}$ can be expressed as a function of p :

$$\begin{cases} b_{i,0} = \left(\frac{p}{1-p}\right)^i b_{0,0} & 0 < i \leq m \\ b_{i,k} = \frac{CW_i - k}{CW_i} b_{i,0} & 0 < i \leq m, \quad 0 \leq k \leq CW_i - 1 \end{cases} \quad (2.10)$$

It should be noticed that this expression is different from the one expressed in [9], due to the proposed backoff strategy. By imposing the classical normalization condition and considering

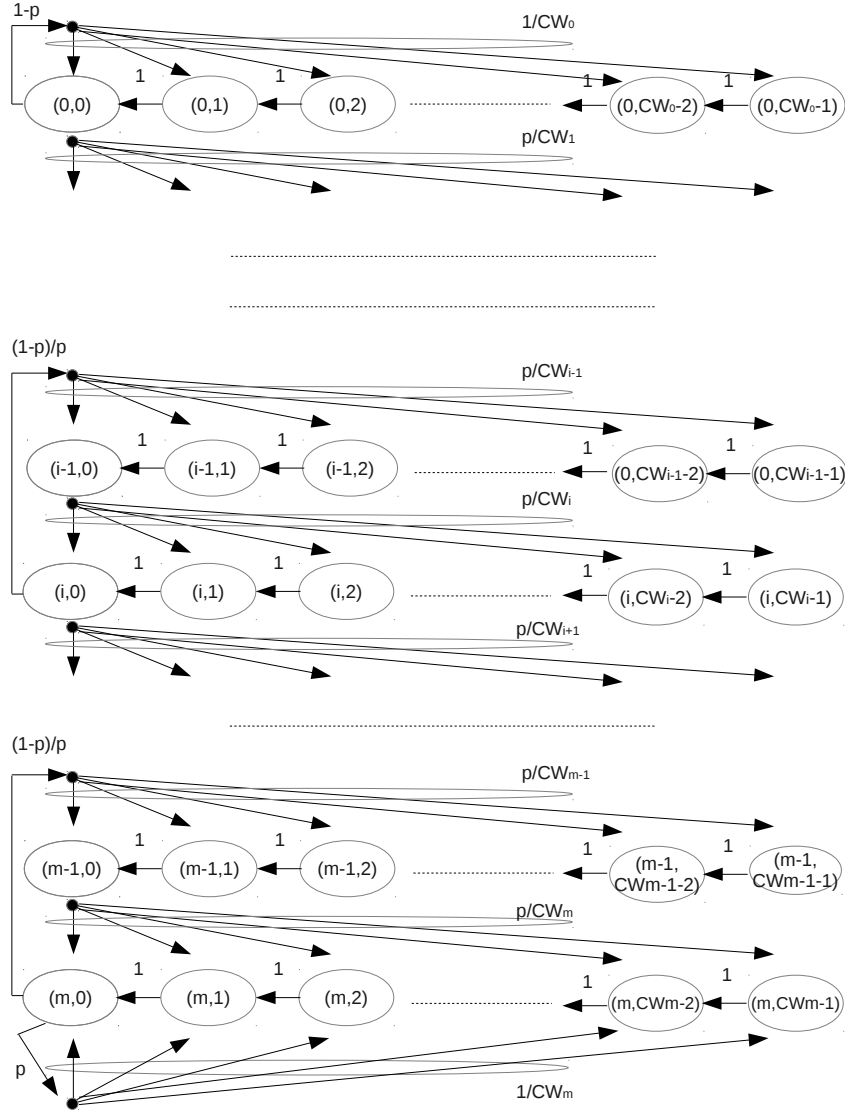


Figure 2.15: Markov chain model of backoff window size in proposed CSMA/CA.

Equation 2.10, $b_{0,0}$ can be expressed as a function of p :

$$\begin{aligned}
 1 &= \sum_{i=0}^m \sum_{k=0}^{CW_i-1} b_{i,k} \\
 &= \frac{b_{0,0}}{2} \left(W_{min} + 1 + W_{min} \frac{(1-p)^m - (2p)^m}{(1-3p)(1-p)^{m-1}} \right. \\
 &\quad \left. + \frac{(1-p)^m - p^m}{(1-2p)(1-p)^{m-1}} \right)
 \end{aligned} \tag{2.11}$$

Where $W_{min} = CW_{min} - 1$. Finally, combining equations (2.9), (2.10), and (2.11), the channel

access probability π is equal to:

$$\begin{aligned}
\pi &= \sum_{i=0}^m b_{i,0} \\
&= \sum_{i=0}^m \left(\frac{p}{1-p} \right)^i b_{0,0} \\
&= b_{0,0} \frac{(1-p)^m - p^m}{(1-2p)(1-p)^{m-1}}
\end{aligned} \tag{2.12}$$

This two equations, (2.8) and (2.12), form a system of two nonlinear equations that has a unique solution and can be solved numerically for the values of p and π .

2.6.1.2 Performance analysis and validation

In this Section we study the validity, the saturation throughput and the delay of the analytical proposed model. The system of two nonlinear equations (2.8) and (2.12) is solved numerically. The protocol and channel parameters adopted are those specified in Table 2.1. However analysis and results can be extended to others PHY layers. The minimal contention window (W_{min}) has been chosen constant and equal to 16.

Packet payload	8184 bits
MAC header	272 bits
PHY header	128 bits
ACK length	112 bits + PHY header
RTS length	160 bits + PHY header
CTS length	112 bits + PHY header
Channel Bit Rate	1 Mbit/s
Propagation Delay	1 μ s
SIFS	28 μ s
Slot Time	50 μ s
DIFS	128 μ s

Table 2.1: PHY layer parameters

2.6.1.2.1 Validation of Analytical Results In order to validate the analytical model, the proposed backoff strategy is simulated for various number of mobile nodes. Saturation throughput is computed for 2 different maximum backoff stages ($m = 3$ and $m = 7$). Figure 2.16 illustrates the relative error expressed by equation (2.13). The difference between the analytical and the simulated model is negligible and it is due to the solve function tolerance as well as to the modeling assumptions¹. Finally, the analytical model is validated.

$$RelativeError = 100 \times \frac{(Theoretical\ Throughput) - (Simulated\ Throughput)}{(Simulated\ Throughput)} \tag{2.13}$$

2.6.1.2.2 System Performance In order to study the performance of the proposed back-off strategy, we compute the saturation throughput (bits/sec) vs. the number of mobile stations for the RTS/CTS mode. RTS/CTS transmission mode is considered as it avoids collision between long data packets especially for high number of mobile stations. Figures 2.17 and 2.18 show that the saturation throughput in the proposed strategy is better than the saturation

¹A complete discussion about the validity of the assumptions will take place in the next Chapter.

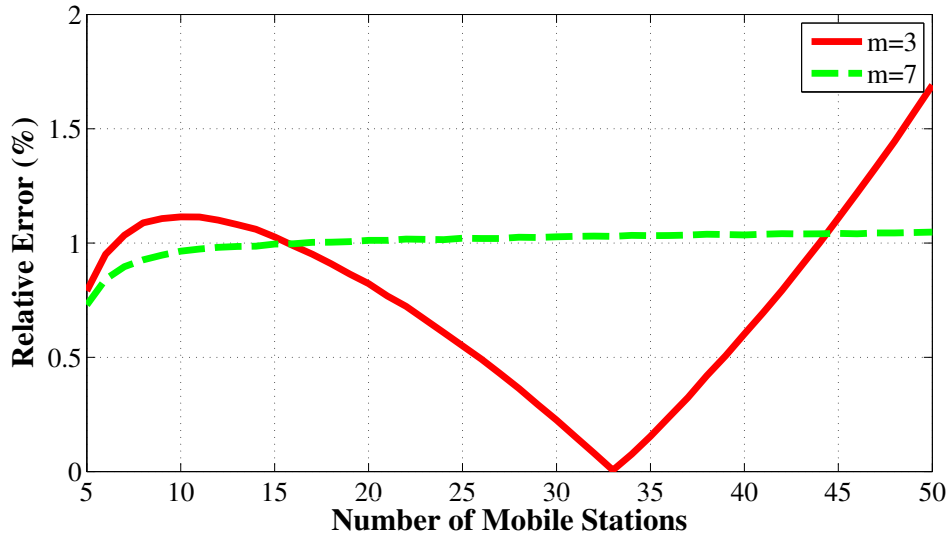


Figure 2.16: Relative error vs. number of mobile stations.

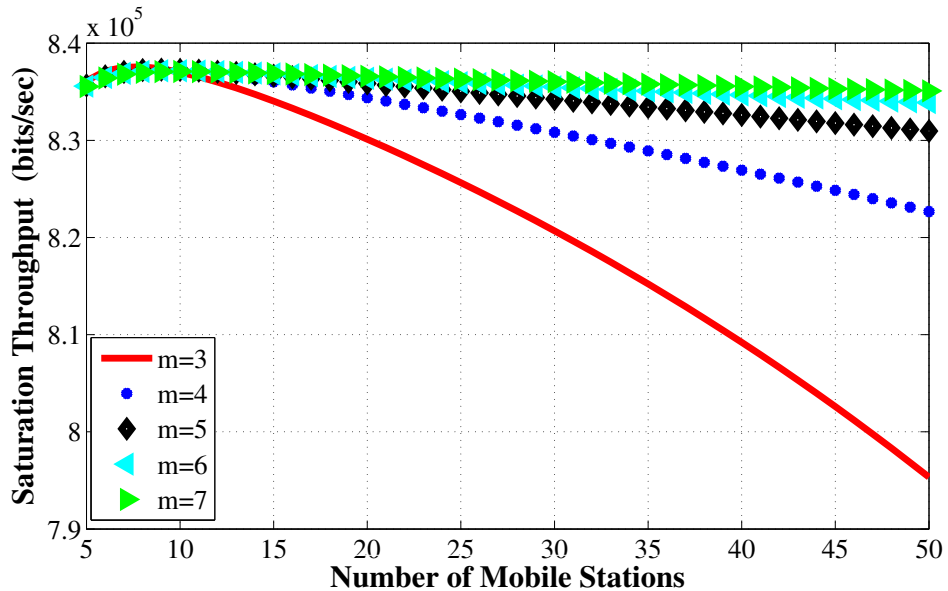


Figure 2.17: Saturation throughput for proposed strategy with RTS/CTS transmission.

throughput in the classical CSMA/CA protocol with 802.11 backoff strategy for RTS/CTS mechanism, and especially in the cases of large CW_{max} (big m) independently from the number of mobile stations. For example, in the proposed model and for $CW_{max} = 511$ ($m = 5$) we can achieve better saturation throughput than the 802.11 model with $CW_{max} = 2047$ ($m = 7$).

Numerical results show, as expected and due to lower probability of collision between transmitters, that the throughput increases when the number of states becomes higher. This fact is due to the distribution of all users within different backoff states, instead to be all located in the first state (bottleneck of classical 802.11 protocol). Note that we didn't take into consideration the retransmission limit and the maximum backoff stage as defined by the IEEE standard specification [47]. It should be mentioned that 802.11 strategy has better performance for large number of users and $m = 3$ and it is due to the lack of spatial degree of liberty.

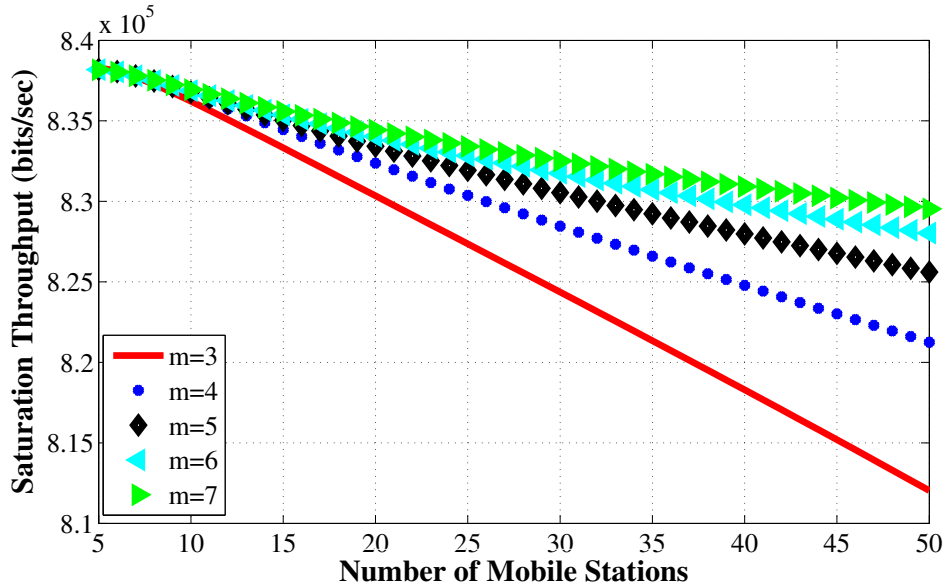


Figure 2.18: Saturation throughput for classical 802.11 with RTS/CTS transmission.

2.6.1.2.3 Statistical Delay Study Many previous works [46,48–50] evaluates the system performance in terms of delay by computing or simulating the average access delay. Since the average access delay isn't always a sufficient metric especially in VoIP applications, we go forward to simulate the cumulative density function (CDF) of the access delay. Figure 2.19 represents the CDF of the access delay for $m = 3$. It's seen clearly from Figure 2.19 that the delay of the proposed strategy is less than the classical one especially in dense mode (large number of mobile stations). It is due to the fact that users are distributed over all the stages instead to be located in the bottleneck (first backoff stage). Also, the proposed backoff strategy is much more robust with high states number (big m) thanks to the offered degree of freedom. Tables 2.2 and 2.3 give different delay values for some CDF with an idea about the gain introduced by our strategy. For instance, for $m = 3$ (resp. $m = 7$) 99% of packets are transmitted with at most 17.6 ms (resp. 13.9 ms) by the classical IEEE backoff while they are sent with at most 15.5 ms (resp 12.5 ms) by our proposed backoff strategy .

CDF	Proposed Backoff (ms)	Classical Backoff (ms)	Gain (%)
99%	15.5	17.6	11.93
98%	14.5	16.4	11.58
95%	13.3	14.6	8.90
90%	12.4	13.4	7.46

Table 2.2: Delay (ms) and gain (%) values in both backoff strategies for many CDF values with $m = 3$

CDF	Proposed Backoff (ms)	Classical Backoff (ms)	Gain (%)
99%	12.5	13.9	10.07
98%	12.0	13.2	9.09
95%	11.4	12.3	7.32
90%	10.9	11.5	5.22

Table 2.3: Delay (ms) and gain (%) values in both backoff strategies for many CDF values with $m = 7$

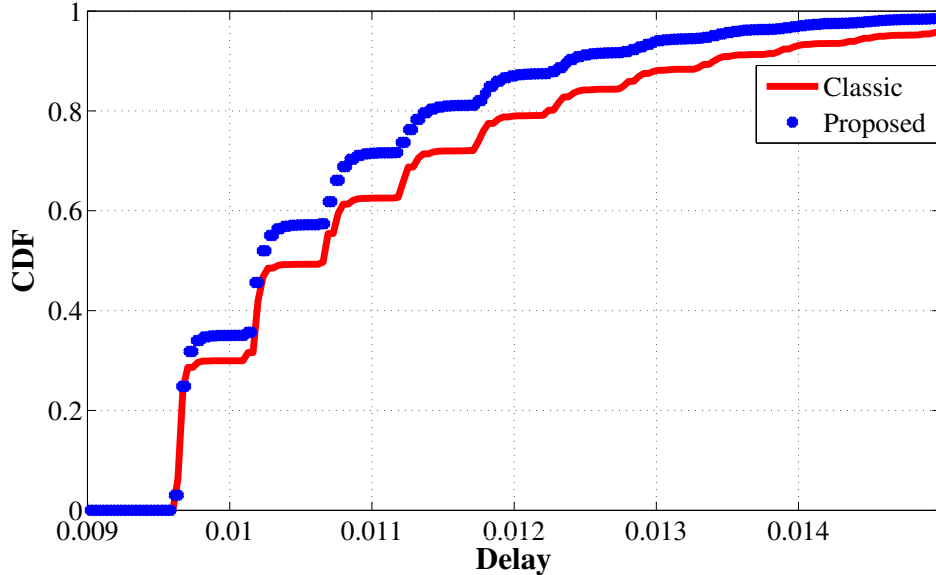


Figure 2.19: CDF of access delay for $m = 3$ with 50 mobile stations. Delay is expressed in second.

2.6.1.3 Conclusion

In this Section, we proposed and developed an analytical model for a new backoff strategy for CSMA/CA-CTS/RTS protocol. We validated the analytical model by simulations and we proved that the saturation throughput performance and the statistical access delay are improved especially in loaded systems. This proposed strategy could be a good candidate to solve the bottleneck problem existing in the classical IEEE 802.11 backoff strategy. Our model assumes a finite number of terminals and ideal channel conditions. The model is suitable for both Basic and RTS/CTS access mechanisms.

2.6.2 CSMA/CA - Enhanced Collision Avoidance

CSMA with Enhanced Collision Avoidance (CSMA/ECA) [20] significantly reduces the number of collisions by using a deterministic backoff after successful transmissions. This deterministic backoff may also be adjusted to prioritize traffic or to accommodate more contenders [51].

Figure 2.20 describes an example in which six saturated nodes contend for the channel. The channel time is divided in numbered slots and the balls on that slots represent the transmissions. The balls are filled with different patterns where each pattern corresponds to a different node [20].

A successful slot contains only one ball. If collision is occurred on a defined time slot, this slot contains more than one ball. The collided nodes will randomly choose a backoff value. Figure 2.20 shows that a collision is happened in slot number 7. The two collided nodes choose backoff values 10 and 20 which lead to two new collisions in slots 17 and 27, respectively.

A node that transmits with success, chooses a deterministic backoff equals to 16 slots. For instance, the node that successfully transmits in slot number 13 it will also transmits in slots 29, 45, 64 and 77. The behavior of the system becomes deterministic and collisions disappear when all nodes have successfully transmitted. In fact, when the number of active nodes is not greater than the value of deterministic backoff, the systems converges to a collision-free operation [52].

Since the number of collisions and the average backoff value are reduced, the throughput achieved by CSMA/ECA is higher [53]. Also CSMA/ECA does not add any additional complexity to the implementation comparing to the CSMA/CA and it can coexist with the

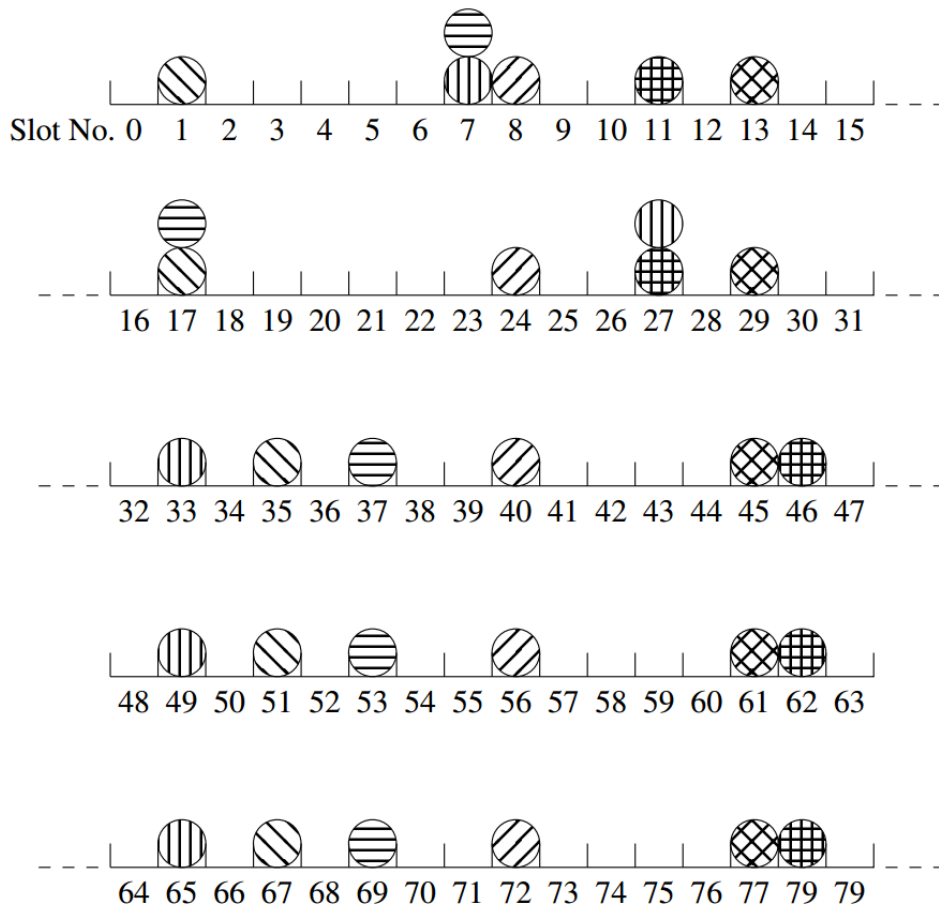


Figure 2.20: CSMA/ECA description [20]

already deployed networks. However, it should be mentioned that for high number of active nodes present in the network (especially if the number of transmitters is greater than the deterministic backoff size) the performance of CSMA/ECA would tend asymptotically to the performance obtained in CSMA/CA [20].

2.6.3 Related Works

All the random access techniques and their enhancements which are described above are based on single channel communication. It means that all the presented works consider one frequency band and try to optimize the access over this band (reducing the number of idle slots, reducing the number of collision,...). Moreover, trying to optimize the access in the frequency domain could introduce a second degree of freedom which can enhance further the MAC performance. For that, the authors of [54] proposed to use the physical layer technologies to improve the MAC layer efficiency. Within this category, the authors of Fine-grained channel access in wireless LAN (FICA) [55] argued that a better way to improve WLAN efficiency is to effectively reduce the channel width and to create more channels. Then, they obtained parallel contention channels without temporal backoff using the RTS/CTS mechanism. The absence of the temporal backoff imposes a dense channel division (to avoid RTS collisions) especially if guard bands are required to control a low level of inter user interference which causes a very high loss of useful frequency spectrum. Also this approach relies on tight time synchronization; it may experience practical challenges in real systems. Different works already proposed to generalize the CSMA/CA to the multiband case [49] [56] [57] in order to increase the global data rate. In these protocols, users are multiplexed through different channels while keeping the classical CSMA/CA strategy in each channel. Other works tried to eliminate collisions

between control and data packets by separating physically the control and the data planes: one band is reserved for control packets and the rest for data transmissions [58] [59] [60]. This scheme provides a higher throughput compared to the classical protocol adopted in 802.11 standard. However, it suffers from two issues when the network is crowded or lightly busy. In crowded situations, the classical CSMA/CA still runs on a common channel and suffers from collisions between control messages. In low traffic conditions, high rates users are penalized because they cannot transmit simultaneously on several channels, even if several ones are free. In [61] the authors proposed the Back2F protocol which migrates protocol operations from the time to the frequency domain and they designed an Orthogonal Frequency-Division Multiplexing (OFDM) based system where a random backoff is realized by transmitting on a selected subcarrier. In [62] a MAC protocol named REPICK was proposed. It distributes information on subcarriers to conduct both channel contention and ACK in the frequency domain concurrently. Above works are unfair when they interoperate with the legacy 802.11 protocol because of the absence of Distributed Inter-Frame Space (DIFS) time needed before participating in a backoff. The major drawback of the presented works is the need for an additional antenna. They assumed that each node has two antennas, one transmitter antenna and one listening antenna. The listening antenna is used to detect which subcarriers are activated by nearby nodes when the transmission antenna is sending packets concurrently. The presence of the listener behind the transmitter may cause self-interference problems which conduct to misdetection and lead to dysfunction of the proposed protocols. Moreover, these protocols are not very suitable for loaded networks and especially in the case of high mobility scenarios with fast joining/leaving events.

In order to take advantage from the frequency bandwidth and to have a fair interoperability with the legacy 802.11 DCF [63] we propose in this thesis a new MAC layer based on multichannel CSMA/CA with RTS/CTS mechanism adapted for dense scenarios. In the next chapters we will investigate the proposed MAC and we will analyze and compare the related system performance (based on some metrics) regarding the single band CSMA/CA-RTS/CTS (current standard).

2.7 Conclusion

In this chapter, we give the state of the art of access protocols. We differentiate two modes of access techniques, the scheduled one and the random one. Then, we switch to analyze the CSMA/CA protocol as described in the literature based on Bianchi model. After that, we proposed and we reported from the literature several works which suggest to improve the current protocol discussing their advantages/disadvantages. Other related works which invoke this protocol and propose to divide the communication channel into several communication channels are also discussed and analyzed.

The CSMA/CA could be adopted for several reasons: it allows to operate in an environment with an unknown number of devices with the entire available bandwidth [4], operates in distributed manner [5] and leads to a cheaper deployment since it doesn't require much planning, interoperability and management complexity [6]. CSMA/CA - RTS/CTS is widely used in many random access wireless networks especially to combat hidden node problem [7] as it can reduce potential collisions and improves the overall network performance.

To conclude in this chapter we discussed the state of the art related mainly to the single band CSMA and we identify the challenges of such access techniques. A novel protocol will be addressed in the next chapter in order to enhance this access technique and to reach better system performance.

Chapter 3

M-CSMA/CA - RTS/CTS

3.1 Introduction

In this chapter, a novel Medium Access Control (MAC) layer protocol based on the division of RTS band is proposed in order to improve the performance of the single band CSMA/CA - RTS/CTS. Hence, the channel is splitted for RTS messages while keeping the whole channel as a single band for CTS, DATA and ACK transmissions. The proposed protocol uses the advantages of both time and frequency resources. This new protocol is described in this chapter. Analytical and simulation results highlight the interest of this approach. We first explain in Section 3.2 the motivations behind the proposed protocol which is described in details in Section 3.3. Then, we present the analytical derivations related to the proposed protocol in Section 3.4 and the achieved gain compared to the single band CSMA/CA - RTS/CTS. The protocol performance is evaluated in Section 3.5. MAC performance study is evaluated in Section 3.6 and two type of allocation methods are described in Section 3.7. Finally we conclude this chapter in Section 3.8.

3.2 Motivations

The CSMA/CA - RTS/CTS protocol efficiency can be analyzed by computing the time repartition for each phase (collision, success and idle). In fact, the time proportion is evaluated by computing the duration spent in each state during the whole simulation time. Let's denote by R_c , R_s and R_i the time proportion passed in collision, success and idle states. If $T_{simulation}$, $T_{collision}$, $T_{success}$ and T_{idle} refers to the simulation time, total collision periods, total success periods and total idle periods during the simulation time. Then,

$$\begin{aligned} R_c &= \frac{T_{collision}}{T_{simulation}} \\ R_s &= \frac{T_{success}}{T_{simulation}} \\ R_i &= \frac{T_{idle}}{T_{simulation}} \end{aligned} \tag{3.1}$$

An analysis of the time repartition vs. the number of mobile stations is depicted in Figure 3.1 to better understand the protocol and to analyze the causes of system performance degradation. When the number of mobile stations increases, the time spent in success period decreases and the time wasted in idle and collision period increases. Hence a high waste of time (40%) is shown for dense network because of collisions. To improve the efficiency of the access method, reducing the probability of collision is crucial. Hence, the multichannel protocol is proposed in this chapter to reduce the time period wasted in collisions and idle.

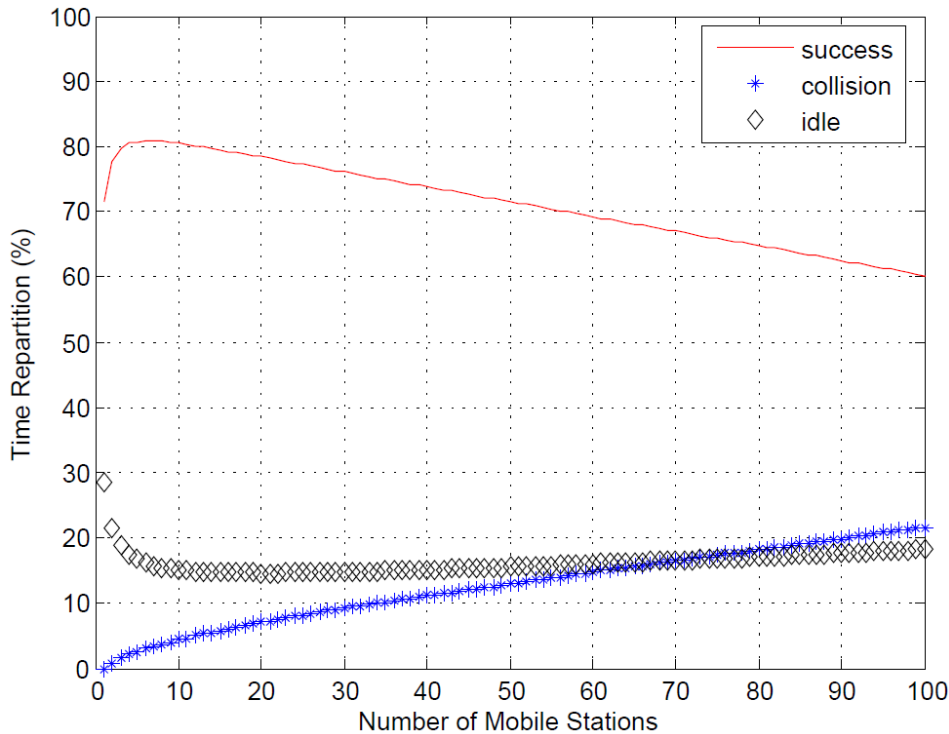


Figure 3.1: Single channel CSMA/CA - RTS/CTS time repartition vs. number of mobile stations.

3.3 Description

3.3.1 System Model

Without loss of generality, we consider a scenario where many nodes transmit packets to an access point (AP). Actually the system performance is closely related to the collision between simultaneous transmitted packets [9]. Considering a symmetrical and ideal channel with RTS/CTS mechanism, collisions may occur only during RTS transmissions. Orthogonal frequency multiplexing for these RTS messages is considered. Hence a single channel is divided into n sub-channels during RTS transmission. It should be mentioned that the duration of a RTS packet is increased by a factor n when the frequency bandwidth is reduced by a factor n to preserve the capacity of the link. Then, due to RTS channel decomposition the transmission duration (T^{new}) of the new RTS message is equal to the time needed for original RTS (T) multiplied by the number of sub-channels (n). Hence, $T^{new} = n \times T$.¹ We assume that both transmitter (TX) and receiver (RX) have the knowledge of the sub-channels size and central frequency. The proposed technique is based on a CSMA/CA protocol with RTS/CTS techniques. The proposed strategy is used to avoid collisions between multiple users (source nodes) which are willing to access at the same time to a common access point (destination node) by introducing an additional degree of freedom in the choice of a sub-channel.

According to this protocol, a source node wishing to transmit data should first sense the communication channel. Note that the receiver listens to all sub-channels simultaneously. Suppose that each node (STA) is allocated in advance to a define RTS sub-channel. If a signal is detected on at least one sub-channel, the channel is declared busy. Then, a period (expressed in number of time slots) of a waiting counter (known as "backoff counter") is chosen randomly in the interval $[0, CW-1]$, where CW is a contention window. Once the channel is detected available for a DIFS duration, the backoff counter is decremented by one (one time slot). The wait counter freezes when the channel is busy, and resumes when the channel is

¹Introducing a real physical layer could relax this equality to become more optimistic. Due to mapping and coding blocks the time needed T^{new} may be lower than $n \times T$. This effect will be discussed in Chapter 5.

available again [64]. When the backoff counter reaches zero, the source (STA) starts to send a request permission message (RTS) to the destination node using its pre-defined sub-channel. It waits for receiving an authorization message (CTS) from the destination node (access point) before transmitting data. The access point (AP) listens simultaneously to all sub-channels. If one or more RTS is detected, the AP broadcasts CTS over all the sub-channels indicating the authorized node to communicate. The chosen STA sends its data and waits for Acknowledge (ACK) from the AP. Both data and ACK messages are sent over all the sub-channels. Upon receipt of all transmitted data (successful transmission), and immediately, after a SIFS duration, the destination node sends an ACK (for "Acknowledgment"). Contention window (CW) is an integer between CW_{min} and CW_{max} . The CW is initially set to the minimum value; $CW=CW_{min}$. Whenever a source node is involved in a RTS collision, it increases the waiting time of transmission by doubling the CW, up to the maximum value $CW_{max} = 2^m \times CW_{min}$. Where m is the number of backoff stages. Conversely, in case of a successful RTS transmission, the source node reduces the CW to CW_{min} .

Let's describe a simple example which consider the case of three STAs, STA3, STA20, STA26 and an AP. Simultaneous transmission cause a collision over the RTS messages and no CTS is received by any node. Figure 3.2 illustrates how this collision can be reduced by dividing the RTS channel into two sub-channels. STA20 and STA26 are allocated to the first sub-channel. STA3 is allocated to the second sub-channel. Each one of the STAs tries to send an RTS on its sub-channel. At the receiver side a collision occurs on sub-channel 1. Therefore, the AP detects RTS from STA3. The AP chooses the STA3 and sends CTS over all present sub-channels indicating that STA3 has gained the channel access. All the STAs receive and decode the CTS and only STA3 tries to send its packets during a defined amount of time (many time slots). Successful communication takes place when the AP responds with ACK over all the sub-channels. If several STA succeed to transmit their RTS (one STA/sub-channel at the most), the AP chooses randomly or not one succeed node. The choice may depend on sub-channels conditions and nodes priorities. It should be mentioned that many allocation techniques are possible. For instance, a preallocation technique consists to allocate nodes to sub-channels in advance (before that their backoff reaches zero). A rather strategy consists in using random allocation technique by allocating randomly the nodes ready to transmit (having backoff equals to zero) to sub-channels.

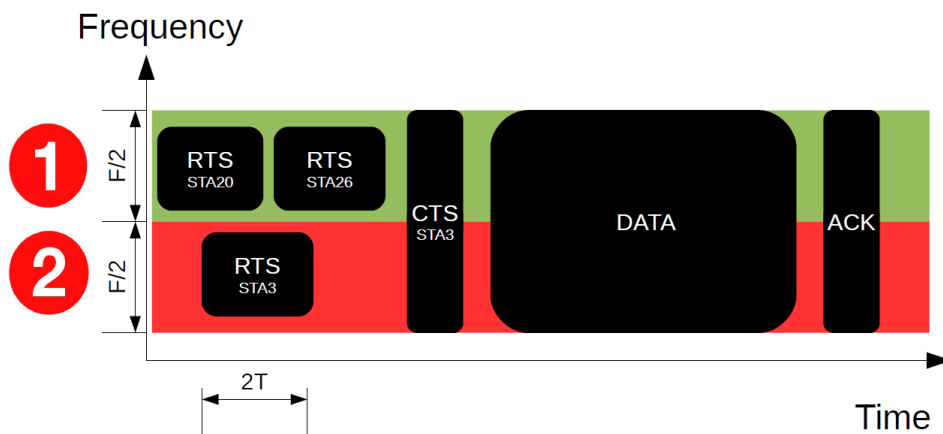


Figure 3.2: Multi channel CSMA/CA - RTS/CTS.

3.3.2 M-CSMA/CA - RTS/CTS Case Study

We now explore the benefits and potential issues of this M-CSMA/CA - RTS/CTS in regards of the classical problems arising with CSMA/CA, such as hidden [7] and exposed nodes [65] [66]).

3.3.2.1 Hidden node

The hidden node problem refers to a configuration of three nodes X, R and Y. X can hear R but not Y and Y can hear R but not X. A "hidden node" scenario results when Y attempts to transmit while X is transmitting to R, since Y has sensed the channel idle. The node configuration is depicted in Figure 3.3. This classical problem is resolved by the handshaking mechanism (RTS/CTS). The use of a virtual carrier sense (also known as Network Allocation Vector (NAV) scheme) provides a way to deal with hidden node problem. When a RTS or CTS is received by non transmitting nodes, they defer their backoff during a time specified into the RTS/CTS messages. In the case of the proposed protocol no additional mechanisms are required at the MAC layer. At the physical layer the receiver must be able to analyze each band independently for RTS messages but also to be able to decode the whole band. This is not an issue with OFDM systems.

Last but not least note that if the classical RTS/CTS mechanism avoids collisions in the hidden node scenario, it cannot deal with collisions between RTS messages themselves. The channel is kept clear only when the CTS has been sent.

3.3.2.2 Exposed node

RTS/CTS handshake mechanism was introduced to deal with the hidden node issue. However this mechanism introduces a new problem, known as exposed node. The issue of exposed node is depicted in Figure 3.3. Exposed node S_E can hear the RTS and DATA packets sent out from node S to D . Consequently, through the virtual carrier sensing, S_E can not initiate transmission despite being out of range of the receiver D . Consequently, the transmission between S_E and D_E is differed introducing a lost in capacity. The same problem exists with the proposed protocol but dealing with this issue is kept out of the scope of this paper. It is worth mentioning that some mechanisms have been proposed in the literature to face the exposed node problem and they could be transposed to the M-CSMA/CA - RTS/CTS protocol (see [65] for instance).

3.3.2.3 New pathologic case

The frequency multiplexing of RTS introduces a new issue that can be easily solved by a basic rule. Let us consider the following scenario including four nodes, two sources and two destinations. Source A sends a RTS to node B using band i and at the same time, source C sends a RTS to node D using band $i + 1$. Node B can hear both A and C , while node D can hear A or C only². In this case no RTS collision occurs since RTS messages are sent on different bands. Without particular rule the two destinations will respond CTS. In some cases, this scenario can introduce a CTS collision (since CTS messages are broadcasted over all the bands). To prevent the CTS collision and its consequences (watchdog timer is required if no data packet arrives ...), we propose to use the destination identity field already present in the RTS message in order to detect what we call virtual RTS collision. When two or more RTS can be decoded, the destination analyzes the identity of the destination node. If at least two different identities are detected then a collision is declared and no CTS is broadcasted over the cell. This case does not exist in the context of per-AP single band CSMA/CA-RTS/CTS with frequency reuse since each AP send its CTS over its own band.

3.4 Analytical Model

In this Section, the proposed protocol is modelled analytically by Markov chain in the case of a finite [67] or infinite [12] retransmission limit. The expressions of saturation throughput

²when all nodes can hear each other the same problem occurs

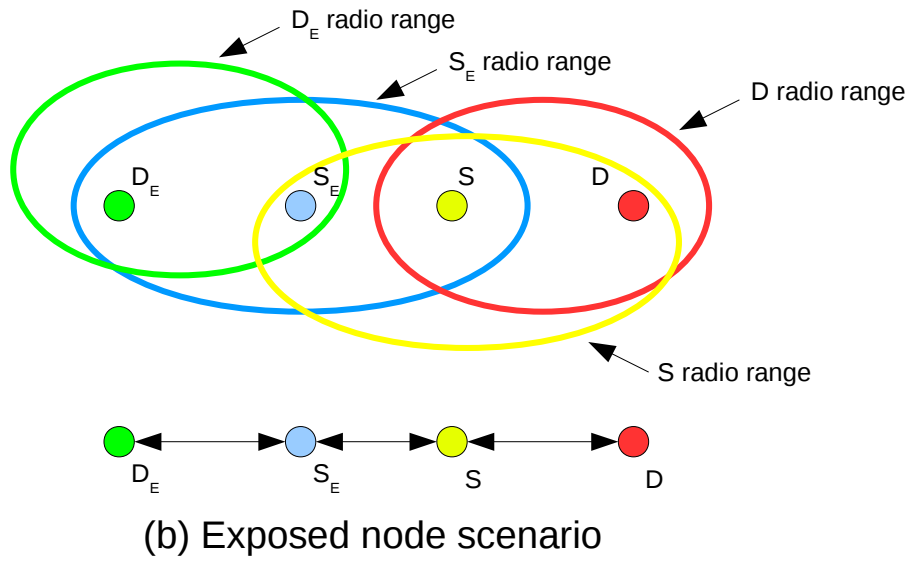
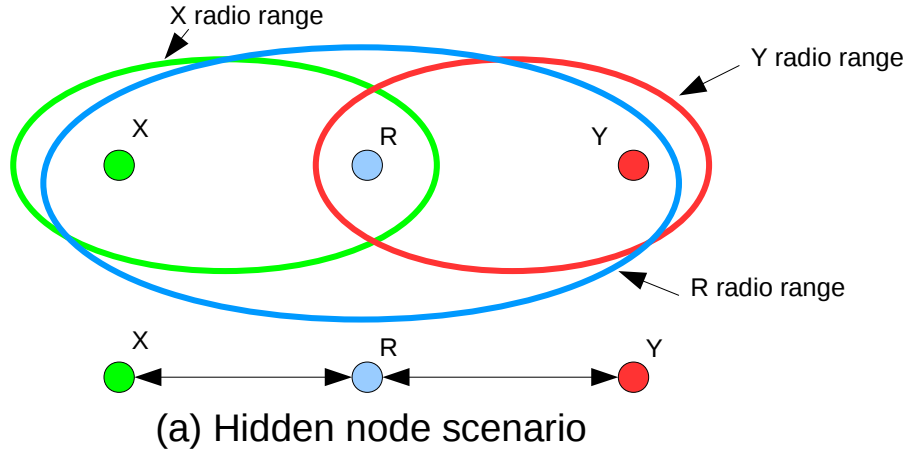


Figure 3.3: Illustration of the hidden and exposed node problem

and the related gain achieved by the proposed protocol compared to a standard single channel protocol is derived based on the analytical model. The packet drop probability is also expressed theoretically in the case of a finite retransmission limit.

3.4.1 Infinite Retry Limit Analysis

We first consider the proposed protocol with infinite retransmission limit [12]. It means that the node retries to transmit the packet until success.

3.4.1.1 Saturation Throughput

In this part we give the analytical calculation of saturation throughput for the proposed protocol (M-CSMA/CA-RTS/CTS). For that, we follow the same approach of Bianchi [10, 13] for the single channel protocol applied to the M-CSMA/CA-RTS/CTS taking into consideration that the RTS band is divided into many sub-channels. The saturation throughput, which is the average information payload in a slot time over the average duration of a slot time, can be expressed using the classical expression [9]:

$$S^n = \frac{E[\text{Payload information transmitted in a slot time}]}{E[\text{Duration of slot time}]} \quad (3.2)$$

$$= \frac{P_s^n \times P_{tr}^n L}{P_s^n \times P_{tr}^n T_s^n + P_{tr}^n \times (1 - P_s^n) T_c^n + (1 - P_{tr}^n) T_{id}}$$

This equation is strictly equivalent to the one given by Bianchi [9] but some of the variables change w.r.t. n . where upperscript n stands for the number of RTS sub-bands; P_{tr}^n is the probability that there is at least one transmission within the global system embedding n RTS sub-channels in the considered slot time; L is the average packet payload size; T_s^n is the average time needed to transmit a packet of size L (including the inter-frame spacing periods [10]); P_s^n is the probability of a successful transmission; T_{id} is the duration of the idle period (a single slot time); and T_c^n is the average time spent in the collision. T_c^n and T_s^n can be calculated for RTS/CTS transmission mode with:

$$\begin{cases} T_s^n = n \times RTS + SIFS + \sigma + CTS + SIFS + \sigma + H \\ \quad + P + SIFS + \sigma + ACK + DIFS + \sigma \\ T_c^n = n \times RTS + DIFS + \sigma \end{cases} \quad (3.3)$$

where H , P , and ACK are the transmission times needed to send the packet header, the payload, and the acknowledgment, respectively. σ is the propagation delay. The main goal is to compute P_{tr}^n and P_s^n .

Theorem 1: The probability of transmission and the probability of success for n RTS sub-channels considered in the system are given by:

$$P_{tr}^n = 1 - \prod_{i=1}^n (1 - \pi_i)^{N_i} \quad (3.4)$$

$$P_s^n = \frac{1 - \prod_{i=1}^n (1 - N_i \pi_i (1 - \pi_i)^{N_i - 1})}{1 - \prod_{i=1}^n (1 - \pi_i)^{N_i}} \quad (3.5)$$

Equations 3.4 and 3.5 show that the probabilities of transmission and success for the whole system are equivalent to have at least one transmission or success on one sub-channel. N_i is the number of active nodes allocated to the sub-channel i and π_i is the probability that a node associated to the sub-channel i transmits in a randomly chosen slot time.

Proof:

$(1 - \pi_i)^{N_i}$ is the probability to have no transmission on the sub-channel i . Then, $\prod_{i=1}^n (1 - \pi_i)^{N_i}$ corresponds to the probability to have neither transmission on the all sub-channels. Hence, equation 3.4 gives the probability to have at least one transmission on the all sub-channels (whole system).

Equation 3.5 is proven by the same methodology by considering that $1 - N_i \pi_i (1 - \pi_i)^{N_i - 1}$ corresponds to the probability to have neither successful transmission on the sub-channel i .

Now, we propose to compute the expression of π_i .

Theorem 2: The channel access probability is given by:

$$\pi_i = \frac{2}{1 + W_{min_i} + p_i W_{min_i} \sum_{k=0}^{m_i-1} (2p_i)^k} \quad (3.6)$$

Proof: We compute this probability (π_i) by assuming the following hypothesis [11]:

- No capture effect.
- Failed transmissions only occur as a consequence of collision (perfect physical channel).
- All nodes are saturated, always having packets to send.
- For any given node, the probability of collision, p_i , is constant and independent of the node's collision history of the node and all other nodes.
- The probability of collision does not depend on the backoff stage at which the transmission is made.
- All users have same bitrates and same amount of time to transmit.
- All users are divided into groups and each group of users is assigned to a predefined sub-channel.

We model the proposed protocol by a Markov chain (for each active node presents in the network) of $m_i + 1$ backoff stages as illustrated in Figure 3.4 [10]. Each stage of the Markov chain modelled the backoff counter. The number of states per stage is equal to the maximum authorized value of the backoff counter, i.e CW_i . It should be mentioned that we use notations described in [9], i.e $CW_{i,j} = 2^j(CW_{min_i} + 1)$.

When a collision occurs a transition from stage j to $(j + 1)$ is considered and a random backoff will be chosen between 0 and $CW_{i,j}-1$ with probability of $\frac{p_i}{CW_{i,j}}$. A successful transmission is modelled by a transition from stage $(j + 1)$ to 0 and a random backoff will be chosen between 0 and $CW_{i0}-1$ with probability of $\frac{1-p_i}{CW_{i0}}$.

Each state of this Markov process is represented by $\{s_i(t), b_i(t)\}$, where $b_i(t)$ is the stochastic process representing the backoff time counter for a given node and $s_i(t)$ is the stochastic process representing the backoff stage $(0, 1, \dots, m_i)$ of the node at time t [9]. A discrete and integer time scale is adopted where $t, (t + 1)$ stands for the beginning of two consecutive slot times.

We define p_i as the probability that, in a slot time, at least one of the $N_i - 1$ remaining nodes transmits. This probability can be expressed by:

$$p_i = 1 - (1 - \pi_i)^{(N_i-1)} \quad (3.7)$$

Where π_i is the probability that a node transmits a packet. It can be written by:

$$\pi_i = \sum_{j=0}^{m_i} b_{j,0} \quad (3.8)$$

Where $b_{j,k} = \lim_{t \rightarrow \infty} P\{s_i(t) = j, b_i(t) = k\}$, $j \in (0, m_i), k \in (0, CW_{i,j} - 1)$ is the stationary distribution of the chain. Only $b_i(j, 0)$ are considered because a transmission occurs when the backoff time counter is equal to zero. By considering the proposed Markov chain, $b_{j,0}$ can be expressed as a function of p_i :

$$\begin{cases} b_{j,0} = p_i^j b_{0,0} & 0 < j < m_i \\ b_{m_i,0} = \frac{p_i^{m_i}}{1-p_i} b_{0,0} \\ b_{j,k} = \frac{CW_{i,j}-k}{CW_{i,j}} b_{j,0} & 0 \leq j \leq m_i, \quad 0 \leq k \leq CW_{i,j} - 1 \end{cases} \quad (3.9)$$

By imposing the classical normalization condition and considering Equation 3.9:

$$\begin{aligned} 1 &= \sum_{j=0}^{m_i} \sum_{k=0}^{CW_{i,j}-1} b_{j,k} \\ &= \frac{b_{0,0}}{2} \left(W_{min_i} \left(\sum_{j=0}^{m_i-1} (2p_i)^j + \frac{(2p_i)^{m_i}}{1-p_i} \right) + \frac{1}{1-p_i} \right) \end{aligned} \quad (3.10)$$

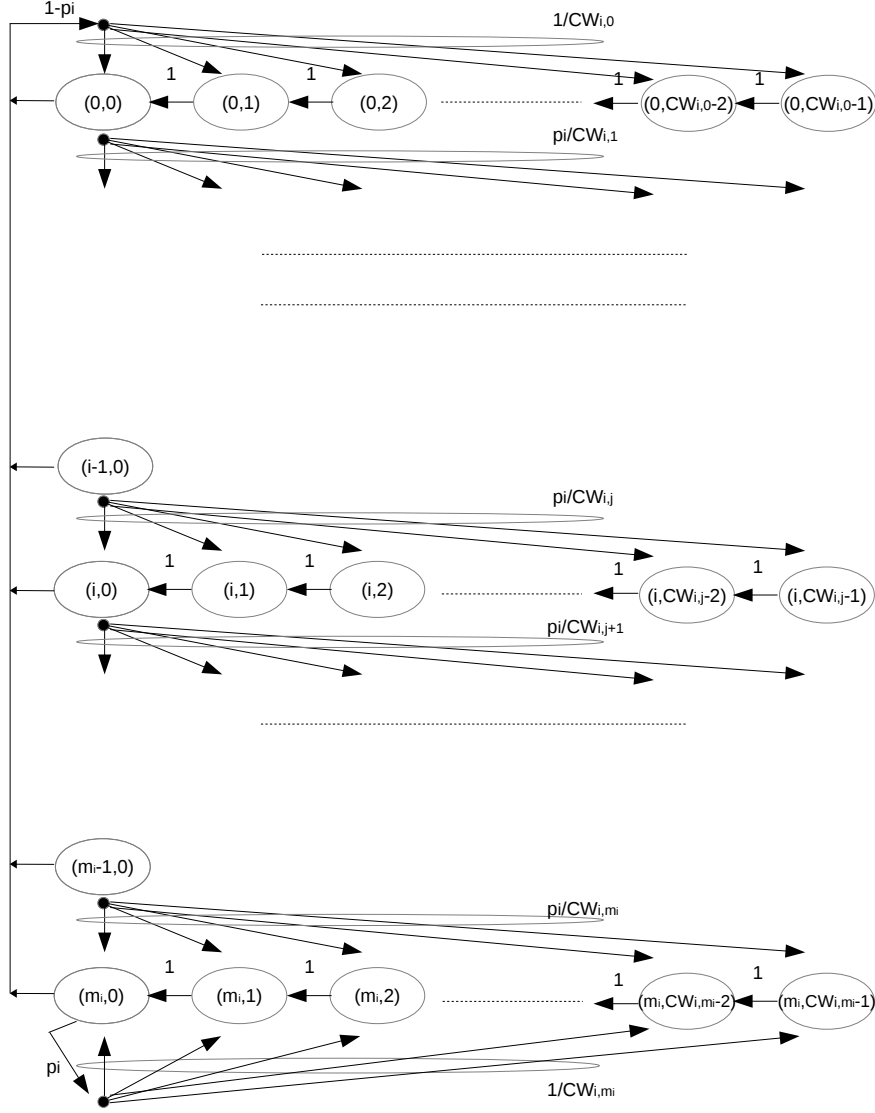


Figure 3.4: Backoff model for the proposed CSMA/CA with infinite retry limit. Compared to Bianchi [9], the probability is p_i instead of p .

Then $b_{0,0}$ can be expressed as a function of p_i :

$$b_{0,0} = \frac{2(1-2p_i)(1-p_i)}{(1-2p_i)(W_{min_i} + 1) + p_i W_{min_i} (1 + (2p_i)^{m_i})} \quad (3.11)$$

Finally, combining equations (3.8), (3.9) and (3.10), the channel access probability π_i is equal to:

$$\pi_i = \frac{2}{1 + W_{min_i} + p_i W_{min_i} \sum_{k=0}^{m_i-1} (2p_i)^k} \quad (3.12)$$

where W_{min_i} is the minimal contention window corresponding to the sub-channel i and p_i is the collision probability between 2 or more active nodes allocated to the sub-channel i .

In the case when the total amount of active user present in the system are distributed equally over all the sub-channels, the probability of transmission and success for the whole system could be expressed by the following equations:

case 1: N is multiple of n :

In that case, $\pi_1 = \pi_2 = \dots = \pi_i = \dots = \pi_n = \pi$ and $N_1 = N_2 = \dots = N_i = \dots = N_{n-1} = N_n = \frac{N}{n}$

$$P_{tr}^n = 1 - (1 - \pi)^N \quad (3.13)$$

$$P_s^n = \frac{1 - (1 - \frac{N}{n}\pi(1 - \pi)^{\frac{N}{n}-1})^n}{1 - (1 - \pi)^N} \quad (3.14)$$

Note that $n = 1$ corresponds to Bianchi [9] results.

case 2: N is not multiple of n :

The repartition of nodes over the bands may be expressed in equation 3.15.

$$\begin{aligned} N_1 &= \left\lfloor \frac{N}{n} \right\rfloor \\ N_2 &= \left\lfloor \frac{N - N_1}{n - 1} \right\rfloor \\ N_i &= \left\lfloor \frac{N - \sum_{k=1}^{i-1} N_k}{n - k} \right\rfloor \\ N_n &= N - \sum_{k=1}^{n-1} N_k \end{aligned} \quad (3.15)$$

The probability of success and transmission related to this case are given by equations 3.4 and 3.5.

3.4.1.2 Gain Analysis

In this Section we compute analytically the gain in terms of saturation throughput introduced by the proposed protocol regarding the single channel one. Let's denotes by G the relative saturation throughput gain between the proposed protocol and the single channel.

$$G = \frac{S^n - S^1}{S^1} = G_1 G_2 \quad (3.16)$$

Where G_1 and G_2 may be expressed as following:

$$G_1 = T_s^1 + \left(\frac{1}{P_s^1} - 1\right) \times T_c^1 + \left(\frac{1}{P_s^1 \times P_{tr}^1} - P_s^1\right) \times T_{id} \quad (3.17)$$

$$\begin{aligned} G_2 &= P_s^1 \times P_{tr}^1 \times P_s^n \times P_{tr}^n \times (T_s^1 - T_s^n) \\ &+ P_{tr}^1 \times P_{tr}^n (P_s^1 \times P_s^n (T_c^n - T_c^1) + P_s^n T_c^1 - P_s^1 T_c^n) \\ &+ (P_{tr}^n (P_s^n + P_s \times P_{tr}^1) - P_{tr}^1 (P_s^1 + P_s^n \times P_{tr}^1)) T_{id} \end{aligned} \quad (3.18)$$

Where P_{tr}^1 is the probability that there is at least one transmission in the considered slot time and P_s^1 is the probability of a successful transmission in the case of single channel protocol (standard). They may be expressed by following expressions [9]:

$$P_{tr}^1 = 1 - (1 - \pi)^N \quad (3.19)$$

$$P_s^1 = \frac{N\pi(1 - \pi)^{N-1}}{1 - (1 - \pi)^N} \quad (3.20)$$

It is clearly seen that the gain G is related directly to the minimal and maximal contention windows (number of backoff stages), number of RTS sub-channels, number of users by sub-channel, average time needed to transmit a packet of size L , average time spent in the collision and the slot time duration.

3.4.2 Finite Retry Limit Analysis

In this Section we consider the proposed protocol with finite retransmission limit. It means, that when the CW for a considered node attains CW_{max} , the node retries to transmit the packets as long as the retry counter (r) is less than a predefined limit.

3.4.2.1 Saturation Throughput

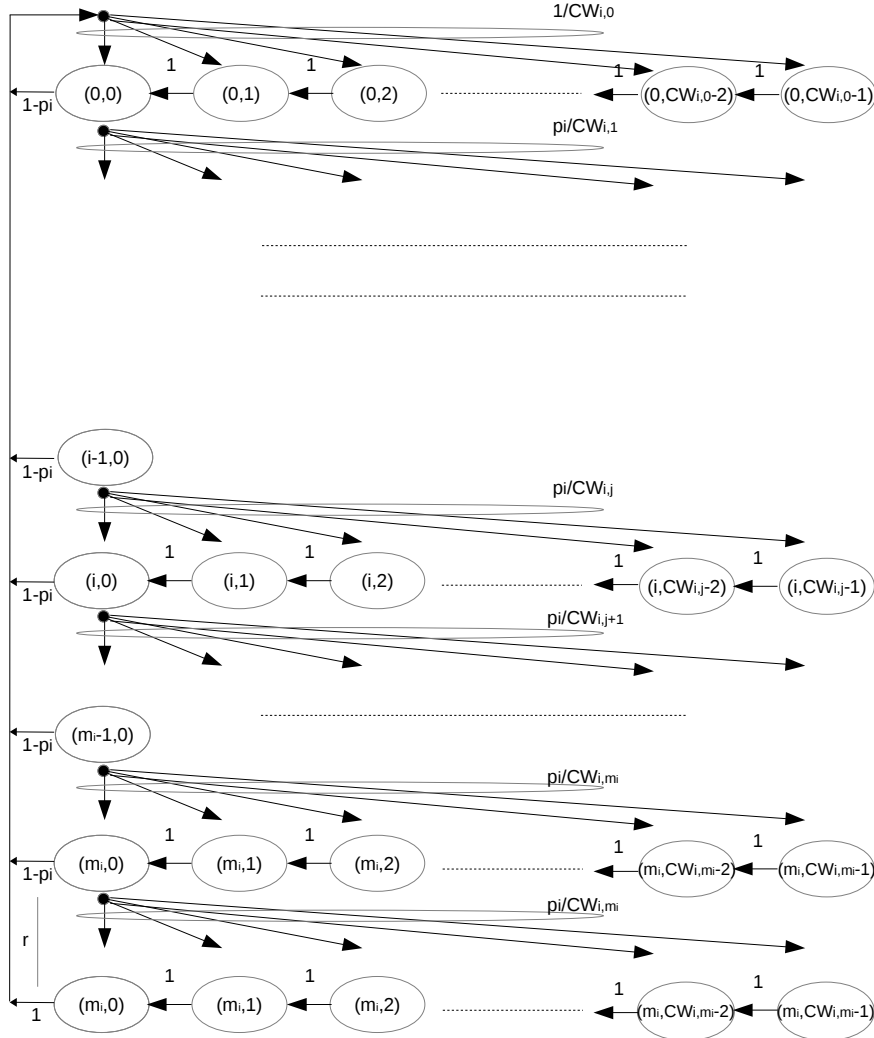


Figure 3.5: Backoff model for the proposed CSMA/CA with finite retry limit.

The analytical calculation of saturation throughput for the proposed protocol with finite retry limit has the same formulation as equation 3.2. The main change is the access probability value. Adopting the same assumptions and derivations as Section 3.4.1.1 we can compute π_i based on the new Markov chain depicted in Figure 3.5 where the last backoff stage is repeated r times. The stationary distribution of the Markov chain may be expressed as following:

$$\begin{cases} b_{j,0} = p_i b_{j-1,0} & 0 < j \leq m_i + r_i \\ b_{j,0} = p_i^j b_{0,0} & 0 < j \leq m_i + r_i \end{cases} \quad (3.21)$$

If the normalization condition is imposed and using the previous analysis, we can derive the probability π_i that a node transmits a packet in a randomly chosen slot time. Since a node transmits when its backoff counter reaches zero, π_i may be expressed by equation 3.22.

Theorem 3:

$$\pi_i = \sum_{j=0}^{m_i+r_i} b_{j,0} = \sum_{j=0}^{m_i+r_i} p_i^j b_{0,0} = b_{0,0} \frac{1 - p_i^{m_i+r_i+1}}{1 - p_i}$$

where,

$$b_{0,0} = \frac{2(1 - 2p_i)(1 - p_i)}{W_{\min_i}(1 - (2p_i)^{m_i+1})(1 - p_i) + (1 - 2p_i)(1 - p_i^{m_i+r_i+1}) + W_{\min_i}2^{m_i}p_i^{m_i+1}(1 - 2p_i)(1 - p_i^{r_i})}$$

$$\pi_i = \frac{2(1 - p_i^{m_i+r_i+1})(1 - 2p_i)}{W_{\min_i}(1 - (2p_i)^{m_i+1})(1 - p_i) + (1 - 2p_i)(1 - p_i^{m_i+r_i+1}) + W_{\min_i}2^{m_i}p_i^{m_i+1}(1 - 2p_i)(1 - p_i^{r_i})}$$
(3.22)

It should be mentioned that the above analysis with transmission limit which tends to infinity leads to the same results obtained with infinite retransmission limit.

$$\begin{aligned} \pi_i^{r_i=\infty} &= \frac{2}{1 + W_{\min_i}2^{m_i}p_i^{m_i+1} + W_{\min_i}(1 - p_i)\frac{1-(2p_i)^{m_i+1}}{1-2p_i}} \\ &= \frac{2}{1 + W_{\min_i} - W_{\min_i} + W_{\min_i}2^{m_i}p_i^{m_i+1} + W_{\min_i}(1 - p_i)\frac{1-(2p_i)^{m_i+1}}{1-2p_i}} \\ &= \frac{2}{1 + W_{\min_i} + W_{\min_i}(2^{m_i}p_i^{m_i+1} - 1) + W_{\min_i}(1 - p_i)\frac{1-(2p_i)^{m_i+1}}{1-2p_i}} \\ &= \frac{2}{1 + W_{\min_i} + \frac{W_{\min_i}}{1-2p_i}((2^{m_i}p_i^{m_i+1} - 1)(1 - 2p_i) + (1 - p_i)(1 - (2p_i)^{m_i+1}))} \\ &= \frac{2}{1 + W_{\min_i} + W_{\min_i}p_i\frac{(1-(2p_i)^{m_i})}{1-2p_i}} \\ &= \frac{2}{1 + W_{\min_i} + p_iW_{\min_i}\sum_{k=0}^{m_i-1}(2p_i)^k} \end{aligned}$$
(3.23)

Equation 3.23 proves that when the retry limit is infinite, equation 3.22 match the probability that a node corresponding to sub-channel i transmits given by equation 3.12 (infinite retransmission limit).

3.4.2.2 Packet drop probability

The packet drop probability is defined, as the probability that a packet is dropped when the retry limit is reached. It can be analytically evaluated by:

$$P_{drop} = \sum_{i=1}^n p_i^{m_i+r_i+1}$$
(3.24)

since a packet is dropped if it encounters $m_i + r_i + 1$ collisions. In the case when the total amount of active user present in the system are distributed equally over all the sub-channels ($N_1 = N_2 = \dots = N_i = \dots = N_n = N/n$), the packet drop probability is expressed as following:

$$P_{drop} = np^{m+r+1}$$
(3.25)

where

$$\begin{aligned}
 p &= p_1 = \dots = p_i = \dots = p_n \\
 m &= m_1 = \dots = m_i = \dots = m_n \\
 r &= r_1 = \dots = r_i = \dots = r_n
 \end{aligned}
 \tag{3.26}$$

3.5 Performance Analysis

In this Section, we validate the analytical model by simulation and we analyze the performance of the M-CSMA/CA-RTS/CTS protocol through different metrics. The results are compared to the single channel protocol (standard) considering the same conditions and same number of nodes allocated to each sub-channel. The scenario of one AP and many mobile stations is considered for simulation. The size of the data packet is considered quite large which corresponds to video or image with high resolution or even an aggregation of several packets. It should be noticed that due to the nature of the protocol, this scenario is equivalent to a plurality of AP. Home-made event-driven simulator was used to model the protocol behavior. The protocol and channel parameters adopted are those specified in Table 3.1. The 802.11n standard parameters are considered during this work because they are employed in the current Wi-Fi technology and without loss of generality this standard has a high channel bitrate which corresponds to the context of this work [68]. Indeed other standards which have a high channel bitrate (i.e. 802.11ac [69]) could also be considered without affecting the performance behavior. The minimal contention window (CW_{min}) has been chosen constant and equal to 16. According to Table 3.1 the time needed to transmit an RTS is less than $4\mu s$, while the time slot is equal to $9\mu s$. Since the time needed to transmit an RTS is less than the time slot, the problem of hidden node at the RTS level is automatically solved.

3.5.1 Model Validation

Packet payload	8184 bits
MAC header	272 bits
PHY header	128 bits
ACK length	112 bits + PHY header
RTS length	160 bits + PHY header
CTS length	112 bits + PHY header
Channel Bit Rate	72.2 Mbit/s
Propagation Delay	1 μs
SIFS	10 μs
Slot Time	9 μs
DIFS	28 μs

Table 3.1: PHY layer parameters for 802.11n 20Mhz

For validation purposes, we consider the case of 2 RTS sub-channels, equal nodes allocation and the 802.11n standard parameters as a physical layer reported in Table 3.1. Figures 3.6 and 3.7 depict the saturation throughput vs. the number of mobile stations for various number of backoff stages (m) computed by the theoretical model (Section 3.4.1.1) and by simulation according to the proposed protocol considering the case of 2 RTS sub-channels. Above a given number of nodes (here typically 10) the saturation throughput decreases linearly with the number of nodes. This decrease is partly compensated with a larger number of backoff stages (when m increases, the collision probability decreases).

Figure 3.8 depicts the error vs. the number of mobile stations between the analytical model and the simulation results of the proposed protocol. The difference between the analytical and

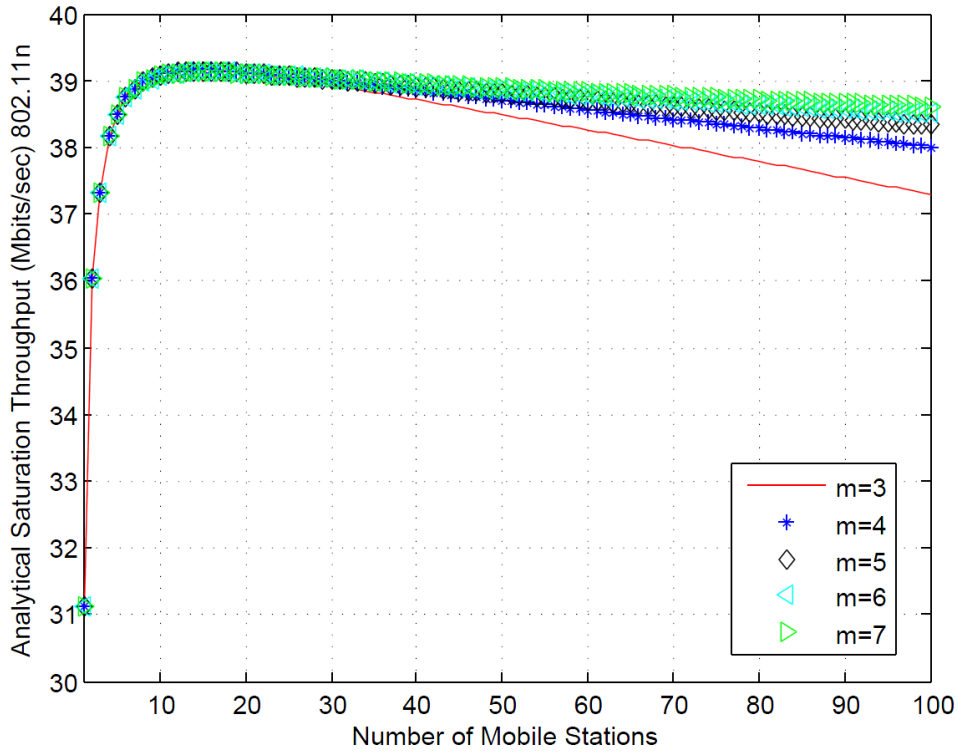


Figure 3.6: Saturation throughput for 2 RTS sub-channels based on the analytical model.

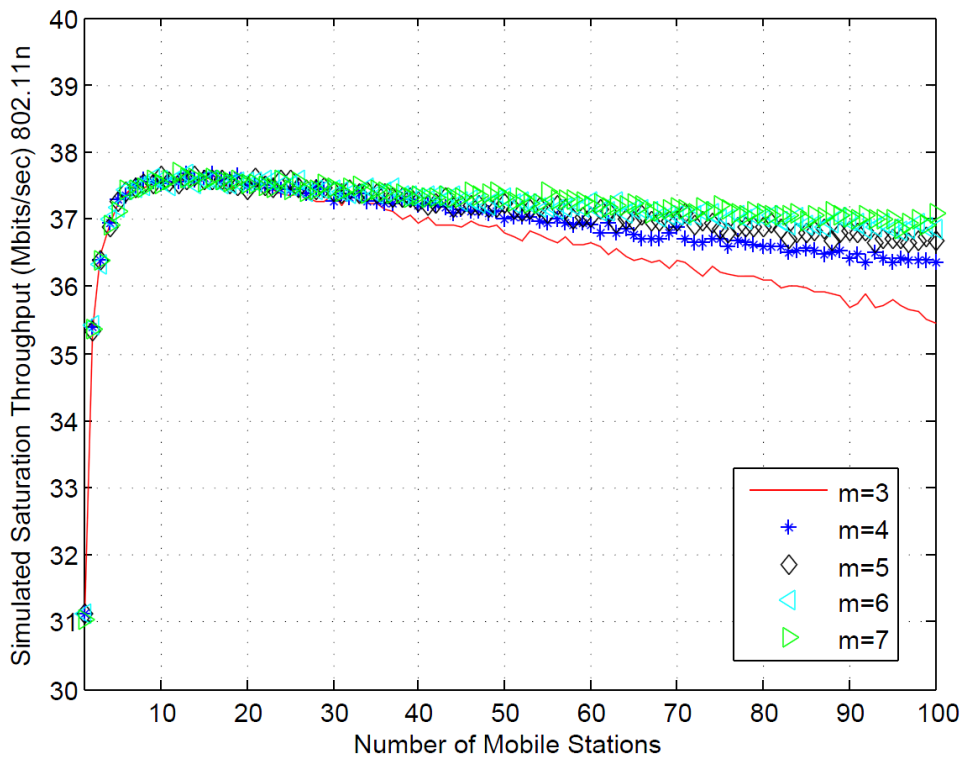


Figure 3.7: Saturation throughput for 2 RTS sub-channels based on simulation.

the simulated model is negligible (less than 5 %) and it is of the same order for the case of single channel. This error is due to the modeling assumptions since we considered that:

- For any given node, the probability of collision, p_i , is constant and independent of the node's collision history of the node and all other nodes.
- The probability of collision does not depend on the backoff stage at which the transmis-

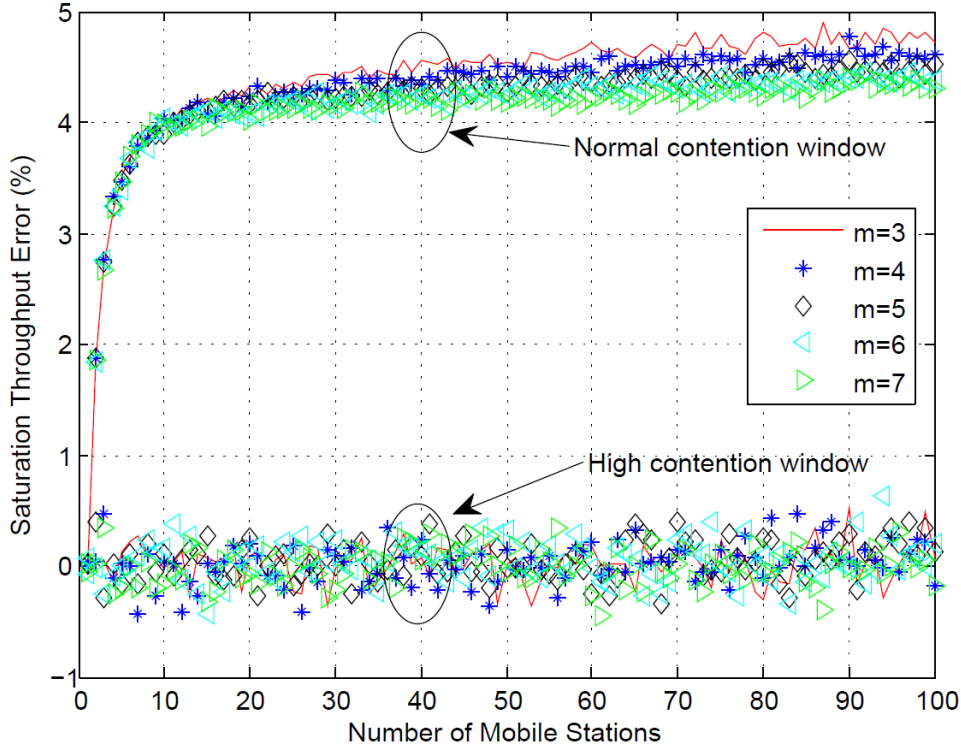


Figure 3.8: Error (%) between analytical model and simulation.

sion is made.

These assumptions may become true in the case of large minimal contention window and in the presence of huge number of mobile stations (based on the law of large numbers).

Note: simulation with high minimal contention window ($CW_{min} = 2^{20}$) was considered in the same conditions and the error converges to zero. The related curves are shown on figure 3.8 for different number of backoff stages and legended by 'high'.

3.5.2 Performance Discussion

Since the proposed model is validated in the previous sub-Section, we will evaluate its performance through different metrics. The M-CSMA/CA - RTS/CTS is compared to the reference single band protocol.

3.5.2.1 Metrics

The relevant metrics considered for protocol evaluation are collision probability, saturation throughput, transmission delay and packet drop probability.

3.5.2.1.1 Collision probability From MAC point of view, the collision probability is the probability that the packet transmitted by a node collides with another packet transmitted simultaneously from another node. For the case of single band CSMA/CA - RTS/CTS, the collision probability is the probability that two RTS messages coming from two different nodes collide. Considering the proposed protocol, a collision takes place if all the RTS transmitted over all the sub-bands are in collisions (more than one RTS over each sub-band). In fact once a collision happens, no CTS will be broadcasted.

3.5.2.1.2 Saturation throughput The saturation throughput is the bitrate in saturated conditions (since high number of nodes are considered to transmit huge amount of packets).

It means that the bitrate is computed considering that there is always at least one packet in the buffer of each node presents in the network. If the node buffers may be empty, we speak then about unsaturation mode. In the case of the CSMA/CA family protocols, the saturation throughput may be obtained by computing the ratio between the useful transmitted information (DATA) over a predefined time interval (the total duration needed to transmit this amount of DATA).

3.5.2.1.3 Transmission delay The transmission delay is the time needed to transmit a packet successfully. This duration contains the whole protocol procedure from sensing the channel idle until receiving the ACK.

3.5.2.1.4 Packet drop probability After each collision the contention window is doubled. When the contention window reaches the maximal contention window size (CW_{max}), this value of contention window will be considered for the next m transmission retries. If after this m retries the node collides, the packet will be rejected and the contention window will be updated by the minimal contention window size (CW_{min}). Then, the counter of rejected packet is increased by one. The packet drop probability is the ratio between the number of rejected packet over the total number of packets considered for transmission (rejected + transmitted).

3.5.2.2 System Evaluation

In this Section we will evaluate numerically the performance of the proposed protocol based on the metrics described above.

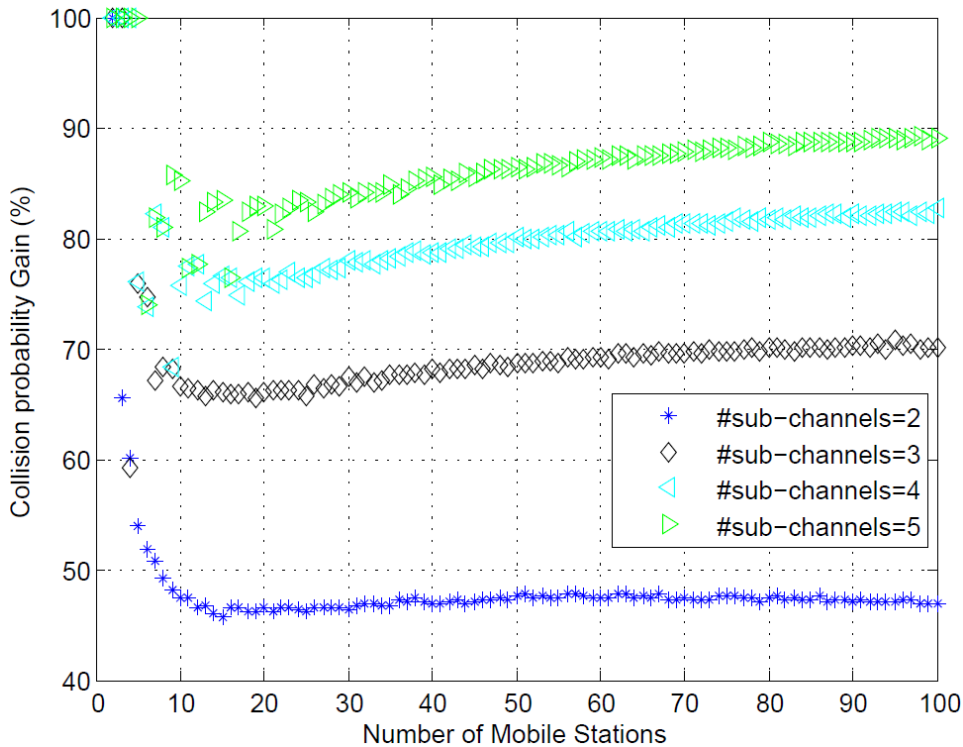


Figure 3.9: Collision probability gain vs. number of mobile stations for various number of RTS sub-channels.

3.5.2.2.1 Collision probability As mentioned above, the 802.11 standard suffers from RTS collisions. In order to clarify the advantages of the proposed protocol, it is interesting to

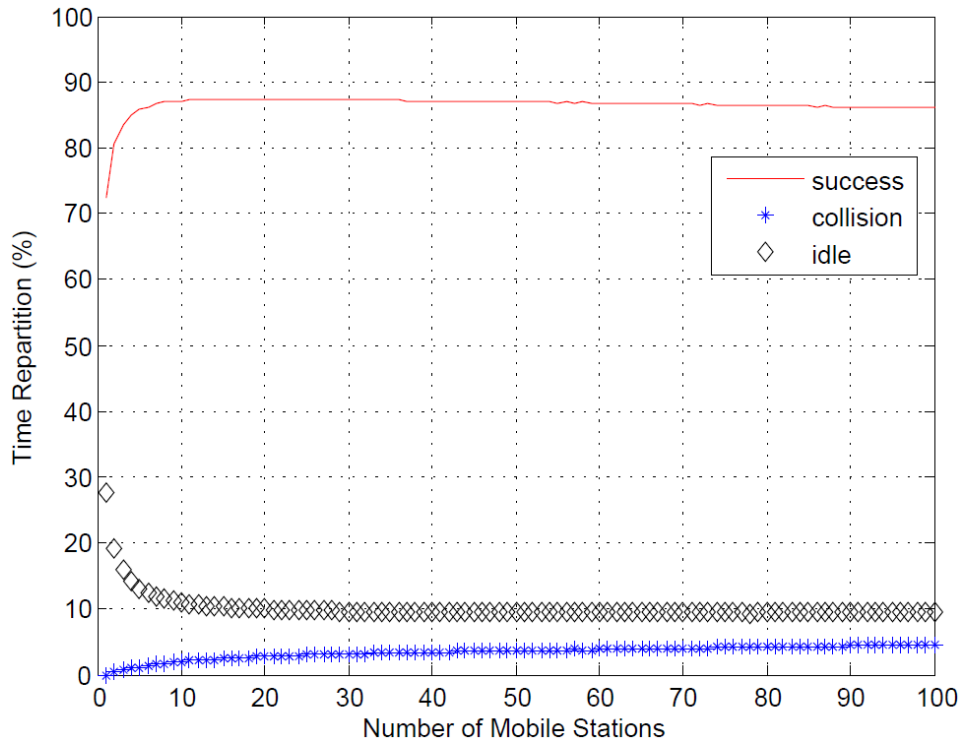


Figure 3.10: CSMA/CA - RTS/CTS time repartition vs. number of mobile stations for 3 RTS sub-bands.

compute the gain in terms of collision probability introduced by the proposed protocol regarding the state of the art (single channel). Figure 3.9 depicts the collision probability gain of the M-CSMA/CA - RTS/CTS protocol w.r.t. to that of the single channel protocol for several sub-channels numbers as function of the number of mobile stations. It is straightforward to notice that the gain increases significantly when the number of subchannels grows. Nodes have more opportunities to transmit on different sub-channels and hence collision probability is reduced. In loaded networks, since the RTS collision probability is very high, the proposed protocol performs very well to reduce dramatically the collision and hence the gain increases linearly. For instance, in the case of 50 nodes present in the network, a gain of 47.58% (86.35%) is achieved when two (five) sub-channels are considered.

3.5.2.2.2 Time Repartition Since collisions only occur on RTS packets ³, reducing the time period wasted in collisions is related to the reduction of the RTS collisions probability.

Based on the proposed protocol, Figures 3.10 and 3.11 depict the time repartition vs. the number of mobile stations for three and five RTS sub-bands. It is clearly seen that the multi-band protocol improves the proportion of time period passed in successful transmission and reduces significantly the time period wasted in collision and non-transmission (idle), especially for loaded network. For example, when 3 RTS sub-bands are considered with 100 nodes, the collision and idle proportions time period are reduced from (22%) to (5%) and from (20%) to (10 %) respectively. The time period spent in successful transmission is improved from (60%) to (87%). The difference between the success proportion is equal to the sum of the difference between the collision and idle proportions, hence the improvement in term of collision and idle (27%) are transformed to success. Moreover, increasing the number of RTS sub-bands leads to better time exploitation (see figure 3.11). Also, it is clearly showed that the time period wasted in collision and idle period decreases especially for loaded scenario. The proportion of success time period tends to 90% which indicates better channel usage. It is also shown that increasing the number of RTS sub-bands decreases the collision probability but the time

³In the case of perfect transmission.

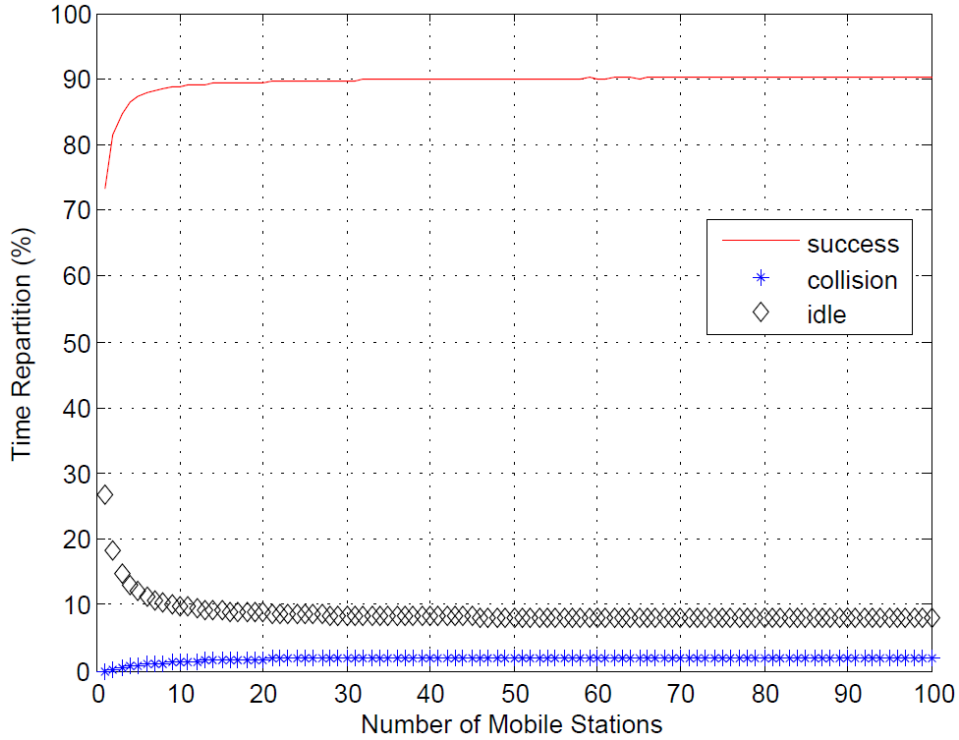


Figure 3.11: CSMA/CA - RTS/CTS time repartition vs. number of mobile stations for 5 RTS sub-bands.

period wasted in idle is quite the same (no major difference for the time period wasted in idle between the use of 3 and 5 sub-bands).

3.5.2.2.3 Saturation throughput Figures 3.12 and 3.14 depict the saturation throughput and its associated gain (equation 3.18) vs. the number of mobile stations presents in the network for various number of RTS sub-channels considering the case of infinite retry limit. Regardless the number of considered sub-channels, the proposed protocol performs always better; and better saturation throughput performance is achieved comparing to the single channel protocol (standard). In dense network (i.e. 50 nodes) the improvement is very important. Based on Figure 3.14, it is more useful to divide the transmission channel into two parts when the number of nodes is less than 20. If the number of nodes increases it becomes better to enhance the channel division. Until 100 nodes present in the network, 3 sub-channels may be enough to get best saturation throughput. For instance, using two sub-channels, the gain is about 10% (25%) for 20 (100) nodes present in the network. However the gain is 5% (30%) for 20 (100) nodes when the number of sub-channels is five. Hence, the proposed protocol introduces high gain in terms of saturation throughput especially in dense networks. Moreover, Figure 3.13 depicts the saturation throughput vs. the number of mobile stations for various number of RTS sub-channels with $m=r=3$ (finite retry limit case). It is shown that the saturation throughput with finite retry limit is lower than the infinite case, and it is due to the packets drop after $m + r$ retries.

3.5.2.2.4 Transmission delay The transmission delay is defined as the time needed to transmit a packet. In order to compare the delay between the two strategies, we extract from simulations the cumulative density function (CDF) of the transmission delay for one network scenario and for many users. We plot the results for CDF=99% in Figure 3.15 for various numbers of RTS sub-channels and many network load varying the number of node from 1 to 100. A delay of x second with CDF of 99% means that a packet should be delivered with a latency lower than x with a probability of 99%. Figure 3.15 depicts the transmission delay gain vs. the number of mobile stations for various number of RTS sub-channels. Despite of

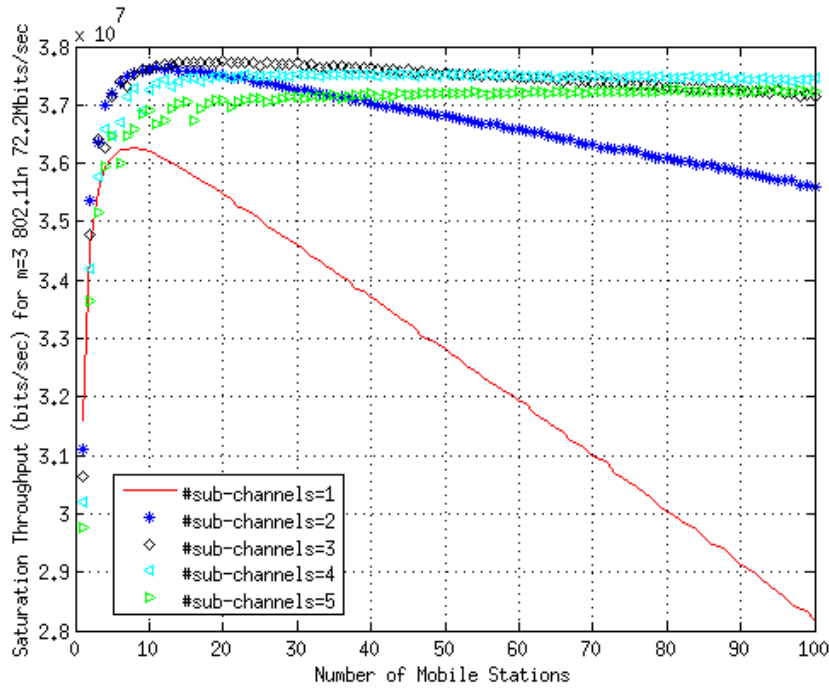


Figure 3.12: Saturation throughput vs. number of mobile stations for various number of RTS sub-channels.

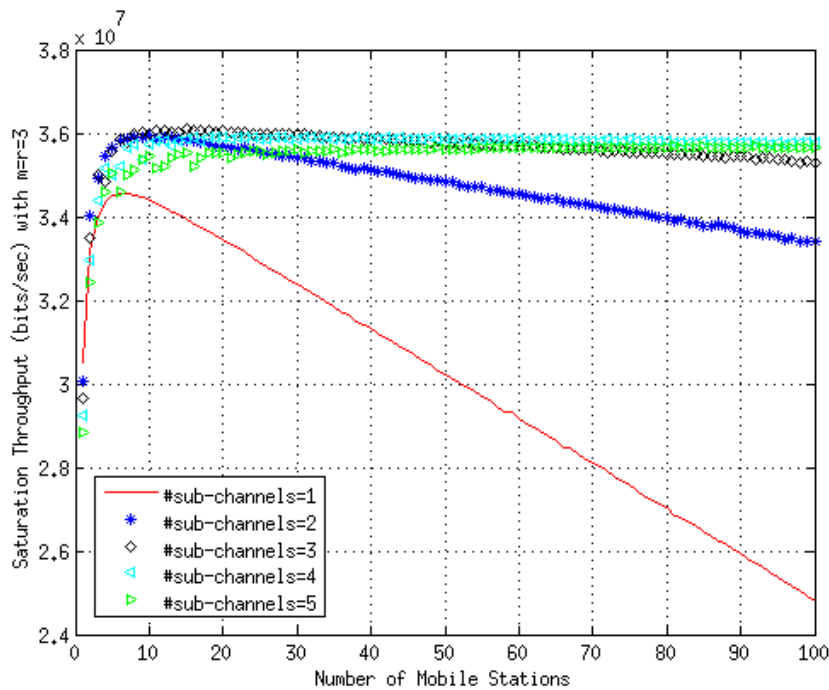


Figure 3.13: Saturation throughput (bits/sec) vs. number of mobile stations for various number of RTS sub-channels with $m=r=3$.

the extended duration of RTS messages due to the channel divisions, Figure 3.15 shows that the transmission delay gain is always positive. It means that the reduction in terms of collision probability is much more efficient comparing to the RTS message extension. The transmission delay gain increases with the number of mobile stations and the number of sub-channels. The gain is very high when the network is loaded (with 100 nodes and 4 sub-channels the gain is of 40%). We can also notice that 4 channels are sufficient for a network size up to 100 nodes.

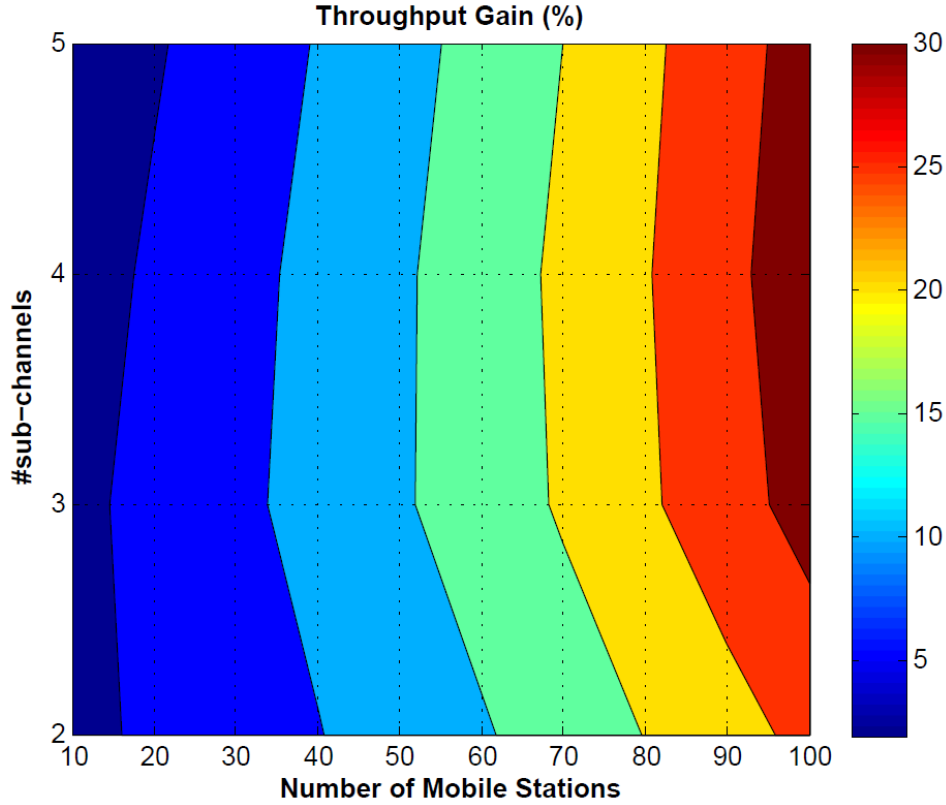


Figure 3.14: Saturation throughput gain vs. number of mobile stations for various number of RTS sub-channels.

As expected, this improvement is achieved because the collision probability is highly reduced.

3.5.2.2.5 Packet drop probability In this Section we simulate the packet drop probability (P_{drop}^{sim}) due to the rejection of packets. The P_{drop}^{sim} which is the ratio between the rejected packets and the total amount of packets to be transmitted (succeed+rejected) is expressed as follow:

$$P_{drop}^{sim} = \frac{R}{S + R} \quad (3.27)$$

where R and S stand for the rejected and succeed packets.

Figures 3.16, 3.17 and 3.18 depict the simulated packet drop probability for single, two and three sub-channels protocols as a function of the number of backoff stages for various maximum retry limits with 100 nodes present in the network. We define the maximum retry limit (r) by the maximum allowed time to stay in the last backoff stage ($CW=CW_{max}$).

Figures 3.16, 3.17 and 3.18 highlight that the number of rejected packets decreases when the number of backoff stages and the retry limit increases. This is due to the fact, that the transmitters have more chance to stay in the system when m and r become high. The P_{drop}^{sim} is approximately reduced by a factor of two (resp. three) when the number of RTS sub-channels is equal to two (three). Since the proposed protocol reduces collisions between transmitters (RTS collisions), the nodes have more chance to have success transmissions and hence the number of nodes with ($CW=CW_{max}$) is reduced. When the number of sub-channels increases, the number of collisions decreases which allows to achieve lower packet drop probability. Using more than three sub-channels doesn't introduce a significant added value because the network size is not very high. It should be mentioned that with network size up to 100 nodes, three sub-channels are enough to obtain the best tradeoff amelioration in terms of saturation throughput, transmission delay and packet drop probability.

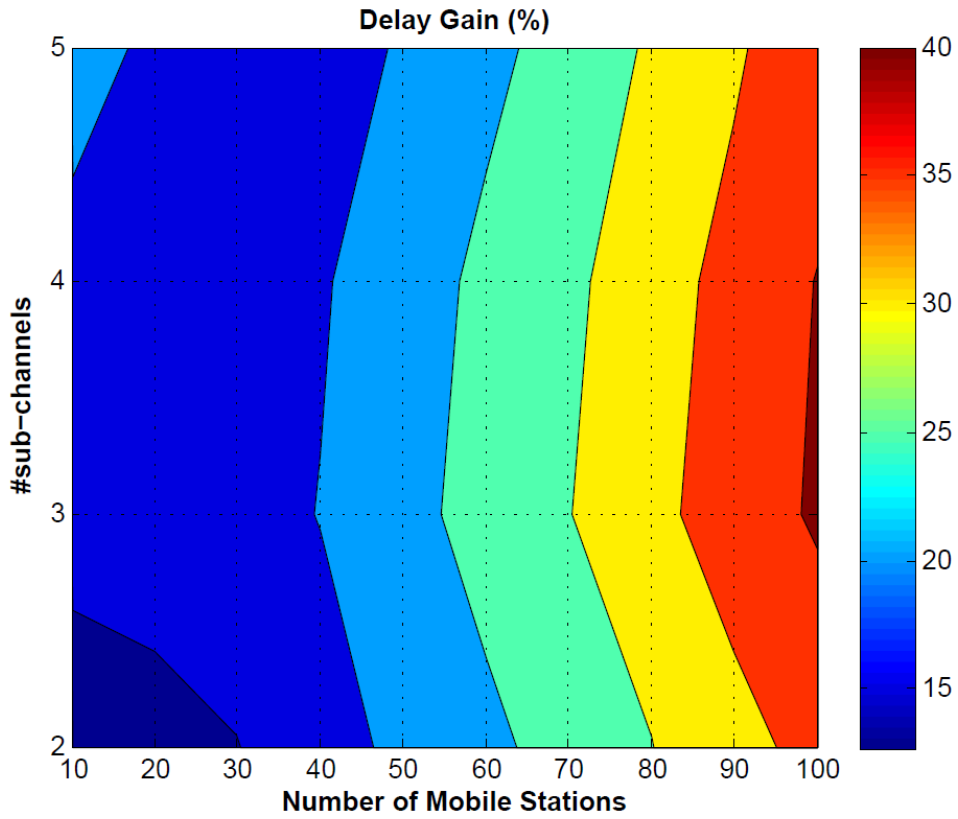


Figure 3.15: Transmission delay gain vs. number of mobile stations for various number of RTS sub-channels.

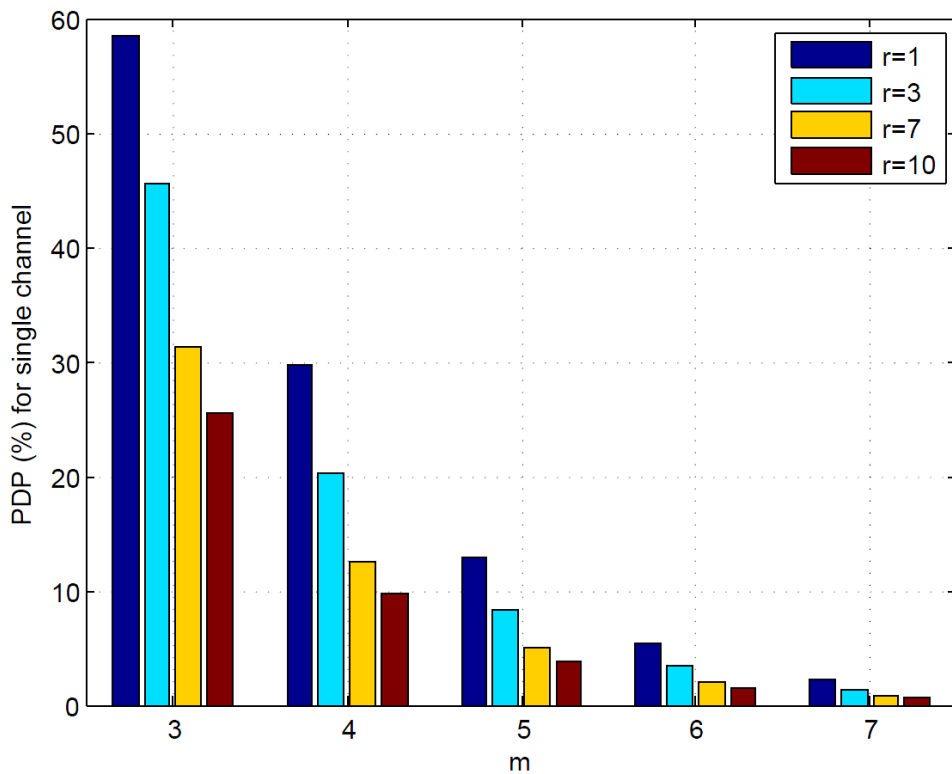


Figure 3.16: Packet drop probability for single channel vs. number of backoff stages for various retransmission limits.

3.6 Upper bounds

In order to understand how much the opportunistic protocols make us looser in terms of performance and to define the maximum achievable throughput that we can get by using

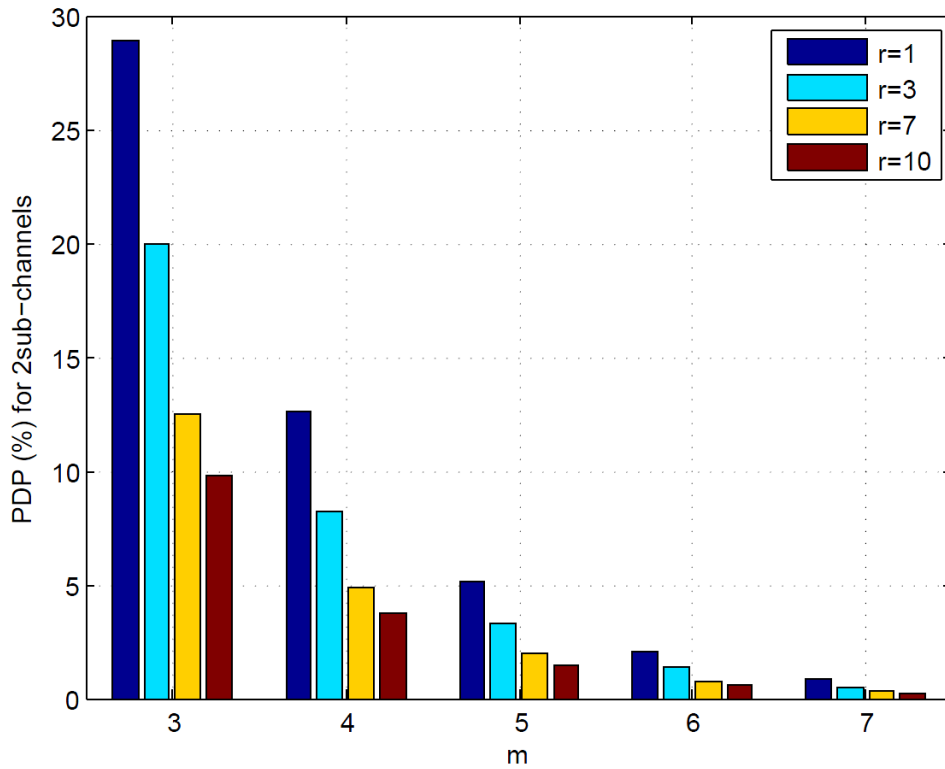


Figure 3.17: Packet drop probability for $\#sub\text{-channels}=2$ vs. number of backoff stages for various retransmission limits.

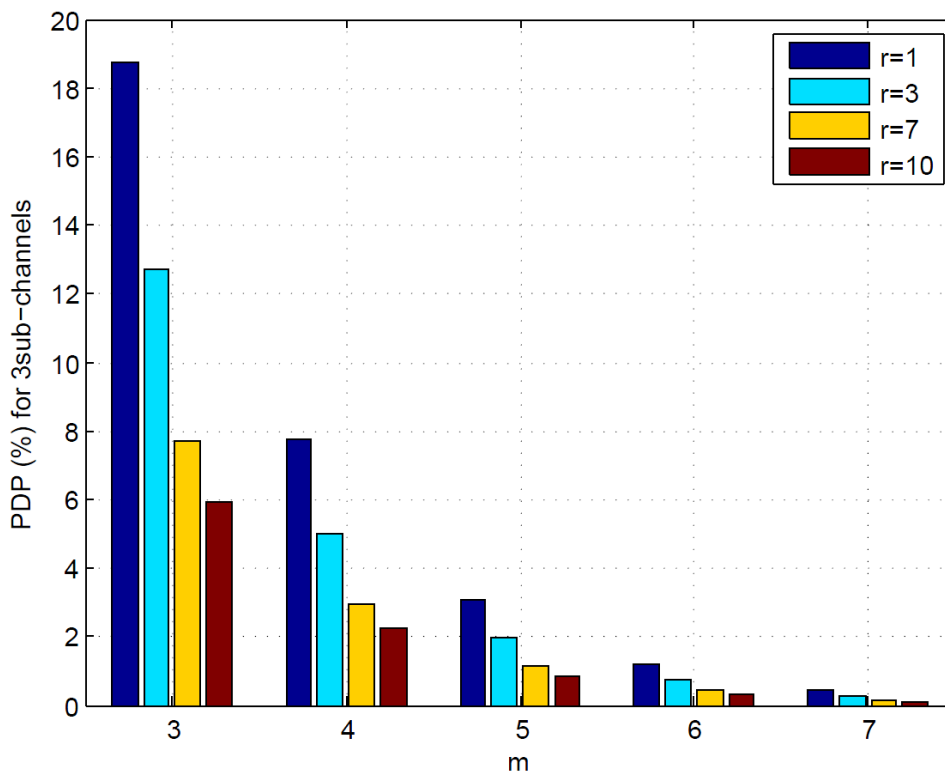


Figure 3.18: Packet drop probability for $\#sub\text{-channels}=3$ vs. number of backoff stages for various retransmission limits.

these protocols, we introduce in this Section the notion of MAC and PHY upper bounds. Full system performance discussion of the contention based MAC comparing to these upper bounds is also integrated. We define the Perfect transmission and Perfect hand shaking upper

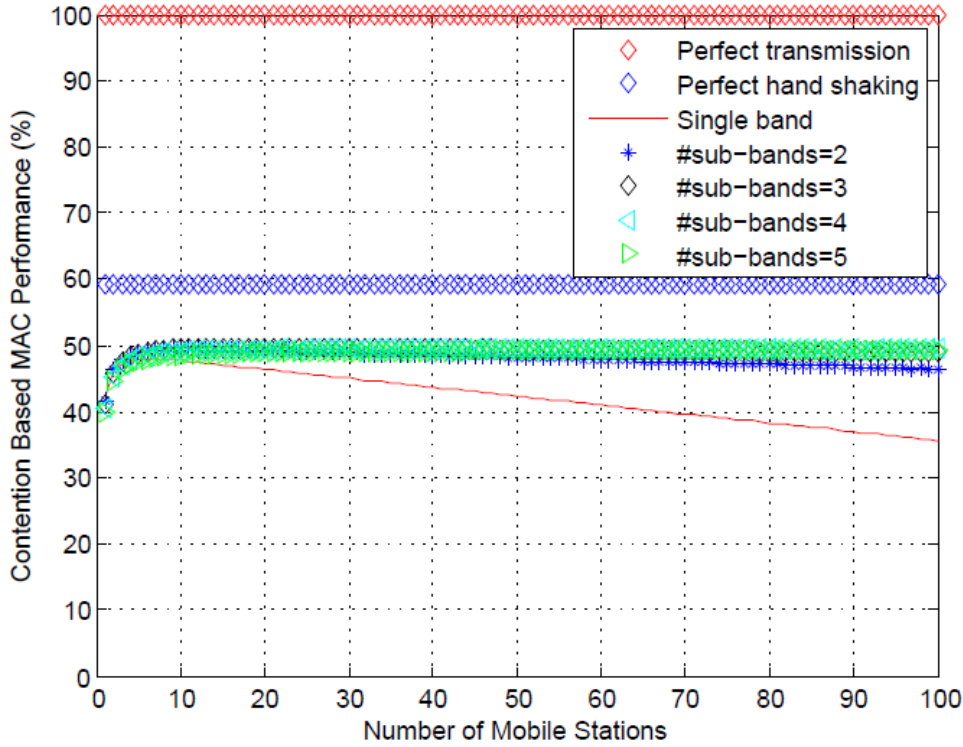


Figure 3.19: Contention Based MAC Performance.

bounds. A perfect transmission is a communication without any added overhead (no signaling, no synchronization, no reservation, no crc, ...). It is a transmission on the physical layer without any access mechanism and without any collision (kind of one user present alone in the network and it will always communicate successfully with the destination). Also, a perfect hand shaking communication refers to the achievable upper bound of the contention based protocol. It is a communication without using the backoff mechanism. Figure 3.19 depicts the normalized saturation throughput vs. the number of mobile stations. The curve related to perfect transmission will serve as a reference to compare the CSMA/CA protocols. A difference of 40% between the perfect transmission and perfect hand shaking is noticed due to the overhead introduced by the nature of the contention based protocol (RTS, CTS and ACK). Hence, with best and ideal communication strategies (no collisions), the maximum achievable performance based contention MAC could reach 60% of the perfect transmission performance. In fact, Figure 3.19 shows that using contention based protocols on a single channel, CSMA/CA - RTS/CTS introduces a 64% of loss in terms of throughput performance for loaded networks. However, such protocols could be adopted for many reasons: they allow to operate in an environment with an unknown number of devices with the entire available bandwidth [4], to operate in a distributed manner [5] and to lead to a cheaper deployment since they don't require much planning, interoperability and management complexity [6]. The investigated multi-channel CSMA/CA - RTS/CTS introduces a 48% of loss in terms of throughput performance for loaded networks. A gain of 16% is noticed regarding the single channel CSMA/CA - RTS/CTS. Also, the proposed multichannel protocol reaches the maximum achievable performance with 8% of difference when the considered number of sub-channels is equal to 5.

3.7 Allocation Methods

In this Section we study the difference between two allocation strategies. We consider a Pre-allocation and Postallocation strategies. As we discussed before, the preallocation technique

is based on a prior users' distribution over the free RTS sub-channels. It means that the total number of users present in the network is grouped into several groups where their number is equal to the number of sub-channel. Then, each group will be attached to a predefined sub-channel and the users belong each group will transmit their RTS over this sub-channel. So the number of RTS messages sent over each sub-channel is related to number of nodes inside the group which is associated to the sub-channel. Indeed, the repartition of nodes into groups is not necessary uniform and may depend on some quality of service (QoS). For instance, we can define different group repartition depending on the QoS. A group with high priority contains lower number of nodes than a group with a lower priority. Where no QoS is addressed, the node's repartition over the groups could be uniform.

Lets define by N_i the number of users preallocated to sub-channel i :

$$N_i = \beta_i \times N \quad (3.28)$$

where β_i is the proportion factor of users allocated to sub-channel i with $\sum_{i=1}^n \beta_i = 1$.

In the case of uniform repartition, the groups will contain the same number of nodes. Then, all the proportion factors are equal to the inverse of the considered number of sub-channels.

$$\forall i \in n, \beta_i = \frac{1}{n} \quad (3.29)$$

The Postallocation technique remains on a random choice of sub-channels for RTS transmission. In that case, the total number of users present in the network are seen as one group and when a node wants to transmit its RTS message, it will choose randomly a sub-channel. Then, the RTS message will be transmitted over the chosen sub-channel. With a random allocation strategy, a node ready to transmit chooses randomly a sub-channel based on a uniform probability law. So let's consider that a user chooses a sub-channel i with a probability α_i . When the number of users tends toward infinity, the probability to choose a sub-channel becomes equal to the proportion factor in the case of uniform repartition ($\lim_{N \rightarrow \infty} \alpha_i = \beta_i$). Hence, both allocation strategies become equivalent. To show that both allocation strategies are asymptotically equivalent, we consider the case of uniform users repartition through sub-channels.

Figure 3.20 depicts the saturation throughput difference (%) between Preallocation and Postallocation techniques vs. the number of mobile station for various number of sub-channels. It is clearly seen that difference converges to zero when the number of nodes present in the networks increases.

3.8 Conclusion

In this chapter, we proposed a novel strategy based on multichannel CSMA/CA-RTS/CTS (M-CSMA/CA-RTS/CTS) which is characterized by dividing a band into sub-channels of known size. The proposed protocol is studied with mathematical modelling and simulations. We proved that the proposed MAC is able to achieve a very high gain in terms of saturation throughput, transmission delay and packet drop probability especially in dense networks. For instance, when considering 3 RTS sub-channels with 100 nodes, we can achieve 70% of gain in terms of collision probability, 30% in terms of saturation throughput and 40% in terms of transmission delay. The packet drop probability is divided by 3 as well. This proposed protocol is very adapted for crowded scenarios with opportunistic access. It could be suitable for M2M scenarios in dense metropolitan or regional networks.

We also compute the upper bounds of opportunistic protocols and we prove that the performance of the proposed protocol becomes closer than the single band CSMA/CA - RTS/CTS to this achievable bound. The proposed protocol reaches the maximum achievable contention

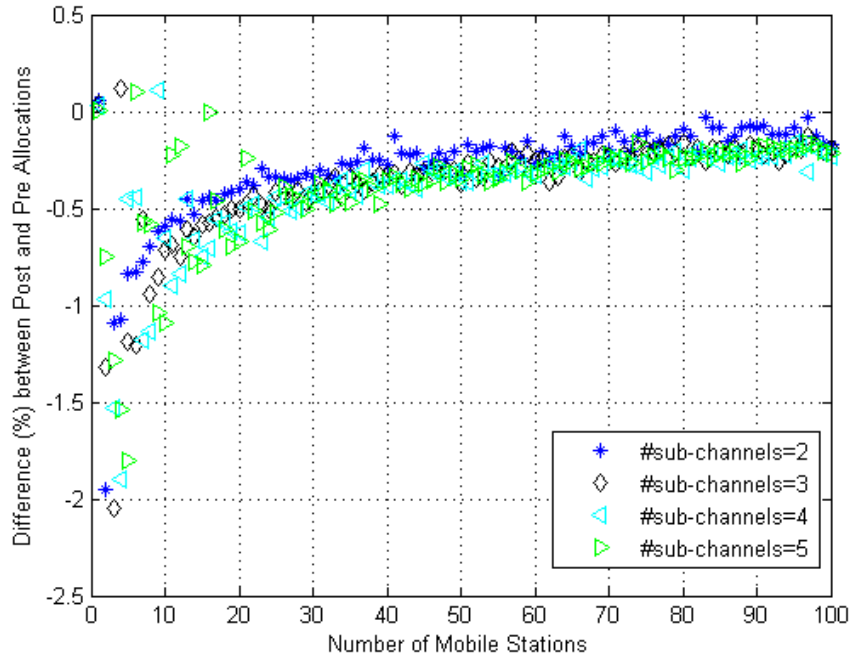


Figure 3.20: Saturation throughput difference (%) between Pre and Postallocation techniques vs. the number of mobile station for various number of sub-channels.

based MAC performance with 8% of difference.

Then, we compare two allocation strategies and we prove that the Preallocation technique with uniform repartition of nodes becomes asymptotically equivalent to the Postallocation strategy when the number of nodes towards to infinity.

To conclude, in this chapter we proposed a new protocol to enhance the MAC layer, but still to find an original technique to schedule the nodes and to serve many winners in order to reach the achievable MAC upper bound which will be the objective of the next chapter.

Chapter 4

Scheduled M-CSMA/CA - RTS/CTS

4.1 Introduction

According to the multiband CSMA/CA-RTS/CTS invoked in the previous chapter, when many RTS messages may be decoded by the AP, the AP can serve only one user which win the channel access and transmit its packets. The non-served users loose the channel access, and have to retry with another RTS transmission after revoking a new backoff procedure. This procedure force the non-served user to transmit a new RTS message and wait for a new CTS message which causes a high MAC overhead. To solve this issue, we propose in this chapter a new strategy which consists to serve many users once the CTS is detected by the transmitters. A scheduler is introduced in the AP and the number of served nodes depends on its size. The maximum number of scheduled nodes is equal to the scheduler size. The strategy is described in Section 4.2. The scheduling technique is evaluated in Section 4.3 and a full MAC performance study is addressed in Section 4.4. Finally Section 4.5 is reserved for conclusion.

4.2 Description

Without loss of generality, we consider the scenario in which many nodes would transmit some packets to an AP. Considering a symmetrical and ideal channel with RTS/CTS mechanism, behind the loss in terms of RTS collision, MAC overhead significantly reduces the system performance. In fact, the RTS and CTS messages introduce a high overhead which makes the system suboptimal. In the case of multiband protocol which is proposed in the previous chapter, many RTS messages may be decoded by the AP simultaneously. For that, it will be interesting to implement a polling mechanism which serves many nodes one after the other¹. The proposed strategy is based on CSMA/CA protocol with RTS/CTS techniques. The corresponding flow chart is depicted in Figure 4.1. According to this strategy, a source node wishing to transmit data should first apply the multiband protocol proposed in the previous chapter. When the RTS is transmitted by the node, the AP decodes the RTS messages and replies with the CTS message which contains the information about the winners (transmitters who gain the channel access). Depending on the priority, the winner either transmits directly (once the CTS is received) or it waits its turn to transmit data over the complete frequency bandwidth. An ACK is transmitted by the AP if the data is successfully decoded.

In the case of finite retransmission limit, the related flow chart is depicted in Figure 4.2, a retry counter per node is incremented after each collision happened at the last backoff stage ($CW = CW_{max}$). After each collision this counter is compared to a define limit in order to decide if the packet should be rejected or not. A packet is rejected when the counter value passes the limit (allowed retry transmission at the last backoff stage).

¹the node for which RTS message does not collide

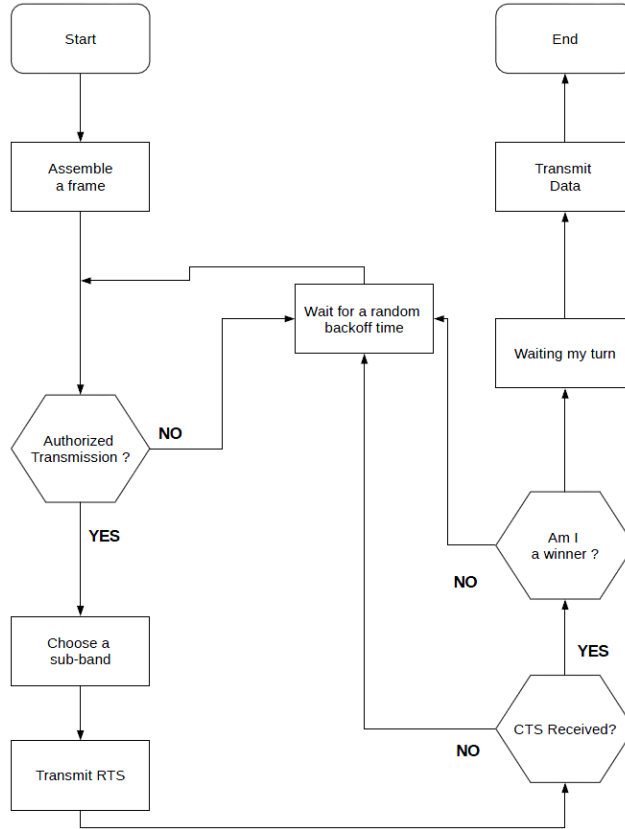


Figure 4.1: Flow chart of the proposed strategy.

Let's consider a simple example composed of four STAs ready to transmit (backoff=0), STA0, STA1, STA2, STA3 and an AP. We illustrate in Figure 4.3 the considered scenario in the case of the proposed strategy. STA1 and STA2 choose the first and third sub-bands respectively. STA0 and STA3 choose the second band. All the nodes, send their RTS messages on the chosen sub-bands. Therefore, the AP detects RTS message from the STA1 and STA2 but it is not able to decode the RTS on sub-band 2 due to collision. The AP chooses to serve the STA1 before STA2 and it broadcasts the CTS message over all the sub-bands. The nodes choice may be random or not (depends on some predefined priority). The number of nodes that could be served by the AP depends on the size of the scheduler. In that case, the scheduler size is equals to two (maximum two nodes can be served successively). All the nodes receive and decode the CTS and only STA1 and STA2 are allowed to transmit. Once the ACK for STA1 is received, the channel becomes clear and STA2 will be authorized to send DATA. The ACK for STA2 is broadcasted indicating successful transmission and the channel becomes free for a new backoff procedure. The proposed strategy allows to serve transmitters successively with reducing the RTS collision and reducing the overhead introduced by the control messages (RTS and CTS) and the backoff. However, it should be mentioned that dividing the band into n sub-bands with bandwidth equals to F/n imposes a duration extension of the RTS messages with factor equals to n . Hence, if T is the duration of the original RTS message, $n \times T$ will be the duration of the extended RTS message ².

The proposed CTS frame format is presented in Figure 4.4 in which an additional field was introduced to indicate the authorized nodes able to transmit data. The size of the authorized band field is equals to 3 bytes which may be divided into 6 blocks of 4 bits. Each block corresponds to a band index. If the block value is 0, it means that the block is not assigned to any band. The priority starts from the right to the left. This field can support up to 15

²Introducing a real physical layer could relax this equality to become more optimistic. Due to mapping and coding blocks the time needed may be lower than $n \times T$. This effect will be discussed in Chapter 5.

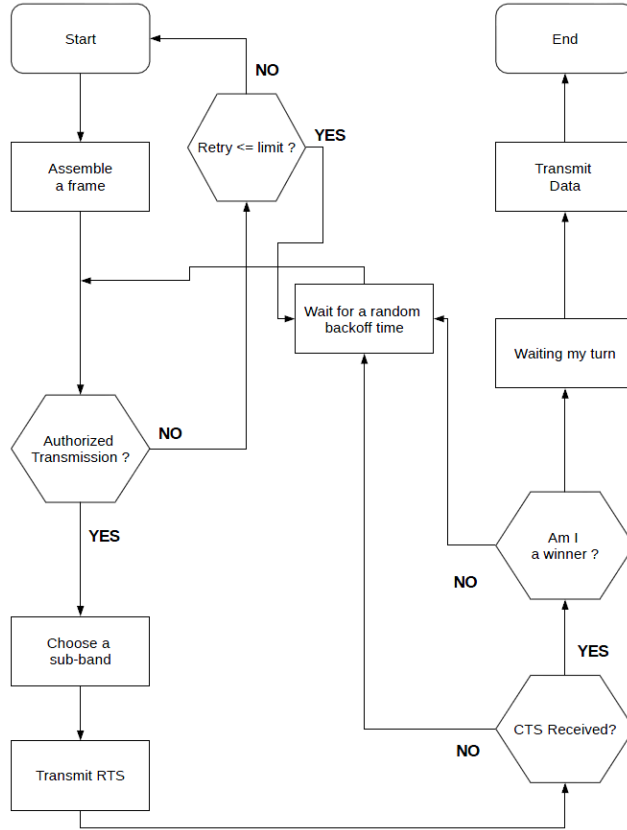


Figure 4.2: Flow chart of the proposed strategy.

sub-bands and serve at most 5 nodes successively. In this case, the authorized band field (00 00 21) indicates that the STA1 is prior to the STA2, hence after the CTS reception the STA1 transmits its packet and waits for acknowledgement.

4.3 Performance Analysis

In this Section, we study the time repartition, saturation throughput, transmission delay and the packet drop probability for the proposed strategy and the related gain compared to the single band and to the multiband protocols in the case of finite and infinite retransmission cases. The scenario of one AP and many nodes is considered for simulation with the same channel parameters as the previous chapter. The minimal and maximal contention window (CW_{min} , CW_{max}) have been chosen constant and equal to 16 and 128 respectively. It is worth mentioning that as the study focuses on the MAC mechanisms, an ideal physical layer (no path loss, no fading, no shadowing, ...) is considered.

4.3.1 Time Repartition

To demonstrate the benefits of the proposed strategy, its time repartition should be analyzed. Figure 4.5 depicts the time repartition vs. the number of mobile stations for 5 RTS sub-bands with scheduler size=2. Comparing Figure 4.5 to the case of multiband proposed in the previous chapter, the time period wasted in collision is the same. As expected the proposed enhancement do not reduce the collision probability. However the time period wasted in idle is decreased by 4% to reach 6% and the time period spent in success transmission is improved by 4% as well to reach 94%. Hence, adopting the overhead reduction strategy we achieve 4% of gain in terms of time spent in successful transmission for loaded network.

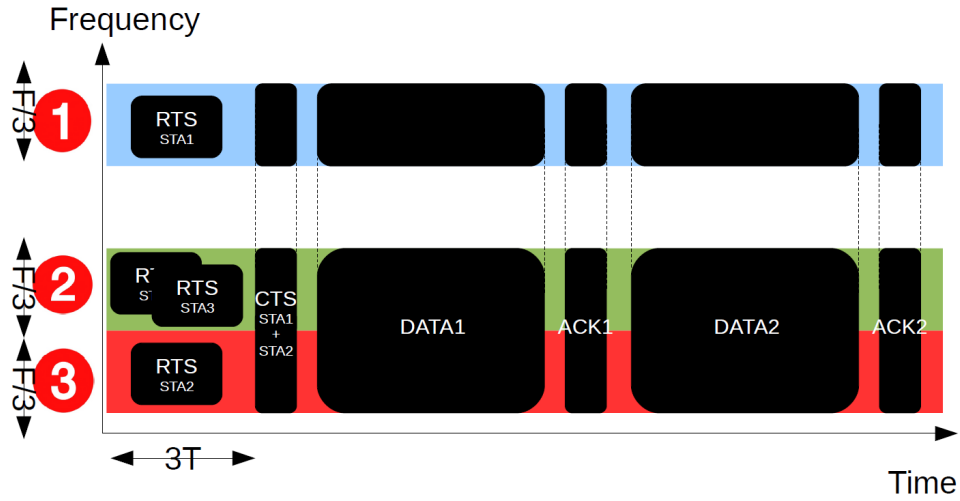


Figure 4.3: Scheduled multiband CSMA/CA with RTS/CTS mechanism with scheduler size=2.

Frame Control	Duration	Receiver Address	Authorized Band	Frame Check
2 byte	2 byte	6 byte	3 byte	4 byte

Figure 4.4: CTS frame format.

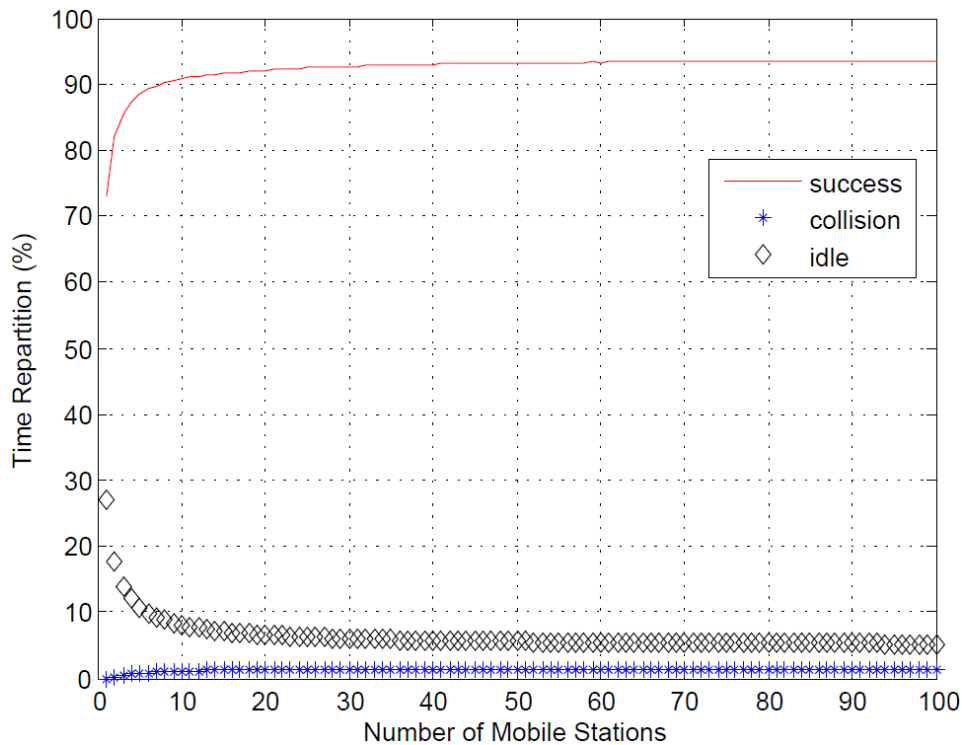


Figure 4.5: CSMA/CA - RTS/CTS time repartition vs. number of mobile stations for 5 RTS sub-bands with scheduler size=3.

4.3.2 Saturation Throughput

In this Section, the throughput of the proposed strategy is evaluated under the saturation conditions (each node has at least one packet ready for transmission) considering a retry limit

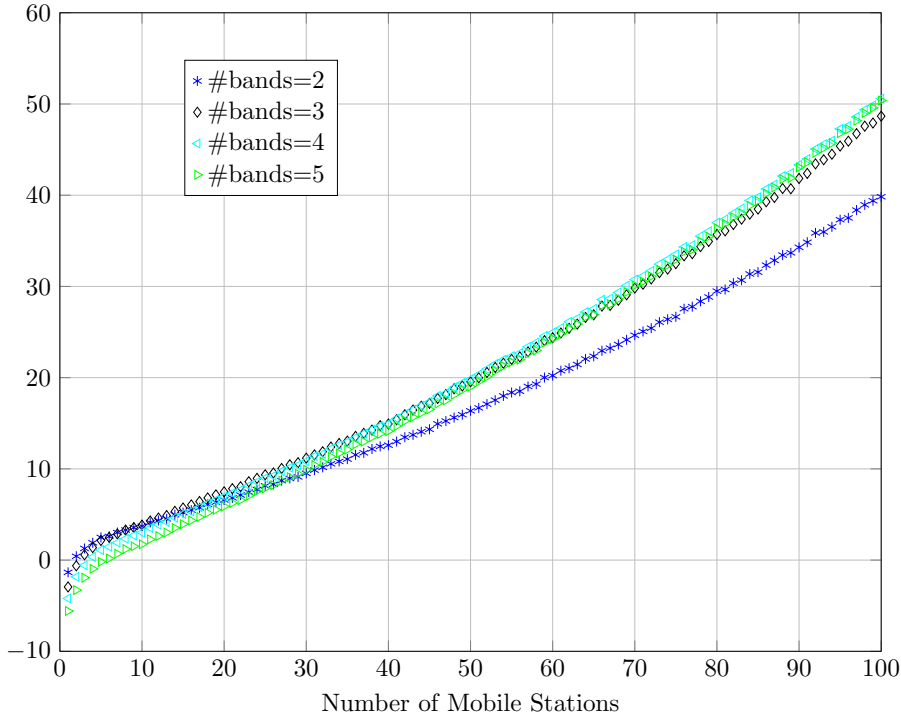


Figure 4.6: Saturation Throughput Gain (%) vs. number of nodes for scheduler size=1.

equals to 3. Figure 4.6, 4.7 and 4.8 depict the saturation throughput gain between the single and multiband protocols vs. the number of mobile stations for various number of RTS sub-bands and scheduler sizes. As expected, the gain is more important when the number of RTS sub-bands is high and especially in the case of loaded networks. This improvement is due to the reduction of the RTS collision probability thanks to the division of the RTS band. Moreover, the use of scheduler sizes greater than one can improve the saturation throughput gain. This is due to the possibility to serve many stations (which correspond to the successful transmitted RTS) without revoking a new backoff procedure (without introducing more overhead). For example, in the case of 5 RTS sub-bands and 50 active nodes, the saturation throughput gain is 20%, 38% and 42% for scheduler size equals to one, two and three. Also, Figures 4.7 and 4.8 show that the gain is the same when the number of RTS sub-bands is lower or equal to the scheduler size (for example: 2 RTS sub-bands with scheduler size equals to two or three). Hence, there is no need to use scheduler sizes larger than the number of RTS sub-bands because a system with n sub-bands can serve at most n nodes one after the other (in the case of non RTS collisions).

Moreover, it is clearly seen that the gain is negative in the case of unloaded networks (number of nodes is less than 5). It can be explained by the fact that RTS message duration is larger if the bandwidth is reduced (the original RTS duration is multiplied by the number of sub-bands to maintain the same quantity of information) which introduces more overhead not amended with the reduction of collision probability.

In the case of infinite retransmission limit, Figures 4.9, 4.10 and 4.11 show that the saturation throughput gain is 17%, 33% and 40% for scheduler size=1, scheduler size=2 and scheduler size=3 respectively. Indeed, when the retry limit tends to infinity the gain becomes lower since the nodes will retry more to transmit which cause more collisions.

Finally, it was showed that the proposed scheduling technique for the M-CSMA/CA-RTS/CTS improves the saturation throughput. The gain becomes higher when the scheduler size is greater due to the reduction of the number of contentions.

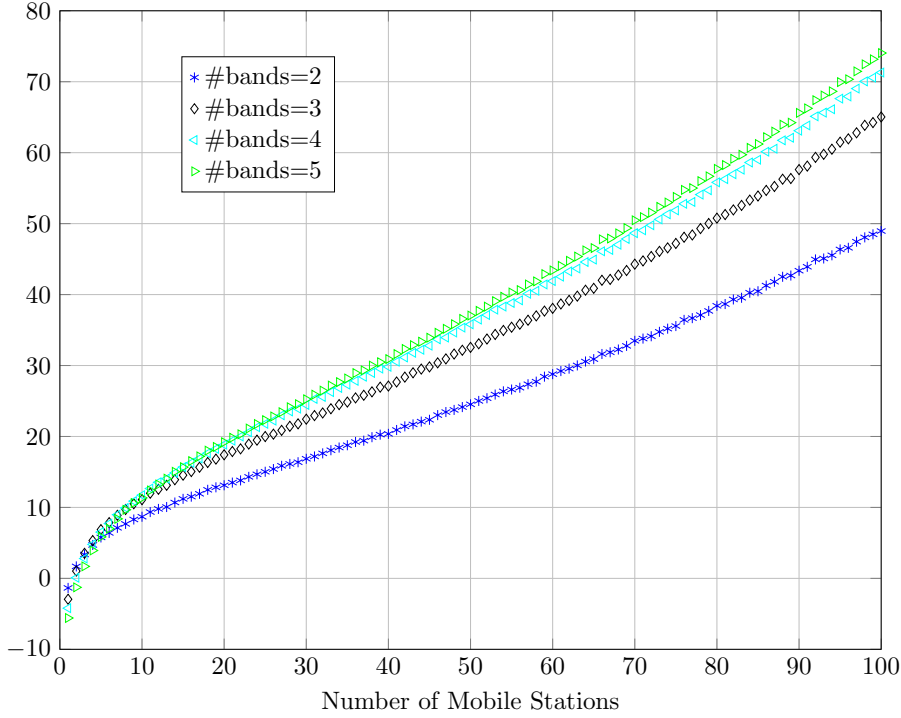


Figure 4.7: Saturation Throughput Gain (%) vs. number of nodes for scheduler size=2.

4.3.3 Transmission Delay

In order to show the effect of the proposed technique, we propose to study the gain in terms of transmission delay between the proposed strategy and the single band protocol for various scheduler size. The transmission delay is defined as the time needed to transmit a packet. In order to compare the delay between the two strategies, we extract from simulation the cumulative density function (CDF) of the delay for various number of nodes. We have plotted the results for a CDF of 99% on Figures 4.12, 4.13 and 4.14 for various number of RTS sub-bands and various number of nodes from 1 to 100 with scheduler sizes equal to 1, 2 and 3 respectively. Despite of the extended duration of the RTS messages due to the RTS band division, These results demonstrate that the delay gain is always positive. It means that the reduction in terms of collision probability is much more efficient comparing to the time extension of the RTS messages. Also, when the size of scheduler is greater than two, the delay gain is more important especially in loaded networks and it is due to the capability to serve many nodes without waiting for next backoff round. Hence, nodes are served one after the other with lower MAC overhead (avoiding losing time due to RTS, CTS and backoff). For instance, considering the case of 50 nodes present in the network with 5 RTS sub-bands. The gain is 17%, 27% and 30% when the scheduler size is equal to 1, 2 and 3 respectively.

Finally, the transmission delay is better when the scheduler size is greater especially for dense scenarios.

4.3.4 Packet Drop Probability

In this Section we analyze the packet drop probability (PDP) for the single band and multiband scenarios for various number of sub-bands and retry limit (r) in the case of 100 nodes present in the network. Figures 4.15, 4.16 and 4.17 depict the packet drop probability (PDP) vs. the number of sub-bands for scheduler size equals 1, 2 and 3 respectively. These figures highlight that the PDP decreases when the value of the retry limit and the number of sub-bands increases. For instance, the PDP is equal to 58% (14%) with $r = 1$ and it will be reduced to 26% (5%) when $r = 10$ for single band (four RTS bands). When the scheduler size

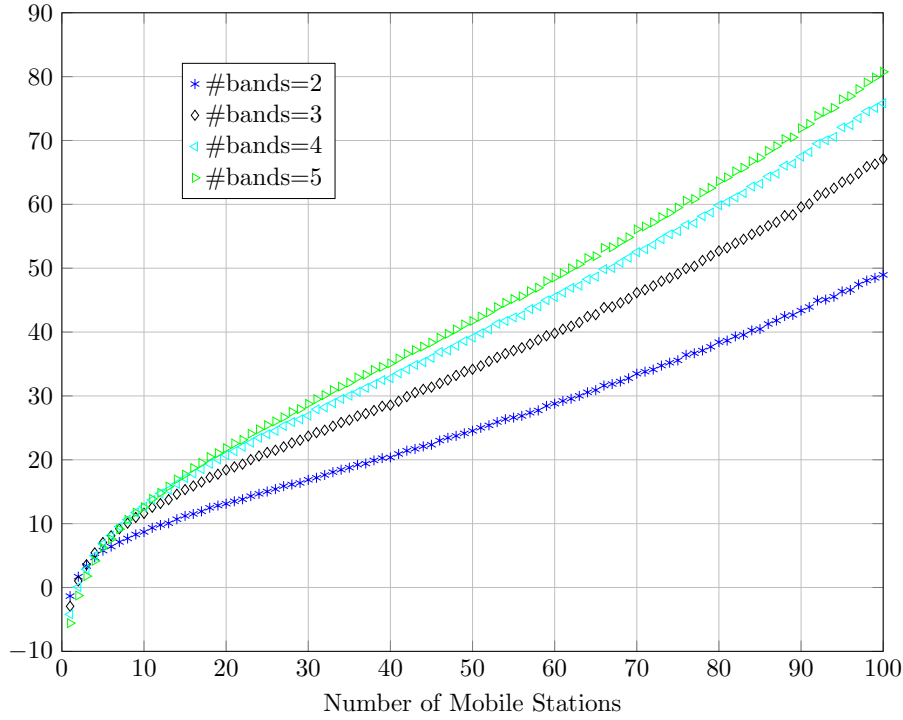


Figure 4.8: Saturation Throughput Gain (%) vs. number of nodes for scheduler size=3.

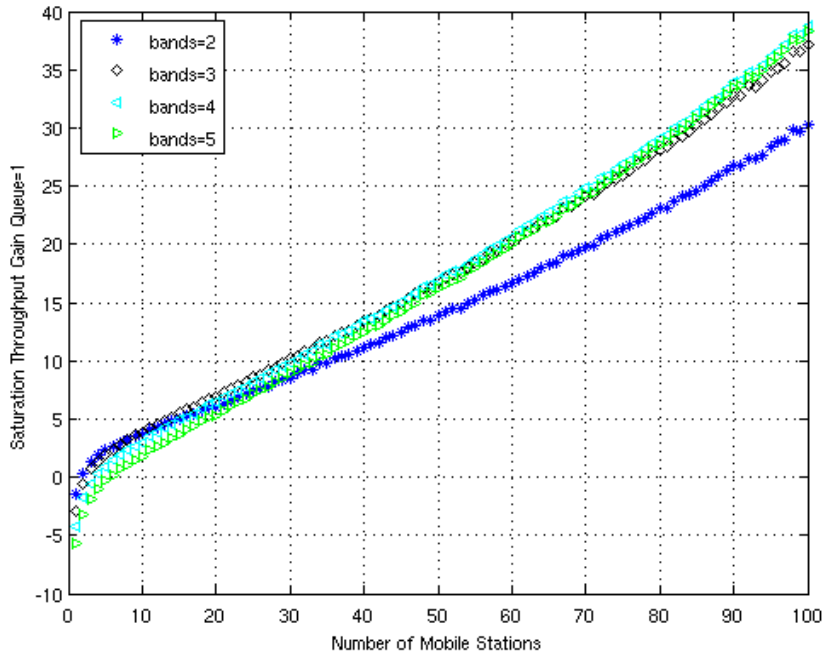


Figure 4.9: Saturation Throughput Gain (%) vs. number of nodes for scheduler size=1.

is greater than or equal to the number of RTS bands, the PDP will be reduced effectively. For the case of 4 RTS bands and $r=1$, the PDP is equal to 14% (10% and 9%) when the scheduler size is equal to 1 (2 and 3). Also, it should be mentioned that there is no need to use scheduler sizes larger than the number of RTS sub-bands (same PDP when using single band for whatever scheduler sizes) because a system with n sub-bands can serve at most n nodes successively (in the case of non RTS collisions). Finally, the proposed strategy helps to reduce drastically the packet drop probability by serving many winners successively.

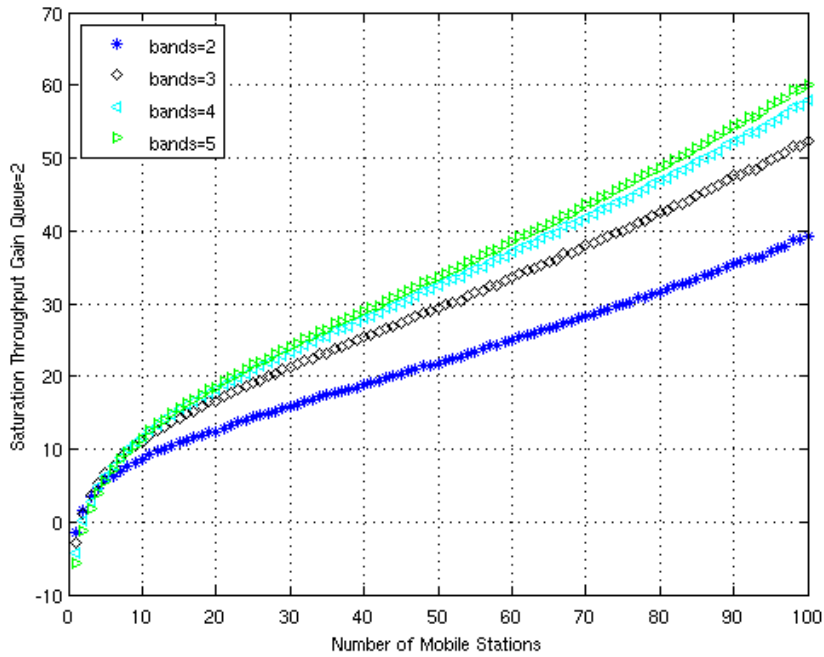


Figure 4.10: Saturation Throughput Gain (%) vs. number of nodes for scheduler size=2.

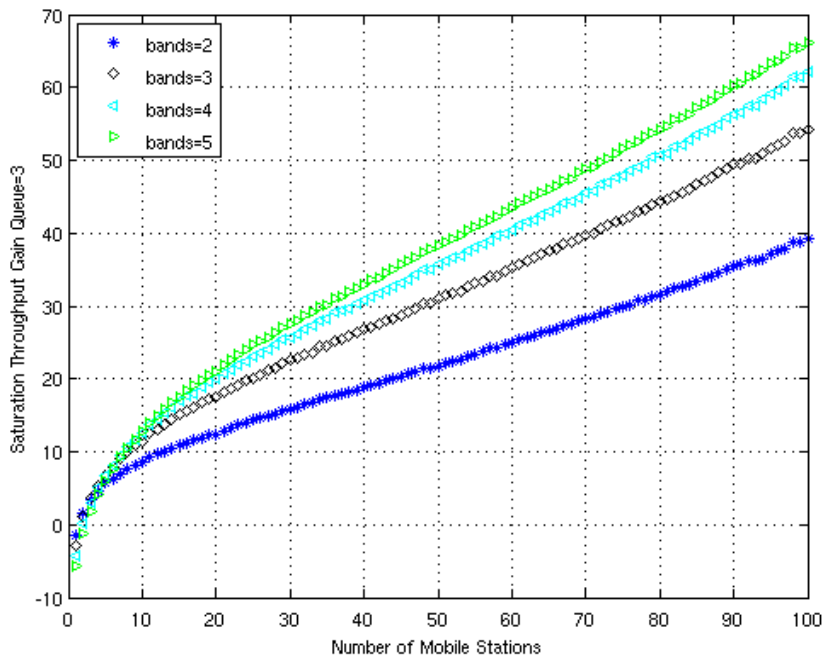


Figure 4.11: Saturation Throughput Gain (%) vs. number of nodes for scheduler size=3.

4.4 Upper bounds

In this Section we investigate the normalized saturation throughput of the scheduled M-CSMA/CA-RTS/CTS strategy and we compare its performance to the PHY and MAC asymptotic throughput already presented in the previous Chapter. Figure 4.18 depicts the normalized saturation throughput vs. the number of mobile stations. Rather than the normalized saturation throughput related to the single band CSMA/CA-RTS/CTS, the normalized saturation throughput of the proposed technique with 5 RTS bands and various scheduler sizes

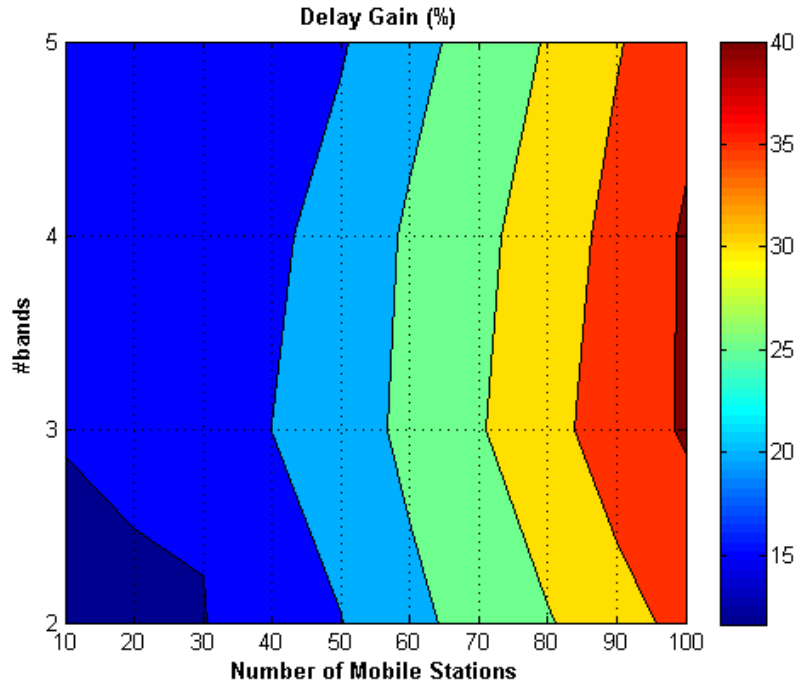


Figure 4.12: Delay Gain (%) vs. number of nodes for various number of sub-bands with scheduler size=1.

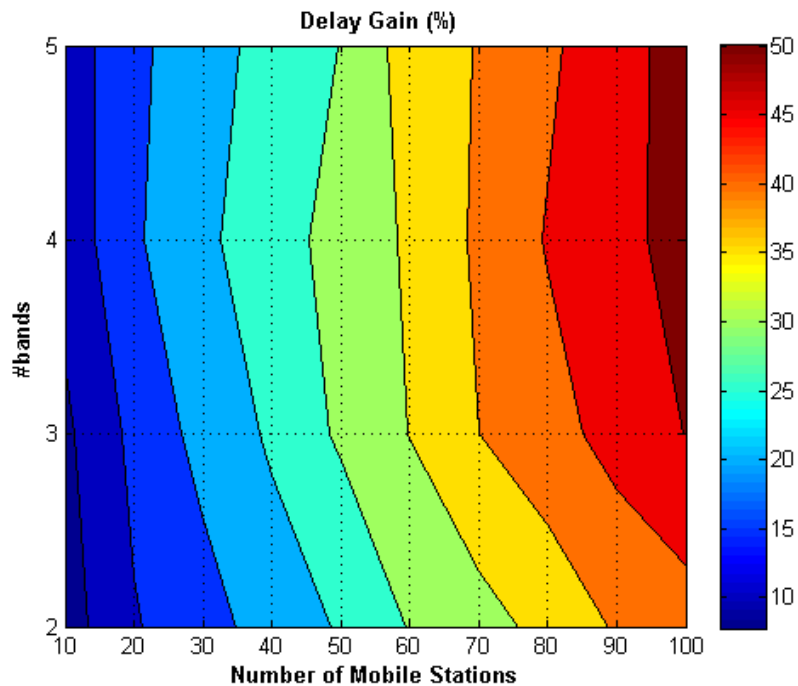


Figure 4.13: Delay Gain (%) vs. number of nodes for various number of sub-bands with scheduler size=2.

are shown on the same figure. However, as mentioned previously, such protocols could be adopted for many reasons: they allow to operate in an environment with an unknown number of devices with the entire available bandwidth [4], operate in distributed manner [5] and leads to a cheaper deployment since they don't require much planning, interoperability and management complexity [6]. Results demonstrate that for loaded network it is possible to achieve the MAC asymptotic throughput bound by considering 5 bands and scheduler size equals to 3.

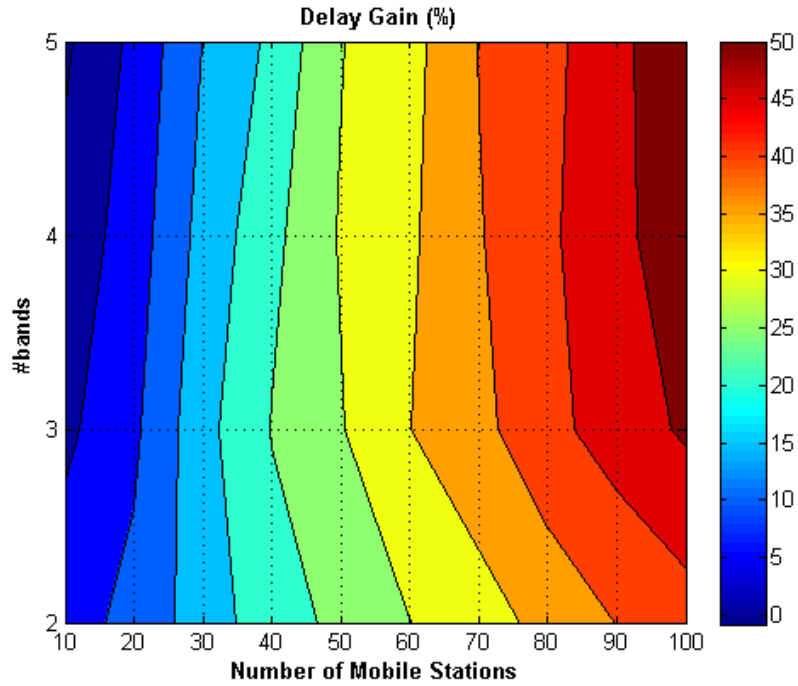


Figure 4.14: Delay Gain (%) vs. number of nodes for various number of sub-bands with scheduler size=3.

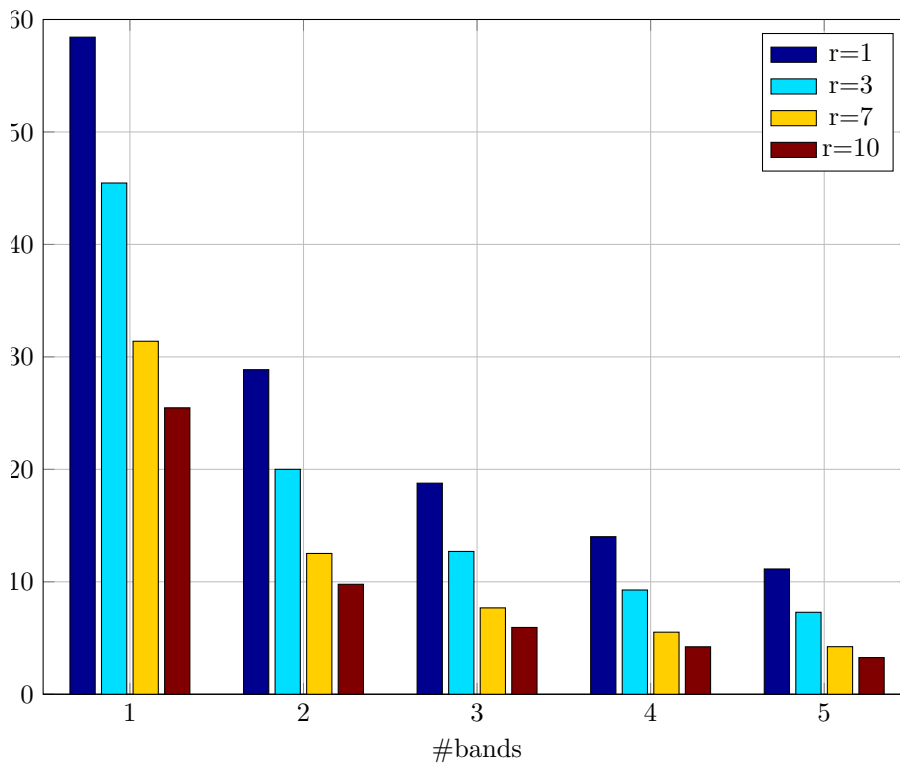


Figure 4.15: Packet Drop Probability for scheduler size=1.

While classical CSMA/CA - RTS/CTS suffers from important loss (64%). The investigated mechanism reaches the maximum achievable performance with 5 RTS bands and scheduler size equals to three for loaded network. Then, the proposed mechanism is a valid approach to achieve the maximum contention based MAC upper bound for loaded scenarios.

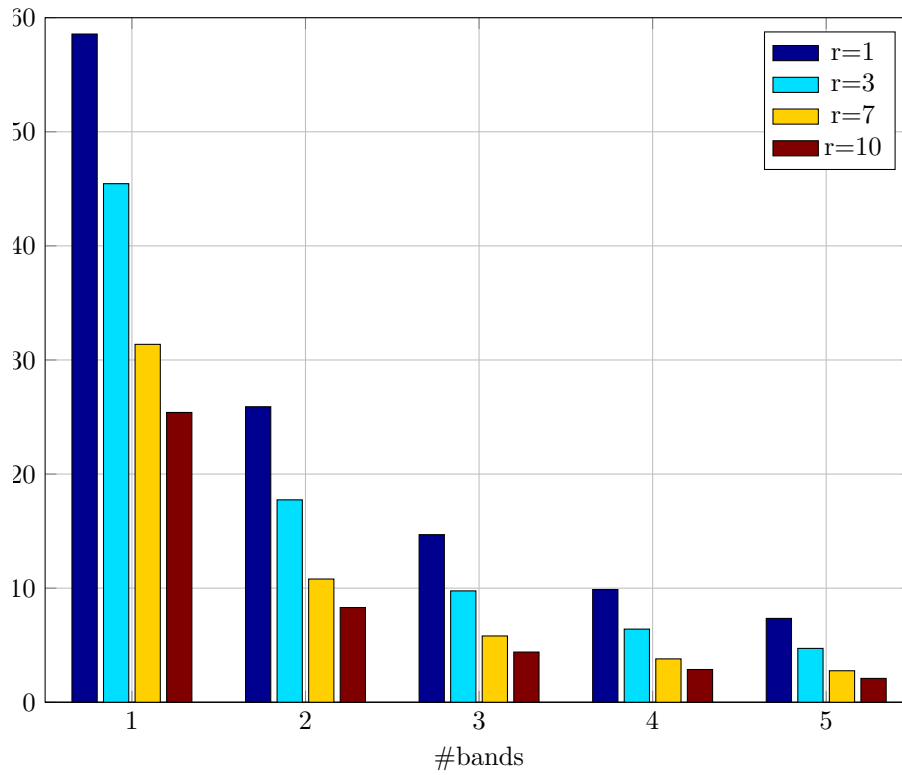


Figure 4.16: Packet Drop Probability for scheduler size=2.

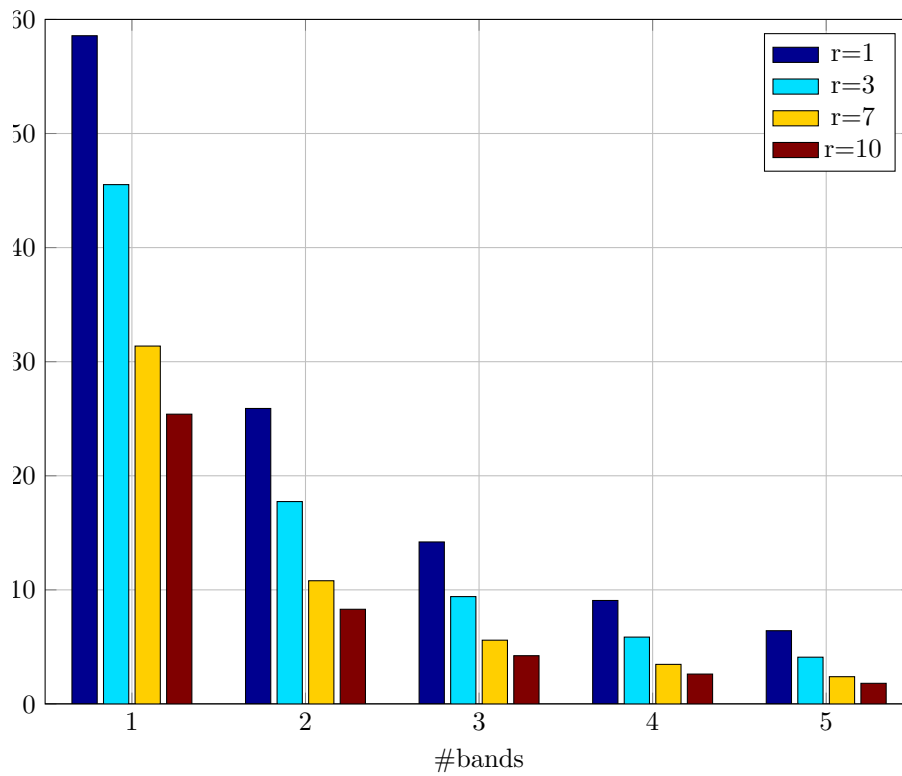


Figure 4.17: Packet Drop Probability for scheduler size=3.

4.5 Conclusion

In this chapter, we proposed a novel strategy based on multiband CSMA/CA-RTS/CTS which is characterized by serving many nodes one after the other to reduce the MAC overhead. We

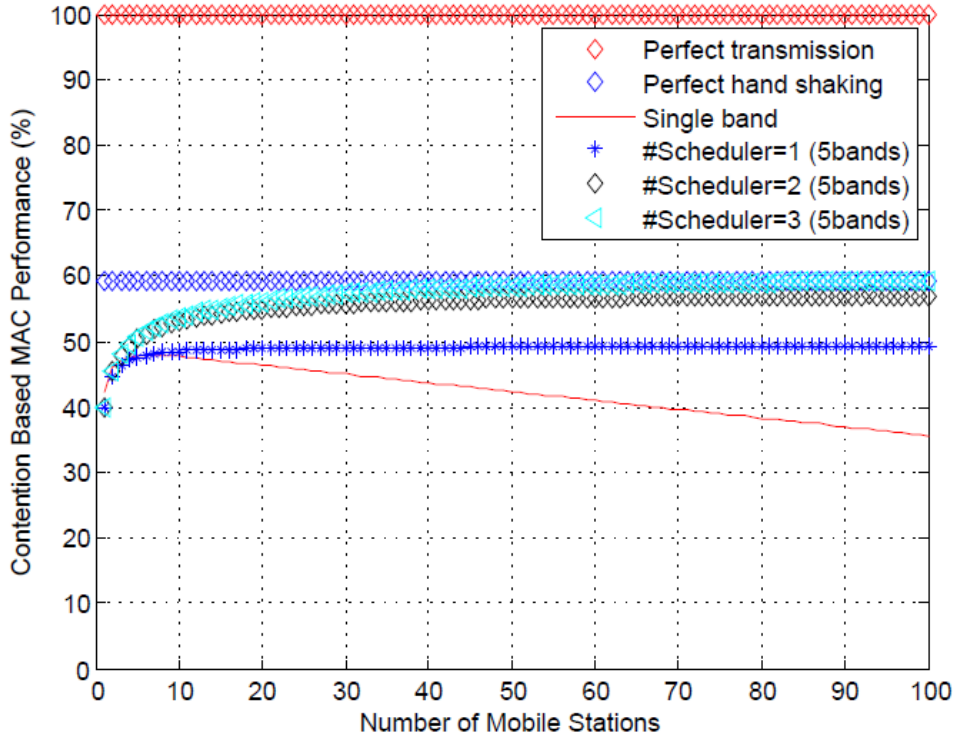


Figure 4.18: Contention Based MAC Performance.

prove by simulations that the proposed strategy reaches the contention based upper bound and is able to achieve very high gain in terms of saturation throughput, transmission delay and packet drop probability. Since the gain is very important in loaded networks, the proposed strategy may be adapted to scenario where very high number of nodes communicate simultaneously. For instance, when considering 4 RTS sub-bands with 100 nodes in saturation conditions, the achieved gain for scheduler size equals to three is 78% in terms of saturation throughput and 35% of gain in terms of packet rejection rate. Since the scheduled M-CSMA/CA-RTS/CTS reduces drastically the RTS collision probability and mitigates significantly the time spent in waiting the channel to be free (idle duration) especially for dense scenarios (where high number of nodes with saturation mode is considered) and as it guarantees a high bitrate for such scenarios, this technique could be very suitable to broadband M2M where high number of nodes want to communicate together with high bitrate.

Finally, in this contribution we proposed a study about the overhead reduction by introducing a scheduler to serve transmitters successively. It should be mentioned that in practical application there is a limit on the scheduler size. For this reason the scheduler size should be reasonable and adapted for each application. Also, the proposed strategy may be easily implemented by allocating many sub-carriers for different RTS messages. Multicarrier waveforms already introduced into latest 802.11 standards can fulfill the requirements for such implementations.

Figures 4.19 and 4.20 depict a comparison between the behaviour of the single band CSMA/CA-RTS/CTS, M-CSMA/CA-RTS/CTS and scheduled M-CSMA/CA-RTS/CTS for loaded scenario. As a conclusion, for loaded networks the M-CSMA/CA-RTS/CTS improves the system velocity (inverse of transmission delay) and has better saturation throughput than the single band CSMA/CA-RTS/CTS. Introducing the scheduled M-CSMA/CA-RTS/CTS the performance is enhanced and the system velocity is further improved especially for loaded networks which is suitable to the context of our proposed work.

In the case of unloaded network, Figure 4.20 depicts that the single band CSMA/CA-RTS/CTS performance outperforms the M-CSMA/CA-RTS/CTS and the scheduled M-CSMA/CA-RTS/CTS.

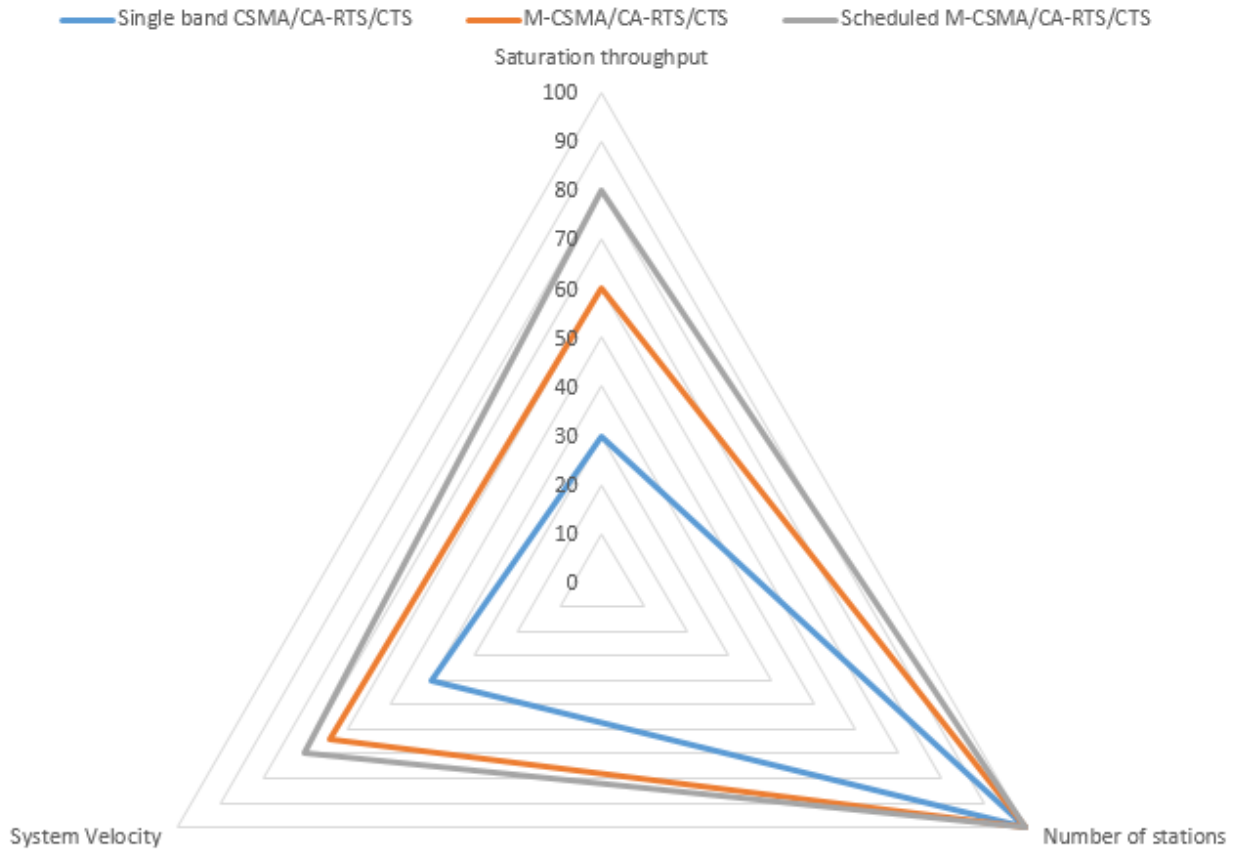


Figure 4.19: CSMA/CA - RTS/CTS synthesis for loaded scenario.

Since the RTS messages in the case of single band CSMA/CA-RTS/CTS are shorter than the RTS messages in the case of M-CSMA/CA-RTS/CTS and scheduled M-CSMA/CA-RTS/CTS, then the system velocity of the single band CSMA/CA-RTS/CTS is higher than the other protocols.

To conclude, the proposed protocol with its enhancement which is based on the scheduling scheme have been studied at MAC level. In order to understand the effects of the physical layer on the protocol performance, a joint PHY-MAC study should be achieved as well. For that we propose to analyze in the next chapter a full cross-layer study of the proposed MAC by introducing a physical layer based on multicarrier waveforms.

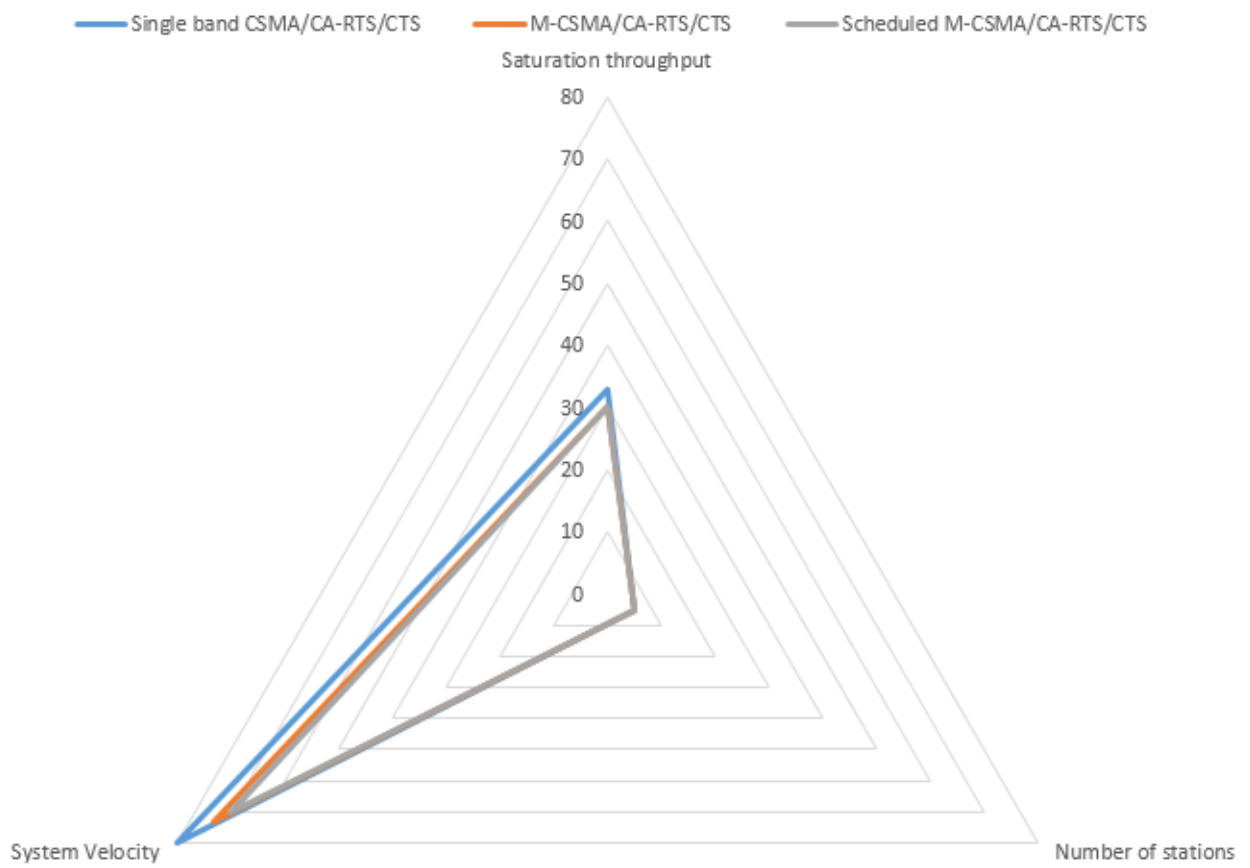


Figure 4.20: CSMA/CA - RTS/CTS synthesis for unloaded scenario.

Chapter 5

Joint PHY-MAC analysis of M-CSMA/CA - RTS/CTS

5.1 Introduction

Until this point, the protocol was studied assuming a perfect PHY layer. In the previous chapters the physical layer effects were not addressed. In order to evaluate its effects we investigate in this chapter the influence of a PHY layer. We will limit our investigation to the effect of PHY frame format as well as capture effect and adjacent channel interference. This latter is specific to the M-CSMA/CA - RTS/CTS as multiple RTS can be received in different sub-bands. In Section 5.2 the physical layer is described where the 802.11n standard is addressed and a complete model related to the physical layer, capture effect and interband interference is derived. Then, the system performance is evaluated in Section 5.3. Finally, the chapter is concluded in Section 5.4.

5.2 Physical layer description

5.2.1 802.11n description

In this chapter, we propose to encapsulate the proposed M-CSMA/CA-RTS/CTS protocol to the physical layer of the 802.11n standard [40]. The IEEE 802.11n standard provides many options to improve the quality of the wireless link and thereby to increase data rate and data range. The performance of IEEE 802.11n is several times greater than legacy standards [70]. According to this standard, the channel is divided into OFDM subcarriers [71]. The OFDM distributes the incoming data bits among the subcarriers, then each of the subcarriers is used as an independent transmission. In 802.11n system, based on the WLAN OFDM system, two new formats are defined for the PHY Layer Convergence Protocol (PLCP): the Mixed Mode and the Green Field [21]. These two formats are called High Throughput (HT) formats. Then, in time domain the 802.11n PHY operates in one of 3 modes: Legacy mode, Mixed Mode and Green Field Mode. As mentioned in [21]: the channel is divided into 64 sub-carriers in legacy mode and HT mode transmission over a 20MHz channel. 4 pilot signals are affected to sub-carriers -21, -7, 7 and 21. Signal is transmitted on sub-carriers -26 to -1 and 1 to 26, with 0 being the center (DC) carrier in the case of legacy mode. While, signal is transmitted on sub-carriers -28 to -1 and 1 to 28 in the case of HT modes .

1. Legacy Mode

In the legacy mode, frames are transmitted in the legacy 802.11a/g OFDM format [38]. Figure 5.1 shows the legacy frame.

2. Mixed Mode

Packets are transmitted with a preamble compatible with the legacy 802.11a/g in the

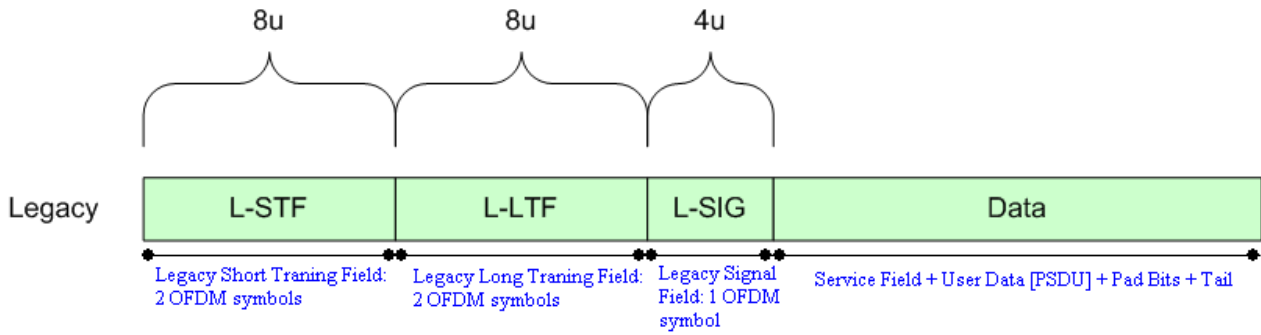


Figure 5.1: 802.11n WLAN frame, Legacy Mode [21].

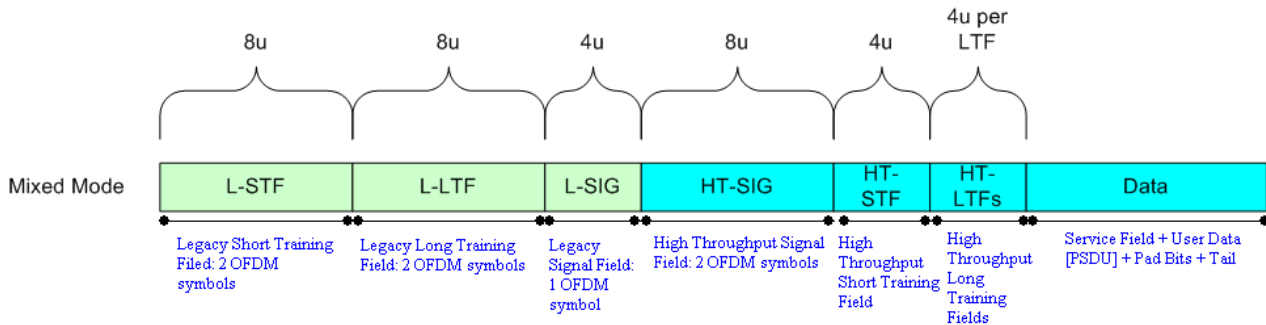


Figure 5.2: WLAN frame modifications to allow for MIMO operation, Mixed Mode [21].

Mixed Mode. The legacy Short Training Sequence, the legacy Long Training sequence and the legacy signal description are transmitted so they can be decoded by legacy 802.11a/g devices. The rest of the packet has a new MIMO training sequence format. Figure 5.2 shows the Mixed Mode format [21].

3. Green Field Mode

In the Green Field mode, high throughput packets are transmitted without a legacy compatible part [21]. Figure 5.3 shows the Green Field format.

As reported in [72]: the legacy short training OFDM symbol is identical to the 802.11a short training OFDM symbol. The L-STF is BPSK modulated at 6 Mbps, it contains no channel coding, and is not scrambled. The period of L-STF is $0.8 \mu s$. The entire short training field includes ten such periods, with a total duration of $8 \mu s$. In the 20 MHz transmission mode: the legacy short training OFDM symbol are assigned to subcarriers -24, -20, -16, -12, -8, -4, 4, 8, 12, 16, 20, 24.

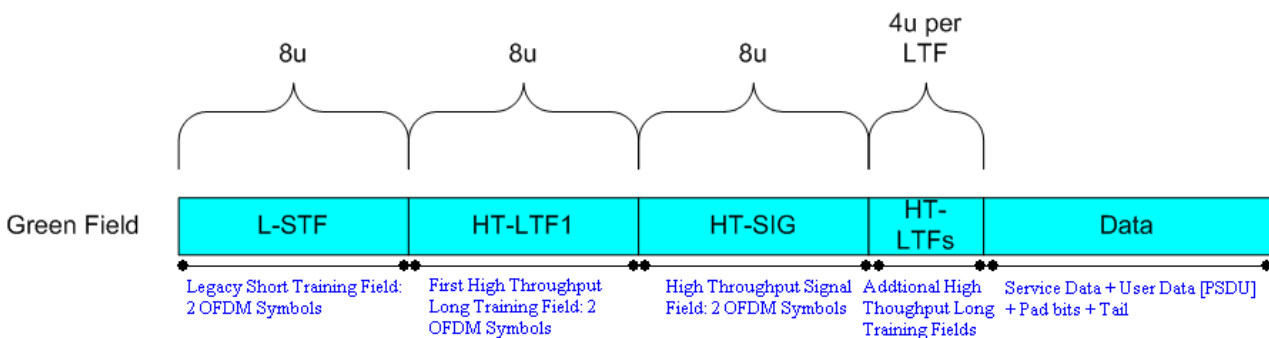


Figure 5.3: 802.11n WLAN frame, Green Field [21].

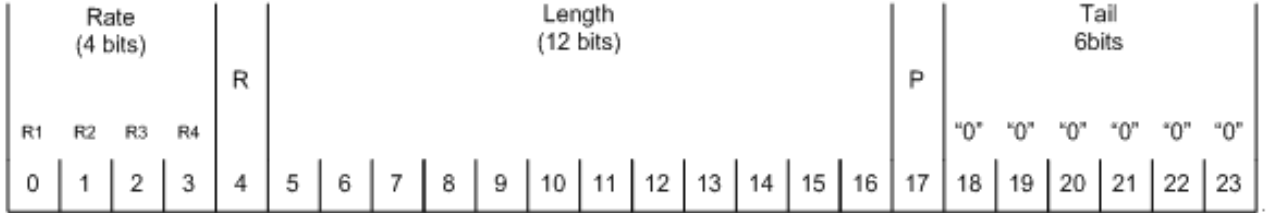


Figure 5.4: Legacy Signal Field (L-SIG) [22].

PHY standard	Subcarrier range	Pilot subcarriers	Subcarriers (total/data)
802.11n, 20MHz	-28 to -1, +1 to +28	$\pm 7, \pm 21$	56 total, 52 usable (7% pilots)

Table 5.1: Channel description attributes for legacy mode.

[73] mentioned that the legacy long training OFDM symbol is identical to the 802.11a long training OFDM symbol. The L-LTF is BPSK modulated at 6 Mbps, it contains no channel coding, and is not scrambled. In the 20 MHz transmission mode: the legacy long training OFDM symbols are assigned to sub-carriers -26 to -1 and 1 to 26 .

As reported in [22] the signal field is used to transfer rate and length information. The L-SIG consists of one OFDM symbol assigned to all 52 subcarriers. This symbol is BPSK modulated at 6 Mbps and is encoded at a $1/2$ rate. L-SIG is interleaved, mapped, not scrambled, and subcarriers -21 , -7 , 7 and 21 are reserved for pilots. L-SIG is transmitted using the same method and meaning as specified in the IEEE 802.11a [38] standard in the case of legacy 20 MHz transmission mode as shown in the below figure 5.4.

The data field includes the service field, the PSDU, the pad bits, and the tail bits. The data field is scrambled. The data rate, encoding rate, and modulation varies.

In this chapter, we will limit our study to the legacy mode [21]. Then, few subcarriers are reserved and are called pilot carriers; they do not carry user data and instead are used to measure the channel. Table 5.1 identifies the OFDM carrier numbering and pilot channels. The range of the subcarriers defines the channel width itself. Each subcarrier has identical data-carrying capacity, and therefore, more is better. Pilot subcarriers are protocol overhead and are used to carry out important measurements of the channel. Figure 5.5 depicts the repartition of subcarriers in the band.

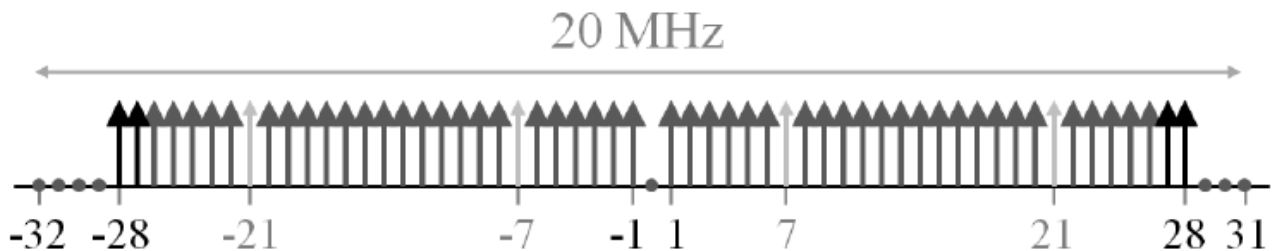


Figure 5.5: WiFi subcarriers according to legacy mode [14].

5.2.2 Physical layer effect

In this Section we propose to study the M-CSMA/CA according to the legacy case description. We consider a simplified version of the 802.11n standard where we take into account the mapping of sub-carriers within the frequency band. For that, we will consider that the data



Figure 5.6: Block diagram of the transmitter.

is transmitted over 52 subcarriers using OFDM modulation. Hence, the time T needed to transmit a packet of size P is given by the following expression:

$$\begin{aligned}
 T &= L - STF + L - LTF + L - SIG + Data \\
 T &= 20\mu s + M(N_c + GI)/B
 \end{aligned} \tag{5.1}$$

where M is the number of OFDM symbols, N_c represents the number of sub-carriers and B is the channel bandwidth.

The block diagram of the proposed transmitter is depicted in Figure 5.6. The transmitter is composed of three elements: forward error correction followed by a data mapping and modulation block. Forward error correction (FEC) is implemented using either a standard convolutional encoder or a Low Density Parity Check (LDPC) code. The convolutional code may be punctured to support variable encoding rates. Various LDPC matrices are considered to support a wide range of block sizes and coding rates. The input bit stream is segmented by blocks of fixed sizes. In case of convolutional coding, the trellis is closed at the beginning and the end of each FEC block. The output of the encoder is forwarded to a bit interleaver of size multiple of the output length of the encoder. The second module, called Mapping and Modulation, maps and modulates the encoded bits to the multicarrier modulation. The coded data are mapped to a QPSK, 16QAM or 64QAM modulation. Symbols are then padded to complete the transmitted burst into an integer multiple of multicarrier symbols. The generated block of data symbols are mapped to the active carriers and modulated through the third block before being transformed into a time domain signal using OFDM waveform. A Modulation and Coding Scheme (MCS) index is defined to describe the combination of the modulation and coding schemes that are used when transmitting data. Hence the number of OFDM symbols (M) may be expressed by the following equation:

$$M = \lceil \frac{\lceil \frac{P}{R} \rceil}{\frac{m}{N_a}} \rceil \tag{5.2}$$

where R is the coding rate, m is the modulation order and N_a is the number of active sub-carriers used to send the packet of length P bits.

Let's first analyze the effect of the division of the RTS band ($B = 20MHz$) into several sub-bands on the RTS duration. Let's denote by x and y_1 the RTS size and the time needed to transmit the RTS message over the complete band (single band CSMA/CA-RTS/CTS case) respectively. y_2 and y_4 correspond to the time duration needed to transmit the RTS message when 2 sub-bands and 4 sub-bands are considered. Concerning control packets, RTS and CTS, the MCS index 0 ($R = 1/2$ and $m = 2$) is considered. As these messages serve for virtual carrier sensing, they should be decoded by all the nodes within the cell. Consequently a robust configuration is set. The number of active sub-carriers used in the case of single, 2 sub-bands and 4 sub-bands are 52, 26 and 13. Hence,

$$\begin{aligned}
 y_1 &= 20\mu s + \lceil \frac{x}{52} \rceil (52 + GI)/20 \\
 y_2 &= 20\mu s + \lceil \frac{x}{26} \rceil (26 + GI)/20 \\
 y_4 &= 20\mu s + \lceil \frac{x}{13} \rceil (13 + GI)/20
 \end{aligned} \tag{5.3}$$

Considering $x=288$ bits (based on the previous chapters), let's compute the above equation for $GI=8$.

$$\begin{aligned} y_1 &= 38\mu s \\ y_2 &= 40.4\mu s = 1.063y_1 \\ y_4 &= 44.15\mu s = 1.16y_1 \end{aligned} \quad (5.4)$$

And for $GI=16$, we get:

$$\begin{aligned} y_1 &= 40.4\mu s \\ y_2 &= 45.2\mu s = 1.12y_1 \\ y_4 &= 53.35\mu s = 1.32y_1 \end{aligned} \quad (5.5)$$

In the previous chapters the assumption of a linear increase of the RTS duration with the number of sub-band was assumed. When the RTS band is divided into n sub-bands the duration needed to transmit the new RTS message duration (y_n) is equal to $n \times y_1$. However, the above values show clearly that the time needed to transmit the RTS message when the band is divided by n is lower than $n \times y_1$. It can be explained by the fact that padding symbol should be add to complete a multicarrier symbol. The effect of the padding is attenuated when the number of active carrier decreases. So we further gain when the band is divided comparing to the MAC study, for instance considering 4 sub-bands the RTS duration is multiplied by 1.16 which is very low comparing to 4.

5.2.3 Capture effect

For wireless communications, when a multiple users share a single wireless channel, they generate interference to each other so their communication quality, characterized by signal-to-interference ratio (SIR) or bit-error-rate (BER), will be severely degraded at the receivers [74]. As we showed in the previous chapter, when multiple nodes send their data packets simultaneously to the same access point, a packet collision occurs. When no power control is integrated, one of the collided packets can still be correctly received, if its SIR seen by the access point is high enough (the SIR at the AP should be higher than a predefined threshold). The desired signal is decoded by treating all the other ongoing signal transmissions as interference. In this case, the packet with the strongest signal is decoded successfully by the receiver. This phenomenon is called the capture effect and is widely exists in cellular networks [75].

We consider a single channel with one AP located at the center of a circular cell. In this cell there are N nodes uniformly distributed and communicating with the AP. Every node in the system and at each time slot will independently send a packet to the AP with the average transmission probability π , which is derived in the previous chapter. The probability of g simultaneous packet transmissions in a typical time slot is given by [74]:

$$R_g = \binom{N}{g} \pi^g (1 - \pi)^{(N-g)} \quad (5.6)$$

when $g = 0$, no packet is transmitted in this time slot and so it is idle; When $g=1$, only one packet is transmitted in this time slot and it will be successfully received and decoded by the AP; Otherwise, i.e. $g \geq 2$, a packet collision occurs [74]. Finally, due to communication distances between the nodes and the AP and to the dynamics of wireless channel conditions, one collided packet with relatively higher SIR may still be correctly decoded by the AP [74]. Let P_i denotes the average power levels received at the AP for the packet transmitted by node

number i . Then, the $SIR(i)$ related to node i will be computed by the following equation:

$$SIR(i) = \frac{P_i}{\sum_{\substack{j=1 \\ j \neq i}}^g P_j} \quad (5.7)$$

The packet transmitted by the node i is considered to be successfully received by the receiver if the received SIR is higher than γ (an appropriate threshold which depends on the modulation and coding scheme) for the whole packet duration. Thus, a packet transmission from node i is successful if

$$SIR(i) \geq \gamma \quad (5.8)$$

In the case of M-CSMA/CA-RTS/CTS with n sub-bands, the AP is able to decode a sub-band k if the SIR related to intended RTS transmitted on the sub-band k is higher than γ_k .

$$SIR(k, i) \geq \gamma_k \quad (5.9)$$

If $P_R(k, i)$ is the power received on the sub-band k from user i the $SIR(k, i)$ could be expressed by:

$$SIR(k, i) = \frac{P_R(k, i)}{\sum_{\substack{j=1 \\ j \neq i}}^{g_k} P_R(k, j)} \quad (5.10)$$

Where g_k presents the number of transmitter nodes (backoff=0) over the sub-band k . A successful communication takes place where at least one sub-band is decodable at the destination side. Based on Friis transmission equation [76], the received power can be expressed in function of the transmitted power by the following equation:

$$\frac{P_r}{P_t} = G_t G_r \left(\frac{\lambda}{4\pi R} \right)^\alpha \quad (5.11)$$

Where G_t and G_r are the antenna gains (with respect to an isotropic radiator) of the transmitting and receiving antennas respectively, λ is the wavelength and R is the distance between the antennas. α is the so-called path loss coefficient which takes several values depending on the network configuration. For instance the authors of [77] have proposed $\alpha = 4$ for short range ($R=25m$), $\alpha = 3.3$ for medium range ($R=50m$) and $\alpha = 2.8$ for long range ($R=100m$). If R_i (R_j) is the distance between the node i (j) and the AP, the $SIR(k, i)$ could be expressed by:

$$SIR(k, i) = \frac{\frac{1}{R_i^\alpha}}{\sum_{\substack{j=1 \\ j \neq i}}^{g_k} \frac{1}{R_j^\alpha}} \quad (5.12)$$

The above equation will serve for simulations purposes.

5.2.4 Interband interference

In this Section we study the effect introduced by the transmitted RTS message over a defined sub-band to all the others RTS sub-bands. For that, we introduce the transmitter-receiver (TX-RX) scheme related to the proposed MAC described in the previous chapters. Once the RTS transmission phase is passed, the protocol works on one channel (complete channel is used for CTS-DATA-ACK). Hence, there is no more interband interference as only one node will use the complete channel to transmit its data. Then, the complete analysis is conducted to analyze the interband interference during simultaneous RTS messages transmission. We start to describe the context and the problematic of the interband interference and we give the equivalent physical model based on OFDM modulation. Then, the effect of asynchronous transmission is studied and the synchronous and asynchronous transmission cases are investigated.

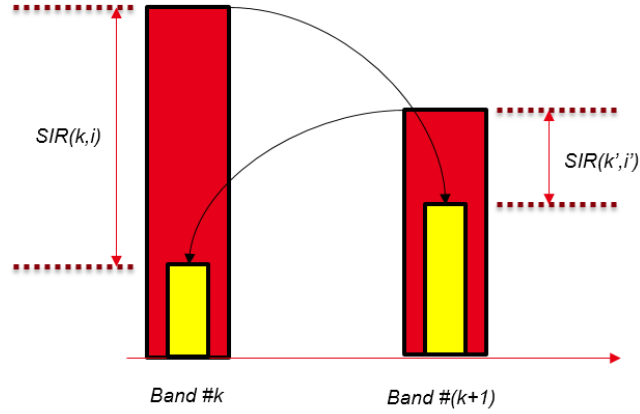


Figure 5.7: Interband Interference.

5.2.4.1 Context and problematic

It is well known that the OFDM modulation is not well localized in frequency [15] (since it is well localized in time) which cause an interference between two parallel transmissions over two consecutive frequency bands when they are not synchronized. Figure 5.7 depicts the case of two parallel transmissions over the bands k and $k + 1$. Since the OFDM modulation is not well localized in frequency a leakage is introduced from each band to the other one. The red and yellow rectangles refer to the signal and interference powers respectively. Higher signal power introduces higher interference on the adjacent band.

The goal of the following parts is to compute the interference caused by an adjacent sub-band on the sub-band of interest in order to evaluate the signal to noise ratio measured on the latter one.

5.2.4.2 Equivalent physical model

We consider a packet (RTS message or whatever ...) which should be transmitted over a sub-band based on OFDM transmission.

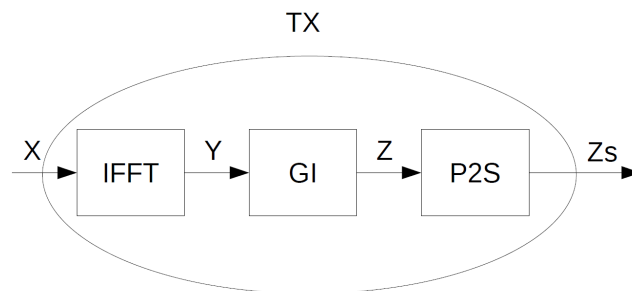


Figure 5.8: Architecture of OFDM transmitter.

Figures 5.8 and 5.9 depict the transmitter and receiver schemes based on OFDM modulation. The transmitter is based mainly on three blocks, the first block is the IFFT (inverse fast fourier transform) followed by adding a guard interval and a parallel to serial conversion. The IFFT block transforms the input signal (X) which contains M symbols mapped over N_a active sub-carriers from frequency domain to time domain. Then, a guard interval is added and a conversion from parallel to serial is required to transmit the formed sequence of data via the communication channel. Actually, if we consider a FFT of size $N=64$ with 56 active sub-carriers ($N_a=56$) the number of usable sub-carriers over all RTS sub-bands is equal to 52.

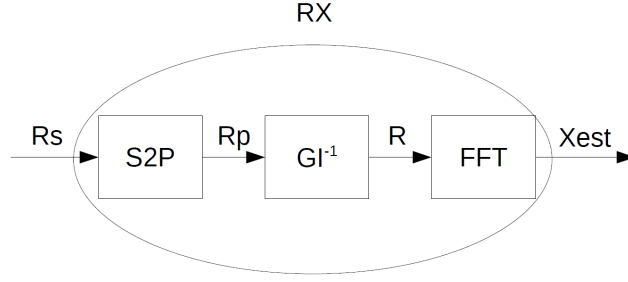


Figure 5.9: Architecture of OFDM receiver.

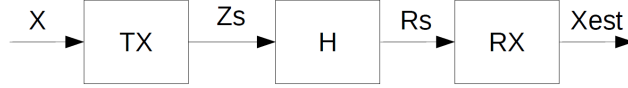


Figure 5.10: Architecture of single band TX-RX.

In the case of 2 RTS sub-bands, each sub-band is formed by 28 active sub-carriers (26 usable sub-carriers and 2 sub-carriers reserved for pilots), hence the size of each OFDM symbol is equal to the number of usable sub-carriers (26).

The receiver is also composed of three main blocks. They are the inverse of the blocks which form the transmitter. The first block is a serial to parallel conversion before removing the guard interval. The last block consists on FFT transform which converts the signal (R) from time to frequency domain.

The equivalent physical layer is depicted in Figure 5.10 where a channel H links the TX with the RX.

Let's consider that the band is divided into two sub-bands and the packet (RTS message) is transmitted over the first sub-band and that no one transmits on the second one. Then, the number of reserved sub-carriers is equal to 32. The number of active and usable sub-carriers is equal to 28 and 26 respectively. The above scenario is a particular case which may be generalized easily to take into consideration several number of sub-bands with different repartition of sub-carriers. Let's denote by A the matrix which contains the OFDM symbols and corresponds to the transmitted message. The first four lines of A are null which corresponds to the sub-carriers -32, -31, -30 and -29.

$$A = \begin{bmatrix} a_{11} & a_{12} & a_{13} & \dots & a_{1M} \\ a_{21} & a_{22} & a_{23} & \dots & a_{2M} \\ \dots & \dots & \dots & \dots & \dots \\ a_{\frac{N}{2}1} & a_{\frac{N}{2}2} & a_{\frac{N}{2}3} & \dots & a_{\frac{N}{2}M} \end{bmatrix} = \begin{bmatrix} 0 & 0 & 0 & \dots & 0 \\ \dots & \dots & \dots & \dots & \dots \\ 0 & 0 & 0 & \dots & 0 \\ a_{51} & a_{52} & a_{13} & \dots & a_{5M} \\ a_{61} & a_{62} & a_{63} & \dots & a_{6M} \\ \dots & \dots & \dots & \dots & \dots \\ a_{N_a1} & a_{N_a2} & a_{N_a3} & \dots & a_{N_aM} \end{bmatrix}$$

Then the transmitted message X of size $N \times M$ can be expressed as following:

$$X = \begin{bmatrix} A \\ 0 \end{bmatrix}$$

Y is the fourrier transform of X of size $N \times M$, then Y may be expressed as following:

$$Y = F^H X \tag{5.13}$$

where F is the quantum Fourier transform matrix of size $N \times N$.

$$F = \frac{1}{\sqrt{N}} \begin{bmatrix} 1 & 1 & 1 & 1 & \dots & 1 \\ 1 & \omega & \omega^2 & \omega^3 & \dots & \omega^{N-1} \\ 1 & \omega^2 & \omega^4 & \omega^6 & \dots & \omega^{2(N-1)} \\ 1 & \omega^3 & \omega^6 & \omega^9 & \dots & \omega^{3(N-1)} \\ \dots & \dots & \dots & \dots & \dots & \dots \\ 1 & \omega^{N-1} & \omega^{2(N-1)} & \omega^{3(N-1)} & \dots & \omega^{(N-1)(N-1)} \end{bmatrix}$$

where $\omega = e^{-j2\pi/N}$. After adding the cyclic prefix, the size of Z is $(N + GI) \times M$ and may be expressed as following:

$$Z = I_{GI}Y = \begin{bmatrix} y_{N-GI+1,1} & y_{N-GI+1,2} & y_{N-GI+1,3} & \dots & y_{N-GI+1,M} \\ \dots & \dots & \dots & \dots & \dots \\ y_{N,1} & y_{N,2} & y_{N,3} & \dots & y_{N,M} \\ y_{1,1} & y_{1,2} & y_{1,3} & \dots & y_{1,M} \\ y_{2,1} & y_{2,2} & y_{2,3} & \dots & y_{2,M} \\ \dots & \dots & \dots & \dots & \dots \\ y_{N,1} & y_{N,2} & y_{N,3} & \dots & y_{N,M} \end{bmatrix}$$

where I_{GI} of size $(N + GI) \times N$ is expressed by the following expression:

$$I_{GI} = \begin{bmatrix} W_{GI} \\ I \end{bmatrix}$$

and $W_{GI} = [0 \ I]$ of size $GI \times N$.

After a parallel to serial conversion Zs could be expressed as following:

$$Zs = [y_{N-GI+1,1} \dots y_{N,1} \ y_{1,1} \ y_{2,1} \dots y_{N,1} \ y_{N-GI+1,2} \dots y_{N,2} \dots y_{N,M}] \quad (5.14)$$

We consider a single input single output channel where the received signal can be written as [78]

$$Rs(t) = \sum_{l=0}^{L-1} c_l(t)Zs(t - \tau_l) \quad (5.15)$$

Where c_l and τ_l are the channel path and the associated delay measured at the receiver side. This may be interpreted as the output of a complex baseband time-varying linear channel with an impulse response equal to

$$c(t, \tau) = \sum_{l=0}^{L-1} c_l(t)\delta(\tau - \tau_l(t)). \quad (5.16)$$

After sampling, the channel can be expressed as:

$$h(k, t) = \sum_{l=0}^{L-1} c_l(t)\delta(kT - \tau_l), \quad (5.17)$$

where T is the sampling period. Note that, in this chapter, we assume slow fading and time invariant channels conditions. The discrete representation of the channel impulse response (CIR) at time k may be modeled as

$$h[k] = \sum_{l=0}^{L-1} h_l\delta[k - l], \quad (5.18)$$

where $h_l = h[l]$ and L represent the l^{th} tap complex amplitude and the number of taps of the channel between the receiver and the transmitter.

After channel convolution the received message Rs can be expressed as following:

$$Rs = h * Zs \quad (5.19)$$

After a serial to parallel conversion the received signal will be mapped in a matrix of size $(N - GI + 1) \times M$ to form the signal Rp . Then, R of size $N \times M$ is obtained by removing the guard interval. The final signal $Xest$ of size $N \times M$ expressed below is computed by applying the FFT on R .

$$Xest = FR \quad (5.20)$$

In the case of one tap channel, $h(t) = \delta(t)(H = 1)$, $R = Y$, then $Xest = FY = FF^H X = X$. The transmitted message is decoded correctly at the transmitter side without any error. What will happen if more than one RTS message are transmitted over the different sub-bands with asynchronous manner? Will the transmitted messages be decoded correctly? In which case? The next part, will study the effect of asynchronous transmission in order to derive theoretically the full expression of SIR related to the signal of interest.

5.2.4.3 Effect of asynchronous transmission on interference level

The multiband CSMA/CA-RTS/CTS envisages a simultaneous RTS transmission at the transmitter side. So the related TX should be able to transmit these RTS messages and the related RX should be able to receive on one shot all these RTS messages and be able to decode them one by one. Then, Figure 5.11 depicts the M-CSMA/CA-RTS/CTS TX-RX for n RTS sub-bands which is able to transmit simultaneously several RTS messages and to decode them. This TX-RX is composed of several OFDM transmitters which are associated in parallel where each OFDM transmitter has its input signal in frequency domain (X_i) and its output signal in time domain (Zs_i). Each of these outputs will be transmitted via a channel (H_i). The channels outputs are summed at the receiver side (Rs). The received signal is converted from serial to parallel and the guard interval is removed. Then, a FFT is needed to convert the signal (R) from time to frequency domain and obtain the estimated signal ($Xest$) of the transmitted one (X). Once the estimated signal is well decoded the receiver could analyze and retrieve the RTS messages.

Considering the case of two RTS sub-bands based on 802.11n physical layer, the equivalent block diagram becomes equivalent to the one depicted Figure 5.12.

Let's compute the different signals at each stage of the transmitter/receiver present in Figure 5.13. Without loss of generality, we show the example of 2 sub-bands but the extension to n sub-bands is also feasible. Let's denote by A_1 and A_2 the matrices which contain the RTS messages information. The size of these matrices is $\frac{N}{2} \times M$ which contains $N_a \times M$ active elements. Since A_1 and A_2 correspond to the first and second part of the considered spectrum, they can be expressed as following:

$$A_1 = \begin{bmatrix} a_{11}^1 & a_{12}^1 & a_{13}^1 & \dots & a_{1M}^1 \\ a_{21}^1 & a_{22}^1 & a_{23}^1 & \dots & a_{2M}^1 \\ \dots & \dots & \dots & \dots & \dots \\ a_{\frac{N}{2}1}^1 & a_{\frac{N}{2}2}^1 & a_{\frac{N}{2}3}^1 & \dots & a_{\frac{N}{2}M}^1 \end{bmatrix} = \begin{bmatrix} 0 & 0 & 0 & \dots & 0 \\ \dots & \dots & \dots & \dots & \dots \\ 0 & 0 & 0 & \dots & 0 \\ a_{51}^1 & a_{52}^1 & a_{53}^1 & \dots & a_{5M}^1 \\ a_{61}^1 & a_{62}^1 & a_{63}^1 & \dots & a_{6M}^1 \\ \dots & \dots & \dots & \dots & \dots \\ a_{N_a1}^1 & a_{N_a2}^1 & a_{N_a3}^1 & \dots & a_{N_aM}^1 \end{bmatrix}$$

The first four lines of A_1 are null which corresponds to the sub-carriers -32, -31, -30 and -29.

$$A_1 = N_1 B_1 \quad (5.21)$$

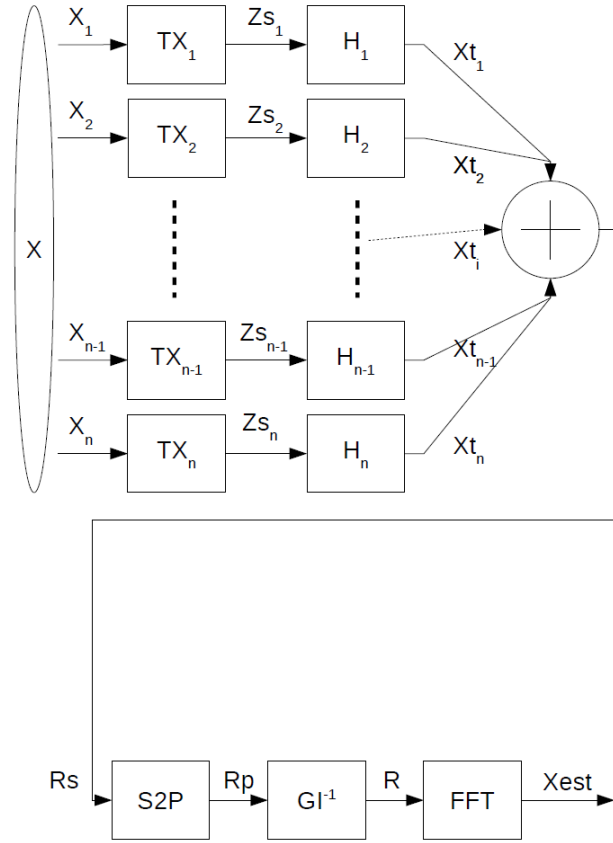


Figure 5.11: Architecture of M-CSMA/CA-RTS/CTS TX-RX with n RTS sub-bands.

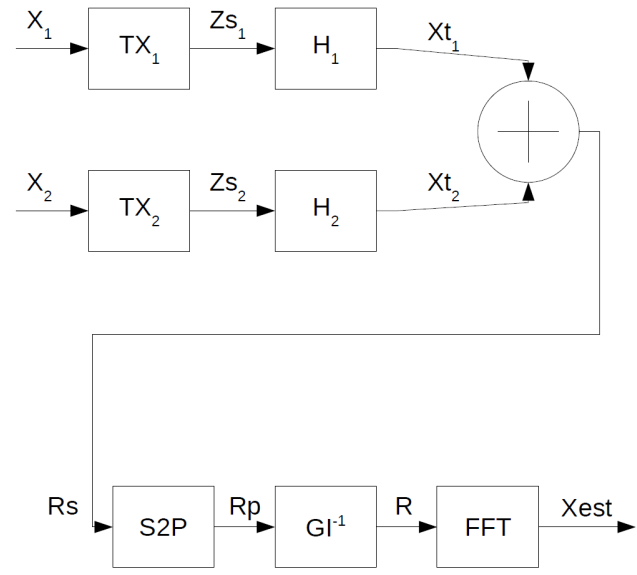


Figure 5.12: Block diagram of M-CSMA/CA-RTS/CTS TX-RX with 2 RTS sub-bands.

$$N_1 = \begin{bmatrix} 0_4 \\ I_{N/2-4} \end{bmatrix}$$

where B_1 corresponds to the non null elements of A_1 and 0_4 is a column of 4 zeros.

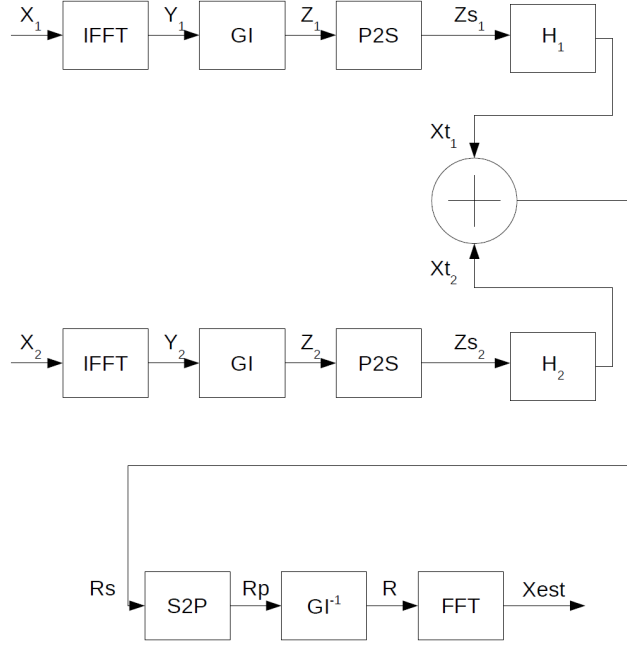


Figure 5.13: Developed M-CSMA/CA-RTS/CTS with 2 sub-bands architecture.

$$A_2 = \begin{bmatrix} a_{11}^2 & a_{12}^2 & a_{13}^2 & \dots & a_{1M}^2 \\ a_{21}^2 & a_{22}^2 & a_{23}^2 & \dots & a_{2M}^2 \\ \dots & \dots & \dots & \dots & \dots \\ a_{\frac{N}{2}1}^2 & a_{\frac{N}{2}2}^2 & a_{\frac{N}{2}3}^2 & \dots & a_{\frac{N}{2}M}^2 \end{bmatrix} = \begin{bmatrix} 0 & 0 & 0 & \dots & 0 \\ a_{21}^2 & a_{22}^2 & a_{23}^2 & \dots & a_{2M}^2 \\ a_{31}^2 & a_{32}^2 & a_{33}^2 & \dots & a_{3M}^2 \\ \dots & \dots & \dots & \dots & \dots \\ a_{N_a1}^2 & a_{N_a2}^2 & a_{N_a3}^2 & \dots & a_{N_aM}^2 \\ 0 & 0 & 0 & \dots & 0 \\ \dots & \dots & \dots & \dots & \dots \\ 0 & 0 & 0 & \dots & 0 \end{bmatrix}$$

The first and the last three lines of A_2 are null which corresponds to the sub-carriers 0, 29, 30 and 31.

$$A_2 = N_2 B_2 \quad (5.22)$$

$$N_2 = \begin{bmatrix} 0 \\ I_{N/2-4} \\ 0_3 \end{bmatrix}$$

where B_2 corresponds to the non null elements of A_2 and 0_3 is a matrix with 3 zeros.

X_1 and X_2 are the matrices of size $N \times M$ which contains A_1 and A_2 . Then, X_1 and X_2 may be expressed as following:

$$X_1 = \begin{bmatrix} A_1 \\ 0 \end{bmatrix}$$

$$X_2 = \begin{bmatrix} 0 \\ A_2 \end{bmatrix}$$

Y_1 and Y_2 are the fourrier transform of X_1 and X_2 respectively of size $N \times M$, then Y_1 and Y_2 may be expressed as following:

$$Y_1 = F^H X_1 \quad (5.23)$$

$$Y_2 = F^H X_2 \quad (5.24)$$

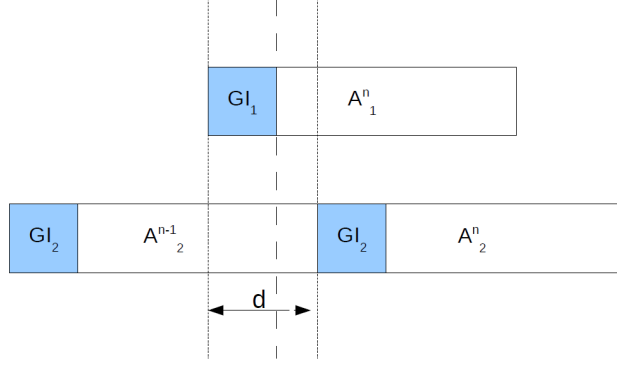


Figure 5.14: Asynchronous RTS messages.

After a parallel to serial conversion Zs_1 and Zs_2 could be expressed as following:

$$Zs_1 = [y_{N-GI+1,1}^1 \cdots y_{N,1}^1 \ y_{1,1}^1 \ y_{2,1}^1 \cdots y_{N,1}^1 \ y_{N-GI+1,2}^1 \cdots y_{N,2}^1 \cdots y_{N,M}^1] \quad (5.25)$$

$$Zs_2 = [y_{N-GI+1,1}^2 \cdots y_{N,1}^2 \ y_{1,1}^2 \ y_{2,1}^2 \cdots y_{N,1}^2 \ y_{N-GI+1,2}^2 \cdots y_{N,2}^2 \cdots y_{N,M}^2] \quad (5.26)$$

After channel convolution the transmitted messages Xt_1 and Xt_2 can be expressed as following:

$$Xt_1 = h_1 * Zs_1 \quad (5.27)$$

$$Xt_2 = h_2 * Zs_2 \quad (5.28)$$

The received signal (R_s) is equal to the sum of both transmitted signals. Then,

$$\begin{aligned} R_s &= Xt_1 + Xt_2 \\ R_s &= h_1 * Zs_1 + h_2 * Zs_2 \end{aligned} \quad (5.29)$$

After a serial to parallel conversion the received signal will be mapped in a matrix of size $(N - GI + 1) \times M$ to form the signal R_p . Then, R of size $N \times M$ is obtained by removing the guard interval. The final signal $Xest$ of size $N \times M$ is computed by applying the FFT on R .

The interference between two RTS sub-bands is equal to the interference between any two consecutive sub-channels. Let's denotes by A_i^n the packet transmitted on the sub-band i during the period n . Figure 5.14 depicts the case of asynchronous RTS transmissions where the two packets arrive to the AP with a delay equals to d . In order to decode the packet transmitted over the first sub-band, the receiver should be synchronized on this packet (packet of interest). So the receiver will start to decode from the beginning of the GI_1 until the end of the packet over all the sub-bands. The receiver decodes A_1^n and a parts of A_2^{n-1} and A_2^n . Then the received signal R_p^1 may be expressed as following:

$$\begin{aligned} R_p &= Z_1^n + U_d Z_2^n + V_{N+GI-d} Z_2^{n-1} \\ R_p &= I_{GI} Y_1^n + U_d I_{GI} Y_2^n + V_{N+GI-d} I_{GI} Y_2^{n-1} \end{aligned} \quad (5.30)$$

Where Y_1^n is related to the packet received (or transmitted in the case of error free transmission) over the first sub-band. $U_d I_{GI} Y_2^n$ and $V_{N+GI-d} I_{GI} Y_2^{n-1}$ correspond to the decoded parts of the $(n-1)^{th}$ and n^{th} packets received on the second sub-band. U_d and V_{N+GI-d} are of size $(N + GI) \times (N + GI)$ and are expressed by the following matrices:

$$U_d = \begin{bmatrix} 0 & I_d \\ 0 & 0 \end{bmatrix}$$

¹We derive the general case where they may exist more than one RTS message on the second RTS sub-band which interferes the RTS message transmitted over the first sub-band. In the case of one RTS interferer the last term related to A_2^{n-1} should be omitted.

$$V_{N+GI-d} = \begin{bmatrix} 0 & 0 \\ 0 & I_{N+GI-d} \end{bmatrix}$$

I_{-GI} is the matrix of size $N \times (N + GI)$ which removes the guard interval, so it is composed of GI columns of zeros followed by an identity matrix. It can be expressed by:

$$I_{-GI} = [0 \quad I]$$

As the receiver is synchronized to the first sub-band, the message sent over the second sub-band is considered delayed comparing to the first message by d . Since only the asynchronism effect is considered, H_1 is equal to identity matrix and H_2 is equal to the shifted identity matrix. Once the guard interval is removed R may be expressed as following:

$$\begin{aligned} R &= Y_1^n + I_{-GI}V_{N+GI-d}I_{GI}Y_2^n + I_{-GI}U_dI_{GI}Y_2^{n-1} \\ R &= F^H X_1^n + I_{-GI}V_{N+GI-d}I_{GI}F^H X_2^n + I_{-GI}U_dI_{GI}F^H X_2^{n-1} \end{aligned} \quad (5.31)$$

At the end, the decoded signal X_{est} may be computed as following:

$$\begin{aligned} X_{est} &= FR \\ X_{est} &= X_1^n + FI_{-GI}U_dI_{GI}F^H X_2^n + FI_{-GI}V_{N+GI-d}I_{GI}F^H X_2^{n-1} \\ X_{est} &= X_1^n + QX_2^n + Q'X_2^{n-1} \end{aligned} \quad (5.32)$$

Where Q and Q' are the interference coefficients introduced by the second sub-channel on the sub-channel of interest. Then, the received signal can be expressed in matrix form as following:

$$\begin{bmatrix} \widetilde{A}_1 \\ \widetilde{A}_2 \end{bmatrix} = \begin{bmatrix} A_1^n \\ 0 \end{bmatrix} + \begin{bmatrix} Q_{11} & Q_{12} \\ Q_{21} & Q_{22} \end{bmatrix} \begin{bmatrix} 0 \\ A_2^n \end{bmatrix} + \begin{bmatrix} Q'_{11} & Q'_{12} \\ Q'_{21} & Q'_{22} \end{bmatrix} \begin{bmatrix} 0 \\ A_2^{n-1} \end{bmatrix}$$

The first matrix is related to signal and the rest present the introduced interference over the sub-channel of interest. The signal of interest can be expressed as following:

$$\widetilde{A}_1 = A_1^n + Q_{12}A_2^n + Q'_{12}A_2^{n-1} \quad (5.33)$$

The power over the sub-channel of interest may be computed as following:

$$\begin{aligned} P_{Signal} &= E[\text{trace}(A_1^n A_1^{nH})] \\ P_{Signal} &= \text{trace}(E[A_1^n A_1^{nH}]) \\ P_{Signal} &= \text{trace}(E[N_1 B_1^n (N_1 B_1^n)^H]) \\ P_{Signal} &= \text{trace}(E[N_1 B_1^n B_1^{nH} N_1^H]) \\ P_{Signal} &= \beta \text{trace}(N_1 N_1^H) = \alpha \end{aligned} \quad (5.34)$$

And the interference power as:

$$\begin{aligned} P_{Interference} &= E[\text{trace}((Q'_{12}A_2^{n-1})(Q'_{12}A_2^{n-1})^H)] + E[\text{trace}((Q_{12}A_2^n)(Q_{12}A_2^n)^H)] \\ P_{Interference} &= \text{trace}(E[(Q'_{12}N_2 B_2^{n-1})(Q'_{12}N_2 B_2^{n-1})^H]) + \text{trace}(E[(Q_{12}N_2 B_2^n)(Q_{12}N_2 B_2^n)^H]) \\ P_{Interference} &= \beta(\text{trace}(E[Q'_{12}N_2 N_2^H Q_{12}^H]) + \text{trace}(E[Q_{12}N_2 N_2^H Q_{12}^H])) \end{aligned} \quad (5.35)$$

Where,

$$\begin{aligned} \beta &= \text{trace}(E[B_1^n B_1^{nH}]) \\ \beta &= \text{trace}(E[B_1^{n-1} B_1^{n-1H}]) \\ \beta &= \text{trace}(E[B_2^n B_2^{nH}]) \\ \beta &= \text{trace}(E[B_2^{n-1} B_2^{n-1H}]) \end{aligned} \quad (5.36)$$

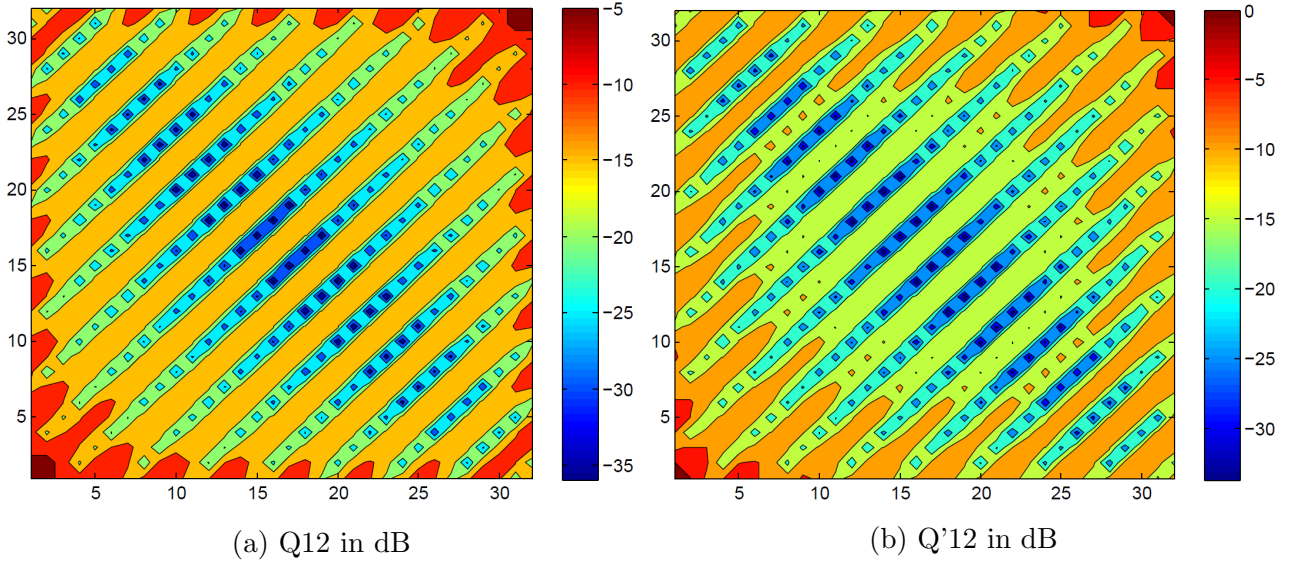


Figure 5.15: Interference matrices

Then the signal to interference ratio (considering only the interband interference) measured on the first sub-band could be expressed by:

$$\begin{aligned}
 SIR_1 &= \frac{P_{Signal}}{P_{Interference}} \\
 SIR_1 &= \frac{\alpha}{\beta(\text{trace}(E[Q'_{12}N_2N_2^H Q'_{12}{}^H]) + \text{trace}(E[Q_{12}N_2N_2^H Q_{12}{}^H]))} \quad (5.37) \\
 SIR_1 &= \frac{\text{trace}(N_2N_2^H)}{\text{trace}(E[Q'_{12}N_2N_2^H Q'_{12}{}^H]) + \text{trace}(E[Q_{12}N_2N_2^H Q_{12}{}^H])}
 \end{aligned}$$

Figure 5.15 depicts the interference matrices Q_{12} and Q'_{12} in dB considering $N=64$, $GI=16$, $M=7$ and $d=N/2$. It is seen clearly that the interference power is high across the border and it is due to the high interference caused by the near sub-carriers from the transmitted message over the second sub-band on the message of interest (transmitted over the first sub-band). Also, the values of Q' are higher than the values of Q because there is more interference coming from A_2^n than A_2^{n-1} on A_1^n .

When the delay (d) is lower than the guard interval the elements of matrices Q_{12} and Q'_{12} are equal to zero, then there is no interference from the messages transmitted over the other sub-band on the message of interest. This case englobes the synchronous and limited asynchronous (where $d \leq GI$) transmissions. Synchronous transmission considers that both RTS messages reach the receiver (AP) at the same time. It means that the transmitters are equidistant from the AP, so they put the same propagation delay to arrive to the AP. A_1^n and A_2^n are considered as RTS messages transmitted over the two RTS sub-bands (see Figure 5.16). In that case, the receiver can decode perfectly both RTS messages without any interference and also the guard interval is considered as an overhead (since both packets reach the AP at the same time).

The quasi synchronous transmission as showed in Figure 5.17 considers that the second RTS message is received after the first one with a delay (d) lower than the guard interval (GI). In that case, the receiver can decode perfectly both RTS messages without any interference and also the guard interval is considered indispensable. Of course it is possible to parametrize the PHY layer (the duration of GI) in order to always be in the case of quasi synchronous transmission. For small cell, it is possible. However if the cell is large then the overhead introduced by a large guard interval may be to the same order of the payload duration. For instance, in the case of cell size equals to 300m (considering the AP in the middle of the cell), the GI is required to be equal or above 20 samples (for a FFT size of 64) in order to combat the interference due to the packets transmissions delay at the receiver level.

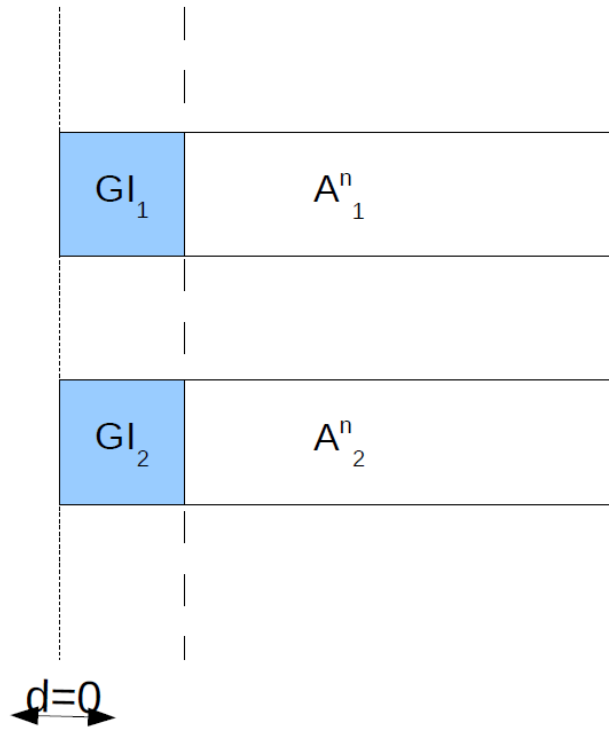


Figure 5.16: Synchronous RTS messages.

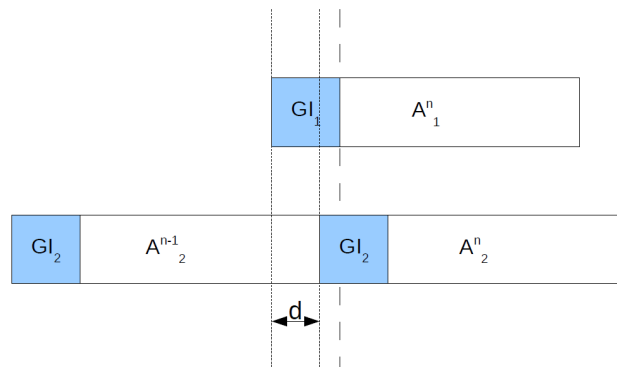


Figure 5.17: Quasi synchronous RTS messages.

Figure 5.18 depicts the SIR (dB) in function of the delay for a scenario with 2 sub-bands and QPSK modulation. It is seen clearly that the SIR tends to infinity (interference is very low) when the delay is less than the guard interval. When the delay becomes higher than GI the message transmitted over the second sub-band introduces a leakage on the first sub-band, then the SIR becomes between 16 dB and 18 dB. It should be mentioned that the nodes are assumed to transmit with the same power and face the same path loss behaviour.

5.2.4.4 Effect of asynchronous transmission and capture effect on interference level

Taking the interband interference and the capture effect into consideration, the signal to interference ratio (SIR) for node i on the sub-band k could be expressed by the below equation:

$$SIR(k, i) = \frac{P_{Signal}}{P_{Capture} + P_{Interference}} \quad (5.38)$$

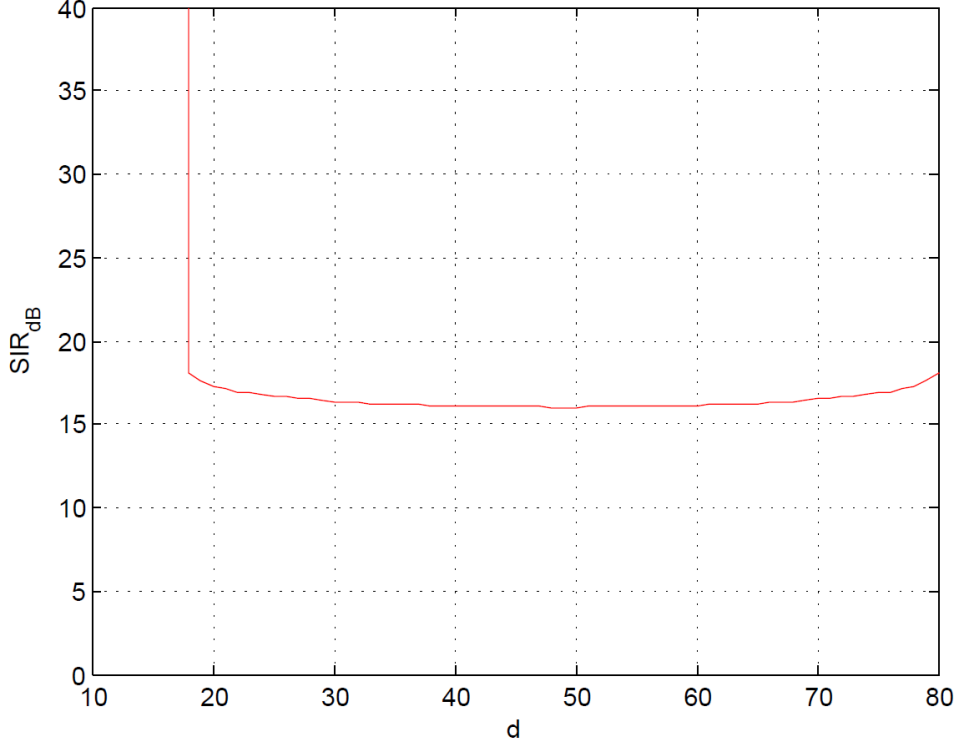


Figure 5.18: SIR (dB) vs. d.

Where P_{Signal} is the received power at the AP of the signal of interest (i) transmitted over the sub-band k , $P_{Capture}$ is the received power of all the interferent signals transmitted over the sub-band k and $P_{Interference}$ is the power of the interferent signals transmitted over the adjacent sub-band ($k-1$ or $k+1$). Hence, the SIR can be expressed by the following equation:

$$SIR(k, i) = \frac{P_R(k, i)}{\sum_{\substack{j=1 \\ j \neq i}}^{g_k} P_R(k, j) + \sum_{\substack{p=1 \\ p \neq k}}^n \sum_{j \in E_p} I(p, j, d_k(j, i))} \quad (5.39)$$

where E_p is the group of transmitters who choose the sub-band p for RTS transmission and $d_k(j, i)$ is the delay between the two RTS transmitted from node i and node j at the receiver side. I is the interference introduced from the band p over the band of interest k . n is the number of sub-bands and g_k is the number of transmitters nodes (backoff=0) over the sub-band k . Considering the case of two sub-bands, the SIR may be expressed as following:

$$SIR(1, i) = \frac{P_R(1, i)}{\sum_{\substack{j=1 \\ j \neq i}}^{g_1} P_R(1, j) + \sum_{j=1}^{g_2} L(2, j) P_R(2, j)} \quad (5.40)$$

Where $L(2, j)$ is the leakage introduced from the sub-band 2 on the sub-band 1 when the node j transmits its message on the sub-band 2. The leakage may be computed as follows:

$$L(2, j) = \frac{\text{trace}(E[Q'_{12} N_2 N_2^H Q'_{12}]) + \text{trace}(E[Q_{12} N_2 N_2^H Q_{12}])}{\text{trace}(N_2 N_2^H)} \quad (5.41)$$

Figure 5.19 depicts the Leakage (dB) introduced by the second sub-band on the sub-band of interest in function of the delay (d). It is seen clearly that there is no leakage when delay is lower than the guard interval ($d \leq GI$).

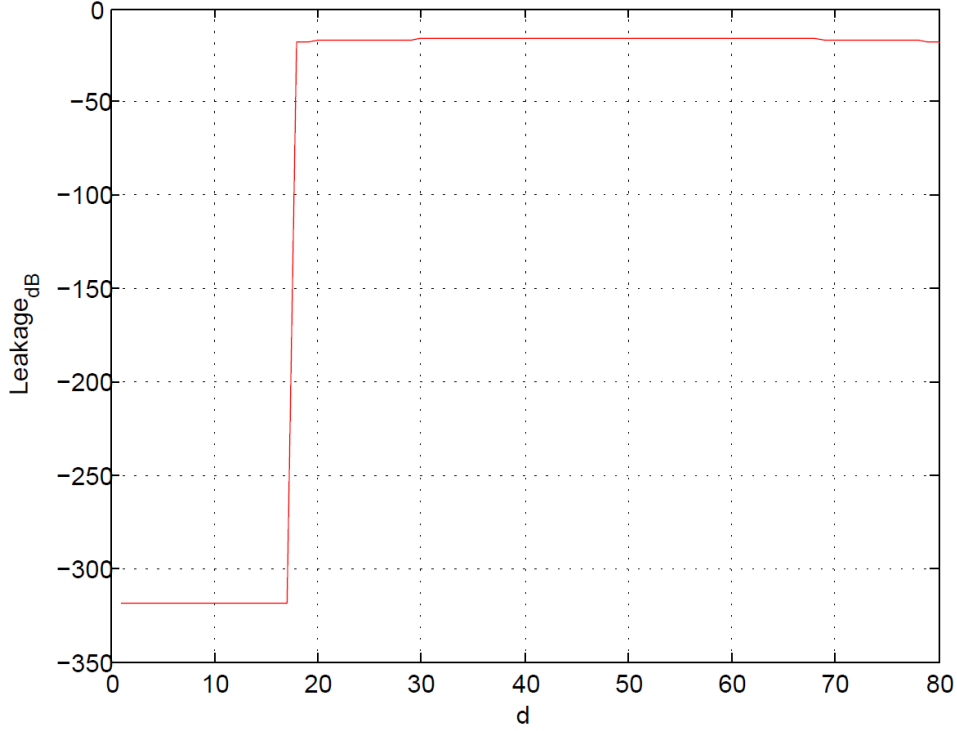


Figure 5.19: Leakage (dB) vs. d.

If the nodes have equal power transmission, the SIR could be expressed by the following equation:

$$SIR(1, i) = \frac{\frac{1}{R_i^\alpha}}{\sum_{\substack{j=1 \\ j \neq i}}^{g_1} \frac{1}{R_j^\alpha} + \sum_{j=1}^{g_2} \frac{L(2,j)}{R_j^\alpha}} \quad (5.42)$$

Where R_i is the distance between the transmitter and the AP and α is the path loss.

5.2.4.4.1 Numerical application on simplified scenario We give in this paragraph a numerical application which explains the theoretical derivations. Figure 5.20 depicts the scenario of a configuration of 5 nodes ready for transmission (backoff=0) enumerated from 1 to 5 and an AP which is located in the center of the cell. The cell radius is equal to 300m and nodes are distributed around the AP with distances equal to $R_1=1m$, $R_2=270m$, $R_3=50m$, $R_4=120m$ and $R_5=300m$. The path loss is equal to $\alpha = 2.8$ and the threshold $\gamma = 10dB$. Let's consider the case of single band CSMA/CA-RTS/CTS with capture effect. Then,

$$\begin{aligned} SIR(1) &= 47.1505dB \\ SIR(2) &= -68.0783dB \\ SIR(3) &= -47.5712dB \\ SIR(4) &= -58.2172dB \\ SIR(5) &= -69.3595dB \end{aligned} \quad (5.43)$$

It is seen clearly from the above SIR values that the closest node to the AP has the highest SIR . Since the node 1 is the only one between the considered nodes which has the SIR higher than 10dB, the AP is able to decode only the RTS message received from node 1. CTS message will be broadcasted to all nodes indicating that node 1 is allowed to transmit its data. All the RTS messages transmitted from the other nodes are considered as noise. In this case a RTS collision is avoided and the other nodes can never success to transmit if node 1 wants to transmit.

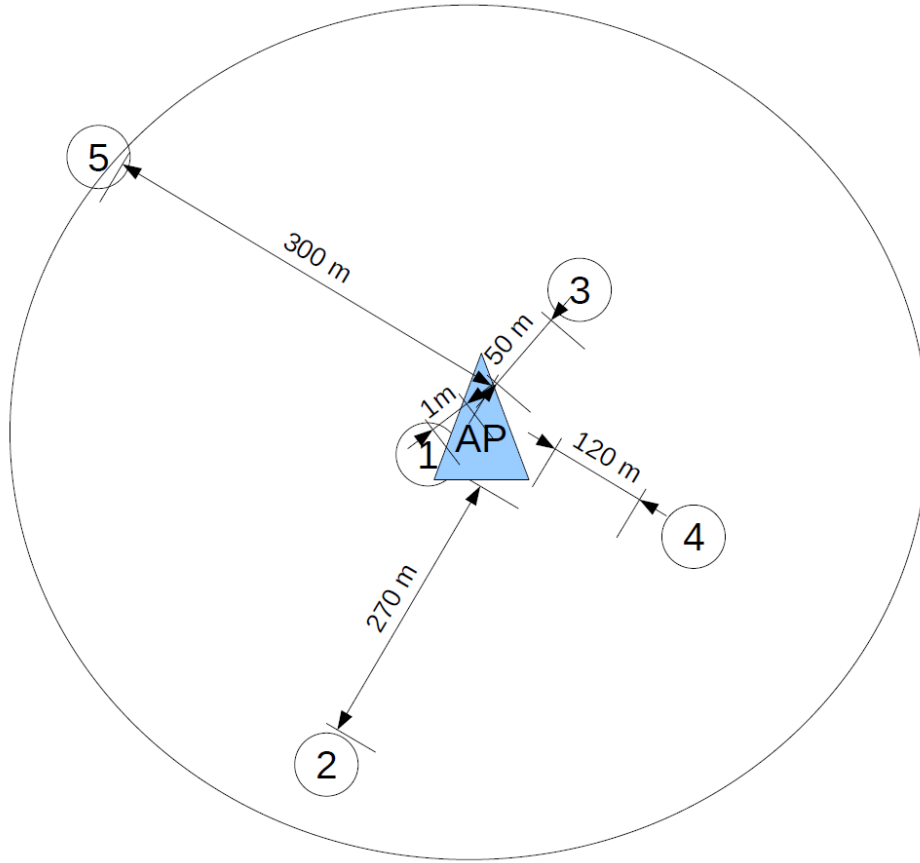


Figure 5.20: Application scenario.

Let's consider the case of M-CSMA/CA-RTS/CTS with 2 sub-bands where the nodes 1 and 2 choose the first sub-band and the other nodes choose the second sub-band. Taking into account the capture effect with the interband interference and $GI=8$, the SIR values are:

$$\begin{aligned}
 SIR(1) &= 68.0064dB \\
 SIR(2) &= -68.0782dB \\
 SIR(3) &= 10.3157dB \\
 SIR(4) &= -10.6752dB \\
 SIR(5) &= -52.8656dB
 \end{aligned}
 \tag{5.44}$$

It is seen clearly that the AP can decode the RTS messages transmitted from node 1 and 3 over the sub-band 1 and 2 respectively. Based on this configuration the AP can serve the node 1 or 3 and not only the node 1 (in the case of single band CSMA/CA). If $GI = 16$ the above SIR values are a little bit higher because the leakage introduced from each sub-band on the other one is lower due to a higher "asynchronous margin". Hence, the SIR can take the following values:

$$\begin{aligned}
 SIR(1) &= 68.0172dB \\
 SIR(2) &= -68.0782dB \\
 SIR(3) &= 10.3243dB \\
 SIR(4) &= -10.6746dB \\
 SIR(5) &= -52.1513dB
 \end{aligned}
 \tag{5.45}$$

The nodes 1 and 3 are decoded at the AP level with lower interference.

According to the above configuration, it is seen that several nodes are able to be decoded at the AP level with the M-CSMA/CA-RTS/CTS. Hence, the winner is not always the same

MCS index	Coding rate	Modulation
0	1/2	QPSK
1	2/3	QPSK
2	3/4	QPSK
3	1/2	16QAM
4	2/3	16QAM
5	3/4	16QAM
6	1/2	64QAM
7	2/3	64QAM
8	3/4	64QAM

Table 5.2: List of MCS Index Values.

(case of single band CSMA/CA-RTS/CTS) because it depends from the choice of nodes to the sub-bands and from the choice of the AP to the winner.

5.3 Performance analysis

In this Section we analyze the system performance taking into consideration the physical layer described in the previous Section. We evaluate by simulations the saturation throughput in Mbits/sec taking into account the capture effect and the asynchronism transmissions. A Modulation and Coding Scheme (MCS) index is defined to describe the combination of the modulation and coding scheme that are used when transmitting data. Table 5.2 illustrated the MCS mapping.

In this study we consider that the MCS related to the RTS and CTS is the same and is equal to 0. In fact, the robust MCS shall be used to guarantee that all users present in the system are capable to decode the synchronization messages without errors related to transmission conditions.

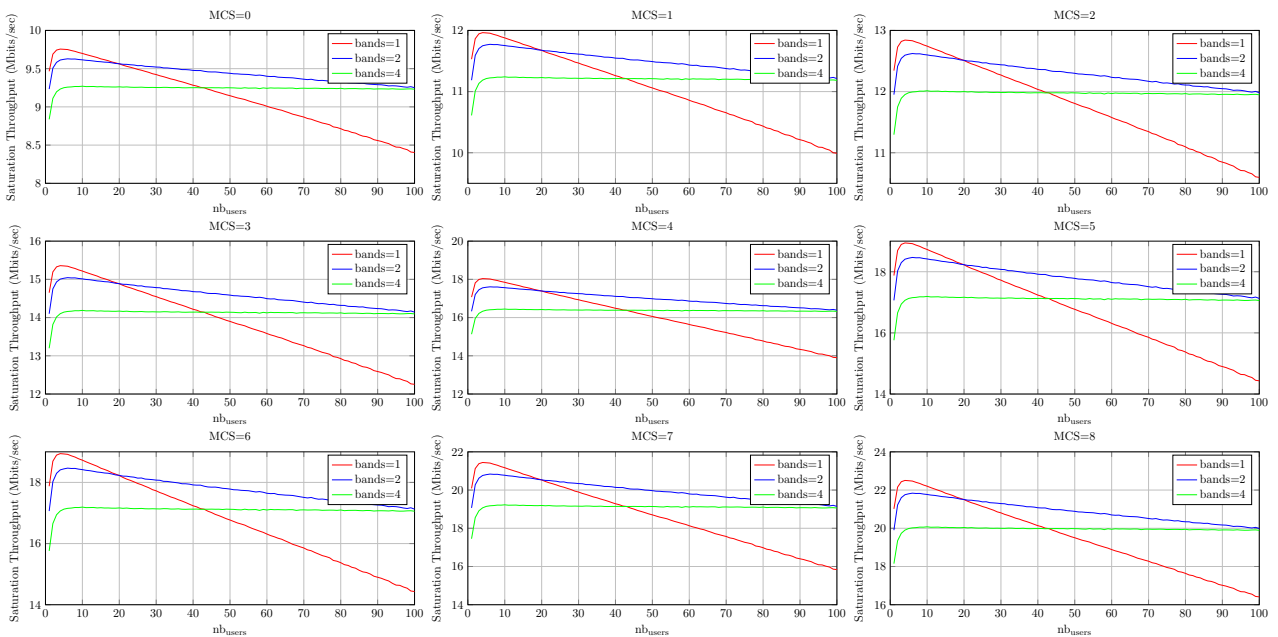


Figure 5.21: Saturation throughput in Mbits/s for various number of users and for all MCS index with GI=8.

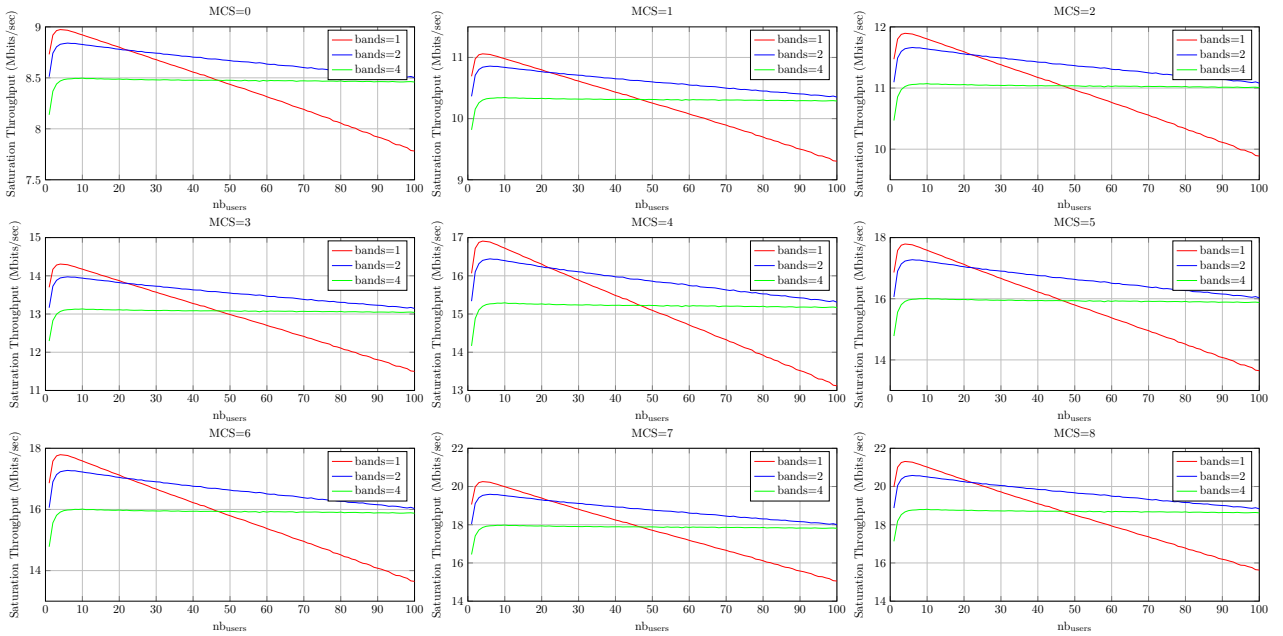


Figure 5.22: Saturation throughput in Mbits/s for various number of users and for all MCS index with GI=16.

5.3.1 Physical layer

Taking into account the effect of the physical layer (perfect transmission but with the exact duration of each packet depending on the MCS), Figures 5.21 and 5.22 depict the achievable physical layer throughput in Mbits/s for various number of users and for all MCS index with GI=8 and GI=16. Like MAC study the throughput degrades drastically when the number of users is high especially for CSMA/CA - RTS/CTS. It is shown that increasing the number of sub-bands the throughput becomes more important than the single band CSMA/CA - RTS/CTS especially for dense networks. For a scenario up to 100 nodes in saturation conditions, two RTS sub-bands are sufficient to reduce the RTS collision probability without introducing high overhead. Also, for lower guard interval and higher MCS the throughput is higher. The presence of large guard interval increases the overhead which reduces the useful bitrate.

5.3.2 Capture effect

In this Section we evaluate the system performance where the capture effect is addressed. The nodes are distributed with a long range scenario ($\gamma = 2.8$ [77]) in a cell of radius equals to 300m. They are supposed to transmit with the same power level. AWGN and fading model D channels [79] are considered in this study. Model D channel [79] is considered for large open space (indoor and outdoor), non-line-of-sight (NLOS) conditions, and 140 ns rms delay spread. In order to decode the packets at the receiver side and considering AWGN channel with Packet Error Rate Target (PERT) equals to 10^{-2} , the SIR should be higher than 4dB (2dB) in the case of convolutional QPSK (LDPC QPSK) modulation with $R = 1/2$ [80]. Knowing that we don't consider any imperfect transmission or noise effect, we can consider that the loss caused by imperfect implementation (front end, linearity,...) is about 1.5dB. Then the new thresholds become $Th_1 = 3.5dB$ and $Th_2 = 5.5dB$. Adding the capture effect on the physical layer, Figures 5.23 and 5.24 (5.25 and 5.26) depict the related saturation throughput in Mbits/s for various number of users and for all MCS index with GI=8 and GI=16 for a threshold equals to $Th_1 = 3.5dB$ ($Th_2 = 5.5dB$). It is shown clearly that using lower guard interval and higher MCS the throughput becomes higher. The presence of large

guard interval increases the overhead which reduces the useful bitrate. Also, when capture effect is introduced the number of RTS collisions is reduced because the receiver (AP) is able to decode the RTS messages if their SIR is higher than the considered threshold. Even if several RTS messages are transmitted over a defined band or sub-band, the probability of decoding at least one RTS correctly is not zero (while it was considered as collision in the case of MAC study). Since the main goal of M-CSMA/CA-RTS/CTS is to reduce the RTS collision probability, capture effect reduces by nature the collision probability, Figures 5.23, 5.24, 5.25 and 5.26 show that there is no need to consider the proposed protocol (only if there is interest in other criteria like fairness,...) for low SIR thresholds (throughput of single band CSMA/CA-RTS/CTS outperforms the M-CSMA/CA-RTS/CTS for a scenario up to 100 nodes in saturation conditions). Moreover, it is clearly seen that when the SIR threshold is higher the throughput becomes lower and it is due to higher number of RTS collision presents in the system. Hence, the M-CSMA/CA-RTS/CTS becomes better than the single band CSMA/CA-RTS/CTS for dense scenarios (where the RTS collision is important).

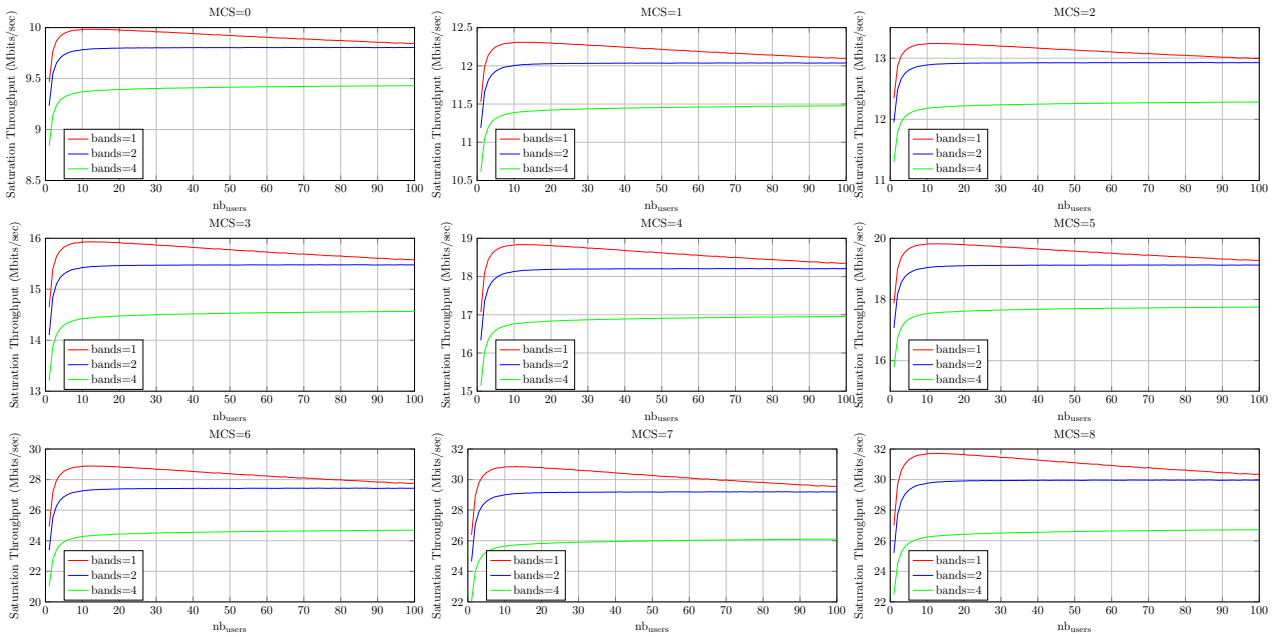


Figure 5.23: Captured saturation throughput in Mbits/s for various number of users and for all MCS index with $GI=8$ and $Th=3.5dB$.

In the case of Fading Channel Model D with power delay profile as defined in [79], NLOS, without simulation of Doppler spectrum, the simulation scenario assumed:

1. Ideal channel estimation
2. All packets detected, ideal synchronization, no frequency offset
3. Ideal front end, Nyquist sampling frequency

the SIR should be higher than $Th_1 = 10dB$ ($Th_2 = 12dB$) in the case of convolutional QPSK (LDPC QPSK) modulation with $R = 1/2$ [80] in order to decode the packets at the receiver side. Adding the loss caused by imperfect implementation, the new thresholds become $Th_1 = 11.5dB$ and $Th_2 = 13.5dB$. Figures 5.27 and 5.28 (5.29 and 5.30) show that when the threshold increases the throughput decreases and it is due to the lower number of decoded RTS (if RTS is not decoded there will be no packet transmission). Having a threshold equals to infinity the decoder cannot decode a captured RTS message, hence the system performance will be the same as the MAC studied in Chapter 3. In that case, it is seen clearly the importance of the M-CSMA/CA-RTS/CTS where the saturation throughput

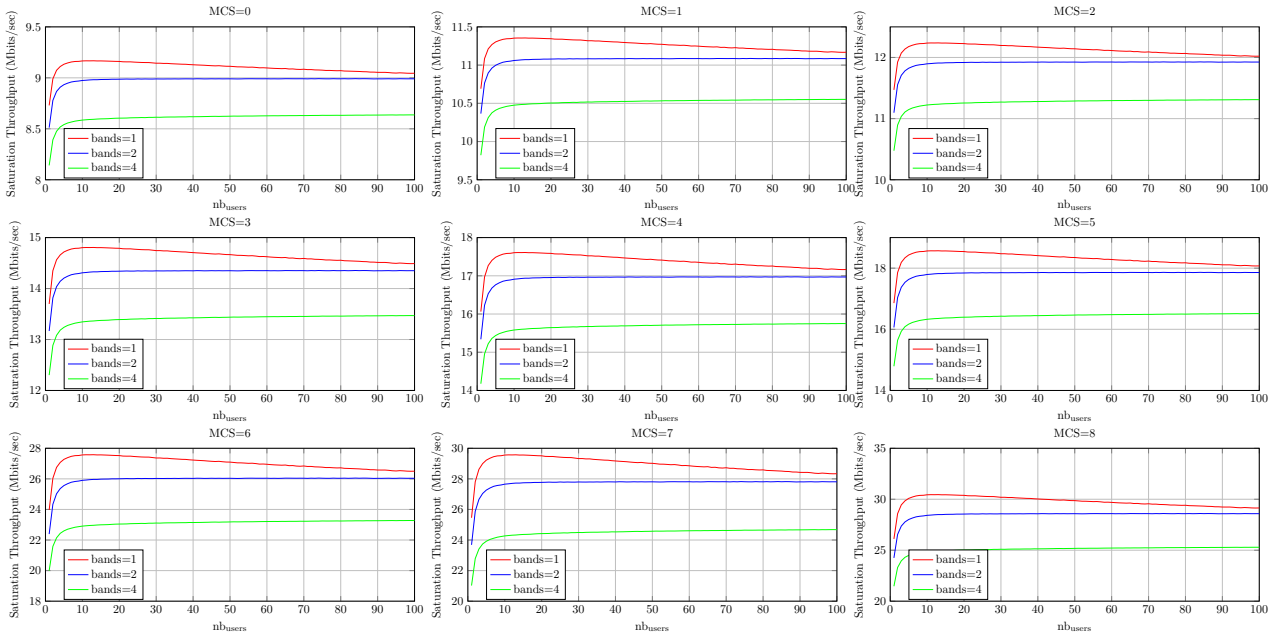


Figure 5.24: Captured saturation throughput in Mbits/s for various number of users and for all MCS index with $GI=16$ and $Th=3.5dB$.

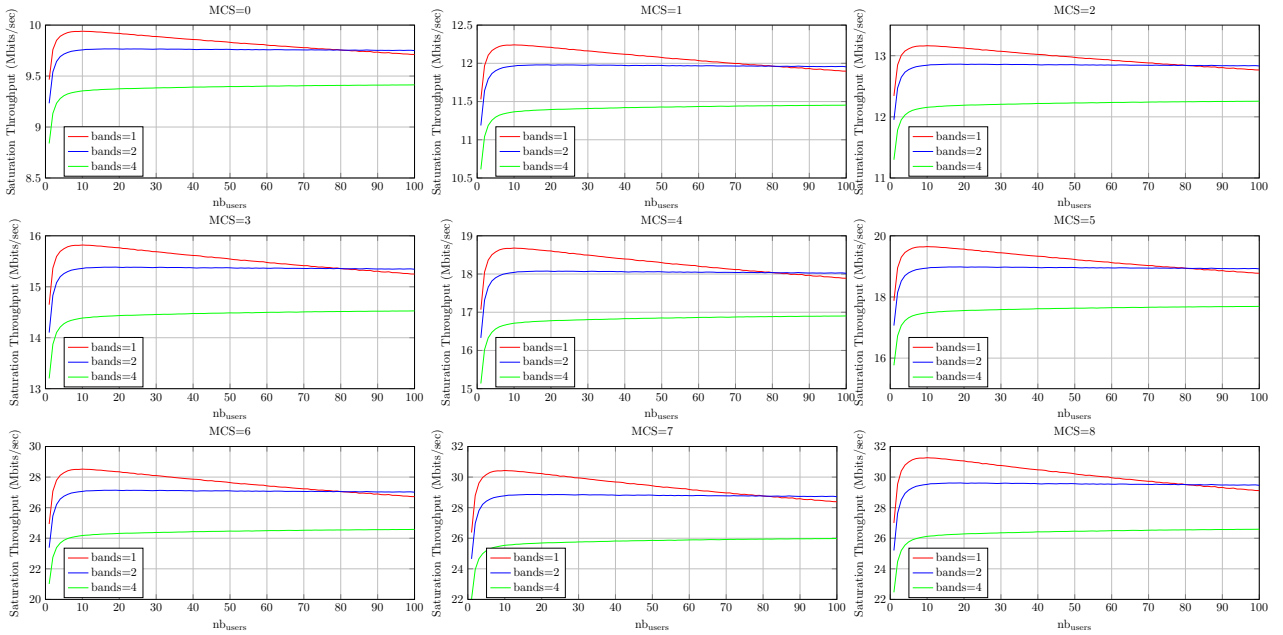


Figure 5.25: Captured saturation throughput in Mbits/s for various number of users and for all MCS index with $GI=8$ and $Th=5.5dB$ for AWGN channel.

is higher by 2Mbits/sec (MCS=8) for dense scenario (100 nodes) comparing to the single band CSMA/CA-RTS/CTS.

5.3.2.1 Successful Transmission Ratio

Considering that all nodes transmit with equal power and due to the path loss, the received power at the AP depends on the position of each node. Due to capture effect, the nodes which are located close to the AP will have higher priority than the far ones to be served due to the channel conditions. For that reason, we propose to compare the ratio of served nodes depending on their positions for the single band and the M-CSMA/CA-RTS/CTS. In

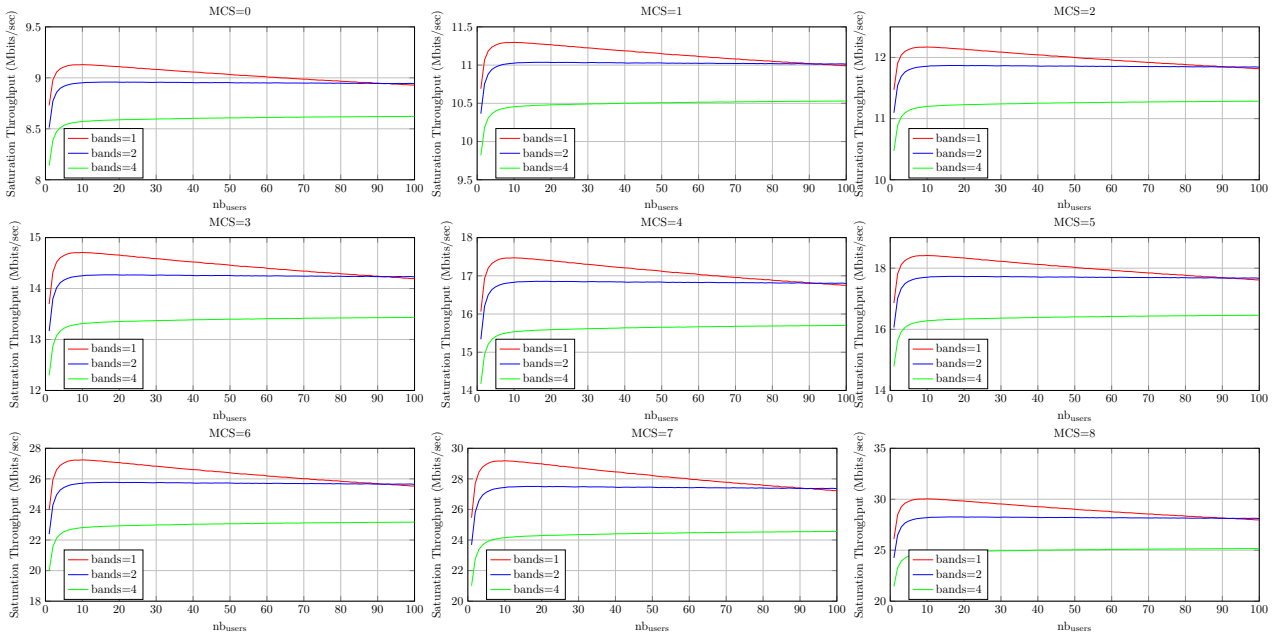


Figure 5.26: Captured saturation throughput in Mbits/s for various number of users and for all MCS index with GI=16 and Th=5.5dB for AWGN channel.

this part, we compare the successful transmission ratio (STR) of the single band and the M-CSMA/CA-RTS/CTS regarding the distance for 100 active nodes (dense scenarios). The STR which is function of the distance between the node and the AP (r) is the average ratio between the number of successful transmission and the number of transmission for a defined distance. It can be expressed by the following equation:

$$STR(r) = E \left[\frac{\text{Number of transmitted DATA}(r)}{\text{Number of transmitted RTS}(r)} \right] \quad (5.46)$$

Considering a circular map of radius equal to 300m, Figures 5.31 and 5.32 depict the STR of the single band and M-CSMA/CA-RTS/CTS with 2 sub-bands for the case of AWGN and D fading channels.

For single band CSMA/CA-RTS/CTS, when r increases the STR decreases. It means that the best STR values correspond to the case when the node is closer to the AP. It can be explained because the closest node captures the channel and all the other transmissions are treated as interference at the receiver side. When the threshold is higher this effect is multiplied. The probability of successful transmission for far nodes is very low which deteriorates their QoS. Since M-CSMA/CA-RTS/CTS allows nodes to transmit their RTS messages on different sub-bands, the nodes which are far from the AP have better probability to transmit with success than the case of single band (i.e. RTS with lower power could arrive alone to a sub-band, hence it has a probability to be served).

It is clear that the M-CSMA/CA-RTS/CTS allows nodes to transmit even if they are at the cell border. Then, the M-CSMA/CA-RTS/CTS can guarantee a better QoS than the single band CSMA/CA-RTS/CTS for far nodes. This analysis is valid for the both channels type: AWGN and D fading. It should be mentioned that the duration of packet transmission is equal for all nodes. It means that the node should adapt its packet size depending on its position and on the channel conditions [81]. Hence, the node which uses higher MCS their packets will be longer than the node using a low MCS. Since the duration is maintained equal for all nodes, the nodes close to the AP will not be affected by the slower nodes.

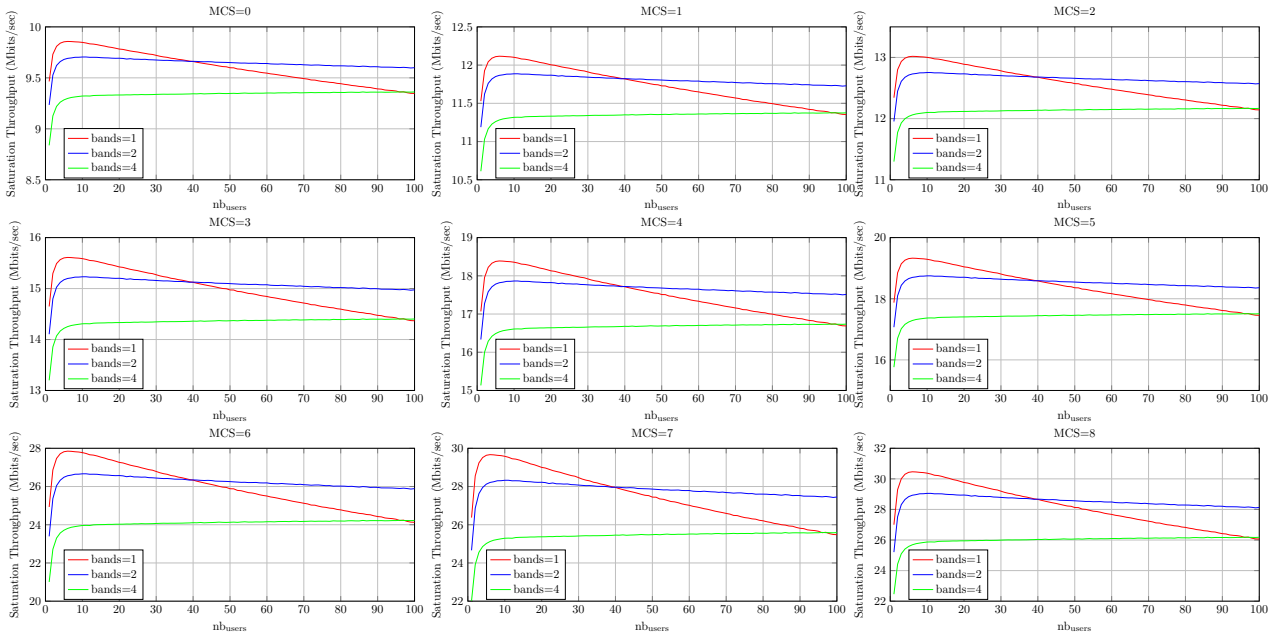


Figure 5.27: Captured saturation throughput in Mbits/s for various number of users and for all MCS index with $GI=8$ and $Th=11.5\text{dB}$ for D fading channel.

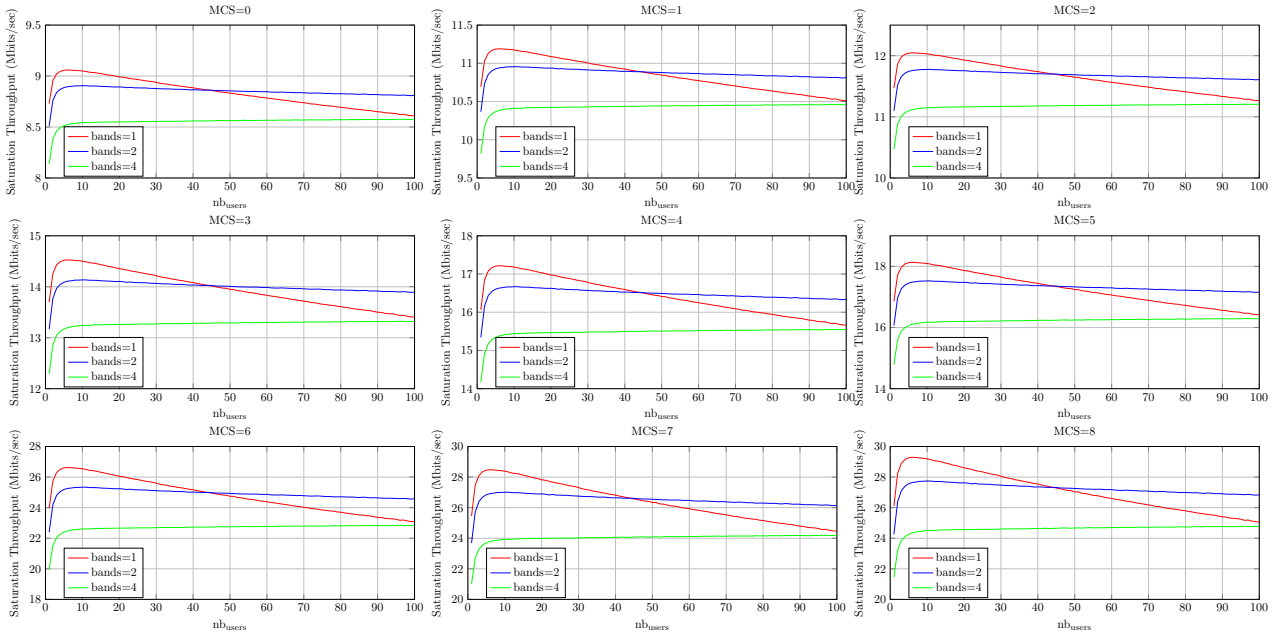


Figure 5.28: Captured achievable throughput in Mbits/s for various number of users and for all MCS index with $GI=16$ and $Th=11.5\text{dB}$ for D fading channel.

5.3.3 Asynchronous transmission

In this part, the effect of asynchronous transmission is evaluated by considering the case of two RTS sub-bands where each sub-band introduces a leakage on the other one. We study the interband interference for the case of AWGN and D fading channels with their related SIR thresholds. Figures 5.33 and 5.34 depict the saturation throughput in Mbits/s in function of the number of users for all MCS index considering interband interference with different guard interval for both type of channels: AWGN and fading D. As discussed in the previous Section, the saturation throughput for AWGN channel is higher than the saturation throughput for D fading channel because the SIR threshold is lower which makes the receiver able to decode

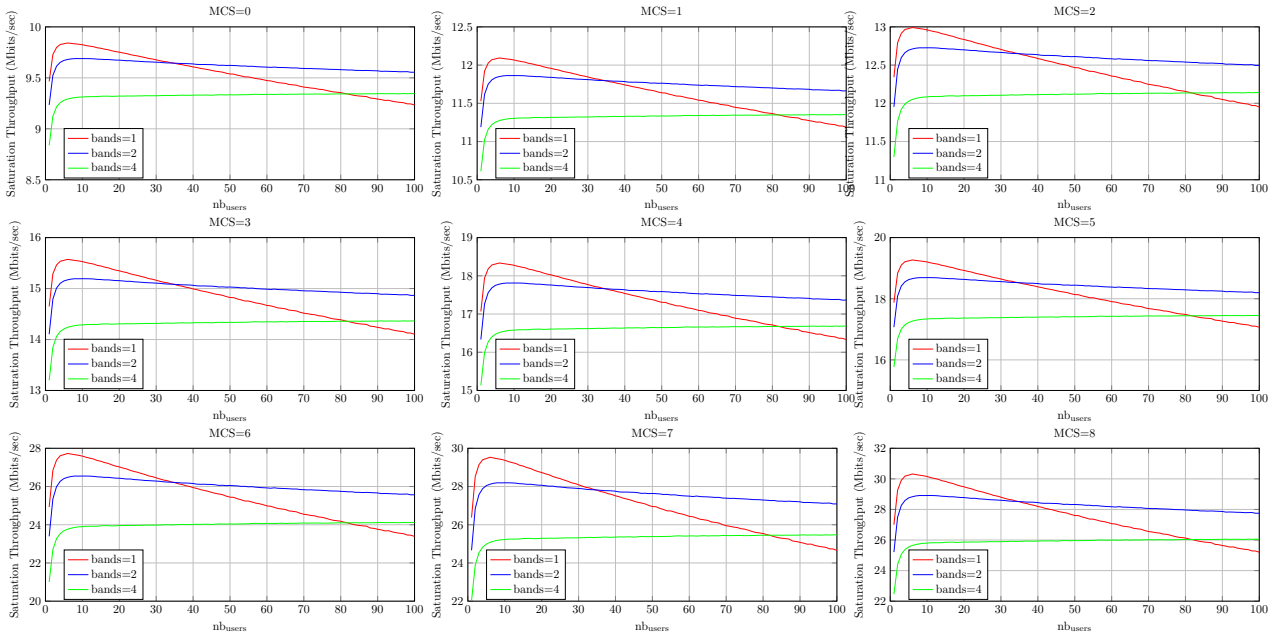


Figure 5.29: Captured saturation throughput in Mbits/s for various number of users and for all MCS index with GI=8 and Th=13.5db.

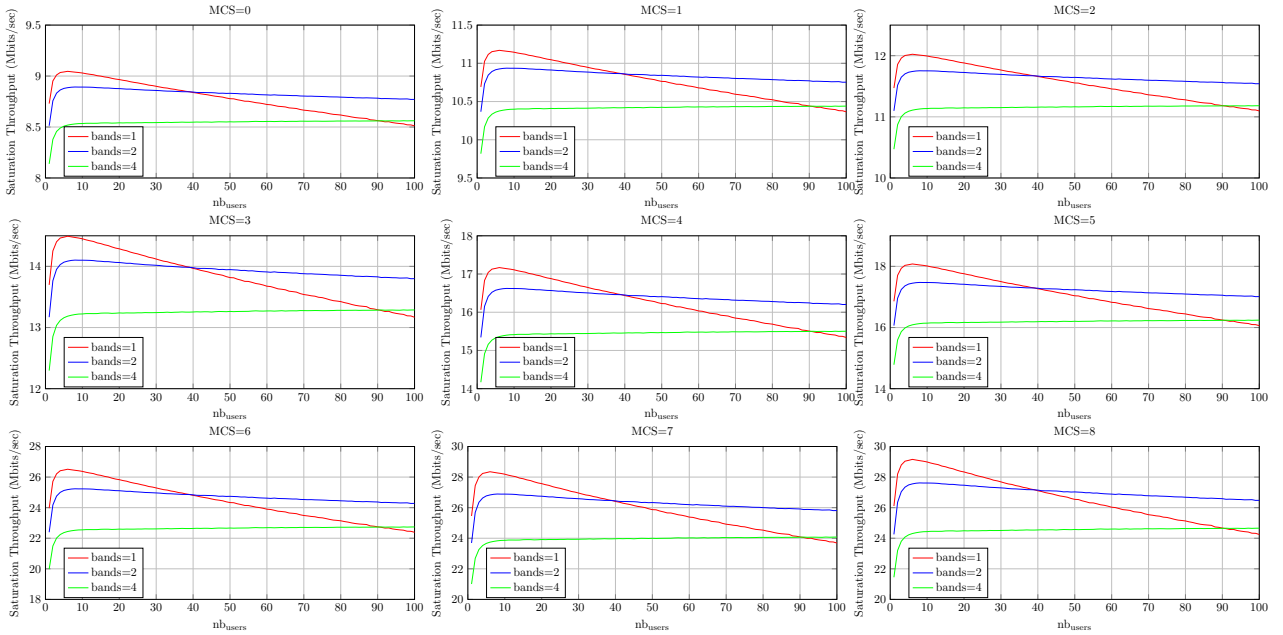


Figure 5.30: Captured saturation throughput in Mbits/s for various number of users and for all MCS index with GI=16 and Th=13.5db.

better the interfered RTS messages. High guard intervals introduce more overhead which reduce the saturation throughput. Also, Figures 5.33 and 5.34 show that when asynchronous transmissions are considered the saturation throughput is a little bit lower than the case of capture effect and it is due to the leakage introduced from each sub-channel to the other one. It is shown as well that even in the case of interband interference the saturation throughput of M-CSMA/CA-RTS/CTS (2 sub-bands are considered) is always higher than the single band CSMA/CA-RTS/CTS in dense network especially for D fading channels.

This study shows that the M-CSMA/CA-RTS/CTS has better performance than the single band CSMA/CA-RTS/CTS especially in the case of dense scenarios and when the *SIR* threshold is high. Moreover, it is clear that considering low guard interval is better in terms of

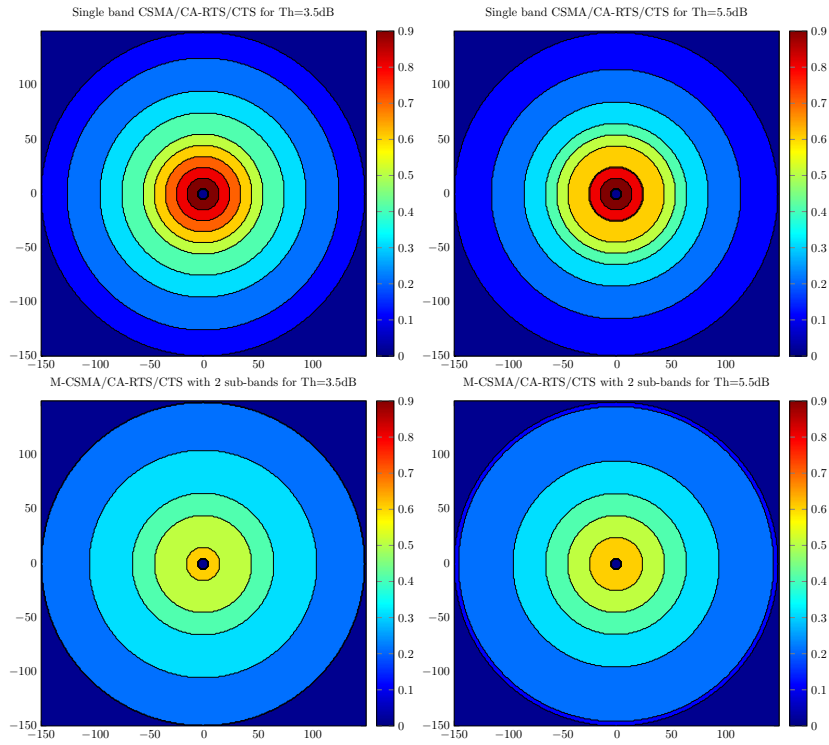


Figure 5.31: STR for AWGN Channel with circular map of radius = 300m, x and y axis presents the cartesian coordinates.

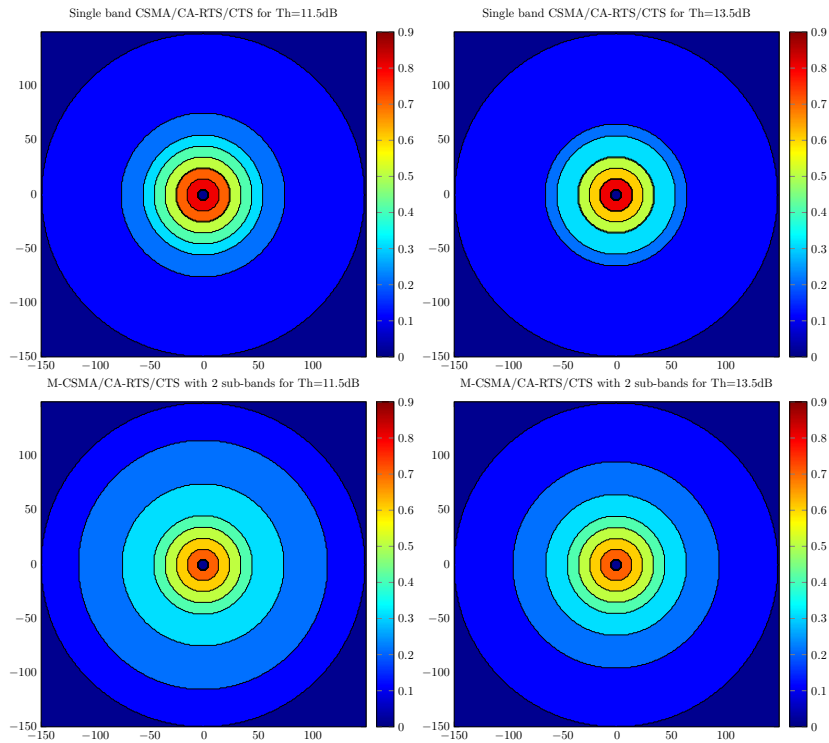


Figure 5.32: STR for D Fading Channel with circular map of radius = 300m, x and y axis presents the cartesian coordinates.

saturation throughput because the interference caused by a sub-band on the other one is not very important. It means that high guard interval deteriorates the performance more than the leakage introduced from sub-bands.

We have also studied other multicarrier waveform which offers a better frequency localiza-

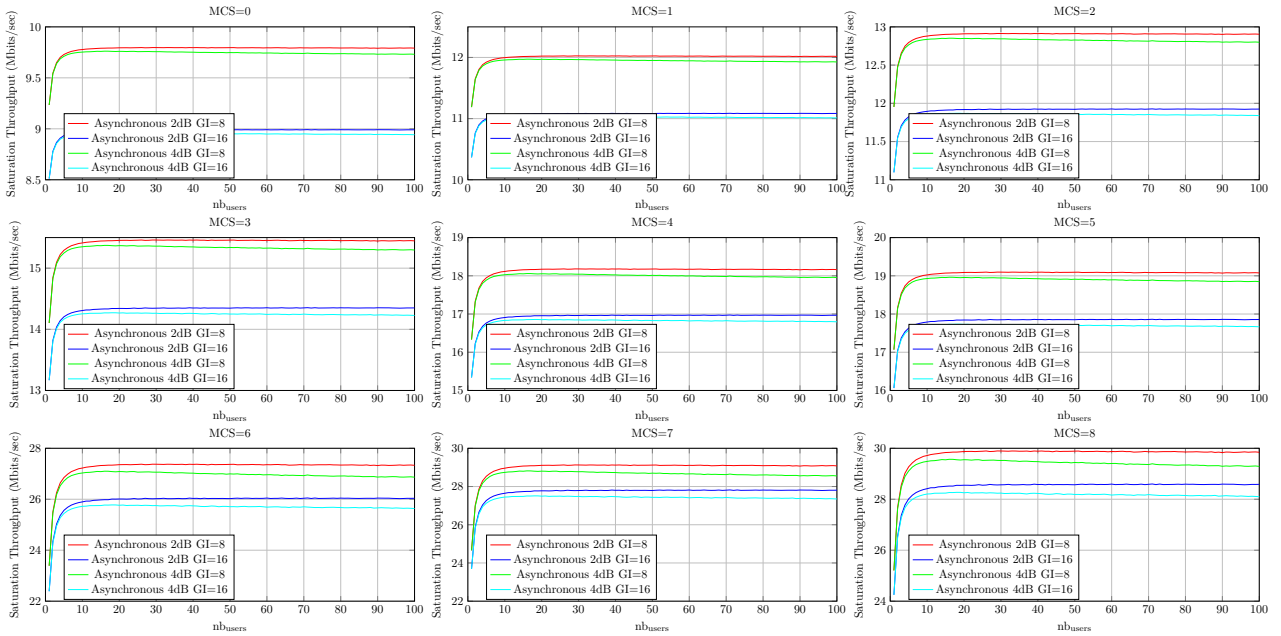


Figure 5.33: Saturation throughput in Mbits/s vs. number of users for all MCS index considering interband interference with different guard interval for AWGN channel.

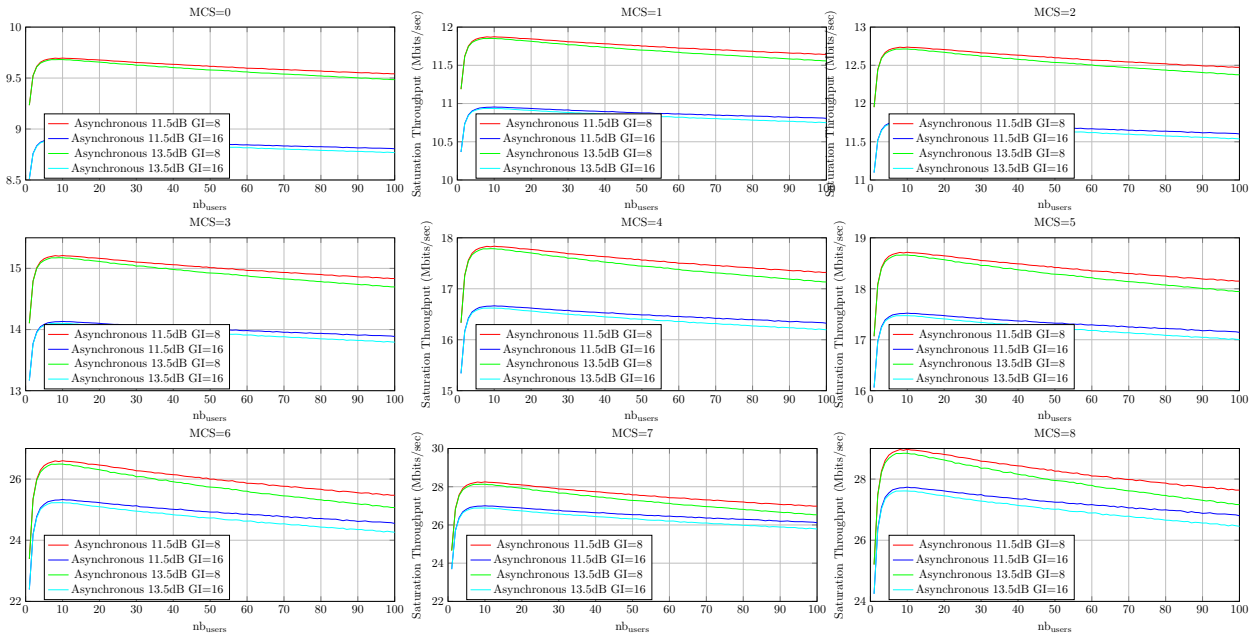


Figure 5.34: Saturation throughput in Mbits/s vs. number of users for all MCS index considering interband interference with different guard interval for D fading channel.

tion and doesn't require a guard interval [82]. This study relies on the Filter Bank Multicarrier Modulations (FBMC) which is not addressed in this thesis [83]. A tradeoff between the time/frequency localization should be studied especially for short packets transmission.

5.4 Conclusion

In this chapter the effect of the physical layer on the M-CSMA/CA-RTS/CTS is investigated and a complete PHY-MAC analytical model is derived. The study considers a physical layer with capture effect and asynchronous transmission. The system performance is evaluated

by simulations and compared to the single band CSMA/CA-CA/RTS-CTS considering two type of channels (AWGN and D fading). Performance analysis has demonstrated that the M-CSMA/CA-RTS/CTS has better performance than the single band CSMA/CA-RTS especially when the SIR is high; it is due to the high number of RTS collisions taken into account. However, for unloaded networks and for low SIR threshold the single band outperforms the M-CSMA/CA-RTS/CTS. Moreover, we show that the M-CSMA/CA-RTS/CTS introduces better QoS for far nodes comparing to the single band CSMA/CA-RTS/CTS since it allows far nodes to transmit even in the presence of closer nodes to the AP while it is not the case for the single band CSMA/CA - RTS/CTS. Also it is shown that the guard interval introduces an important overhead which reduces the saturation throughput. Hence, it is suggested to use different multicarrier modulations which don't require a guard interval. To conclude, the M-CSMA/CA-RTS/CTS introduces a real improvement of the current standard 802.11 and allows to guarantee better throughput especially in dense scenarios and where the SIR threshold is high.

Chapter 6

Conclusions and Future works

6.1 Conclusions

This thesis analyzes the behavior of CSMA/CA - RTS/CTS access methods when a large number of nodes try to communicate simultaneously. In the first part of the thesis, we have introduced the research motivations and the background that resulted in the different contributions of this dissertation. Since the CSMA/CA protocol is the heart of this work, the theory of CSMA/CA has been introduced as a basis for the rest of the thesis. Additionally, several contributions to enhance the CSMA/CA performance have been discussed in Chapter 2.

In Chapter 3, we have illustrated that the high number of nodes presents in the network can cause a performance degradation when the CSMA/CA - RTS/CTS is considered. This loss of performance can be explained by the high level of probability of collision. In order to reduce this collision probability we have proposed a novel access method. The proposed model relies on the Multiband CSMA/CA - RTS/CTS protocol based on orthogonal RTS transmissions over different channels. According to this model, we have derived the closed-form expressions of the saturation throughput under some conditions for both case: finite and infinite retransmission limit. The analytical model has been validated by numerical simulations. Then, the system performance has been analyzed in terms of saturation throughput, transmission delay and packet drop probability. The results have showed that the proposed scheme is able to increase the saturation throughput, decrease transmission delay and packet drop probability especially in scenario of dense networks. For instance, when considering 3 RTS sub-channels with 100 nodes, we can achieve 70% of gain in terms of collision probability, 30% in terms of saturation throughput and 40% in terms of transmission delay. The packet drop probability is divided by 3 as well. This scheme seems to be adapted for crowded scenarios with random access. It could be suitable for M2M scenarios in dense metropolitan or regional networks. We have also evaluated the upper bounds of CSMA/CA access methods and we have proven that the performance of the proposed scheme could bridge the gap. Then, we have compared two allocation strategies and we have proven that the pre-allocation technique with uniform repartition of nodes becomes asymptotically equivalent to the post-allocation strategy when the number of nodes towards to infinity.

In Chapter 4, the Multiband CSMA/CA - RTS/CTS has been enhanced and a scheduling technique has been introduced to serve several winners. This scheme has the advantage of reducing the overhead introduced by the channel access round. We have proven by simulations that the proposed strategy reaches the contention based upper bound and is able to achieve very high gain in terms of saturation throughput, transmission delay and packet drop probability. It mitigates the overhead (additional time needed to transmit the data packet) and it also decreases the number of idle slots. Since the gain is very important in loaded networks, the proposed strategy may be adapted to scenarios where very high number of nodes communicate simultaneously. Eventually, a synthesis was given to compare the behavior of

the classical, Multiband CSMA/CA - RTS/CTS and the scheduled Multiband CSMA/CA - RTS/CTS in loaded and unloaded network scenarios. In the case of loaded networks the M-CSMA/CA-RTS/CTS reduces the overhead and has better system performance (i.e. saturation throughput, transmission delay ...) than the CSMA/CA-RTS/CTS. Introducing the scheduled M-CSMA/CA-RTS/CTS the performance is enhanced and the overhead is further reduced especially for loaded networks which is suitable to the context of our proposed work. In the case of unloaded network, the overhead introduced by the CSMA/CA-RTS/CTS is lower than the others because the RTS messages in the case of CSMA/CA-RTS/CTS are shorter than the RTS messages in the case of M-CSMA/CA-RTS/CTS and scheduled M-CSMA/CA-RTS/CTS. The Multiband CSMA/CA - RTS/CTS and its scheduled version have been investigated respectively in Chapter 3 and 4 assuming a perfect physical layer. In order to understand the effects of the physical layer on the performance, a joint PHY-MAC study should be achieved as well.

Chapter 5 relies on a joint PHY-MAC study of the Mutiband CSMA/CA - RTS/CTS. First, we have described the physical layer according to the IEEE 802.11n standard. Then, we have derived a complete model related to the physical layer, capture effect and interband interference caused by asynchronous transmission. The performance of the system has been evaluated by simulations and has been compared to the CSMA/CA-CA/RTS-CTS considering two types of channels (AWGN and D fading). Performance analysis has showed that the M-CSMA/CA-RTS/CTS keeps better performance compared to CSMA/CA-RTS for dense scenarios and especially when the *SIR* threshold is high. Moreover, we have demonstrated that the M-CSMA/CA-RTS/CTS is more “spatially fair” compared to the CSMA/CA-RTS/CTS. It allows far nodes to transmit even in the presence of closer nodes to the AP with more probability of success; it is not the case for the CSMA/CA - RTS/CTS. To conclude, the M-CSMA/CA-RTS/CTS introduces a real improvement of the current 802.11 access method and allows to guarantee better throughput especially in dense scenarios.

6.2 Suggestions for future works

A number of interesting topics, based on the research issues studied in this thesis, could be addressed. We provide some suggestions of possible extensions to the work presented in this dissertation:

1. The analytical model derived in chapter 3 assumes that collisions happened only at the MAC level “Binary Collision” and it does not take into consideration the effect of imperfect channel transmission. It may be interesting to extend the model to take into consideration the effects of more realistic communications.
2. The proposed scheduling technique in chapter 4 has been evaluated by simulations only. It will be great to propose an analytical model and to derive closed form expressions of the metrics related to system performance evaluation.
3. The proposed protocol considers only the single input single output (SISO) communications. It is wise to extend this work to a global model that takes into account other communication technologies like multiple input single output (MISO), single input multiple output (SIMO) and even multiple input multiple output (MIMO). The spatial diversity could give additional degree of freedom to reduce the collision probability.
4. We have shown in this thesis that the Multiband CSMA/CA - RTS/CTS could be encapsulated to the multicarrier modulations like OFDM. It seems important to restudy the system by considering the FBMC modulation [84] [85]. Recently, many researchers have focused on this type of modulation to remove the guard interval and since it is well localized in frequency it could reduce further the interband interference [86].

Bibliography

- [1] G. I. Team, “5G White Paper,” in *NGMN 5G Initiative*, February 2015.
- [2] M. Iwamura, “NGMN View on 5G Architecture,” in *Vehicular Technology Conference (VTC Spring), 2015 IEEE 81st*, May 2015, pp. 1–5.
- [3] A. Annunziato, “5G Vision: NGMN - 5G Initiative,” in *Vehicular Technology Conference (VTC Spring), 2015 IEEE 81st*, May 2015, pp. 1–5.
- [4] C.-S. Hwang and J. Cioffi, “Opportunistic CSMA/CA for achieving multi-user diversity in wireless LAN,” *Wireless Communications, IEEE Transactions on*, vol. 8, no. 6, pp. 2972–2982, 2009.
- [5] J. Ni and R. Srikant, “Distributed CSMA/CA algorithms for achieving maximum throughput in wireless networks,” in *Information Theory and Applications Workshop, 2009*, 2009, pp. 250–250.
- [6] H. Xiaoben, “Self-Organized and Distributed Radio Resource Management Scheme for CSMA/CA Based IEEE 802.11 WLAN,” in *Wireless Communications, Networking and Mobile Computing, 2007. WiCom 2007. International Conference on*, 2007, pp. 2048–2053.
- [7] F. Tobagi and L. Kleinrock, “Packet Switching in Radio Channels: Part II—The Hidden Terminal Problem in Carrier Sense Multiple-Access and the Busy-Tone Solution,” *Communications, IEEE Transactions on*, vol. 23, no. 12, pp. 1417 – 1433, dec 1975.
- [8] “IEEE Draft STANDARD for Information Technology—Telecommunications and information exchange between systems—Local and metropolitan area networks—Specific requirements Part 11: Wireless LAN Medium Access Control (MAC) and Physical Layer (PHY) specifications Amendment 5: Enhancements for Higher Throughput,” *IEEE Unapproved Draft Std P802.11n/D9.0*, Mar 2009, pp. –, 2009.
- [9] M. H. Manshaei and J.-P. Hubaux, “Performance Analysis of the IEEE 802.11 Distributed Coordination Function: Bianchi Model,” March 2007.
- [10] G. Bianchi, “Performance analysis of the IEEE 802.11 distributed coordination function,” *Selected Areas in Communications, IEEE Journal on*, vol. 18, no. 3, pp. 535 –547, march 2000.
- [11] M. Fang, “Power Evaluation and Performance Enhancement of CSMA/CA based WLANs,” in *Masters Thesis, Hamilton Institute*, June 2010.
- [12] P. Chatzimisios, A. Boucouvalas, and V. Vitsas, “IEEE 802.11 packet delay-a finite retry limit analysis,” in *Global Telecommunications Conference, 2003. GLOBECOM '03. IEEE*, vol. 2, Dec 2003, pp. 950–954 Vol.2.
- [13] G. Bianchi, “IEEE 802.11-saturation throughput analysis,” *Communications Letters, IEEE*, vol. 2, no. 12, pp. 318 –320, dec. 1998.

- [14] G. Redieteab, “Cross-layer Optimization for Next Generation Wi-Fi,” in *PhD thesis National Institute of Applied Sciences (INSA) of Rennes*, October 2012.
- [15] Y. Medjahdi, “Interference modeling and performance analysis of asynchronous OFDM and FBMC wireless communication systems,” in *PhD thesis CONSERVATOIRE NATIONAL DES ARTS ET MÉTIERS*, January 2014.
- [16] I. Grigorik, *High Performance Browser Networking*. O’Reilly, 2013. [Online]. Available: <http://chimera.labs.oreilly.com/books/1230000000545/index.html>
- [17] “Access technologies,” <http://www.itu.int/osg/spu/ni/3G/technology/>.
- [18] “Random access protocols,” <http://fr.slideshare.net/MrSMAk/common-protocols>.
- [19] S. Chen, *ELEC3030 Computer Networks Lectures*. O’Reilly. [Online]. Available: <http://users.ecs.soton.ac.uk/sqc/EL336/CNL-7.pdf>
- [20] J. Barcelo, B. Bellalta, A. Sfaïropoulou, C. Cano, and M. Oliver, “CSMA with Enhanced Collision Avoidance: A Performance Assessment,” in *Vehicular Technology Conference, 2009. VTC Spring 2009. IEEE 69th*, April 2009, pp. 1–5.
- [21] “802.11 signal structure,” rfmw.em.keysight.com/wireless/helpfiles/n7617a/mimo_ofdm_signal_structure.htm.
- [22] “Legacy signal field,” http://rfmw.em.keysight.com/wireless/helpfiles/n7617a/legacy_signal_field.htm.
- [23] M. Starsinic, “System architecture challenges in the home M2M network,” in *Applications and Technology Conference (LISAT), 2010 Long Island Systems*, May 2010, pp. 1–7.
- [24] E. Perahia and R. Stacey, “Next generation wireless lans. throughput, robustness and reliability in 802.11n.” in *Cambridge*, 2008.
- [25] F.-N. Pavlidou, *Frequency-Division Multiple Access (FDMA): Overview and Performance Evaluation*. John Wiley and Sons, Inc., 2003. [Online]. Available: <http://dx.doi.org/10.1002/0471219282.eot112>
- [26] D. Falconer, F. Adachi, and B. Gudmundson, “Time division multiple access methods for wireless personal communications,” *Communications Magazine, IEEE*, vol. 33, no. 1, pp. 50–57, Jan 1995.
- [27] L. Hanzo, L. Yang, E. Kuan, and K. Yen, *CDMA Overview*. Wiley-IEEE Press, 2004, pp. 35–80. [Online]. Available: <http://ieeexplore.ieee.org/xpl/articleDetails.jsp?arnumber=5732958>
- [28] P. Flikkema, “Spread-spectrum techniques for wireless communication,” *Signal Processing Magazine, IEEE*, vol. 14, no. 3, pp. 26–36, May 1997.
- [29] T. Kortequee, W. Li, and D. Kazakos, “Performance evaluation of a soft hand off scheme in CDMA cellular networks,” in *Wireless Communications and Networking Conference, 2006. WCNC 2006. IEEE*, vol. 1, April 2006, pp. 171–176.
- [30] C. H. Foh and M. Zukerman, “A new technique for performance evaluation of random access protocols,” in *Communications, 2002. ICC 2002. IEEE International Conference on*, vol. 4, 2002, pp. 2284–2288 vol.4.
- [31] T.-Y. Yan and L. Clare, “Performance analysis of replication aloha for fading mobile communications channels,” *Communications, IEEE Transactions on*, vol. 34, no. 12, pp. 1256–1259, Dec 1986.

- [32] C. Namislo, "Analysis of mobile radio slotted aloha networks," *Selected Areas in Communications, IEEE Journal on*, vol. 2, no. 4, pp. 583–588, July 1984.
- [33] C. Salati, "An analysis of collisions in 1-persistent CSMA and a simple yet effective method to reduce them," in *Telecommunications, 1991. Third IEE Conference on*, Mar 1991, pp. 240–244.
- [34] S. Glisic, R. Rao, and L. Milstein, "The effect of imperfect carrier sensing on nonpersistent carrier sense multiple access," in *Communications, 1990. ICC '90, Including Supercomm Technical Sessions. SUPERCOMM/ICC '90. Conference Record., IEEE International Conference on*, Apr 1990, pp. 1266–1269 vol.3.
- [35] C.-S. Hwang, K. Seong, and J. Cioffi, "Opportunistic p-persistent CSMA in wireless networks," in *Communications, 2006. ICC '06. IEEE International Conference on*, vol. 1, June 2006, pp. 183–188.
- [36] Y.-C. Liu and G. Wise, "Performance of a CSMA/CD Protocol for Local Area Networks," *Selected Areas in Communications, IEEE Journal on*, vol. 5, no. 6, pp. 948–955, Jul 1987.
- [37] T.-S. Ho and K.-C. Chen, "Performance analysis of IEEE 802.11 CSMA/CA medium access control protocol," in *Personal, Indoor and Mobile Radio Communications, 1996. PIMRC'96., Seventh IEEE International Symposium on*, vol. 2, Oct 1996, pp. 407–411 vol.2.
- [38] "ISO/IEC Standard for Information Technology - Telecommunications and Information Exchange Between Systems - Local and Metropolitan Area Networks - Specific Requirements Part 11: Wireless LAN Medium Access Control (MAC) and Physical Layer (PHY) Specifications (Includes IEEE Std 802.11, 1999 Edition; IEEE Std 802.11A.-1999; IEEE Std 802.11B.-1999; IEEE Std 802.11B.-1999/Cor 1-2001; and IEEE Std 802.11D.-2001)," *ISO/IEC 8802-11 IEEE Std 802.11 Second edition 2005-08-01 ISO/IEC 8802 11:2005(E) IEEE Std 802.11i-2003 Edition*, pp. 1–721, 2005.
- [39] A. Athanasopoulos, E. Topalis, C. Antonopoulos, and S. Koubias, "Evaluation Analysis of the Performance of IEEE 802.11b and IEEE 802.11g Standards," in *Networking, International Conference on Systems and International Conference on Mobile Communications and Learning Technologies, 2006. ICN/ICONS/MCL 2006. International Conference on*, April 2006, pp. 141–141.
- [40] "IEEE Standard for Information technology–Telecommunications and information exchange between systems Local and metropolitan area networks–Specific requirements Part 11: Wireless LAN Medium Access Control (MAC) and Physical Layer (PHY) Specifications," *IEEE P802.11-REVmb/D12, November 2011 (Revision of IEEE Std 802.11-2007, as amended by IEEE Std 802.11k-2008, 802.11r-2008, 802.11y-2008, 802.11w-2009, 802.11n-2009, 802.11p-2010, 802.11z-2010, 802.11v-2011, 802.11u-2011, and 802.11s-2011)*, pp. 1–2910, March 2012.
- [41] J. Yun and S. Bahk, "Parallel contention algorithm with CSMA/CA for OFDM based high speed wireless LANs," in *Personal, Indoor and Mobile Radio Communications, 2003. PIMRC 2003. 14th IEEE Proceedings on*, vol. 3, sept. 2003, pp. 2581 – 2585 vol.3.
- [42] Y. Xu, M. Huang, M. Lin, and Y. Zheng, "A self-adaptive minimum contention window adjusting backoff algorithm in IEEE 802.11 DCF," in *Consumer Electronics, Communications and Networks (CECNet), 2012 2nd International Conference on*, april 2012, pp. 1577 –1582.

- [43] W. Ru-yan, W. Da-peng, and W. Mian, "Contention Awarred Adaptive Backoff Mechanism in IEEE 802.11 Wireless LAN," in *Computational Intelligence and Software Engineering, 2009. CiSE 2009. International Conference on*, dec. 2009, pp. 1–4.
- [44] Z. Haas and J. Deng, "On optimizing the backoff interval for random access schemes," *Communications, IEEE Transactions on*, vol. 51, no. 12, pp. 2081–2090, Dec 2003.
- [45] G. Bianchi and I. Tinnirello, "Kalman filter estimation of the number of competing terminals in an IEEE 802.11 network," in *INFOCOM 2003. Twenty-Second Annual Joint Conference of the IEEE Computer and Communications. IEEE Societies*, vol. 2, March 2003, pp. 844–852 vol.2.
- [46] S.-W. Kang, J.-R. Cha, and J.-H. Kim, "A Novel Estimation-Based Backoff Algorithm in the IEEE 802.11 Based Wireless Network," in *Consumer Communications and Networking Conference (CCNC), 2010 7th IEEE*, jan. 2010, pp. 1–5.
- [47] "IEEE Standard for Information Technology- Telecommunications and Information Exchange Between Systems- Local and Metropolitan Area Networks- Specific Requirements- Part 11: Wireless LAN Medium Access Control (MAC) and Physical Layer (PHY) Specifications," *ANSI/IEEE Std 802.11, 1999 Edition (R2003)*, pp. i–513, 2003.
- [48] J. W. Chong, D. K. Sung, and Y. Sung, "Cross-Layer Performance Analysis for CSMA/CA Protocols: Impact of Imperfect Sensing," *Vehicular Technology, IEEE Transactions on*, vol. 59, no. 3, pp. 1100–1108, march 2010.
- [49] Hojoong Kwon and Hanbyul Seo and Seonwook Kim and Byeong Gi Lee, "Generalized CSMA/CA for OFDMA systems: protocol design, throughput analysis, and implementation issues," *Wireless Communications, IEEE Transactions on*, vol. 8, no. 8, pp. 4176–4187, august 2009.
- [50] Jo Woon Chong and Youngchul Sung and Dan Keun Sung, "Analysis of CSMA/CA Systems under Carrier Sensing Error: Throughput, Delay and Sensitivity," in *Global Telecommunications Conference, 2008. IEEE GLOBECOM 2008. IEEE*, 30 2008-dec. 4 2008, pp. 1–6.
- [51] J. Barcelo, B. Bellalta, C. Cano, A. Sfaïropoulou, M. Oliver, and J. Zuidweg, "Traffic prioritization for carrier sense multiple access with enhanced collision avoidance," in *Communications Workshops, 2009. ICC Workshops 2009. IEEE International Conference on*, June 2009, pp. 1–5.
- [52] J. Barcelo, A. Toledo, C. Cano, and M. Oliver, "Fairness and Convergence of CSMA with Enhanced Collision Avoidance (ECA)," in *Communications (ICC), 2010 IEEE International Conference on*, May 2010, pp. 1–6.
- [53] J. Barcelo, B. Bellalta, C. Cano, A. Sfaïropoulou, and M. Oliver, "Carrier sense multiple access with enhanced collision avoidance: A performance analysis," in *Proceedings of the 2009 International Conference on Wireless Communications and Mobile Computing: Connecting the World Wirelessly*. ACM, 2009, pp. 733–738.
- [54] K. Wu, H. Tan, H.-L. Ngan, Y. Liu, and L. Ni, "Chip Error Pattern Analysis in IEEE 802.15.4," *Mobile Computing, IEEE Transactions on*, vol. 11, no. 4, pp. 543–552, April 2012.
- [55] Ji Fang and Kun Tan and Yuanyang Zhang and Shouyuan Chen and Lixin Shi and Jiansong Zhang and Yongguang Zhang and Zhenhui Tan, "Fine-Grained Channel Access in Wireless LAN," *Networking, IEEE/ACM Transactions on*, vol. 21, no. 3, pp. 772–787, June 2013.

- [56] J. W. Chong, Y. Sung, and D. K. Sung, "RawPEACH: Multiband CSMA/CA-based cognitive radio networks," *Communications and Networks, Journal of*, vol. 11, no. 2, pp. 175–186, 2009.
- [57] H. Kwon, S. Kim, and B. G. Lee, "Opportunistic multi-channel CSMA protocol for OFDMA systems," *Wireless Communications, IEEE Transactions on*, vol. 9, no. 5, pp. 1552–1557, 2010.
- [58] S. Basagni, C. Petrioli, R. Petroccia, and M. Stojanovic, "Multiplexing data and control channels in random access underwater networks," in *OCEANS 2009, MTS/IEEE Biloxi - Marine Technology for Our Future: Global and Local Challenges*, 2009, pp. 1–7.
- [59] N. Jain, S. Das, and A. Nasipuri, "A multichannel CSMA MAC protocol with receiver-based channel selection for multihop wireless networks," in *Computer Communications and Networks, 2001. Proceedings. Tenth International Conference on*, 2001, pp. 432–439.
- [60] J. Deng, Y. S. Han, and Z. Haas, "Analyzing split channel medium access control schemes," *Wireless Communications, IEEE Transactions on*, vol. 5, no. 5, pp. 967–971, 2006.
- [61] S. Sen, R. Roy Choudhury, and S. Nelakuditi, "No Time to Countdown: Migrating Backoff to the Frequency Domain," in *Proceedings of the 17th Annual International Conference on Mobile Computing and Networking*, ser. MobiCom '11. New York, NY, USA: ACM, 2011, pp. 241–252. [Online]. Available: <http://doi.acm.org/10.1145/2030613.2030641>
- [62] X. Feng, J. Zhang, Q. Zhang, and B. Li, "Use your frequency wisely: Explore frequency domain for channel contention and ACK," in *INFOCOM, 2012 Proceedings IEEE*, March 2012, pp. 549–557.
- [63] Y. Xiao and J. Rosdahl, "Throughput and delay limits of IEEE 802.11," *Communications Letters, IEEE*, vol. 6, no. 8, pp. 355–357, Aug 2002.
- [64] B. N. Bhandari, R. V. R. Kumar, and S. L. Maskara, "A modified back-off algorithm for the IEEE 802.11 DCF," in *Networks, 2005. Jointly held with the 2005 IEEE 7th Malaysia International Conference on Communication., 2005 13th IEEE International Conference on*, vol. 1, Nov 2005, pp. Z000 836–Z00 089E.
- [65] A. Qayyum, M. U. Saleem, Tauseef-Ul-Islam, M. Ahmad, and M. Khan, "Performance increase in CSMA/CA with RTS-CTS," in *Multi Topic Conference, 2003. INMIC 2003. 7th International*, 2003, pp. 182–185.
- [66] J. Yao, T. Xiong, and W. Lou, "Elimination of exposed terminal problem using signature detection," in *Sensor, Mesh and Ad Hoc Communications and Networks (SECON), 2012 9th Annual IEEE Communications Society Conference on*, 2012, pp. 398–406.
- [67] P. Chatzimisios, V. Vitsas, and A. Boucouvalas, "Throughput and delay analysis of IEEE 802.11 protocol," in *Networked Appliances, 2002. Liverpool. Proceedings. 2002 IEEE 5th International Workshop on*, Oct 2002, pp. 168–174.
- [68] T. Paul and T. Ogunfunmi, "Wireless LAN Comes of Age: Understanding the IEEE 802.11n Amendment," *Circuits and Systems Magazine, IEEE*, vol. 8, no. 1, pp. 28–54, First 2008.
- [69] Z. Chang, O. Alanen, T. Huovinen, T. Nihtila, E. H. Ong, J. Knecht, and T. Ristaniemi, "Performance analysis of iee 802.11ac dcf with hidden nodes," in *Vehicular Technology Conference (VTC Spring), 2012 IEEE 75th*, May 2012, pp. 1–5.

- [70] “IEEE Standard for Telecommunications and Information Exchange Between Systems - LAN/MAN Specific Requirements - Part 11: Wireless Medium Access Control (MAC) and physical layer (PHY) specifications: High Speed Physical Layer in the 5 GHz band,” *IEEE Std 802.11a-1999*, pp. 1–102, Dec 1999.
- [71] P.-J. Bouvet, “Récepteurs itératifs pour systèmes multi-antennes,” in *PhD thesis National Institute of Applied Sciences (INSA) of Rennes*, December 2005.
- [72] “Legacy short training field,” http://rfmw.em.keysight.com/wireless/helpfiles/n7617a/legacy_short_training_field.htm.
- [73] “Legacy long training field,” http://rfmw.em.keysight.com/wireless/helpfiles/n7617a/legacy_long_training_field.htm.
- [74] X. Ge, Y. Yang, H.-H. Chen, and Y. Zhu, “Cross-layer Throughput Analysis with Capture Effect in Wireless Local Area Networks,” in *Wireless Communications and Networking Conference, 2007. WCNC 2007. IEEE*, March 2007, pp. 4161–4165.
- [75] M. Parvej, S. Chowdhury, N. Hia, and M. Uddin, “Capture effect on the optimal contention window in IEEE 802.11 based WLANs,” in *Informatics, Electronics Vision (ICIEV), 2013 International Conference on*, May 2013, pp. 1–5.
- [76] “The Friis equation,” www.antenna-theory.com.
- [77] Z. Jia, X. He, and F. Li, “Enable concurrent transmissions with beamforming for broadband wireless access in CSMA/CA-based WLANs,” in *Globecom Workshops (GC Workshops), 2014*, Dec 2014, pp. 1075–1080.
- [78] M. Debbah, “Tutorial on MIMO technologies,” *Alcatel-Lucent Radio on Flexible Radio, Supélec*, [Online] Available: <http://flexible-radio.com/teaching/course-materials>, 2008.
- [79] IEEE 802.11-03/940r1, “Tgn channel models,” *TGn Channel Models Special Committee*, November 2003.
- [80] S. S. Aleksandar Purkovic, Nina Burns and L. Demirekler, “LDPC vs. Convolutional Codes for 802.11n Applications: Performance Comparison,” *Nortel Networks, IEEE 802.11-04/0071r1*, January 2004.
- [81] M. Heusse, F. Rousseau, G. Berger-Sabbatel, and A. Duda, “Performance anomaly of 802.11b,” in *INFOCOM 2003. Twenty-Second Annual Joint Conference of the IEEE Computer and Communications. IEEE Societies*, vol. 2, March 2003, pp. 836–843 vol.2.
- [82] B. Farhang-Boroujeny, “OFDM Versus Filter Bank Multicarrier,” *Signal Processing Magazine, IEEE*, vol. 28, no. 3, pp. 92–112, May 2011.
- [83] Baher Mawlawi, Jean-Baptiste Doré and Vincent Berg, “Optimizing Contention Based Access Methods for FBMC Waveforms,” in *International Conference on Military Communications and Information Systems ICMCIS (former MCC)*, May 2015.
- [84] M. Bellanger, “Specification and design of a prototype filter for filter bank based multicarrier transmission,” in *Acoustics, Speech, and Signal Processing, 2001. Proceedings. (ICASSP '01). 2001 IEEE International Conference on*, vol. 4, 2001, pp. 2417–2420 vol.4.
- [85] Y. Medjahdi, M. Terre, D. Le Ruyet, D. Roviras, and A. Dziri, “The Impact of Timing Synchronization Errors on the Performance of OFDM/FBMC Systems,” in *Communications (ICC), 2011 IEEE International Conference on*, June 2011, pp. 1–5.

- [86] Y. Medjahdi, M. Terre, D. Le Ruyet, and D. Roviras, “Asynchronous OFDM/FBMC interference analysis in selective channels,” in *Personal Indoor and Mobile Radio Communications (PIMRC), 2010 IEEE 21st International Symposium on*, Sept 2010, pp. 538–542.